

Dissertation zur Erlangung des Doktorgrades
der Fakultät für Chemie und Pharmazie
der Ludwig-Maximilians-Universität München

EXPLORING IN VIVO CONSEQUENCES OF
C-REL OVEREXPRESSION IN TERMINAL
B CELL DIFFERENTIATION

Anne Maike Margrete Kober

aus
Hamburg, Deutschland

2016

Erklärung

Diese Dissertation wurde im Sinne von §7 der Promotionsordnung vom 28. November 2011 von Herrn Prof. Dr. Matthias Mann betreut.

Eidesstattliche Versicherung

Diese Dissertation wurde eigenständig und ohne unerlaubte Hilfe erarbeitet.

München, 16.08.2016

Anne Maike Margrete Kober

Dissertation eingereicht am: 16.08.2016

1. Gutachter: Prof. Dr. Matthias Mann
2. Gutachter: Prof. Dr. Marc Schmidt-Supprian

Mündliche Prüfung am: 19.10.2016

Summary

Lymphoid B cells are part of the adaptive branch of the incredibly elaborate mammalian immune system that evolved as a defensive barrier to protect organisms against pathogenic invasion. The key characteristic of B cells is their highly diverse B cell receptor repertoire. Upon antigen encounter, naive B cells form germinal centers (GC), where they terminally differentiate into antibody-secreting plasma cells. During GC reactions, B cells undergo somatic hypermutation and isotype class switch recombination of their B cell receptor to improve pathogen recognition and clearance. These processes essentially require DNA breaks. Consequently, physiology can turn into pathology as these mechanisms bear the detrimental potential not only of self-recognition underlying autoimmunity but also of undesired somatic DNA alterations causing malignant transformation. Indeed, the majority of human B cell lymphomas arises from GC or post-GC B cells.

While constitutive NF- κ B transcription factor activation is a hallmark of various human lymphoid cancers, it is remarkable that c-Rel is the only of five NF- κ B family members that malignantly transforms lymphoid chicken cells *in vitro*. Interestingly, the *REL* gene locus is frequently amplified in human B cell lymphomas and a c-Rel splice variant lacking exon 9 has been exclusively detected in diffuse large B cell lymphoma patients but not in healthy individuals. Besides these implications of c-Rel in human lymphomas, single nucleotide polymorphisms within the *REL* gene locus are associated with human autoimmune diseases. Despite this evidence, no mouse model to investigate c-Rel gain-of-function in immune cells existed to date and the distinct role of c-Rel in B cells remains enigmatic.

In this thesis, I present the first conditional c-Rel transgenic mouse models with the aim of elucidating the precise *in vivo* consequences of c-Rel overexpression and aberrant splicing in B cells and germinal center B cells. These novel mouse models allow for Cre-inducible expression of transgenic c-Rel or a GFP-c-Rel fusion protein under control of a strong CAG promoter. In addition, flippase recombinase-mediated excision of exon 9 from this modified *REL* gene locus enables conditional expression of the c-Rel splice variant that has been identified in B cell lymphoma patients.

Induction of c-Rel transgene expression specifically in B cells (CD19Cre) or GC B cells (C γ 1Cre) causes a significant expansion of spontaneous GC B cells in lymphoid tissues of young mice, comprising spleen, lymph nodes and gut-associated mesenteric lymph

nodes and Peyer's patches. This dramatic phenotype is accompanied by an increase of specialized follicular helper T cells that provide crucial signals for GC B cells during GC reactions. Moreover, antibody-secreting plasma cells significantly accumulate in spleen and bone marrow upon c-Rel overexpression. These plasma cells are highly isotype class-switched consistent with elevated serum antibody titers. Although aged c-Rel transgenic mice do not spontaneously develop overt lymphoma or autoimmunity, aged mice produce class-switched autoantibodies, indicating that the GC reactions are driven by self-antigens. Cell cycle analysis suggests that higher proliferation of GC B cells could contribute to the observed GC B cell expansion. In the same line, I also found that in the human primary mediastinal B cell lymphoma cell line MedB-1 shRNA-mediated c-Rel downregulation causes robust cell cycle deceleration without affecting cell viability.

On the basis of comprehensive quantitative assessment of c-Rel protein expression levels in c-Rel transgenic and control mice, I demonstrate that c-Rel levels are B cell subtype-dependent. In both control and c-Rel transgenic mice moderate c-Rel expression levels are present in naive B cells, whereas c-Rel expression is dramatically upregulated in GC B cells and strongly reduced in plasma cells. In addition, this analysis revealed that c-Rel levels strikingly correlate with GC B cell and plasma cell expansion. During this study, I further discovered a fundamental tight regulation of c-Rel levels in naive B cells. Remarkably, proteasomal inhibition causes upregulation of c-Rel levels in naive B cells but not in GC B cells, indicating that proteasome-mediated pathways are responsible for the restricted c-Rel level in naive B cells in both c-Rel transgenic and control mice.

In conclusion, these first conditional c-Rel transgenic mouse models have not only contributed to the knowledge of c-Rel function in B cells and GC B cells so far, but they can be prospectively applied to further advance the understanding of the particular role of c-Rel in immune cells and beyond.

Contents

I	Introduction	1
1	B cells	1
1.1	B cell lymphopoiesis	2
1.1.1	Early B cell development	2
1.1.2	B cell maturation	4
1.2	B cell activation and terminal differentiation	6
1.2.1	The germinal center reaction	7
1.2.2	Germinal center exit: plasma cells and memory B cells	14
2	c-Rel – an NF-κB family transcription factor	17
2.1	Canonical and non-canonical NF- κ B activation	17
2.2	The role of c-Rel in B cells	18
2.2.1	c-Rel protein	19
2.2.2	c-Rel expression in B cells	20
2.2.3	c-Rel activation and regulation	22
2.2.4	Transcriptional activation by c-Rel	25
2.2.5	c-Rel target genes	28
2.2.6	Functional consequences of c-Rel signaling in B cells	31
3	c-Rel signaling in B cell pathology	38
3.1	Malignant transformation of B cells	38
3.2	<i>REL</i> amplification in human B cell lymphoma	39
3.2.1	Diffuse large B cell lymphoma	40
3.2.2	Primary mediastinal B cell lymphoma	43
3.2.3	Classical Hodgkin lymphoma	44
3.2.4	<i>REL</i> amplification and c-Rel protein expression and localization	44
3.2.5	Co-amplification of <i>BCL11A</i> with <i>REL</i>	46
3.3	Human B cell lymphoma cell lines	47
3.4	Disease associations of c-Rel beyond lymphoma	49
3.5	c-Rel as a therapeutic target	50

II	Aim of the thesis	51
III	Materials and Methods	52
1	Standard materials and methods	52
2	Generation and characterization of mouse lines	52
2.1	Mouse generation	52
2.1.1	BAC transgenesis and construct verification	52
2.1.2	Embryonic stem cell culture	53
2.1.3	Southern blot	54
2.1.4	PCR for ES cell screening and genotyping	55
2.2	Genetically modified mice	55
2.3	Flow cytometry and imaging flow cytometry	56
2.4	Magnetic activated cell sorting (MACS)	56
2.5	Primary mouse cell culture	58
2.6	Western blot	58
2.7	Immunization	58
2.8	ELISA	59
2.9	Data analysis, statistical evaluation and visualization	59
3	Manipulation of human B cell lymphoma cell lines	60
3.1	Generation of shRNA constructs by Golden Gate cloning	60
3.2	Cell culture: transfection, selection and induction	60
3.3	Western blot	61
3.4	Flow cytometry	62
3.5	Cell count assay	62
3.6	Competitive co-culture assay	62
3.7	Cell cycle analysis	62
3.8	Active caspase assay	63
3.9	Data analysis and visualization	63

IV	Results	64
1	The first conditional c-Rel transgenic mouse models to investigate enhanced c-Rel function in B cells	64
1.1	Generation of novel c-Rel transgenic mouse lines	64
1.2	Developmental and naive mature B cell physiology is largely unaltered . . .	67
1.3	c-Rel overexpression causes expansion of GC B cells and plasma cells . . .	71
1.3.1	Expansion of germinal center B cells	71
1.3.2	Activated T cells	74
1.3.3	Expansion of class-switched plasma cells	77
1.4	Validation of phenotype in GFP-c-Rel CD19Cre ^{I/+} mice	80
1.5	Induced GC reactions and acute expression of c-Rel at the GC B cell stage	82
1.5.1	Expansion of GC B and plasma cells upon immunization	82
1.5.2	c-Rel C γ 1Cre ^{I/+} mice phenocopy c-Rel CD19Cre ^{I/+} mice	84
1.6	Aged c-Rel CD19Cre ^{I/+} mice	87
1.7	c-Rel levels are B cell subtype-dependent and correlate with cellular expansion	89
1.7.1	c-Rel is upregulated in GC B cells and decreased in plasma cells . .	89
1.7.2	c-Rel level switches are not caused by transgenic promoter regulation	94
1.7.3	Higher c-Rel nuclear translocation in germinal center B cells	96
1.7.4	Strong correlation of c-Rel level with GC B cells and plasma cells .	102
1.7.5	Higher proliferation could contribute to expansion of GC B cells . .	104
1.8	c-Rel levels are tightly regulated	106
1.8.1	c-Rel levels are limited in GC B cells of double transgenic mice . . .	106
1.8.2	c-Rel level in B cells is sensitive to proteasomal inhibition	109
1.9	Expression of the novel c-Rel Δ Ex9 splice variant	111
2	Consequences of c-Rel knockdown in human B cell lymphoma cell lines	112
2.1	Strategy for c-Rel knockdown	112
2.2	Efficient c-Rel knockdown in human lymphoma cell lines	113
2.3	c-Rel knockdown in MedB-1 cells reduces cellular expansion	117
2.4	c-Rel knockdown causes a clear disadvantage in competitive co-cultures . .	118
2.5	c-Rel knockdown reduces proliferative cell cycle phases	120

V	Discussion	122
1	Generation of the first conditional c-Rel transgenic mouse models	122
2	c-Rel in terminal B cell differentiation	123
3	c-Rel protein expression and regulation	126
4	c-Rel in lymphoma and autoimmunity - a yet unresolved question	129
5	Concluding remarks and outlook	132
	Supplemental Figures	133
	References	189
	Abbreviations	209
	Acknowledgements	213

Part I

Introduction

1 B cells

The highly complex mammalian immune system has evolved elaborate mechanisms to protect an organism against intruding pathogens. The two branches of immunity, the innate and adaptive immune response, intertwine to form an effectively organized network to combat these infectious agents. While innate immune cells recognize conserved structures through germline-encoded pattern recognition receptors, lymphoid B cells and T cells are characterized by a highly diverse somatically assembled receptor repertoire [Murphy et al., 2007]. The principal defensive mechanism provided by the B lineage is the secretion of antibodies after B cells have terminally differentiated into plasma cells, also known as humoral immunity [Nutt et al., 2015]. Furthermore, B cell memory enables a rapid response against previously encountered pathogens [Kurosaki et al., 2015]. Although the protective role for antibodies had already been described in the late 19th century, it was not until 1965 that B cells and T cells were recognized as functionally and developmentally distinctive lineages [Von Behring and Kitasato, 1890; Cooper et al., 1965; Cooper, 2015]. Today, research focuses on unraveling the molecular mechanisms underlying tightly regulated processes that enable lymphoid cells to fulfill their immune cell function.

The tremendously variable B cell receptor (BCR) repertoire is generated in the bone marrow where B cells undergo sequential DNA rearrangements of their immunoglobulin (Ig) gene loci [Clark et al., 2014]. This initial repertoire is further diversified through the mechanism of somatic hypermutation (SHM) within the germinal center structures that are formed following B cell activation upon encounter with a foreign antigen. During this affinity maturation process, the BCR is modified and subsequently selected for an improved fit to the initially recognized antigen [Peled et al., 2008]. In addition, mature B cells undergo isotype class switch recombination (CSR) in order to refine the antibody's effector function [Stavnezer et al., 2008; Xu et al., 2012]. These activated B cells give rise to memory B cells and plasma cells that provide both primary and long-lived humoral protection [Shlomchik and Weisel, 2012].

1.1 B cell lymphopoiesis

Cells of the hematopoietic lineages have their developmental origin in pluripotent hematopoietic stem cells (HSC) that reside in the fetal liver during early embryogenesis and in the bone marrow during postnatal life [Dorshkind and Montecino-Rodriguez, 2007]. HSC give rise to multipotent progenitors (MPP) that lose long-term self-renewal capacity – a unique property of HSC [Wilson and Trumpp, 2006; Cabezas-Wallscheid et al., 2014]. Lineage determination is initiated as MPPs further differentiate into oligopotent common myeloid progenitors (CMP) or common lymphoid progenitors (CLP) that give rise to cells of the myeloid and lymphoid lineages, respectively [Akashi et al., 1999; Murphy et al., 2007]. Although it has been suggested recently that CMPs might be composed of several unipotent progenitors rather than representing one population, it is evident that these myeloid precursors are able to develop into granulocytes (neutrophils, eosinophils, basophils), monocytes and macrophages as well as mast cells or erythroid cells and megakaryocytes [Kondo et al., 2003; Cabezas-Wallscheid and Trumpp, 2016]. CLPs can commit not only towards the B cell lineage but also to T cell, NK cell and dendritic cell populations [Akashi et al., 1999].

1.1.1 Early B cell development

Early B cells develop in the microenvironment of the bone marrow. In these so called bone marrow niches, B cells closely interact with stromal cells that secrete various cytokines and provide essential signals for B cell development. Amongst these factors FLT3 ligand (FLT3L), interleukin-7 (IL-7), stem-cell factor (SCF) and CXC-chemokine ligand 12 (CXCL12) have been shown to be indispensable [Nagasawa, 2006]. Moreover, studies in mice demonstrated that several transcription factors are required to transition through distinct early B cell developmental stages, including B cell lymphoma/leukemia 11a (Bcl-11a) [Liu et al., 2003], E2A [Bain et al., 1994; Zhuang et al., 1994], early B cell factor (EBF) [Lin and Grosschedl, 1995] and paired box protein 5 (Pax5) [Urbánek et al., 1994; Nutt et al., 1999]. While Bcl-11a acts upstream of E2A and EBF that initiate B lymphopoiesis, Pax5 is required to confer restricted B cell fate commitment [Rolink et al., 2000; Singh et al., 2005; Fuxa and Skok, 2007].

Stages of B cell development are defined by expression of cell surface molecules and status of somatic recombination of Ig gene segments. Somatic recombination provides the

framework of the enormous B cell receptor diversity. During this process the variable (V), diversity (D) and joining (J) gene segments encoding for the variable region of the Ig heavy (IgH) and light (IgL) chain are rearranged sequentially to form a functional BCR [Murphy et al., 2007; Hozumi and Tonegawa, 1976; Tonegawa, 1983]. Pro-B cells initiate assembly of the IgH chain (Ig μ) locus, first by D to J_H , followed by V_H to DJ_H segment rearrangement [Clark et al., 2014]. Successful rearrangements of one IgH chain allele results in arrest of rearrangement of the second allele to ensure that a single B cell only expresses one unique IgH chain, a mechanism referred to as allelic exclusion [Melchers, 2015]. The rearranged IgH chain is transiently expressed on the cell surface together with a surrogate light chain that is composed of VpreB and $\lambda 5$. In combination with the signaling subunits Ig α and Ig β they form the pre-BCR complex [Clark et al., 2014]. Signaling through the correctly assembled pre-BCR constitutes an important checkpoint during B cell development and provides signals that induce proliferation and allow cells to proceed to the subsequent pre-B cell stage. Pre-BCR-expressing large pre-B cells undergo several rounds of cell division before they become resting small pre-B cells that initiate rearranging the V_L and J_L segments of the IgL chain gene loci (Ig κ and Ig λ) [Clark et al., 2014; Melchers, 2015].

Gene locus rearrangements require expression of the lymphocyte-specific recombination activation genes *RAG1* and *RAG2* in B cells as well as in T cells that rearrange the T cell receptor (TCR)-encoding genes during development in the thymus [Schlissel, 2003; Schatz and Ji, 2011]. RAG-deficient mice lack mature B and T cells emphasizing the crucial relevance of these enzymes [Mombaerts et al., 1992; Shinkai et al., 1992]. Tightly restricted RAG expression and the DNA-encoded recombination signal sequences (RSS) that flank rearranging gene segments combined with regulated DNA accessibility by germline transcription and chromatin structure modifications safeguard the temporally and spatially restricted execution of locus rearrangements [Schlissel, 2003; Schatz and Ji, 2011]. In addition, ubiquitous non-homologous end joining (NHEJ) repair pathway proteins are involved in lymphocyte somatic gene rearrangement. These factors include DNA-dependent protein kinase (DNA-PK) consisting of Ku (Ku70:Ku80) and a catalytic subunit DNA-PKcs, X-ray repair cross complementing protein 4 (XRCC4), Artemis as well as DNA ligase IV [Bassing et al., 2002; Schlissel, 2003].

Upon productive rearrangement of both IgH and IgL chains, immature B cells express the rearranged IgM on the cell surface. B cells emerging from these processes potentially

recognize auto- or self-antigens and need to undergo a selection process to avoid exit of autoreactive B cells into the periphery in order to prevent autoimmunity [Nemazee, 2006]. This checkpoint in B cell development is crucial in establishing central B cell tolerance as it has been reported that the majority of human and mouse B cells initially recognize self-antigens [Grandien et al., 1994; Wardemann et al., 2003; Pelandra and Torres, 2012]. Autoreactive B cells can undergo receptor editing, i.e. these B cells proceed through additional rounds of IgL chain rearrangements. B cells that retain strong self-antigen binding despite receptor editing face elimination by apoptotic cell death, a process referred to as clonal deletion [Nemazee, 2006]. An alternative fate for autoreactive B cells is escape to and persistence in the periphery with simultaneous conversion to an anergic state. Anergic B cells are silenced and non-responsive to antigen stimulation, thus representing another mechanism by which tolerance is sustained [Merrell et al., 2006; Cambier et al., 2007].

1.1.2 B cell maturation

Tolerance-selected cells egress from the bone marrow to enter the periphery as transitional B cells. Transitional B cells are identified by expression of the surface marker AA4.1/CD93 and can be subdivided into three groups. Transitional T1 B cells express IgM. Upon maturation to the T2 stage, B cells start surface IgD expression in addition to IgM mediated by alternative splicing. T2 B cells enter splenic B cell follicles and are able to recirculate through the bone marrow [Allman et al., 2001; Stavnezer et al., 2008; Pillai and Cariappa, 2009]. The population of T3 B cells was shown to consist of B cells with an anergic phenotype and was suggested to be re-defined as An1 B cells [Merrell et al., 2006; Allman and Pillai, 2008]. B cells are not only subject to negative selection during maturation in the periphery but also depend on positive selection signals [Allman and Pillai, 2008; Stadanlick and Cancro, 2008]. From the transitional stages onwards, tonic BCR- and BAFF(B cell-activating factor belonging to TNF family)-mediated survival signals become crucial for peripheral B cell maturation and maintenance [Sasaki et al., 2004; Stadanlick and Cancro, 2008; Srinivasan et al., 2009].

Transitional B cells differentiate into follicular (FO) B cells or into marginal zone precursor (MZP) that further develop into marginal zone (MZ) B cells. FO B cells are able to recirculate through blood and lymph stream to the bone marrow and home to B cell follicles in secondary lymphoid organs, such as spleen, lymph nodes and Peyer's patches,

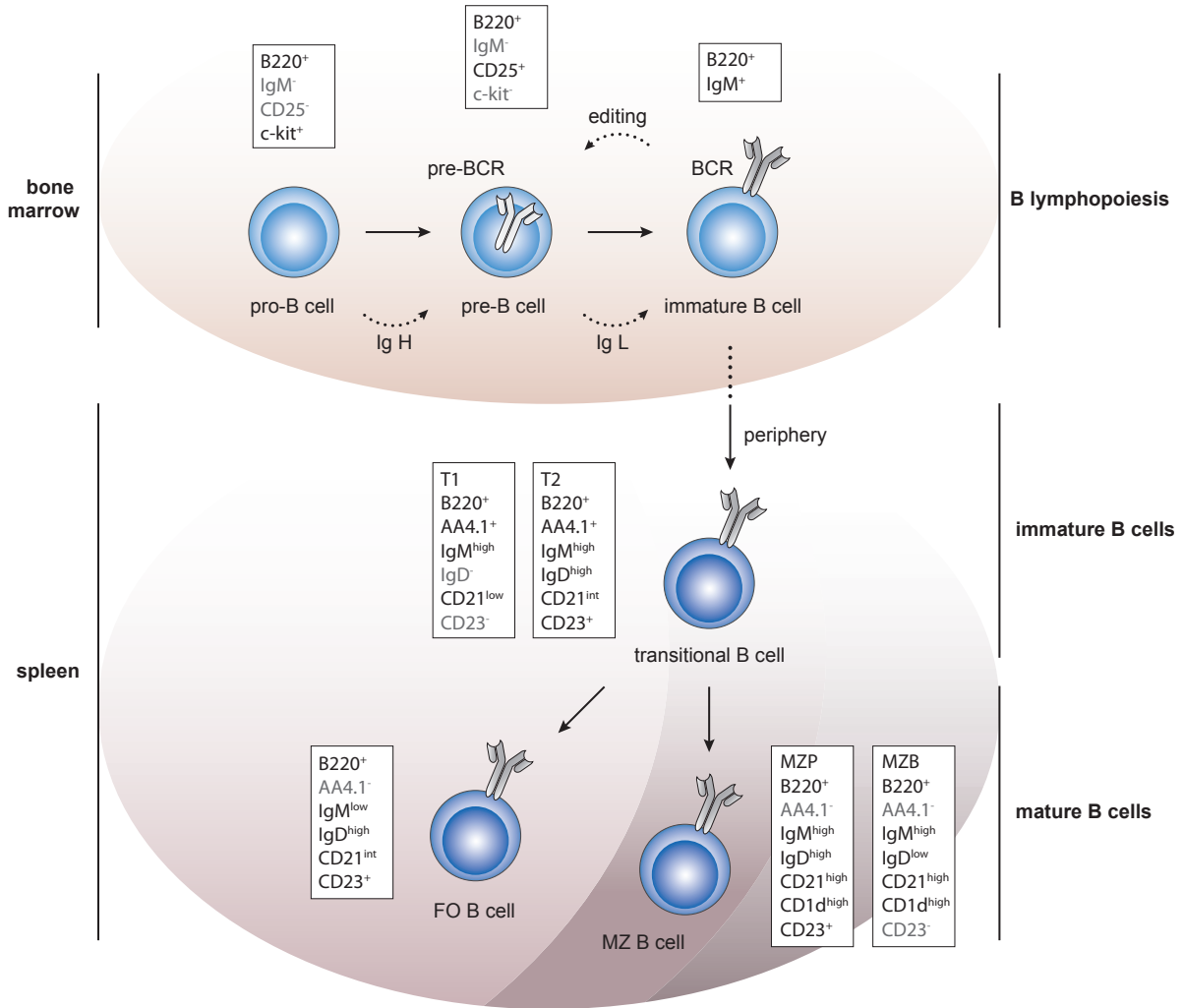


Figure 1: Simplified illustration of early B cell development and B cell maturation. In the bone marrow B cells begin rearrangement of the immunoglobulin (Ig) heavy (H) chain locus during the pro-B cell stage. Successfully rearranged IgH is expressed together with a surrogate light chain as the pre-B cell receptor (pre-BCR) allowing the B cell to proceed to the subsequent pre-B cell stage. Pre-B cells rearrange the Ig light (IgL) chain loci eventually resulting in mature BCR expression that characterizes the immature B cell stage. These cells egress from the bone marrow and enter the periphery as transitional B cells. In the spleen transitional B cells differentiate into follicular (FO) B cells or into marginal zone precursor (MZP) and further into marginal zone (MZ) B cells. Important mouse surface expression markers are given for each subset. The content of this figure is based on Pillai and Cariappa, 2009, and Cambier et al., 2007.

where they become central mediators of T cell-dependent (TD, also thymus-dependent) immune responses. In contrast, MZ B cells reside in the outer white pulp adjacent to the marginal sinus of the spleen and rapidly respond to blood-borne pathogens in a T cell-independent (TI, also thymus-independent) manner, although they are also involved in TD immune responses. MZ B cells have the ability of self-renewal and are characterized by longevity, whereas FO B cells have a limited lifespan [Allman and Pillai, 2008; Pillai and Cariappa, 2009; Cerutti et al., 2013]. While a complex interplay of BCR signaling

strength, BAFF-mediated survival signals and downstream activation of NF- κ B signaling contributes to MZ versus FO B cell fate decisions [Pillai and Cariappa, 2009], Delta-like-1 (DL1) induced Notch2 signaling is a key linear factor for splenic MZ B cell development [Tan et al., 2009].

Both FO and MZ B cells belong to the B-2 line of mature B cells. Besides these populations, B-1 cells, which develop earlier in ontogeny than B-2 cells, constitute another peripheral mature B cell population in the mouse. B-1 cells are rare in spleen and lymph nodes but frequent in peritoneal and pleural cavity and produce natural IgM antibodies, which are polyreactive antibodies that are present prior to antigen exposure. They are involved in tissue homeostasis and TI immune responses and provide immune protection against mucosal pathogens. While the pool of B-2 cells is continuously replenished by B cells developed in the bone marrow, B-1 cells are mainly derived from fetal precursors and are to a large extent sustained by self-renewal thereafter. A distinct population representing a human functional counterpart of mouse B-1 cells remains under debate [Dorshkind and Montecino-Rodriguez, 2007; Baumgarth, 2011].

1.2 B cell activation and terminal differentiation

Activation of mature naive B cells is initiated upon encounter with an antigen. BCR ligation by specific antigen binding assembles a BCR proximal signaling cascade that culminates in B cell activation-associated gene expression [Reth and Wienands, 1997; Kurosaki and Wienands, 2015]. These signaling events lead to internalization of the BCR-antigen complex that is subsequently processed for loading on major histocompatibility complex class II (MHC-II). Upon presentation in context of MHC-II on the cell surface, the antigen peptide can be recognized by cognate CD4⁺ helper T cells [Pierce, 2002; Harwood and Batista, 2010]. Formation of an immunological synapse during B cell-T cell interaction at the border region of the B cell follicle and the T cell zone provides secondary signals, including CD40 ligand (CD40L) and stimulatory cytokine signaling, that lead to full activation of a B cell [Batista and Harwood, 2009; Crotty, 2015]. Activated B cells can then rapidly become plasmablasts that secrete antibodies in extrafollicular foci [MacLennan et al., 2003] or found germinal centers (GC). B cells can also be activated in the absence of T cells by TI antigens [Balázs et al., 2002; MacLennan et al., 2003].

1.2.1 The germinal center reaction

Following the phase of antigen encounter and subsequent B cell activation, B cells undergo extensive proliferation in the center of the B cell follicle, thus forming an activated initial GC B cell cluster surrounded by a mantle zone of naive follicular B cells [Victora and Nussenzweig, 2012; De Silva and Klein, 2015]. GC B cells upregulate B cell lymphoma 6 (Bcl-6) that is considered to be the master transcriptional regulator of GC B cells [De Silva and Klein, 2015]. Subsequently, the GC extends towards maturity as it polarizes into a dark zone (DZ) and a light zone (LZ). These terms originate from historic conventional histologic descriptions of the GC but are still used today [Röhlich, 1930; Nieuwenhuis and Opstelten, 1984; Allen et al., 2004; Victora and Nussenzweig, 2012]. The DZ/LZ differentiation of mature GCs represents a polarization into functional states as delineated in detail in the following subsections. B cells of the DZ and LZ are often referred to as centroblasts and centrocytes, respectively. The CXC-chemokine receptors CXCR4 and CXCR5 mediate the DZ/LZ polarization and spatial structure of the GC [Allen et al., 2004]. DZ B cells are characterized by high CXCR4 and low CXCR5 and CD83/CD86 surface expression, whereas LZ B cells appear low in CXCR4 but express high levels of CXCR5 and CD83/CD86 [Allen et al., 2004; Victora et al., 2010, 2012]. Moreover, recent studies identified the transcription factor forkhead box O1 (FOXO1) as a crucial regulator in establishing the GC DZ phenotype that is antagonized by phosphatidylinositol 3-kinase (PI3K) signaling in the LZ [Dominguez-Sola et al., 2015; Sander et al., 2015]. In addition, GC B cells express high levels of CD95/Fas and n-glycolylneuraminic acid that is recognized by the GL7 antibody, bind peanut agglutinin (PNA) and lose IgD expression. While mouse GC B cells downregulate CD38, human GC B cells upregulate CD38 [Hauser et al., 2010; Victora and Nussenzweig, 2012]. In mice the temporal dynamics of GC reactions have been well-described. Induced by antigen encounter, the GC matures within approximately 8 days and dissolves after several weeks – depending on the experimental immunization [Victora, 2014; De Silva and Klein, 2015]. Also in mice housed under specific-pathogen-free conditions GCs spontaneously occur without prior immunization through chronic triggering by commensal bacteria in gut-associated lymphoid tissues [Casola and Rajewsky, 2006].

Germinal center cell types GC B cells are not the only cell type within the GC. T cells, stromal cells and macrophages provide essential cues and are engaged in spatial

organization and structure of the GC [Victora and Nussenzweig, 2012]. The DZ is densely populated by GC B cell blasts and few recently described reticular cells that express CXCL12, the ligand for CXCR4 [Bannard et al., 2013]. In contrast, B cells in the LZ are more sparse and surrounded by a dense network of follicular dendritic cells (FDC) as well as specialized follicular helper T cells (T_{fh}). Tingible body macrophages (TBM) that phagocytose apoptotic GC B cells are localized throughout the GC [Victora and Nussenzweig, 2012].

FDCs produce CXCL13 that functions as a chemoattractant for B cells and T_{fh} cells as it is the ligand for CXCR5 that is expressed on these lymphocytes. FDCs also represent a source of IL-6 and BAFF that foster B cell survival [Wang et al., 2011; Aguzzi et al., 2014; Heesters et al., 2014]. Moreover, FDCs are able to capture and display immune complexes, which has been suggested to preserve antigens and serve as an antigen depot in GCs [Allen and Cyster, 2008; Suzuki et al., 2009].

T_{fh} cell marker proteins include CXCR5, programmed cell death 1 (PD-1), high levels of inducible T cell co-stimulator (ICOS) and CD69 as well as Bcl-6, the pivotal transcriptional regulator of T_{fh} cell differentiation. By expression of CD40L as well as secretion of IL-4 and IL-21, T_{fh} cells promote GC B cell survival [Fazilleau et al., 2009; Vinuesa et al., 2010; Crotty, 2011]. The importance of T_{fh} cell interaction with GC B cells is emphasized by long-standing studies showing that blockade of the CD40-CD40L interaction [Han et al., 1995; Foy et al., 1994] or deficiency for CD40 or CD40L [Xu et al., 1994; Kawabe et al., 1994] abrogates GC formation. Despite the GC reaction being a typical event during TD immune responses, it has been shown that GCs can initially form without T_{fh} cell help to B cells in mice; however, these GCs do not persist [de Vinuesa et al., 2000; Lentz and Manser, 2001].

GC B cell competition and selection Fully matured GCs are the site of clonal GC B cell expansion, somatic hypermutation (SHM) and affinity maturation as well as class switch recombination (CSR) (see page 12). During the process of SHM, point mutations are introduced into gene segments encoding for the variable regions of the BCR (see page 11). These mutations can alter antigen binding affinity or selectivity of the respective BCR, thus potentially improving antigen recognition. Positive selection of GC B cells with enhanced recognition properties results in an enrichment of specifically antigen-affine GC B cells over time – the phenomenon referred to as affinity maturation [Berek et al.,

1991; Victora and Nussenzweig, 2012; De Silva and Klein, 2015]. GC B cells that have decreased antigen binding capacities after mutation or recognize self-antigens, which is consequently presented on MHC-II to T_{fh} cells, are eliminated by apoptotic cell death. Indeed, high expression of death inducing CD95/Fas receptor on GC B cells as well as low expression of the pro-survival protein Bcl-2 makes apoptosis the default fate of a GC B cell [Victora and Nussenzweig, 2012]. The exact mechanism of a process of negative selection opposed to mere death by neglect due to the lack of positive selection signals in GCs is under debate [Vinuesa et al., 2009; Brink, 2014; Allen, 2015]. T cell populations of the GC are implicated in mediating negative selection of GC B cells. First, overactivated T_{fh} cells are associated with deregulated GC reactions and autoimmunity. Second, newly identified follicular regulatory T cells (T_{fr}) are proposed to have suppressive effects on T_{fh} cells as well as GC B cells and represent a novel candidate cellular population involved in negative selection [Ramiscal and Vinuesa, 2013; Vinuesa et al., 2016]. Although the exact role of CD95/Fas signaling in elimination of self-reactive GC B cells and the cell types providing CD95L/FasL signals remain elusive, it is evident that defects in the CD95/Fas-CD95L/FasL pathway perturb selection processes and are associated with autoimmunity [Hao et al., 2008; Victora and Nussenzweig, 2012; Allen, 2015; Butt et al., 2015]. Moreover, it is established that GC B cells highly depend on survival signals supplied by the GC microenvironment, hence allowing these selection processes to proceed [Victora and Nussenzweig, 2012].

This premise entails a scenario in which GC B cells compete for limited signals that enable their positive selection. The model of competition for antigen binding suggests that high affinity GC B cells sequester available antigen, consequently leading to the expansion of these clones via induction of BCR signaling [Victora and Nussenzweig, 2012]. Feedback from newly produced antigen-specific antibodies was shown to limit antigen access and was suggested to influence GC B cell selection pressure [Zhang et al., 2013]. However, accumulating evidence supports the hypothesis that T_{fh} cells are the predominant mediators of selection. *In vivo* imaging studies visualizing GC B cell-T cell interactions and lymphocyte motility in the GC [Allen et al., 2007b; Schwickert et al., 2007; Victora et al., 2010] as well as mathematical modeling [Meyer-Hermann et al., 2006, 2012] corroborate the theory of competition for T cell help. Targeting T_{fh} cells to a subpopulation of GC B cells by increasing the surface density of peptide-MHC-II independent of BCR cross-linking results in the expansion of specifically this subpopulation of GC B cells [Victora

et al., 2010]. Furthermore, GC B cells with high surface density of peptide-MHC-II form the most lasting and highest number of contacts with T_{fh} cells. These GC B cell- T_{fh} cell contacts are accompanied by an increase in T_{fh} cell intracellular Ca^{2+} as well as IL-4 and IL-21 expression [Shulman et al., 2014]. As these models are not mutually exclusive, integration of both BCR and T_{fh} cell signals could contribute to GC B cell selection [Allen et al., 2007a; Victora and Nussenzweig, 2012; De Silva and Klein, 2015].

Cyclic re-entry and germinal center dynamics While proliferation for clonal expansion and SHM take place in the DZ of the GC, selection mainly occurs in the LZ of the GC [Victora et al., 2010]. A model of cyclic re-entry had been proposed early [Kepler and Perelson, 1993], but only studies using intravital microscopy could eventually demonstrate that GC B cells migrate between DZ and LZ and vice versa [Allen et al., 2007b; Hauser et al., 2007a; Schwickert et al., 2007; Victora et al., 2010]. Whilst these groups present comparable results, the groups around Michel Nussenzweig and Jason Cyster conclude that their findings are in support of iterative cycles between the zones [Allen et al., 2007b; Schwickert et al., 2007; Victora et al., 2010], whereas Hauser et al. propose a model of a predominantly intrazonal circulation pattern [Hauser et al., 2007a]. However, as explained by Hauser et al. all data can be regarded in accordance with a cyclic re-entry model depending on the frequency of selection [Hauser et al., 2007b, 2010]. Half of the GC B cells transit from the DZ to the LZ within 4-6 hours, while around 15% migrate from LZ to DZ within this time frame. According to mathematical modeling these experimental observations translate into a total fraction of 10-30% of cells that re-enter the DZ after being in the LZ [Victora et al., 2010; Victora, 2014]. A bi-directional interzonal migration allows antibody affinity maturation to take place as GC B cells repeatedly undergo proliferation and SHM in the DZ followed by selection in the LZ. Cellular homolog of myelocytomatosis oncogene (c-Myc)-expressing LZ GC B cells have been proposed to represent a population of cells positively selected for DZ re-entry [Calado et al., 2012; Dominguez-Sola et al., 2012]. A recent report indicates that the switch from DZ to LZ cellular state is independent of signals received in the DZ. The authors suggest that the centroblast to centrocyte transition occurs according to a timed cell-intrinsic program. This cellular 'timer' could be pre-set by LZ signals before cyclic re-entry [Bannard et al., 2013]. This is in agreement with studies demonstrating that T_{fh} cells can influence cell cycle dynamics in GC B cells [Gitlin et al., 2015] and that the amount of antigen captured

by GC B cells and presented to T_{fh} cells positively correlates with the extent of subsequent cell divisions and hypermutation [Gitlin et al., 2014].

The GC structure is a highly dynamic environment as both T_{fh} cells [Shulman et al., 2013] and B cells [Schwickert et al., 2007] – including B cells specific for an unrelated antigen [Schwickert et al., 2009] – can enter and invade pre-existing GCs. In addition, recent studies describing the population dynamics of affinity maturation conclude that clonal diversity is a feature of immune responses elicited by complex antigens and that polyclonality can be maintained in parallel to homogenous clonal dominance [Kuraoka et al., 2016; Tas et al., 2016]. Together, these studies on GC dynamics hint at mechanisms evolved to warrant diversity, thus ensuring broad protective immune response also against variable or fast evolving pathogens.

Somatic hypermutation During somatic hypermutation (SHM) point mutations in Ig variable gene regions are introduced at an estimated frequency of 10^{-3} per base pair per generation/division [Rajewsky et al., 1987; Berek et al., 1991; Jacob et al., 1991]. The nucleotide substitutions can lead to both transition mutations, which refers to the exchange of a purine with a purine or a pyrimidine with a pyrimidine base, and transversion mutations, where a purine base is exchanged for a pyrimidine base or vice versa. These mutations are enriched within complementarity determining regions (CDR), the Ig site of specific antigen contact, that contain preferred mutational hotspot DNA motifs [Odegard and Schatz, 2006; Di Noia and Neuberger, 2007; Hwang et al., 2015].

The first step of SHM is triggered by activation-induced cytidine deaminase (AID) that deaminates deoxycytidine on single-stranded DNA converting it to deoxyuridine. These AID-catalyzed U:G lesions are substrates for enzymes of the ubiquitous base excision repair (BER) and mismatch repair (MMR) pathways. Mutations at C:G pairs are attributed to activity of uracil DNA glycosylase (UNG) of BER, whereas mutations at A:T pairs are associated with MutS protein homolog (MSH) complexes and exonuclease 1 (Exo1) function of MMR [Di Noia and Neuberger, 2007; Teng and Papavasiliou, 2007]. Ultimately, error-prone DNA polymerases including translesion polymerase Rev1 and low-fidelity polymerases θ (pol θ) and η (pol η) contribute to SHM [Martomo and Gearhart, 2006; Teng and Papavasiliou, 2007].

AID is required in both SHM and CSR as further described below [Muramatsu et al., 1999, 2000]. It has been suggested that co-factors interacting specifically with either the amino-

or carboxy-terminus of AID are involved in mediating AID function and localization in SHM or CSR, respectively [Barreto et al., 2003; Ta et al., 2003; Shinkura et al., 2004]. SHM is known to be closely linked to transcription [Teng and Papavasiliou, 2007] and AID targeting to particular loci in combination with balancing error-prone and high-fidelity DNA repair has been suggested to protect the genome during SHM [Liu et al., 2008; Liu and Schatz, 2009]. Nevertheless, the exact mechanisms of AID targeting remain largely unresolved [Odegard and Schatz, 2006; Daniel and Nussenzweig, 2013; Hwang et al., 2015].

Class switch recombination Ig class or isotype switching is the process in which activated B cells couple their rearranged variable antibody determining genetic region with an alternative heavy chain constant gene fragment. As different antibody classes are characterized by distinct functional properties, class switch recombination (CSR) alters the effector functions of an antibody while conserving the antibody's antigen specificity. The five major antibody classes IgM, IgD, IgG, IgE and IgA are encoded by the heavy chain isotype loci μ , δ , γ , ϵ and α respectively. Class switching involves an intrachromosomal deletional recombination event between donor and acceptor switch (S) regions located upstream of these constant heavy chain genes [Chaudhuri and Alt, 2004; Stavnezer et al., 2008].

CSR requires DNA double strand breaks (DSB) in S regions. Initiation of this process is promoted by AID-mediated deamination of deoxycytidine to deoxyuridine [Muramatsu et al., 1999, 2000; Delker et al., 2009]. Subsequently, enzymes of the ubiquitous BER pathway, such as UNG and apurinic/aprimidinic endonucleases (APE), generate DNA single strand breaks (SSB). DSB formation occurs in case SSBs are in close proximity to each other on opposite strands or is facilitated by enzymes of the MMR pathway, including MSH complexes and Exo1. The resulting DSB in S regions are then fused by non-homologous or alternative end-joining, thus linking the antibody's variable segment to an alternative heavy chain isotype [Stavnezer et al., 2008; Xu et al., 2012].

Germline transcription through a specific S region is essential for and directs class switch to the respective isotype, predominantly by conferring accessibility for factors involved in CSR, first and foremost AID [Xu et al., 2012; Matthews et al., 2014]. Moreover, proliferation is crucial for CSR [Stavnezer et al., 2008]. CSR is triggered by CD40 signaling or an interplay of BCR, Toll-like receptor (TLR) as well as transmembrane activator and calcium-modulating cyclophilin-ligand interactor (TACI) signaling [Xu et al., 2012]. In

cooperation with specific cytokines, such as IL-4, transforming growth factor- β (TGF β) and interferon- γ (IFN γ) that drive class switching to preferential isotypes, these stimuli activate multiple transcription factors leading to effective AID expression, germline transcription at S regions and histone modifications. Transcription factors involved in these processes include NF- κ B, signal transducer and activator of transcription (STAT) proteins, homeobox C4 (HoxC4), Pax5 and basic leucine zipper transcription factor ATF-like (BATF) [Xu et al., 2012; Matthews et al., 2014].

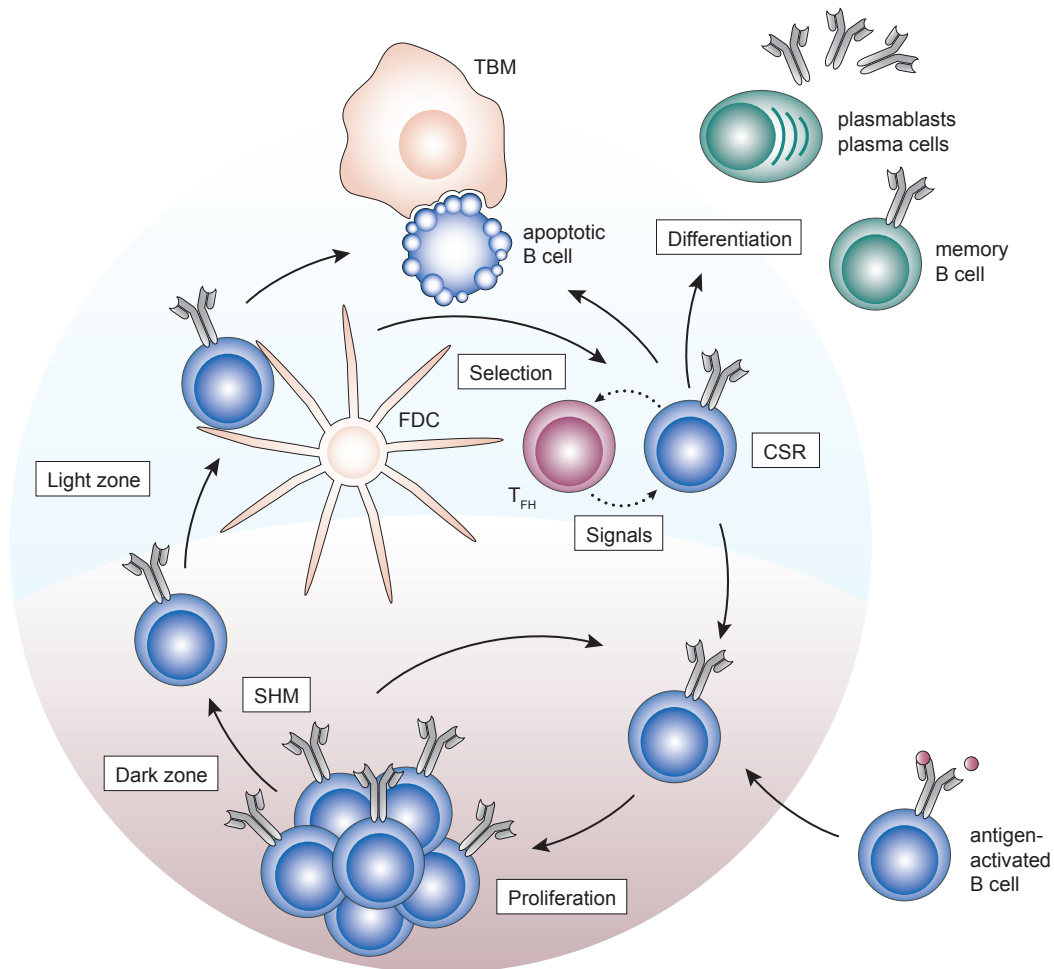


Figure 2: Simplified illustration of the germinal center reaction. Upon antigen encounter, activated B cells form germinal centers (GC) where they undergo extensive proliferation. GCs are the site of somatic hypermutation (SHM) and class switch recombination (CSR). Repeated cycles of these processes combined with competitive selection involving follicular dendritic cells (FDC) and follicular helper T cells (T_{fh}) culminates in affinity maturation of the B cell receptor. GC B cells differentiate into antibody-secreting plasma cells and memory B cells. TBM, tingible body macrophage. This figure is based on Heesters et al., 2014, De Silva and Klein, 2015, and Vinuesa et al., 2009.

1.2.2 Germinal center exit: plasma cells and memory B cells

Both plasma cells and memory B cells contribute to persistent, long-lasting immune protection. While long-lived plasma cells are an incessant supplier of circulating antibodies, thus sustaining serum antibody titers, memory B cells are rapidly re-activated following antigen re-exposure [Shapiro-Shelef and Calame, 2005; McHeyzer-Williams et al., 2012]. Although memory B cells and short-lived plasmablasts can develop outside of GCs, GCs represent the established source of class-switched affinity-matured plasma cells and memory B cells [Radbruch et al., 2006; McHeyzer-Williams et al., 2012; Shlomchik and Weisel, 2012; Kurosaki et al., 2015]. Fate decisions of B cell terminal differentiation and GC exit still remain enigmatic and a variety of models – that are not mutually exclusive – have been proposed. Differentiation into the plasma cell or memory B cell pool could be determined by extrinsic instructive stimuli or by an automatic, intrinsically programmed response. Furthermore, stochastic or temporal-defined mechanisms have been suggested to influence the memory or plasma cell fate choice [Shlomchik and Weisel, 2012; Nutt et al., 2015]. A recent report demonstrated a timed switch for GC output of memory B cells and plasma cells [Weisel et al., 2016]. However, the exact molecular cues leading to this switch are to date unknown. BCR affinity or BCR isotype class have been suggested to drive B cells towards either plasma cells or memory B cells [Shlomchik and Weisel, 2012; Zotos and Tarlinton, 2012; Gitlin et al., 2016]. Moreover, there is evidence that IL-21 influences GC B cell fate as it is involved in driving plasma cell differentiation [Zotos and Tarlinton, 2012].

Plasma cells Antibody-secreting cells that appear early during an immune response are referred to as plasmablasts. Plasmablasts typically secrete antibodies with moderate affinity and are comparably short-lived, yet dividing. In contrast, long-lived plasma cells secrete class-switched high-affinity antibodies and are quiescent in terms of cell cycling [Radbruch et al., 2006; Nutt et al., 2015]. Plasma cells are entirely dedicated to secretion of large amounts of antibody reflected by their characteristic morphology of an extended endoplasmic reticulum [Grootjans et al., 2016]. The switch from surface BCR expression in B cells to antibody production in plasma cells demands major adaptations in gene regulatory networks [Radbruch et al., 2006; Nutt et al., 2015]. This identity conversion involves silencing of B cell and GC B cell lineage commitment transcription factors, namely Pax5 and Bcl-6. In addition, BTB and CNC homolog 2 (BACH2) and E twenty-six (ETS)

transcription factor family members are downregulated in plasma cells [Shapiro-Shelef and Calame, 2005; Nutt et al., 2015]. The pivotal transcription factors activated in plasma cells are B lymphocyte-induced maturation protein 1 (Blimp-1), X-box-binding protein 1 (XBP-1) and interferon regulatory factor 4 (IRF4) [Nutt et al., 2011]. The transcriptional repressor Blimp-1 is essential in terminating distinctive B cell properties by antagonizing Pax5 and Bcl-6 [Lin et al., 2002; Shaffer et al., 2002a; Shapiro-Shelef et al., 2003] and setting the stage for antibody secretion, including XBP-1 upregulation [Shaffer et al., 2004; Minnich et al., 2016; Tellier et al., 2016]. XBP-1 induces the unfolded protein response (UPR) to enable plasma cells to cope with the endoplasmic reticulum stress that accompanies extensive antibody production [Reimold et al., 2001; Shaffer et al., 2004; Todd et al., 2009]. In contrast to Blimp-1 and XBP-1, IRF4 executes its functions in both GC B cells and plasma cells in a dose-dependent manner with high levels of IRF4 promoting plasma cell fate [Klein et al., 2006; Sciammas et al., 2006; Ochiai et al., 2013]. Long-lived plasma cells reside in a limited number of bone marrow niches, where their longevity is maintained by survival factors, including IL-6, tumor necrosis factor (TNF) and a proliferation inducing ligand (APRIL), the ligand for B cell maturation antigen (BCMA) that is expressed on plasma cells. In addition, surface molecules CXCR4, very late antigen 4 (VLA4), CD44, CD28 and CD93 as well as the transcription factor Aiolos are thought to contribute to plasma cell homing or survival [Cortés and Georgopoulos, 2004; Radbruch et al., 2006; Nutt et al., 2015]. Moreover, plasma cells can be identified by surface expression of CD138 (syndecan-1) [Radbruch et al., 2006].

Memory B cells In contrast to plasma cells, memory B cells conserve a B cell profile through Pax5 maintenance which is embodied by continuation of surface BCR expression and absence of antibody secretion. However, upon antigen re-challenge, memory B cells can rapidly expand and differentiate into antibody-secreting plasma cells. This recall response involves help provided by memory T cells [McHeyzer-Williams et al., 2012; Kurosaki et al., 2015]. Memory B cells can also re-enter GCs allowing them to re-diversify their BCRs within these secondary GCs [McHeyzer-Williams et al., 2015; Seifert et al., 2015]. Both unswitched IgM-expressing as well as switched IgG-expressing memory B cells can be found in mice and human [Shlomchik and Weisel, 2012].

This section has highlighted how B cells exert their function as central mediators of the adaptive immune response based on the evolution of antigen recognition. While the

BCR diversity has its origin in somatic recombination during B cell development in the bone marrow, the highly elaborate GC reaction in peripheral immune organs provides the structure for B cells to specifically adapt to a pathogen and provide long-lasting protection by giving rise to hypermutated class-switched plasma cells as well as memory B cells.

2 c-Rel – an NF- κ B family transcription factor

The nuclear factor κ -light-chain-enhancer of activated B cells (NF- κ B) is a universal player in both innate and adaptive immune responses [Baltimore, 2011]. In general, NF- κ B transcription factors are activated through a plethora of stimuli and induce the expression of a broad diversity of genes. Nevertheless, particular target gene expression triggered by a defined stimulus in a distinct cell-type is tightly regulated on multiple layers, thus highlighting the complexity of NF- κ B signaling [Sen and Smale, 2010; Smale, 2011]. Common activators of NF- κ B include not only inflammatory cytokines, antigen receptor signaling and viral or bacterial mediators of infection but also genotoxic stress [Oeckinghaus and Ghosh, 2009]. The subsequent downstream signals following NF- κ B activation contribute to cell survival, differentiation and proliferation and control central mechanisms of immune responses including inflammation [Hayden and Ghosh, 2008; Ghosh and Hayden, 2008].

c-Rel is one of the five members of the NF- κ B family of transcription factors. Besides c-Rel the mammalian NF- κ B family consists of RelA/p65 and RelB as well as p50/NF- κ B1 and p52/NF- κ B2. NF- κ B transcription factors exert their function as regulators of gene expression forming hetero- or homodimers. The amino-terminal Rel homology domain (RHD) is shared amongst all NF- κ B family members and is involved in dimerization, DNA binding, inhibitor interaction and nuclear localization. While RelA, RelB and c-Rel possess a carboxy-terminal transactivation domain (TAD), p50 and p52 lack a TAD. Instead the precursor proteins of the latter, p105 and p100, contain a domain of inhibitory ankyrin repeats that is proteolytically processed to form the DNA-binding molecules p50 and p52. Hence, p50 and p52 rely on pairing with TAD-containing family members for positive regulation of target genes and are implicated in repressing transcription as homodimers [Perkins and Gilmore, 2006; Ghosh and Hayden, 2008; Hayden and Ghosh, 2008; Vallabhapurapu and Karin, 2009].

2.1 Canonical and non-canonical NF- κ B activation

Under inactive steady state conditions NF- κ B dimers are sequestered in the cytoplasm by interaction with ankyrin repeat-containing inhibitor of κ B ($I\kappa$ B) proteins or the precursors p100 and p105. Triggering the canonical or also referred to as the classical NF- κ B signaling cascade leads to activation of the trimeric $I\kappa$ B kinase (IKK) complex that consists of

IKK α /IKK1, IKK β /IKK2 and the regulatory subunit IKK γ /NEMO (NF- κ B essential modulator). The IKK complex phosphorylates I κ B proteins, thus targeting the inhibitors for polyubiquitination followed by proteasomal degradation. The released NF- κ B dimers, mainly RelA:p50 and c-Rel:p50, can subsequently translocate into the nucleus and activate target genes. The non-canonical or also termed alternative NF- κ B pathway is mediated by NF- κ B-inducing kinase (NIK)-dependent IKK α dimer activation. Phosphorylation of p100 by activated IKK α dimers induces partial proteolytic processing of p100 to p52 which primarily heterodimerizes with RelB [Perkins and Gilmore, 2006; Hayden and Ghosh, 2008; Vallabhapurapu and Karin, 2009]. In concert with co-activators or co-repressors, NF- κ B dimers act on κ B sites within promoters or enhancers of target genes [Ghosh and Hayden, 2008]. The typical 9-11 base pair κ B target sequence is 5'-GGGRNWYYCC-3' (R: purine (A, G); Y: pyrimidine (C, T); W: weak (A, T); N: any nucleotide); however, the κ B site sequence is highly degenerate [Natoli et al., 2005; Karin, 2011; Siggers et al., 2012].

The resolution of the NF- κ B response is in part governed by negative feedback loops as NF- κ B target genes include negative regulators, for instance de novo synthesis of I κ B proteins or expression of the negative regulator A20. Other mechanisms negatively regulating NF- κ B activation involve dissociation of the signaling complexes, displacement of NF- κ B from DNA or direct NF- κ B degradation. Many of these processes are influenced by post-translational modifications, in particular phosphorylation and ubiquitination [Wertz and Dixit, 2010; Ruland, 2011].

2.2 The role of c-Rel in B cells

c-Rel was discovered as the cellular homolog of the transforming viral gene v-Rel of reticuloendotheliosis virus strain T (Rev-T), an oncogenic avian retrovirus that causes aggressive lymphoma/leukemia [Chen et al., 1981; Gilmore, 1999]. Indeed, first descriptions of c-Rel in avian species precede the discovery of the general NF- κ B transcription factor family. Characterization of c-Rel in turkey [Wilhelmsen et al., 1984; Wilhelmsen and Temin, 1984] and chicken [Chen et al., 1983; Hannink and Temin, 1989] had been initiated in the early nineteen-eighties and was soon followed by findings in human [Brownell et al., 1985] and mouse [Brownell et al., 1986; Grumont and Gerondakis, 1989; Bull et al., 1990]. In the mid nineteen-eighties, independent studies led to the discovery of NF- κ B, which was found as a nuclear factor that binds to the κ light chain enhancer in B cells during attempts to

unravel mechanisms of DNA rearrangement [Sen and Baltimore, 1986b,a]. Sequence and functional comparisons between c-Rel and different κ B-binding factors [Gilmore, 1990; Ghosh et al., 1990; Kieran et al., 1990; Bours et al., 1990; Nolan et al., 1991] as well as the drosophila dorsal protein [Steward, 1987] substantiated the notion that these proteins in fact belong to the same family of transcription factors.

An increasing number of publications thereafter demonstrated that NF- κ B/Rel transcription factors by far exceed a sole function in B cells. Especially mouse models have advanced our understanding in this regard [Gerondakis et al., 2006; Pasparakis et al., 2006]. In contrast to RelA knockout in mice which is embryonic lethal, c-Rel knockout mice are viable and show defects primarily in lymphocytes during immune responses [Kontgen et al., 1995; Harling-McNabb et al., 1999; Gerondakis et al., 2006]. In brief, c-Rel-deficient B cells are characterized by impaired proliferative and survival responses to mitogenic stimuli *in vitro* and by abrogated germinal center reactions and antibody production *in vivo* (for details see 2.2.6). Despite the enormous research efforts performed to understand NF- κ B in general and numerous studies concentrating on c-Rel in particular, the complexity of subunit and cell type specificity still raises puzzling questions. The following subsections summarize the current knowledge of c-Rel with a particular focus on B cells.

2.2.1 c-Rel protein

The human and murine *REL* gene loci – on chromosome 2 and chromosome 11 – encode for the c-Rel protein with a length of 587 and 588 amino acids (aa), respectively, and an approximate molecular weight of 65 kDa [Brownell et al., 1985, 1986; Grumont and Gerondakis, 1989; Bull et al., 1990; Leeman et al., 2008]. Human and mouse c-Rel share 75% total aa sequence identity and more than 94% identity in the first 300 aa containing the highly conserved amino-terminal RHD¹. Besides the primary human c-Rel transcript, the original publication reported a transcript containing an exonized Alu element between exon 8 and 9 identified in a human B cell lymphoma cell line (Daudi) that could encode for a 619 aa protein [Brownell et al., 1989; Leeman and Gilmore, 2008]. In addition, a lymphoma-specific spliced version of human c-Rel lacking the entire exon 9 (aa 308-330) with a higher *in vitro* transactivation activity has been described [Leeman et al., 2008] (see also 3.2). Furthermore, this study defined the protein sequence of aa 323-422

¹Application of BLASTP search on www.ensembl.org aligning parts or whole protein sequences for transcripts ENSMUST00000102864 (mouse GRCm38.p4) and ENST00000394479 (human GRCh38.p5)

upstream of the TAD as the Rel inhibitory domain (RID) based on biochemical analyses demonstrating that mutants lacking this region show enhanced transactivation and DNA binding *in vitro* [Leeman et al., 2008]. Within the carboxy-terminal TAD c-Rel harbors two subdomains referred to as TAD1 and TAD2 that map to aa 425-490 and aa 518-587, respectively [Martin et al., 2001; Starczynowski et al., 2003; Gilmore and Gerondakis, 2011]. c-Rel contains a nuclear localization signal (NLS), but in contrast to RelA it does not have a nuclear export signal (NES) [Tam et al., 2001; Fagerlund et al., 2008]. c-Rel is able to form homodimers or heterodimeric complexes with RelA, p50 and p52 [Bonizzi and Karin, 2004; Gilmore and Gerondakis, 2011]. The molecular protein structures of different NF- κ B subunits have been resolved [Chen and Ghosh, 1999] including that of chicken c-Rel homodimers [Huang et al., 2001].

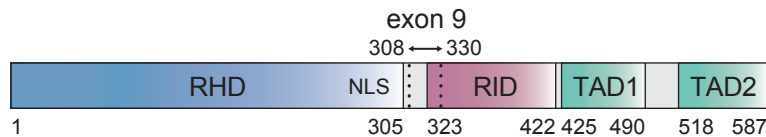


Figure 3: Schematic representation of the human c-Rel protein. Numbers below the scheme are amino acid start and end points of indicated protein domains. Dotted lines mark the position of the amino acid sequence encoded by exon 9 (aa 308-330). RHD, Rel homology domain; RID, Rel inhibitory domain; TAD, transactivation domain; NLS, nuclear localization signal. This figure is based on Gilmore and Gerondakis, 2011, and Leeman et al., 2008. Other references assign the RHD to aa 8-290 [Perkins, 2012] or aa 8-297 (UniProt database, UniProtKB, Q04864 REL (human), www.uniprot.org).

2.2.2 c-Rel expression in B cells

The murine c-Rel promoter contains several κ B sites and octamer (Oct) transcription factor binding sites. It is not only recognized by other NF- κ B subunits, but the c-Rel promoter can also be transactivated by c-Rel itself [Grumont et al., 1993]. Furthermore, there are PU.1/Spi-B Ets family transcription factor binding sites in the c-Rel promoter that are elementary for its transactivation in B cells as c-Rel expression is markedly reduced in PU.1^{+/-} Spi-B^{-/-} mouse splenic B cells [Grumont et al., 1993; Viswanathan et al., 1996; Hu et al., 2001].

In contrast to RelA that is expressed ubiquitously in mice [Sen and Smale, 2010], c-Rel expression is under healthy conditions mainly restricted to the hematopoietic lineage [Carrasco et al., 1994]. Already the earliest studies analyzing c-Rel expression in mouse tissues demonstrated high c-Rel abundance particularly in lymphocytes, with exceedingly

elevated levels in splenic B cells but low levels in bone marrow B cells [Brownell et al., 1987; Carrasco et al., 1994]. This is in accordance with a predominant NF- κ B complex composition of c-Rel and p50 in mature B cells [Grumont and Gerondakis, 1994; Wuerzberger-Davis et al., 2011], accompanied by indications that in pre-B cells p50 and RelA could be the major subunits [Grumont and Gerondakis, 1994; Liou et al., 1994; Miyamoto et al., 1994]. These early studies also found that expression of c-Rel can be induced by activating stimuli, e.g. by lipopolysaccharide (LPS) [Grumont and Gerondakis, 1994; Carrasco et al., 1994] (see also 2.2.3). Based on biochemical analyses by Grumont and Gerondakis, it has been inferred that in mature B cells c-Rel is primarily nuclear [Grumont and Gerondakis, 1994; Gilmore et al., 2004a]. In contrast, Carrasco et al. observed heterogeneous localization of c-Rel in the nucleus and cytoplasm of B cells applying immunofluorescence [Carrasco et al., 1994]. More recent quantitative immunofluorescence studies demonstrate that c-Rel nuclear translocation can be detected in around 20% of mature resting B cells [Ferch et al., 2007; Wuerzberger-Davis et al., 2011].

B cells of mice deficient for the B cell adaptor for PI3K (BCAP) exhibit much lower transcript and protein levels exclusively of c-Rel but not any of the other NF- κ B family members [Yamazaki and Kurosaki, 2003]. In line with this, c-Rel protein levels are strongly decreased in total and mature B cells of mice with genetic disruption of PI3K activity, whereas RelA is only mildly reduced. Furthermore, PI3K inhibition of wild-type B cells leads to a decrease in c-Rel protein levels [Suzuki et al., 1999; Matsuda et al., 2008]. These findings indicate that PI3K activity, which is thought to be downstream of tonic BCR survival signaling in resting mature B cells [Srinivasan et al., 2009], plays a role in maintaining c-Rel levels in B cells. Moreover, c-Rel expression is strongly reduced in splenocytes of mice with a functionally mutant form of NIK, suggesting that c-Rel levels are also dependent on the alternative NF- κ B pathway [Yamada et al., 2000].

To date of publication of this thesis, there are no comprehensive quantitative studies on c-Rel protein levels in activated or terminally differentiated primary B cells. A compendium of microarray-based gene expression analyses of immune cells conclude that a typical NF- κ B signature is absent in GC B cells [Shaffer et al., 2001, based on data in Alizadeh et al., 2000]. On the contrary, an NF- κ B signaling signature was reported to be enhanced in LZ GC B cells in comparison to DZ GC B cells also based on microarray gene expression analysis [Victora et al., 2010]. In addition, there are studies indicating that c-Rel is expressed in GC B cells. First, basic studies using *in situ* hybridization detected *REL*

transcripts in GCs in spleen and lymphoid follicles of lymph nodes and Peyer's patches in mouse [Carrasco et al., 1994]. Second, Barth et al. mention that they found high c-Rel expression in GC cells in non-neoplastic lymphoid tissue with predominant cytoplasmic but also rare nuclear localization [Barth et al., 2003]. Third, Basso et al. detected c-Rel in the majority of GC B cells in the cytoplasm and only in a fraction of centrocytes of the LZ nuclear c-Rel was observed [Basso et al., 2004], a finding that is in agreement with data presented by that group in a later publication [Saito et al., 2007]. Beyond these limited experiments on GC B cells, transcriptional profiling of mouse mature B cell and plasma cell populations suggests a decrease of *REL* transcript level in plasmablast and plasma cell stages in comparison to mature B cell subsets [Shi et al., 2015]. In conclusion, despite the strong phenotype of c-Rel-deficient mice in activated and terminally differentiated B cells (see 2.2.6), c-Rel protein expression levels have not been quantitatively investigated in these B cell subsets.

2.2.3 c-Rel activation and regulation

c-Rel is activated by diverse stimuli and regulated on multiple layers. The regulatory mechanisms include nuclear shuttling and sequestration by $I\kappa B$ proteins as well as post-translational modifications that are implicated in modifying c-Rel transactivation and transforming activity as well as in regulating c-Rel protein levels. In addition, *REL* mRNA is controlled on the post-transcriptional level.

c-Rel activation The cardinal triggers of canonical NF- κ B signaling in B cells are ligands to the BCR, TNF-receptor (TNFR) superfamily member CD40 and TLRs, namely TLR4 and TLR9, all of which can activate c-Rel [Gilmore and Gerondakis, 2011; Kaileh and Sen, 2012]. Several knockout mouse models provide evidence for factors involved in the cascade of c-Rel activation downstream of the BCR. c-Rel nuclear translocation downstream of BCR signaling in mature B cells specifically requires the paracaspase mucosa-associated lymphoid tissue protein 1 (MALT1). Together with caspase activation and recruitment domain (CARD)-containing membrane-associated guanylate kinase 1 (CARMA1) and Bcl-10, MALT1 forms the CBM signal transduction complex upon BCR stimulation [Ferch et al., 2007; Jaworski and Thome, 2016]. In MALT1-deficient B cells c-Rel, unlike RelA, remains in complex with $I\kappa B\alpha$ and $I\kappa B\beta$ following anti-IgM BCR stimulation and does not translocate to the nucleus. This MALT1-dependence is specific

for signals downstream of the BCR as c-Rel nuclear translocation upon LPS stimulation triggering TLR4 is not impaired [Ferch et al., 2007]. Moreover, an irreversible direct inhibitor of MALT1 protease activity, MI-2, was shown to inhibit c-Rel nuclear translocation in human lymphoma cell lines *in vitro* and in a xenograft mouse model [Fontan et al., 2012]. Data obtained in B cells lacking Bruton’s tyrosine kinase (Btk) indicate that also this signaling molecule plays a role in c-Rel activation as c-Rel DNA binding is strongly reduced in Btk-deficient B cells upon stimulation, despite unchanged c-Rel protein levels [Shinners et al., 2007].

When comparing NF- κ B kinetics upon IgM stimulation of B cells Damdinsuren et al. found that pulsed, single round IgM stimulation results in transient nuclear translocation of both c-Rel and RelA for up to 6 hours. In contrast, only continuous IgM stimulation leads to de novo c-Rel induction and long-term nuclear c-Rel accumulation between 6 and 24 hours, while nuclear quantities of RelA are negligible during this time period. Combination of anti-CD40 stimulation following pulsed or continuous anti-IgM treatment causes enhanced c-Rel nuclear expression, whereas RelA remains unaffected [Damdinsuren et al., 2010]. These experiments demonstrate a dominant role of c-Rel in sustained NF- κ B responses in B cells.

Nuclear shuttling and I κ B In contrast to RelA, c-Rel does not contain an NES. As a consequence, RelA containing dimers are more efficiently shuttled out of the nucleus than c-Rel complexes *in vitro* [Tam et al., 2001]. Taken into consideration that initial NF- κ B activation can induce de novo c-Rel expression, this mechanism could contribute to a prolongation of the NF- κ B response executed by c-Rel [Damdinsuren et al., 2010; Sen and Smale, 2010].

I κ B proteins represent a fundamental layer of negative NF- κ B regulation. It has been proposed that in pre-B cell lines c-Rel is mainly associated with I κ B β , whereas c-Rel is associated with both I κ B α and I κ B β in mature B cells, implicating that these differential associations could be related to selective activation of subunits in particular B cell stages [Tam et al., 2001; Liou and Hsia, 2003]. The significance of I κ B α in c-Rel regulation is demonstrated in a mouse model expressing a mutant I κ B α lacking a functional I κ B α NES (Nfkb α ^{NES/NES}). In these mice c-Rel accumulates in the nucleus in mature B cells accompanied by a compromised c-Rel DNA-binding activity. As a consequence Nfkb α ^{NES/NES} mice show severe defects in the B cell lineage that in part phenocopy c-Rel^{-/-} mice (see

2.2.6). These findings emphasize the importance of $I\kappa B\alpha$ degradation achieved by proper $I\kappa B\alpha$ localization for c-Rel function in mature B cells [Wuerzberger-Davis et al., 2011]. Interestingly, a partial shift of preferential c-Rel association from $I\kappa B\beta$ to $I\kappa B\alpha$ has been proposed during priming of naive T cells with pro-inflammatory cytokines. Subsequent TCR stimulation is thought to allow c-Rel-mediated effector cytokine production to occur more rapidly [Banerjee et al., 2005]. A third $I\kappa B$ protein, $I\kappa B\epsilon$, has been shown to have crucial regulatory impact on c-Rel in lymphocytes. B cells from $I\kappa B\epsilon$ -deficient mice are characterized by an increase in basal nuclear c-Rel and enhanced nuclear DNA-binding activity of c-Rel-containing complexes upon anti-IgM or LPS treatment [Clark et al., 2011; Alves et al., 2014]. Intriguingly, this higher c-Rel activity is associated with a phenotype that correlates inversely with some aspects of the c-Rel^{-/-} mouse phenotype [Mémet et al., 1999; Clark et al., 2011; Alves et al., 2014] (see 2.2.6).

Post-transcriptional regulation c-Rel is regulated on the post-transcriptional level by control of *REL* mRNA stability. In T cells *REL* mRNA has been shown to be a substrate for Regnase-1 that is thought to cleave 3'UTRs of target mRNAs [Uehata et al., 2013]. As reported by Roquin-1/2 ablation in T cells, *REL* is also a target of the RNA-binding and -regulating Roquin proteins that induce mRNA decay by binding to 3'UTRs of target mRNAs [Jeltsch et al., 2014]. Both Regnase-1 [Uehata et al., 2013] and Roquin proteins [Bertossi et al., 2011] are also expressed in B cells. However, the precise *in vivo* impact of these mRNA-destabilizing pathways on c-Rel function in B cells has not been described yet.

Post-translational modifications c-Rel can be modified by various post-translational modifications [Perkins, 2006; Gilmore and Gerondakis, 2011]. Several publications provide evidence for protein phosphorylation of c-Rel within its carboxy-terminal TAD. *In vitro* studies suggest that NIK [Sánchez-Valdepeñas et al., 2006] or TNFR-associated factor family member-associated NF- κ B activator (TANK)-binding kinase 1 (TBK1) and IKK ϵ [Harris et al., 2006] can phosphorylate c-Rel, which is associated with enhanced transactivation or nuclear accumulation, respectively. c-Rel phosphorylation is not only implicated in transactivation by further studies [Martin and Fresno, 2000; Martin et al., 2001; Fognani et al., 2000] but also in strengthening transforming activity of lymphoid chicken cells measured in colony formation and outgrowth assays [Starczynowski et al.,

2005, 2007]. In addition, the redox status of a cysteine residue in the RHD correlates with c-Rel phosphorylation and DNA-binding abilities [Glineur et al., 2000] and mutations in the RHD within a putative protein kinase A (PKA) recognition site were proposed to render c-Rel temperature-sensitive [Gapuzan et al., 2003].

Ubiquitination followed by proteasomal degradation as a means of regulating c-Rel turnover was first reported in *in vitro* studies that suggested that a carboxy-terminal part of c-Rel is important in promoting degradation [Chen et al., 1998]. A more recent study in mice identified the E3 ligase Peli1 of the Pellino family as a catalyst of c-Rel lysine-48(K48)-linked ubiquitination and subsequent proteasomal degradation in T cells [Chang et al., 2011]. Upon TCR stimulation, c-Rel accumulates in the nucleus of Peli1-deficient T cells that have a hyper-responsive phenotype. Remarkably, Peli1-ablated mice develop syndromes of autoimmunity establishing Peli1 as an essential negative regulator during T cell activation [Chang et al., 2011]. In macrophages c-Rel turnover is influenced by IKK α , possibly through phosphorylation within the carboxy-terminal domain and proteasomal-dependent degradation [Lawrence et al., 2005]. Furthermore, Jin et al. present results on c-Rel proteasomal degradation in macrophages by a mechanism involving TNFR-associated factor 2 (TRAF2) and TRAF3 and the E3 ubiquitin ligase cellular inhibitor of apoptosis (cIAP) [Jin et al., 2015].

Albeit most prominently described, phosphorylation and ubiquitination are not the only post-translational modifications of c-Rel. The peptidyl-prolyl cis/trans isomerase, NIMA interacting (Pin1) catalyzes isomerization of proline amide bonds. Pin1 was shown to associate with c-Rel and influence c-Rel nuclear translocation in human B cell lymphoma cell lines as pharmacologic inhibition or knockdown of Pin1 decreased c-Rel nuclear translocation [Fan et al., 2009]. In addition, c-Rel can be modified by glycosylation, namely the addition of O-linked β -N-acetyl-glucosamine (O-GlcNAcylation) to Serine 350 *in vitro*, which was suggested to activate transcription of c-Rel target genes [Ramakrishnan et al., 2013].

2.2.4 Transcriptional activation by c-Rel

c-Rel has been suggested to associate with TATA-box-binding protein (TBP) and transcription factor II B (TFIIB) of the basal transcriptional machinery [Kerr et al., 1993; Xu et al., 1993] as well as with the histone acetyltransferase p300 that is a co-factor for various transcription factors [Garbati et al., 2010]. A direct interaction or indirect interaction

through complex formation of c-Rel with other transcription factors has also been proposed [Gilmore and Gerondakis, 2011]. These transcription factors include IRF4 [Shindo et al., 2011], IRF8 [Liu and Ma, 2006], nuclear factor of activated T cells 1 (NFAT1) [Ruan et al., 2009], NFAT2 [Pham et al., 2005] and forkhead box P3 (FoxP3) [Loizou et al., 2011].

Several reports illustrate how c-Rel might orchestrate chromatin remodeling processes. Chromatin accessibility of the IL-2 promoter is dependent on c-Rel in T cells upon CD3/CD28 TCR stimulation [Rao et al., 2003] and strongly correlates with nuclear c-Rel expression and *Il2* transcription [McKarns and Schwartz, 2008]. More detailed insights have been obtained with regard to the conserved non-coding DNA sequences (CNS) of the FoxP3 locus that is pivotal for regulatory T cell (T_{reg}) development. The CNS3 element is considered to be the pioneer element in FoxP3 expression due to the permissive histone marks in T cells indicative of a poised chromatin state [Zheng et al., 2010]. c-Rel has the ability to bind to the CNS3 even in a DNA-methylated state, while other transcription factors can only bind in the demethylated state that is characteristic of committed natural T_{reg} cells and is associated with stable FoxP3 expression, suggesting that c-Rel facilitates locus opening [Long et al., 2009; Zheng et al., 2010]. Indeed, c-Rel is amongst the first transcription factors recruited to the FoxP3 promoter in T cells [Ruan et al., 2009]. In addition, in primary mouse dendritic cells c-Rel was demonstrated to bind weakly to promoters in unstimulated cells prior to the action of the histone demethylase Aof1 that can remove silencing methylation marks of lysine 9 on histone H3 (H3K9). Upon stimulation c-Rel is essential for Aof1 recruitment via direct interaction and subsequent gene expression [van Essen et al., 2010]. Finally, a recent study identified c-Rel as an activator of histone methyltransferase enhancer of zeste homolog 2 (Ezh2) expression in stimulated murine B and T cells [Neo et al., 2014]. This cumulative evidence supports the idea that c-Rel is a pioneer of transcriptional activation by functioning as an auxiliary factor in epigenetic remodeling.

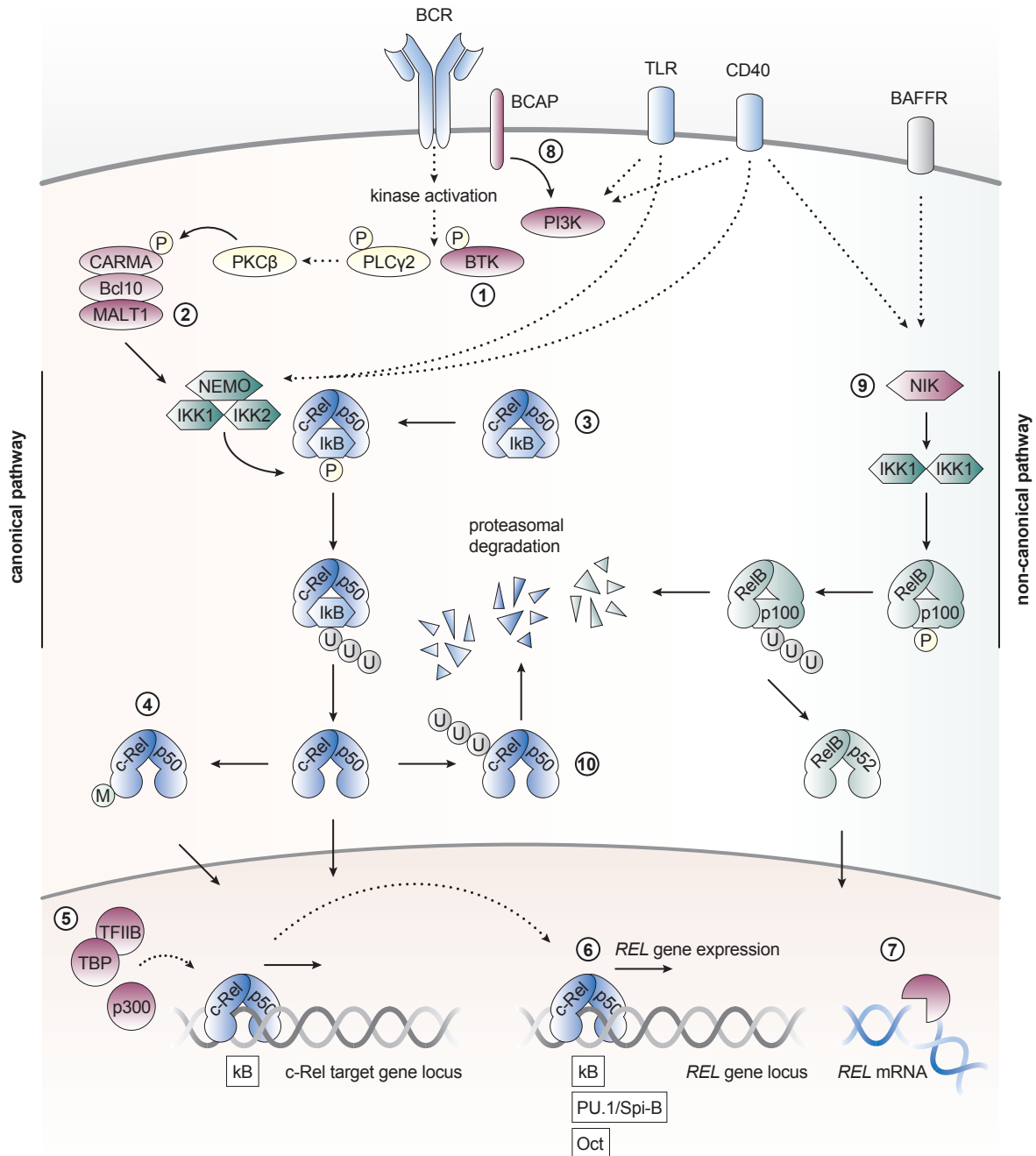


Figure 4: Simplified illustration of c-Rel activation in B cells. Both the canonical NF- κ B pathway (left) triggered by B cell receptor (BCR), toll-like receptor (TLR) or CD40 stimulation as well as the non-canonical NF- κ B pathway (right) downstream of CD40 and BAFF receptor (BAFFR) are displayed. (1) c-Rel DNA-binding activity is strongly reduced in Btk-deficient B cells upon stimulation (page 23). (2) MALT1 is specifically required for c-Rel nuclear translocation downstream of BCR signaling (page 22). (3) The predominant NF- κ B dimers in mature B cells are composed of c-Rel and p50 (page 21). In general the canonical pathway also leads to activation of RelA-containing complexes. c-Rel is associated with I κ B α , I κ B β and I κ B ϵ (page 23). (4) c-Rel can be modified by post-translational modifications (M) which influence c-Rel transactivation and transforming activity (page 24). (5) c-Rel has been proposed to associate with factors of the basal transcriptional machinery (page 25). (6) The *REL* gene locus contains a κ B site and c-Rel has been shown to activate its own transcription. The *REL* locus also contains octamer (Oct) and PU.1/Spi-B Ets family transcription factor binding sites (page 20). (7) *REL* mRNA is regulated on a post-transcriptional level (page 24). (8) PI3K signaling is implicated in maintaining c-Rel levels in B cells (page 21). (9) Also non-canonical NF- κ B signaling could play a role in maintaining c-Rel expression levels (page 21). (10) c-Rel has been shown to be controlled by ubiquitination and subsequent proteasomal degradation (page 25). For further details, references and abbreviations the reader is referred to indicated paragraphs of the main text. In addition to references provided in section 2, the content of this figure is based on Okkenhaug and Vanhaesebroeck, 2003, Siebenlist et al., 2005, and Murphy et al., 2007. P, phosphorylation; U, ubiquitination.

2.2.5 c-Rel target genes

Numerous conditions influence target gene selectivity during the NF- κ B response. The selectivity is defined by stimulus and cell type that can influence the kinetics of the response. On a molecular level, regulatory principles of selectivity range from gene expression levels or post-translational modifications of subunits and dimer composition to differential co-factor recruitment and chromatin accessibility [Sen and Smale, 2010; Smale, 2011] (see also 2.2.3). Distinctive target gene expression is also conferred by κ B site sequence. Remarkably, several studies demonstrate that c-Rel homodimers bind to a broader range of κ B sites with a higher overall affinity in comparison to RelA or p50 homodimers suggesting a lower stringency and higher flexibility for c-Rel binding motifs [Kunsch et al., 1992; Sanjabi, 2005; Siggers et al., 2012]. A comparison of κ B site motifs for all NF- κ B members corroborates these observations as the c-Rel motif is distinguished by particularly high degeneracy in its 5'-half-site [Zhao et al., 2014].

As mentioned above, *REL* is a target gene of itself as c-Rel transactivates its own promoter in a murine B cell line 129B [Grumont et al., 1993]. Nevertheless, as for the majority of potential target genes substantial overlap and compensation between the NF- κ B subunits complicate the identification of exclusive c-Rel target genes. Mice deficient for c-Rel (c-Rel^{-/-}) are a basic source for target gene discovery, although indirect mechanisms accounting for changes in gene expression cannot be excluded.

Survival factors c-Rel target genes include survival factors. Studies in B and T cells derived from c-Rel^{-/-} or wild-type mice and cell lines provide evidence for the prosurvival Bcl-2 family member *A1* (*Bcl2A1/Bfl1*) as a direct c-Rel target gene [Grumont et al., 1999; Edelstein et al., 2003]. It should be noted that despite being significantly reduced, minor A1 transcript and protein levels could be detected in c-Rel^{-/-} B cells upon stimulation of IgM or CD40 suggesting partial compensation [Owyang et al., 2001]. In contrast, induction of Bcl-x_L, another Bcl-2 family member, is abrogated on both protein and transcript level in c-Rel^{-/-} B cells upon the same stimuli [Owyang et al., 2001; Castro et al., 2009]. Interestingly, B cells deficient in MALT1 that mediates c-Rel nuclear translocation (see 2.2.3) also fail to upregulate Bcl-x_L upon anti-IgM stimulation [Ferch et al., 2007]. *In vitro* work suggests binding of c-Rel, p50 and to a marginal extent RelA to a κ B site in the *Bclx* promoter and its transactivation by c-Rel [Chen et al., 2000]. Both A1 and Bcl-x_L proteins are not efficiently induced under stimulus conditions precluding sustained

c-Rel nuclear translocation in B cells [Damdinsuren et al., 2010]. Furthermore, data obtained in human B cell lymphoma cell lines suggests a cooperation of c-Rel with NFAT transcription factors in activating expression of CD40L (CD154) [Pham et al., 2005] and potentially BAFF [Fu et al., 2006].

Cell cycle and proliferation c-Rel target genes are also involved in cell cycle and proliferation. While a strong reduction of cyclin D3, E and A proteins has been observed in anti-IgM-treated c-Rel^{-/-} B cells, only *CCNE* (encoding cyclin E) but not *CCND3* (encoding cyclin D3) mRNA levels were affected [Hsia et al., 2002]. Notably, absence of sustained nuclear c-Rel upon pulsed IgM stimulation of B cells coincides with a failure to trigger typical features of cell cycle progression, including expression of cyclins D2 and E [Damdinsuren et al., 2010]. Moreover, c-Rel^{-/-} B cells show almost no *CCND2* (encoding cyclin D2) mRNA expression upon anti-CD40 or LPS stimulation [Zarnegar et al., 2004] but only delayed kinetics of cyclin D2 protein induction upon continuous anti-IgM stimulation [Hsia et al., 2002]. *CCND2* has also been suggested to be a target gene of c-Myc [Pelengaris et al., 2002]. In correlation with these results, a strong reduction of *Myc* mRNA upon anti-CD40 or LPS treatment of c-Rel^{-/-} B cells was observed [Zarnegar et al., 2004], but no substantial change in c-Myc protein expression was detected upon anti-IgM [Grumont et al., 1998] or combined anti-IgM/LPS stimulation in c-Rel^{-/-} B cells [Grumont et al., 2002]. As *Myc* induction upon LPS stimulation is higher in MZ B cells compared to FO B cells [Meyer-Bahlburg et al., 2009], these results could be influenced by the reduction of MZ B cells in c-Rel^{-/-} mice [Cariappa et al., 2000] (see also 2.2.6). Nevertheless, *in vitro* experiments suggests that an upstream regulatory element of the c-Myc promoter is bound by c-Rel and p50 upon anti-CD40 stimulation and that this site can be transactivated by c-Rel or c-Rel:p50 in luciferase reporter assays [Siebelt et al., 1997; Grumont et al., 2002]. As much as these findings emphasize complex transcriptional interconnections and the possibility of multiple upstream regulators of a single target gene, they first and foremost highlight the impact of distinctive stimuli on c-Rel-regulated gene expression. Furthermore, although these data implicate c-Rel in cyclin regulation, these cell cycle regulators might not be direct c-Rel target genes. Alternatively, also E2F transcription factors that are pivotal to cell cycle regulation [Bertoli et al., 2013] – including E2F1, E2F2, E2F3, E2F4 and E2F5 – are not efficiently induced in c-Rel^{-/-} B cells [Hsia et al., 2002]. Results obtained in c-Rel^{-/-} B cells and cell lines suggest that

c-Rel directly activates transcription of *E2f3a* [Cheng et al., 2003]. Interestingly, *CCNE* and *CCNA* are target genes of E2F transcription factors [Bertoli et al., 2013] providing a putative explanation for the reduction of cyclin E and cyclin A observed in c-Rel^{-/-} B cells [Hsia et al., 2002; Cheng et al., 2003].

Germinal center B cells Several findings hint to a function of c-Rel target genes in GC B cells. IRF4 expression is not activated in c-Rel^{-/-} lymphocytes upon diverse stimuli. Both c-Rel:p50 heterodimers and c-Rel homodimers bind to κ B sites within the IRF4 promoter in T cells upon anti-CD3/CD28 stimulation. The authors note that equivalent results were obtained in B cells upon anti-IgM stimulation [Grumont and Gerondakis, 2000]. Further evidence for a contribution of c-Rel to IRF4 induction is provided by work in a B cell lymphoma line (P3HR1) [Saito et al., 2007]. *In vitro* c-Rel^{-/-} B cells fail to upregulate AID mRNA upon anti-CD40 stimulation [Zarnegar et al., 2004]. Nevertheless, abrogated AID induction is also a prominent phenotype of IRF4-deficient GC B cells *in vivo* [Klein et al., 2006; Sciammas et al., 2006] pointing to an indirect mechanism for the lack of AID transcription as a consequence of insufficient IRF4 levels in c-Rel^{-/-} B cells. In addition, γ 1 germline transcription is strongly decreased in c-Rel^{-/-} B cells following diverse *in vitro* stimuli [Kaku et al., 2002] and c-Rel, but not RelA or p50, was proposed to bind to the human γ 4 germline promoter in response to IL-4/anti-CD40 treatment of a human lymphoma cell line (BL-2) [Agresti and Vercelli, 2002]. As cited above, c-Rel activates expression of the histone methyltransferase Ezh2 in activated lymphocytes [Neo et al., 2014]. Remarkably, not only is Ezh2 highly expressed in GC B cells, but also GC B cell-specific Ezh2 deficiency is associated with compromised GC formation and antibody responses [Caganova et al., 2013]. When investigating consequences of c-Rel deletion selectively in GC B cells, Heise et al. found that a set of genes involved in cellular metabolism is downregulated in c-Rel^{-/-} GC B cells. The authors provide further experimental evidence for corrupted metabolic functions in c-Rel^{-/-} cells. Notably, gene expression profile analysis of this work does not show a change in *Aicda* and *Ezh2* levels in c-Rel^{-/-} GC B cells [Heise et al., 2014].

Mediators of immune signaling in B cells and beyond c-Rel knockout mice show a reduction in a diversity of cytokines. Expression of the cytokines IL-6, IL-10, and IL-15 is reduced in c-Rel^{-/-} B cells upon stimulation with anti-IgM or anti-CD40 *in vitro* [Tumang

et al., 2002]. $c\text{-Rel}^{-/-}$ T cells are impaired in production of IL-2, IL-3, IL-21 and granulocyte macrophage colony-stimulating factor (GM-CSF) [Kontgen et al., 1995; Gerondakis et al., 1996; Chen et al., 2010]. With regard to IL-2 and IL-21 a direct requirement for c-Rel in regulating *Il2* and *Il21* gene transcription has been described [Rao et al., 2003; Chen et al., 2010]. c-Rel has also been established as a central mediator of *FoxP3* transcription in T_{reg} cells [Long et al., 2009; Ruan et al., 2009; Zheng et al., 2010] and was shown to activate *Rorc* (retinoic acid-related orphan receptor γ encoding ROR γ /ROR γ t) transcription that is crucial for Th17 differentiation and function [Chen et al., 2011; Ruan et al., 2011]. A general study of c-Rel target gene identification in T cells was carried out by Bunting et al., 2007. Beyond lymphocytes, publications support a direct involvement of c-Rel in expression of *Il12b* [Sanjabi et al., 2000] in macrophages and *Il23a* [Carmody et al., 2007], *Il12a* [Grumont et al., 2001] and *Il12b* as well as *Mdc/Ccl22* [van Essen et al., 2010] in dendritic cells. Two further studies using a monocytic cell line or mouse embryonic fibroblasts aimed at elongating the list of NF- κ B subunit-specific or distinctively c-Rel target genes, respectively [Schreiber et al., 2006; Wei et al., 2008].

2.2.6 Functional consequences of c-Rel signaling in B cells

Analyses of genetically modified mice yield invaluable knowledge of lymphocyte functions in a systemic *in vivo* context. The following paragraphs highlight the functional consequences of c-Rel signaling in B cells primarily based on selected mouse model studies.

B cell development and maturation The first publication of c-Rel knockout mice described no defects in hematopoietic progenitors and lymphopoiesis in the bone marrow of $c\text{-Rel}^{-/-}$ mice [Kontgen et al., 1995]. Both the classical and alternative NF- κ B pathway are implicated in B cell maturation following immature B cell egress from the bone marrow [Gerondakis and Siebenlist, 2010; Sasaki and Iwai, 2016]. c-Rel expression can be induced by anti-IgM stimulation in T2 and mature but not in T1 B cells and BAFF receptor – that is thought to be crucial for transitional B cell development [Sasaki and Iwai, 2016] – is not efficiently produced in $c\text{-Rel}^{-/-}$ B cells. Based on these findings, it was proposed that c-Rel activation plays a role in transitional T2 B cells in providing survival signals, possibly downstream of BCR signaling [Castro et al., 2009]. Nevertheless, no significant differences were reported for T1 (B220⁺AA4.1⁺IgM⁺CD23⁻) or T2/T3 (B220⁺AA4.1⁺IgM⁺CD23⁺) splenic B cell populations in $c\text{-Rel}^{-/-}$ mice [Almaden et al., 2016].

Although FO B cell numbers are normal in $c\text{-Rel}^{-/-}$ mice, MZ B cells were found to be markedly reduced [Cariappa et al., 2000]. Similar results were observed for RelA or p50 and also for RelB or p52, suggesting that several NF- κ B subunits are involved in MZ B cell development [Cariappa et al., 2000; Weih et al., 2001; Siebenlist et al., 2005; Pillai and Cariappa, 2009]. Opposed to Cariappa et al. in a recent publication Almaden et al. did not find a difference in MZ B cells in $c\text{-Rel}^{-/-}$ mice [Almaden et al., 2016]. However, while Cariappa et al. based their flow cytometry analysis on $\text{IgM}^{\text{high}}\text{IgD}^{\text{low}}\text{CD21}^{\text{high}}$ MZ B cells, the authors of the latter publication defined MZ B cells exclusive of IgD as $\text{B220}^+\text{AA4.1}^-\text{CD21}^{\text{high}}\text{IgM}^+$.

Mice deficient in the adaptor protein BCAP that binds to PI3K show a reduction of mature B cell numbers with impaired survival and proliferation. Remaining B cells have prominently lower levels exclusively of $c\text{-Rel}$. In addition, this phenotype was rescued in $c\text{-Rel}$ -retrovirus-transduced BM chimeras implicating a contribution of $c\text{-Rel}$ to the $\text{BCAP}^{-/-}$ phenotype [Yamazaki and Kurosaki, 2003]. A similar phenotype of decreased mature B cell numbers and accompanying reduction in $c\text{-Rel}$ level is observed in B cells of $\text{PU.1}^{+/-}\text{Spi-B}^{-/-}$ mice lacking Ets family transcription factors. Again $c\text{-Rel}$ reconstitution could counterbalance the defects [Hu et al., 2001]. Therefore, $c\text{-Rel}$ could in part be involved in late-stage peripheral B cell maturation or survival, although other factors most probably act in concert with $c\text{-Rel}$ or partially compensate for $c\text{-Rel}$ deficiency in $c\text{-Rel}^{-/-}$ mice.

Mature B cells The most remarkable consequences of $c\text{-Rel}$ -deficiency are observed in mature B cells, especially following activation and terminal differentiation during immune responses. $c\text{-Rel}^{-/-}$ B cells show strong proliferative defects in response to mitogenic stimuli, including LPS, CD40 ligand and anti-IgM [Kontgen et al., 1995] and reduced survival upon anti-IgM or LPS treatment [Grumont et al., 1998] *in vitro* as further discussed below (see page 34).

Upon immunization GC B cells are barely present in $c\text{-Rel}^{-/-}$ mice coinciding with a strong reduction of T_{fh} cells and IL-21 levels [Tumang et al., 1998; Chen et al., 2010]. While administration of IL-21 restores T_{fh} cells, it does not revert the almost complete absence of GC B cells [Chen et al., 2010]. $\text{C}\gamma 1\text{-Cre}$ -mediated GC B cell-specific $c\text{-Rel}$ ablation in conditional $c\text{-Rel}^{\text{fl/fl}}$ knockout mice recently demonstrated that the loss of GC B cells is indeed B cell-intrinsic [Heise et al., 2014]. Splenic GC B cells initially form upon im-

munization of $c\text{-Rel}^{\text{fl/fl}}$ $C\gamma 1\text{-Cre}$ mice with sheep red blood cells (SRBC), but these GCs begin to collapse starting at day 8 post-immunization. In this model, the polarization of GC LZ and DZ is established at day 7 and thereafter GC LZ and DZ B cells are equally affected when $c\text{-Rel}$ -deleted GC B cells steadily cease to exist. It is noteworthy that $Bcl\text{-}2$ transgene expression does not rescue the compromised GC B cells pointing towards a role of $c\text{-Rel}$ in GC B cells beyond mere survival. As indicated above (see 2.2.5), the authors conclude that $c\text{-Rel}$ establishes a cellular state providing high metabolic conditions essential to GC B cell growth and maintenance [Heise et al., 2014]. The observation that single round anti-IgM and subsequent anti-CD40 stimulation synergize in activating nuclear $c\text{-Rel}$ and expression of pro-survival proteins $Bcl\text{-}x_L$ and $A1$, led to the hypothesis that $c\text{-Rel}$ could be involved in priming naive B cells to receive T cell help – a model that could be relevant to the role of $c\text{-Rel}$ in GC reactions [Damdinsuren et al., 2010].

$c\text{-Rel}^{-/-}$ mice have strikingly low IgG1 and undetectable IgG2a as well as partially reduced IgM, IgG2b and IgG3 naive antibody titers. Specific IgM and IgG1 titers are also reduced after immunization [Kontgen et al., 1995]. Upon intranasal influenza infection or subcutaneous influenza vaccination, $c\text{-Rel}^{-/-}$ mice show a strongly impaired antiviral antibody response with reductions of all tested Ig subclasses comprising IgM, IgA, IgG1, IgG2a, IgG2b and IgG3. $c\text{-Rel}^{-/-}$ mice develop no significant levels of virus-neutralizing antibodies with essentially equal neutralizing antibody titers in naive and infected $c\text{-Rel}^{-/-}$ mice. In spite of these clear disadvantages, $c\text{-Rel}^{-/-}$ mice successfully clear pulmonary influenza infection – albeit with delayed kinetics – due to an effective cytotoxic T cell response [Harling-McNabb et al., 1999]. Correspondingly, GC B cell-specific $c\text{-Rel}$ deletion in NP(4-hydroxy-3-nitrophenyl acetyl)-KLH(keyhole limpet hemocyanin)-immunized $c\text{-Rel}^{\text{fl/fl}}$ $C\gamma 1\text{-Cre}$ mice results in a near complete absence of specific IgG1-secreting cells as well as anti-NP-IgG1 serum titers, which is not restored by $Bcl\text{-}2$ transgene expression [Heise et al., 2014]. Interestingly, the impaired $c\text{-Rel}$ DNA-binding activity seen in $Nfkb\text{ia}^{\text{NES/NES}}$ mice expressing $I\kappa B\alpha$ lacking an NES similarly correlates with a significant reduction in IgA, IgG1 and IgG2b serum antibody titers [Wuerzberger-Davis et al., 2011]. Conversely, the higher nuclear $c\text{-Rel}$ activity in $I\kappa B\epsilon$ -deficient mice results not only in an expansion of mature B cells in lymph nodes and MZ B cells in spleen, but it is also associated with increased B cell proliferation and survival in the presence or absence of stimulation as well as augmented naive and post-immunization IgG1 and IgM serum titers [Mémet et al., 1999; Clark et al., 2011; Alves et al., 2014]. Although $c\text{-Rel}^{-/-}$ B cells can

be driven towards a CD138⁺ plasmablast stage *in vitro* [Heise et al., 2014], the exact role of c-Rel in B cell terminal differentiation *in vivo* remains unknown as the c-Rel-ablated mouse models described so far are immensely compromised in their GC response, thus impeding independent investigation of subsequent memory or plasma cell stages.

Carrasco et al. generated mice that instead of wild-type c-Rel express a carboxy-terminal-truncated form of c-Rel devoid of the TAD (c-Rel^{ΔCT/ΔCT}), which leaves the RHD and consequently DNA binding and dimer formation intact. These mice develop a complex phenotype involving diverse hematopoietic tissues and cell types, including B cell hyperplasia and enlarged spleen and lymph nodes. This multilayered immune phenotype hinders distinction of primary from secondary effects [Carrasco et al., 1998]. c-Rel^{ΔCT/ΔCT} B cells have been analyzed separately *in vitro* [Zelazowski et al., 1997] (see page 36).

In summary, the studies describing consequences of c-Rel-deficiency highlight the particular role of c-Rel in activated B cells and GC B cells. The central processes in these B cell subsets during which c-Rel exerts its function are delineated in the following paragraphs.

B cell survival Both the canonical and alternative NF-κB pathway are implicated in the maintenance of mature B cells *in vivo* [Senftleben et al., 2001; Kaisho et al., 2001; Pasparakis et al., 2002; Li et al., 2003; Sasaki and Iwai, 2016]. Mature B cell survival is controlled by BAFF, which can activate the alternative pathway, but constitutive canonical NF-κB activation uncouples B cell survival from BAFF signals [Sasaki et al., 2006, 2008; Sasaki and Iwai, 2016]. Although c-Rel expression is strongly reduced in NIK mutant mice [Yamada et al., 2000], mice with stabilized high expression of NIK via truncation of the domain mediating TRAF3-dependent proteasomal degradation in B cells do not show an increase in nuclear c-Rel level [Sasaki et al., 2008]. The unaltered mature B cell numbers in c-Rel^{-/-} mice (see 2.2.6) and the observation that apoptosis is not accelerated when culturing c-Rel^{-/-} B cells in the absence of stimuli [Grumont et al., 1998] indicate that c-Rel is not essential for mere maintenance survival of resting mature B cells.

On the contrary, apoptosis is markedly enhanced in c-Rel^{-/-} B cells in comparison to control cells upon stimulation, including anti-IgM and LPS [Grumont et al., 1998]. Similarly, MALT1-ablated B cells, which are deficient in BCR-initiated c-Rel nuclear translocation, present reduced survival *in vitro* upon anti-IgM treatment [Ferch et al., 2007]. Furthermore, in the presence of stimuli, c-Rel^{-/-} B cells are more sensitive to cell death *in vitro* induced by γ-irradiation or the glucocorticoid dexamethasone that is used as an immuno-

suppressive [Owyang et al., 2001]. As discussed above (see 2.2.5), there is substantial evidence that c-Rel is involved in activation of the survival factors A1 and Bcl-x_L following stimulation. Intercrosses of c-Rel^{-/-} mice with transgenic Bcl-2 or Bcl-x_L mice demonstrate restoration of c-Rel^{-/-} B cell survival *in vitro* conferred by Bcl-2 [Grumont et al., 1998] or Bcl-x_L [Owyang et al., 2001] transgene expression. In the same line, loss of Bcl-2 interacting mediator of cell death (Bim), a pro-apoptotic antagonist of Bcl-2 family pro-survival proteins [Strasser, 2005], can counteract stimulus-induced apoptosis of c-Rel^{-/-} B cells [Banerjee et al., 2008].

Cell cycle c-Rel^{-/-} or c-Rel^{ΔCT/ΔCT} B cells are impaired in their proliferative response to *in vitro* stimulation [Kontgen et al., 1995; Tumang et al., 1998; Carrasco et al., 1998]. In addition, c-Rel^{-/-} B cells are more sensitive to the anti-proliferative effects of IFNs, which is likely a consequence of impaired IRF4 expression in c-Rel^{-/-} B cells upon stimulation [Grumont and Gerondakis, 2000]. Importantly, Bcl-2 or Bcl-x_L transgene expression that restores c-Rel^{-/-} B cell survival does not rescue the proliferative defects and c-Myc upregulation is not altered in c-Rel^{-/-} B cells upon anti-IgM stimulation pointing to an independent role of c-Rel in cell cycle regulation [Grumont et al., 1998; Owyang et al., 2001].

Indeed, several studies provide evidence for a failure of c-Rel^{-/-} B cells to transit to cell cycle S phase as a result of a block in early G1 phase. c-Rel^{-/-} B cells synthesize reduced amounts of RNA and DNA as well as protein in response to stimulation indicating defective progression through late G1 and S phase [Grumont et al., 1998; Tumang et al., 1998]. As mentioned above (see 2.2.5), the expression of multiple E2F transcription factors and cyclins that are key cell cycle regulators is impaired in c-Rel^{-/-} B cells [Hsia et al., 2002; Cheng et al., 2003]. In addition, c-Rel^{-/-} B cells show decreased activity of G1 cyclin-dependent kinases CDK4 and CDK6 that are central to G1/S transition despite unaltered CDK4/6 protein levels [Hsia et al., 2002]. This is accompanied by reduced expression and phosphorylation of retinoblastoma protein (Rb) [Hsia et al., 2002], which is thought to be mediated by G1-CDKs and important for releasing activator E2F transcription factors from inhibition by Rb [Bertoli et al., 2013]. In contrast, degradation of the CDK inhibitor p27 and the E2F inhibitory protein p130, which is expressed in quiescent cells [Bertoli et al., 2013], does not appear to be strongly affected in c-Rel^{-/-} B cells, suggesting that c-Rel^{-/-} cells are able to exit the G0 resting state [Hsia et al., 2002]. In agreement

with these data, only stimulative conditions resulting in sustained c-Rel nuclear translocation correlate with signs of G1 progression, including expression of cyclin D2 and E as well as CDK4, phosphorylation of Rb, and degradation of p27 [Damdinsuren et al., 2010]. Moreover, c-Rel – but also RelA – has been proposed to associate with CDKs [Perkins et al., 1997; Chen and Li, 1998]. Notwithstanding the multilayered feedback-loop control of cell cycle progression that complicates identification of cause and consequences, these findings clearly demonstrate that the hallmarks of G1 progression are dependent on c-Rel in B cells.

The block in cell cycle G1 phase in c-Rel^{-/-} B cells can only be partially overcome by combination of mitogenic stimuli or addition of cytokines, indicating that also c-Rel-independent pathways can promote cell cycle progression in B cells given certain conditions *in vitro* [Grumont et al., 1998; Tumang et al., 1998]. Moreover, cyclin E protein transduction into c-Rel^{-/-} B cells that additionally express the Bcl-x_L transgene can resolve G1 cell cycle arrest to a certain degree [Cheng et al., 2003].

Class switch recombination The decreased *in vivo* serum Ig titers described upon c-Rel ablation in mice [Kontgen et al., 1995; Harling-McNabb et al., 1999; Heise et al., 2014] (see 2.2.6) are consistent with deficits of c-Rel^{-/-} or c-Rel^{ΔCT/ΔCT} B cells in class switch assays *in vitro* [Zelazowski et al., 1997; Kaku et al., 2002; Heise et al., 2014]. The central role of c-Rel in proliferation and GC responses probably underlies these observations at least in part as CSR depends on proliferation [Hodgkin et al., 1996]. The identification of IRF4 as a central coordinator of CSR [Klein et al., 2006; Sciammas et al., 2006] together with the finding that induction of IRF4 fails in c-Rel^{-/-} lymphocytes [Grumont and Gerondakis, 2000] represent another pathway for involvement of c-Rel in CSR.

Besides c-Rel also other NF-κB subunits are implicated in class switching to distinct Ig isotypes [Snapper et al., 1996a; Doi et al., 1997; Snapper et al., 1996b]. Evidence for a direct role for c-Rel and other subunits is provided with regard to germline transcription through Ig constant heavy chain loci that directs CSR to distinct isotypes [Stavnezer et al., 2008; Xu et al., 2012]. The murine γ1 promoter has been shown to be bound by c-Rel, RelA, p50 and RelB in response to CD40 stimulation *in vitro* [Lin et al., 1998]. Based on an *in vitro* transactivation assay the authors suggest that RelA:p50 or RelB:p50 heterodimers can activate the γ1 promoter, whereas c-Rel:p50 or p50:p50 dimers fail to activate it

[Lin et al., 1998]. Opposed to this notion, $p50^{-/-}$, $p50^{-/-} RelA^{-/-}$ and $RelB^{-/-}$ B cells are still able to efficiently switch to IgG1 [Snapper et al., 1996b,a; Horwitz et al., 1999]. Additionally, in accordance with almost undetectable IgG1 serum titers and abrogated *in vitro* class switch to IgG1 of c-Rel-ablated B cells [Heise et al., 2014], Kaku et al. show that germline $\gamma 1$ transcription is considerably reduced in c-Rel $^{-/-}$ B cells accompanied by a strong reduction of IgG1 secretion *in vitro* [Kaku et al., 2002]. Further evidence for an involvement of c-Rel in germline transcription is provided by *in vitro* analysis of B cells from c-Rel $^{\Delta CT/\Delta CT}$ mice that lack the c-Rel TAD. The observation of abolished switching to IgG1, IgG3 and IgE but unaltered IgA class switch in c-Rel $^{\Delta CT/\Delta CT}$ B cells is corroborated by undetectable germline transcripts of $\gamma 1$ or $\gamma 3$ but normal levels of $\gamma 2b$, $\gamma 2a$, ϵ and α germline transcripts, pointing out that germline transcription is required but not sufficient for class switching [Zelazowski et al., 1997]. Nevertheless, also RelA was shown to be important for $\gamma 3$ germline transcription and IgG3 class switching [Horwitz et al., 1999]. Finally, a role for c-Rel, but not RelA or p50, has been suggested for human $\gamma 4$ germline transcription [Agresti and Vercelli, 2002]. The discrepancies or NF- κ B subunits delineated above could in part be explained by the differential use of single or combinatorial stimuli applied to induce class switch in these studies – exemplified also by stimuli-dependent regulation of the Ig heavy chain enhancer complex located 3' to the IgA locus by p50 and c-Rel [Zelazowski et al., 2000]. Nevertheless, these experiments clearly demonstrate the role of NF- κ B in germline transcription and emphasize the importance of c-Rel in CSR, especially in class switch to IgG1. However, these results also hint to a partial functional redundancy between the NF- κ B subunits.

This section has illustrated distinct characteristics of the c-Rel transcription factor amongst the NF- κ B family members. c-Rel has a unique role in mature B cells that is of central relevance during immune responses. In particular, c-Rel is required for proliferation during B cell activation and is essential for pivotal processes in GC B cells during GC reactions.

3 c-Rel signaling in B cell pathology

Aberrant constitutive NF- κ B activation is a hallmark of numerous cancers including lymphoid tumors [Staudt, 2010; Lim et al., 2012]. Intriguingly, c-Rel is the only member of the NF- κ B family that has the capacity to malignantly transform lymphoid chicken cells *in vitro* [Gilmore et al., 2001]. This section focuses on literature that lays the foundation for the proposed role of c-Rel in human B cell lymphomas.

3.1 Malignant transformation of B cells

Following activation upon antigen encounter, B cells initiate the formation of GCs, where the fundamental immunological mechanisms of SHM and CSR require DNA breaks in GC B cells (see 1.2.1). Higher tolerance of DNA damage is an essential condition for progression through SHM and CSR rendering GC B cells more permissive to incidents of genetic instability that can promote lymphomagenesis. Hence, at this stage physiological processes can turn into pathology once DNA missarrangements or aberrant somatic mutations occur. These translocations, deletions, mutations or amplifications alter the function or regulation of proto-oncogenes or result in their ectopic expression [Küppers, 2005; Klein and Dalla-Favera, 2008; Basso and Dalla-Favera, 2015]. Notably, deregulated GC reactions are also implicated in development of autoimmunity [Vinuesa et al., 2009]. Indeed, approximately 95% of human lymphomas arise from B cells, the majority of which carry somatically mutated Ig genes indicative of GC or post-GC origin [Küppers, 2005]. Chromosomal translocations involving Ig genes are a common feature of human B cell lymphomas [Küppers, 2005] and somatic hypermutation has been shown to affect many genes, including proto-oncogenes, besides the actually targeted Ig loci [Pasqualucci et al., 2001; Shen et al., 1998; Liu et al., 2008]. Interestingly, B cells with Ig loci translocations are present in healthy mice and human at very low frequency. This observation is consistent with the clinical presentation of lymphomas with a variety of oncogenic lesions that finally trigger malignant transformation [Küppers and Dalla-Favera, 2001]. These driving genetic aberrations typically provide a B cell with enhanced proliferative capacities and viability that is often accompanied by a block in differentiation [Küppers and Dalla-Favera, 2001; Shaffer et al., 2002b]. Beyond these intrinsic determinants, the microenvironment is of relevance to tumor cell proliferation and survival [Küppers, 2005] and the malignantly transformed cells need to escape or break immune surveillance that is for instance exerted

by T cells [Zhang et al., 2012; Afshar-Sterle et al., 2014].

3.2 *REL* amplification in human B cell lymphoma

Gains or amplifications of the genetic locus containing the human *REL* gene that maps to chromosome 2 to band p16.1² are frequently found in human B cell lymphomas. As described in detail below (see page 40) and summarized in Table 1, these most predominantly include classical Hodgkin lymphoma (cHL) and B cell non-Hodgkin lymphomas (B-NHL), specifically diffuse large B cell lymphoma (DLBCL) and primary mediastinal B cell lymphoma (PMBCL). Many reports distinguish amplifications that refer to high copy number increases within the total number of reported gains that may also include moderate genomic overrepresentations. While most studies define an amplification as a gene copy number ≥ 4 , an extreme case of DLBCL was diagnosed with more than 100 copies of the *REL* locus [Houldsworth et al., 2004]. *REL* amplifications were also discovered in follicular lymphoma (FL) and the respective successively transformed DLBCL counterparts [Goff et al., 2000; Martinez-Climent et al., 2003]. Gains of the *REL*-including gene segment were additionally found in two other types of B cell lymphoma, namely nodular lymphocyte predominant Hodgkin lymphoma (NLPHL) and T cell/histiocyte rich large B cell lymphoma (THRLBCL) [Hartmann et al., 2015]. Interestingly, gains of 2p16.1 were also observed in peripheral T cell lymphoma, not otherwise specified (PTCL NOS) [Hartmann et al., 2010] and enhanced c-Rel expression was associated with poor response to therapy in adult T-cell leukemia/lymphoma (ATLL) [Ramos et al., 2007]. Other discovered genetic *REL* aberrations are *REL*-positive double minute chromosomes in FL [Reader et al., 2006] and *REL* translocations in cHL [Martin-Subero et al., 2002, 2006].

Besides the discovery of these genetic variations, c-Rel protein alterations were shown to influence c-Rel *in vitro* transactivation and transforming capabilities. A c-Rel splice variant devoid of Exon 9 (c-Rel Δ Ex9) has a higher *in vitro* transactivation activity compared to full length c-Rel. Remarkably, this c-Rel Δ Ex9 splice variant has been detected in primary DLBCL patient material and lymphoma cell lines but not in normal lymphoid tissue [Leeman et al., 2008]. Furthermore, point mutations of serine residues in the c-Rel TAD1 into residues that preclude phosphorylation enhance c-Rel transforming activity. Conversely, mutation into a phosphomimetic residue have a positive effect on c-Rel trans-

²Genomic location of REL ENSG00000162924 accessible on www.ensembl.org (human GRCh38.p5)

activation [Starczynowski et al., 2005]. Interestingly, an identical point mutation resulting in a change of serine 525 to proline in the c-Rel TAD2 that also strengthens c-Rel transformation *in vitro* has been discovered in one patient with FL and another patient with PMBCL [Starczynowski et al., 2007]. Finally, deletion of either of the two c-Rel TADs or introduction of substitution of acidic residues with alanine in the TAD2 decreases c-Rel transactivation ability while increasing transforming potency [Starczynowski et al., 2003; Fan and Gelinas, 2007].

Due to the lack of suitable *in vivo* models, the proposed lymphoma-promoting role of *REL* amplification and aberrant splicing has not been investigated in any mouse studies until today. Opposed to that, a recent publication reported an unexpected earlier disease onset in the E μ -Myc and pE μ -B29-TCL1 lymphoma/leukemia mouse models upon loss of c-Rel. The authors suggest that the results could be explained by the observed downregulation of the tumor suppressor Bach2 in E μ -Myc c-Rel-deficient mice [Hunter et al., 2015]. However, it remains unclear whether the phenotypes are B cell-intrinsic and in contrast to the human cHL and B-NHL disease entities mentioned above, the E μ -Myc mouse strain mainly develops pre-B cell tumors [Harris et al., 1988].

3.2.1 Diffuse large B cell lymphoma

DLBCL is the most frequent form of B-NHL representing roughly 40% of all B-NHL diagnoses [Basso and Dalla-Favera, 2015]. DLBCL is considered an aggressive lymphoma of rather broad heterogeneity and despite initial therapy response in most patients, durable remission is accomplished only in a minority [Alizadeh et al., 2000; Küppers, 2005]. The origin of DLBCL is thought to be GC- or post-GC-derived B cells [Küppers, 2005]. Two early studies identified *REL* copy number amplifications of 4 or more copies in 23% of DLBCL cases when analyzing a cohort of 111 [Houldsworth et al., 1996] or 96 [Rao et al., 1998] patients, respectively, that is for the most part redundant.

Based on gene expression profiling, Alizadeh et al. defined subgroups of DLBCL that were classified according to molecular phenotypes. The germinal center B cell-like (GCB) cluster expresses a gene signature associated with GC B cells, whereas the gene profile of the activated B cell-like (ABC) cluster resembles *in vitro* activated peripheral blood cells [Alizadeh et al., 2000]. A third subgroup termed type 3 DLBCL identified in a large cohort of 240 patients expresses neither genes of the ABC nor the GCB profiling set at high levels [Rosenwald et al., 2002]. In these studies, the subgroups were related to clinical

Table 1: Frequency of 2p *REL* gains in selected human B cell lymphomas. Frequencies of gains including amplifications are displayed. Total or the respective fraction of patient numbers are given in parentheses. Average calculation was performed considering patient numbers and average for DLBCL includes data from GCB- and ABC-DLBCL subgroups. This table summarizes the literature cited in this thesis with no claim to completeness of published datasets. ^{*1}largely redundant cohorts; numbers displayed as given in Houldsworth et al. [1996]. ^{*2}6/21 GCB- and 10/21 ABC-DLBCL, 5/21 unclassified. ^{*3}based to large extent on same cohort. ^{*4}Weniger et al. selected 5 samples with and 15 samples without gain/amplification from the Bentz et al. cohort. ^{*5}Barth et al. studied samples from the Joos et al. cohort.

Reference	DLBCL	GCB-DLBCL	ABC-DLBCL	PMBCL	cHL
Houldsworth et al. [1996] Rao et al. [1998]	23% (26/111) ^{*1}				
Bea et al. [2004]	14% (9/64)				
Jardin et al. [2010]	18% (21/114) ^{*2}				
Rosenwald et al. [2002] ^{*3}		15% (17/115)	0% (0/73)		
Bea et al. [2005] ^{*3}		17% (15/87)	15% (12/77)	47% (9/19)	
Lenz et al. [2008] ^{*3}		35% (72)	12% (74)	26% (31)	
Houldsworth et al. [2004]		28% (5/18)	17% (2/12)		
Feuerhake et al. [2005]		17% (10/57)	5% (1/22)	3% (1/34)	
Tagawa et al. [2005]		33% (6/18)	7% (2/28)		
Joos et al. [1996]				27% (7/26)	
Bentz et al. [2001] ^{*4}				19% (8/43)	
Weniger et al. [2007] ^{*4}				75% (15/20)	
Palanisamy et al. [2002]				36% (4/11)	
Martin-Subero et al. [2002]					35% (11/31)
Joos et al. [2002] ^{*5}					54% (22/41)
Barth et al. [2003] ^{*5}					41% (7/17)
Steidl et al. [2010]					28% (53)
Salipante et al. [2016]					40% (8/20)
Average	17%	21%	9%	28%	39%

parameters and the authors detected a superior clinical outcome for the GCB-DLBCL subgroup [Alizadeh et al., 2000; Rosenwald et al., 2002]. This was, however, not confirmed in reports of 58 [Shipp et al., 2002] or another 46 [Houldsworth et al., 2004] DLBCL samples. Nevertheless, a significantly better survival rate for GCB-DLBCL patients was again determined for 2 of the data sets [Rosenwald et al., 2002; Shipp et al., 2002] by Wright et al. using a new subgroup prediction algorithm designed to be independent of the microarray platform that differed in the two original publications [Wright et al., 2003]. In agreement with this, a correlation of the GCB-DLBCL phenotype with better overall survival was found in an independent cohort [Curry et al., 2009]. Monti et al. suggested a DLBCL classification that focuses on cell-intrinsic signaling pathways and response to the microenvironment rather than the cell of origin. When clustering their data according to Wright et al., these authors also found extended survival rates for the GCB-DLBCL subgroup [Monti et al., 2005].

Rosenwald et al. detected a *REL* amplification exclusively within the GCB-DLBCL subgroup at a frequency of 15% (17/115) using quantitative polymerase chain reaction [Rosenwald et al., 2002]. On the contrary, applying comparative genomic hybridization (CGH) on the same patients, a DNA gain or amplification in 2p14-p16 ranks as the second most frequent overrepresentation observed and is distributed with 17% in GCB-DLBCL (15/87) and 15% in ABC-DLBCL (12/77). Of these gains, amplifications are more frequent in GCB- (8/14) than in ABC-DLBCL (2/11) [Bea et al., 2005]. Partially the same cohort was evaluated using array-based CGH (aCGH). Considering both gains and amplifications of 2p, Lenz et al. detected this genomic alteration in 35% of GCB- and 12% of ABC-DLBCL. Restricting the analysis to amplifications, the authors still found copy number changes > 3.5 in 28% and 5% of all samples for the GCB and ABC subgroup, respectively [Lenz et al., 2008].

In agreement with a higher abundance of *REL* overrepresentation in the GCB-DLBCL subgroup, Feuerhake et al. found 17% (10/57) and 5% (1/22) *REL* amplifications in GCB- and ABC-DLBCL-classified samples, respectively [Feuerhake et al., 2005]. In another published patient group, 28% of GCB (5/18), 17% of ABC (2/12) and 15% of type 3 DLBCL (2/13) display *REL* amplifications with at least 4 copies [Houldsworth et al., 2004], hence further corroborating this tendency. Similarly, an additional study observed an association with the GCB-DLBCL subtype with gains of 2p15-p16.1 in 33% (6/18) of GCB-DLBCL patients and in only 7% (2/28) of ABC-DLBCL patients [Tagawa et al.,

2005]. In a cohort of 114 DLBCL cases, Jardin et al. observed *REL* gains in 18% (21/114) of all samples with a distribution amongst the GCB and ABC cluster of 6/21 and 10/21, respectively, while the remaining 5 samples were not classified. Bea et al. did not distinguish subtypes by gene expression profile and found 5/64 gains and 4/64 amplifications summing up to 14% (9/64) of DLBCL patients with 2p14-p16 overrepresentation [Bea et al., 2004].

In summary, gains or amplifications in 2p16.1 containing the *REL* locus are highly abundant in DLBCL with a somewhat higher prevalence in the GCB-DLBCL compared to the ABC-DLBCL subset.

3.2.2 Primary mediastinal B cell lymphoma

PMBCL originates in the mediastinum, probably with involvement of the thymus [Barth et al., 2002]. Thus, it appears that thymic medullary B cells are the proposed cells of origin [Küppers, 2005; Savage, 2006]. Originally grouped within the DLBCL lymphoma entity, PMBCL was recognized as a distinguishable separate lymphoma type later on [Barth et al., 2002]. Subsequently, the use of gene expression profiling to identify PMBCL by molecular diagnosis has been suggested [Rosenwald et al., 2003; Savage, 2003]. Both of these studies conclude that PMBCL shares characteristics with cHL on the molecular phenotype level [Rosenwald et al., 2003; Savage, 2003].

Two of the publications cited above for DLBCL also assessed 2p overrepresentations in PMBCL samples. While Bea et al. detected gains in 47% of analyzed samples, Lenz et al. report gains including amplifications for 26% and sole amplifications for 19% of all PMBCL cases [Bea et al., 2005; Lenz et al., 2008]. In an independent cohort, a gain in 2p was detected in 27% (7/26) PMBCL biopsies. Two of these cases display high level *REL* amplifications of 5- and 10-fold as quantified by Southern blot [Joos et al., 1996]. Moreover, Southern blot quantification for a small number of 11 PMBCL patients showed copy numbers ≥ 4 in 36% (4/11) of samples [Palanisamy et al., 2002]. Using CGH another study detected an overrepresentation of 2p14-16 in 19% (8/43) of PMBCL cases [Bentz et al., 2001]. Interphase cytogenetics employing fluorescence *in situ* hybridization (FISH) analysis of material from 20 of these patients substantiated 2 gains and 3 amplifications previously found by CGH in this selected sample set and revealed 8 gains and 2 amplifications in addition, which amounts to a total number of 15 *REL* copy number changes in 20 samples [Weniger et al., 2007].

3.2.3 Classical Hodgkin lymphoma

cHL accounts for about 10% of human mature B cell lymphomas [Küppers, 2005]. A hallmark of cHL are mononucleated Hodgkin cells and multinucleated Reed-Sternberg cells. Remarkably, these Hodgkin and Reed-Sternberg (HRS) cells constitute only 1% of tumor cells. Although HRS cells have lost major B cell gene expression characteristics and even acquired markers of other lineages, they originate from GC B cells based on their rearranged and somatically mutated Ig gene loci [Küppers, 2009, 2012].

In a study of 41 cHL tumors, Joos et al. detected gains in 2p by CGH as the most frequent alteration in 54% of cases [Joos et al., 2002]. Interphase cytogenetic analysis of 17 samples from the same cohort by FISH demonstrates 5 gains and 3 amplifications. Only in 1 case the amplification contradicted the CGH data summing up to an overrepresentation of the *REL* locus in 41% (7/17) of cHL patients substantiated by both methods [Barth et al., 2003]. A similar assessment of interphase cytogenetic by FISH of 31 cHL biopsies showed *REL* locus gains in 35% (11/31) including 8 cases with high-level amplifications (26% of total cases) [Martin-Subero et al., 2002]. Applying aCGH profiling on 53 cHL specimens Steidl et al. detected gains in the 2p15-16.1 genomic locus in 28% of patients [Steidl et al., 2010]. In a recent publication, whole genome sequencing determined significant copy number gains ≥ 4 of the chromosomal segment containing the *REL* locus in 40% (8/20) of cHL patients [Salipante et al., 2016]. Finally, the 2p16.1 *REL* locus was identified as a susceptibility locus for cHL in a genome-wide association study (GWAS) [Enciso-Mora et al., 2010].

3.2.4 *REL* amplification and c-Rel protein expression and localization

REL amplification is a highly frequent event in GC-derived human B cell lymphomas, but the functional consequences remain elusive. Several studies investigated the relation of *REL* genomic status and c-Rel expression level and localization.

DLBCL In the large cohort of 224 DLBCL patients, *REL* is significantly higher expressed in GCB-DLBCL samples with 2p14-p16 gains, whereas in ABC-DLBCL samples with 2p14-p16 gains *REL* levels are only slightly increased and this trend is insignificant [Bea et al., 2005]. Similarly, two other studies observed augmented *REL* mRNA levels in specimens with *REL* locus gains in DLBCL patient cohorts of 127 [Feuerhake et al., 2005] and 114 [Jardin et al., 2010] subjects, respectively. Other publications focused on

assessment of c-Rel nuclear protein level. Houldsworth et al. observed heterogeneity with regard to c-Rel nuclear accumulation based on immunofluorescence and no correlation with *REL* amplification. At least 70% positive c-Rel nuclei were found in 44% (17/39) of cases with a higher prevalence in the ABC-DLBCL subgroup despite the higher percentage of *REL* amplifications within the GCB-DLBCL subgroup of this cohort [Houldsworth et al., 2004]. With nuclear positivity in 64% of 113 DLBCL samples, c-Rel was found to be the most frequently expressed nuclear subunit when comparing the five NF- κ B family members for which positivity was reached when more than 30% of tumor cells exhibited nuclear staining. In this cohort, positive nuclear c-Rel expression is equally distributed amongst the GCB- and ABC-DLBCL subgroups and correlates with favorable prognosis [Odqvist et al., 2014]. Curry et al. set a cutoff for positivity of c-Rel nuclear protein in 20% of neoplastic cells, which results in a comparable frequency of 65% (44/68) of DLBCL cases that fall into this category. The authors did not observe a significant correlation of nuclear c-Rel with the DLBCL subgroups or overall survival of patients. Nevertheless, this data set suggests a trend for worse survival of patients with positive nuclear c-Rel expression within the GCB-DLBCL cluster [Curry et al., 2009]. Despite an even lower cutoff of 5% of tumor cells with c-Rel-stained nuclei considered positive, Li et al. found only 26% (137/460) of DLBCL patients with positive nuclear c-Rel staining and similar distribution of cases amongst the subclasses. *REL* mRNA levels and nuclear positivity show no correlation in this large cohort, but *REL* mRNA is significantly higher in the GCB-DLBCL group [Li et al., 2015]. Moreover, Rodig et al. found nuclear c-Rel staining only in 18% (28/160) of DLBCL samples that were not further subclassified [Rodig et al., 2007]. Finally, in a small group of 9 GCB- and 5 ABC-DLBCL patient samples and 19 DLBCL-derived cell lines, c-Rel DNA binding was found to be more prominent in the GCB-DLBCL subtype [Pham et al., 2011].

PMBCL In order to study the relation of genomic *REL* gains and c-Rel protein level on a single cell basis, Weniger et al. combined FISH interphase cytogenetics with immunofluorescence staining (FICTION, fluorescence immunophenotyping and interphase cytogenetics as a tool for investigation of neoplasms). This analysis demonstrated a positive correlation of *REL* genomic overrepresentation and c-Rel nuclear staining for the 10 analyzed PMBCL samples [Weniger et al., 2007]. In two other studies, c-Rel nuclear localization was observed by immunohistochemistry in 5 of 6 PMBCL patient samples

[Savage, 2003] and in all of 7 PMBCL biopsies [Feuerhake et al., 2005]. In a considerable cohort of 48 PMBCL patients, 65% (31/48) of samples were characterized by the presence of nuclear c-Rel [Rodig et al., 2007].

cHL In a cohort of 25 cHL patients, Barth et al. demonstrated a strong correlation of *REL* gain with nuclear c-Rel staining in HRS cells. While the 12 cases with *REL* copy number gains show positive nuclear c-Rel staining in at least 30% of HRS cells in 5/12 and more than 70% of HRS cells in 7/12 specimens, the majority of samples with balanced *REL* loci displayed less than 30% of positive HRS cells [Barth et al., 2003]. In addition, nuclear c-Rel was detected in two independent studies in 80% (23/25) [Rodig et al., 2005] and even 86% (51/59) [Xiao et al., 2004] of cHL patient material.

In summary, the publications cited above provide evidence for a positive correlation of *REL* gene locus amplification and c-Rel expression level accompanied by frequent observations of nuclear c-Rel protein accumulation for both PMBCL and cHL. This contrasts with the heterogeneity amongst the DLBCL cases, which is illustrated by a broad spectrum of varying frequencies for nuclear c-Rel staining and in part inconsistent conclusions with regard to subtype distribution and relation of *REL* locus overrepresentation and expression levels. As indicated above, it is noteworthy that gene expression analyses demonstrate that PMBCL is related to cHL with closer resemblance than to other DLBCL subtypes [Rosenwald et al., 2003; Savage, 2003]. Interestingly, shared features of cHL and PMBCL are an association with high NF- κ B activity as well as lack of detectable BCR expression [Savage, 2003; Weniger et al., 2007; Küppers, 2009]. It is worth mentioning that cell line-based studies suggest that predominant nuclear or cytoplasmic c-Rel localization is not necessarily a prognostic clue for malignant transformation [Gilmore et al., 2004b]. Finally, c-Rel localization and expression level could be characteristic and specific for the lymphoma cell of origin [Gilmore and Gerondakis, 2011].

3.2.5 Co-amplification of *BCL11A* with *REL*

Especially studies that did not find a positive correlation between *REL* gene amplification and c-Rel protein expression questioned whether *REL* is indeed the target of the 2p16.1 locus gains and amplifications. In fact, *REL* is not the only gene in the commonly amplified genetic region. Amongst others, the *BCL11A* gene also maps to 2p16.1 and is

located only within 300 kB of *REL*³. The Krüppel zinc finger transcription factor Bcl-11a is essential for lymphocyte development and in particular B cells are virtually absent in Bcl11a-deficient mice [Liu et al., 2003]. Intriguingly, Bcl-11a is highly expressed in the GC and a translocation involving *BCL11A* and the Ig heavy chain locus has been discovered in B cell malignancies [Satterwhite, 2001; Küppers et al., 2002].

Several studies provide evidence for a frequent co-amplification of the *REL* and *BCL11A* loci in the B cell lymphoma subtypes introduced above. In 4 of 7 DLBCL cases analyzed by Fukuhara et al. using aCGH both *REL* and *BCL11A* are gained, whereas 3 cases show an exclusive *REL* gain and these genomic gains correlate with mRNA expression levels [Fukuhara et al., 2006]. On the contrary, in a study by Bea et al., all 9 DLBCL patients with 2p14-p16 gains or amplifications show elevated copy numbers for both *REL* and *BCL11A* assessed by real-time quantitative polymerase chain reaction (RQ-PCR) [Bea et al., 2004]. Similarly, in a large cohort of 224 patients, the vast majority of cases of GCB- and ABC-DLBCL as well as PMBCL show concomitant copy number changes of *REL* and *BCL11A* according to RQ-PCR [Bea et al., 2005]. Also in a series of 15 PMBCL cases, copy numbers for *BCL11A* and *REL* were shown to be simultaneously increased [Weniger et al., 2006b, 2007]. Weniger et al. observed nuclear Bcl-11a protein in 88% (14/16) of analyzed PMBCL. However, only in 25% (4/16) of cases, *BCL11A* copy number alterations, transcript levels and nuclear protein clearly correlate [Weniger et al., 2006b]. Lastly, more than 90% (10/11) of cHL cases with *REL* amplification and gains show concomitant *BCL11A* amplification and gains, respectively. In two cases (2/21) of this cohort with balanced *BCL11A* status, the authors found indications for modifications of the *REL* locus without affecting *BCL11A* [Martin-Subero et al., 2002]. These studies demonstrate that in the majority of analyzed lymphoma cases the *BCL11A* gene is indeed frequently co-amplified with the *REL* gene. Hence, both c-Rel and Bcl-11a represent interesting candidates for prospective gain-of-function studies, in particular with regard to investigation of compound effects.

3.3 Human B cell lymphoma cell lines

Patient-derived B cell lymphoma cell lines constitute a versatile tool box to discover lymphoma-associated signaling pathways and have been applied as an approach to deci-

³Genomic location of BCL11A ENSG00000119866 accessible on www.ensembl.org (human GRCh38.p5)

pher the role of c-Rel in this context. A decrease in viability upon short hairpin RNA (shRNA) knockdown of c-Rel, RelA or RelB in 3 cHL cell lines, including U-HO1, has been shown [Ranuncolo et al., 2012]. Also in a murine B cell lymphoma cell line and primary mouse B cells, si(small interfering)RNA-mediated c-Rel knockdown negatively affects cell survival and cell cycle progression [Tian and Liou, 2009]. Similarly, treatment of human B cell lymphoma cell lines with the synthetic compound calafianin monomer CM101 that inhibits DNA binding of c-Rel and RelA lowers proliferation and cell viability correlating with a diminished c-Rel DNA-binding activity in certain sensitive cell lines, including the cHL cell line L-428 [Yeo et al., 2015]. In addition, inhibition of MALT1 protease activity selectively reduces viability and proliferation in ABC- but not GCB-DLBCL cell lines that is accompanied by decreased nuclear c-Rel and basal Bcl-x_L expression [Ferch et al., 2009].

Based on the consistent correlation of *REL* amplification and c-Rel expression in PMBCL and cHL, human B cell lines derived from these lymphoma subtypes represent suitable candidates to further investigate the consequences of c-Rel signaling. Therefore, two PMBCL and two cHL cell lines were chosen for a c-Rel loss-of-function approach in the present work and are introduced in the following paragraphs.

The cell line MedB-1 was established from a PMBCL tumor followed by an initial immunophenotypic description [Moller et al., 2001; Bentz et al., 2001]. Weniger et al. reported that in MedB-1 the *REL* and *BCL11A* gene loci are amplified in 20% of cells and observed a higher transcript level of *REL* but not *BCL11A*. While 30% of MedB-1 cells show c-Rel nuclear translocation, nuclear Bcl-11a is not detectable in this cell line [Weniger et al., 2006b, 2007]. Karpas1106P is also classified as a PMBCL cell line and was established and initially characterized by Nacheva et al. [Nacheva et al., 1994]. Karpas1106P was described to have a gain in *REL* and *BCL11A* without increased transcription of these two genes. However, 70% of Karpas1106P cells show nuclear c-Rel staining but no detectable nuclear Bcl-11a [Weniger et al., 2006b, 2007]. Wessendorf et al. observed a gain in 2p by aCGH in Karpas1106P but not in MedB-1 [Wessendorf et al., 2007]. This 2p gain in Karpas1106P was also detected in a recent publication, but the gained region does not include the *REL* locus [Dai et al., 2015]. Accordingly, no consistent rearrangement or copy number alterations of either the *REL* or *BCL11A* locus in MedB-1 or Karpas1106P were determined, but yet *REL* expression levels are high in both PMBCL cell lines in comparison to numerous other B cell lymphoma cell lines [Dai et al., 2015]. In addition,

Karpas1106P and MedB-1 show high NF- κ B DNA-binding activity [Weniger et al., 2007]. The cell line L-428 was established from a cHL patient sample [Schaadt et al., 1979]. L-428 shows a gain of the 2p16 chromosomal band by CGH [Joos et al., 2003; Mader et al., 2007]. FISH analysis indicated that L-428 harbors chromosomal translocation breakpoints within 2p15-p16 as well as a duplication of the *REL* and *BCL11A* genomic region [Joos et al., 2003]. L-428 expresses an inactive truncated form of I κ B α [Krappmann et al., 1999] and c-Rel is predominantly localized to the nucleus in this cell line [Bargou et al., 1996; de Oliveira et al., 2016]. U-HO1 was established from a cHL patient. FISH analysis demonstrated that U-HO1 carries a six-fold amplification of the *REL* and *BCL11A* locus coinciding with a strong nuclear c-Rel staining [Mader et al., 2007].

3.4 Disease associations of c-Rel beyond lymphoma

Genome wide association studies found associations of single nucleotide polymorphisms (SNPs) within the *REL* gene locus for several human diseases with immunological etiology, including rheumatoid arthritis [Gregersen et al., 2009; Eyre et al., 2010], psoriasis [Strange et al., 2010], ulcerative colitis [McGovern et al., 2010] and celiac disease [Trynka et al., 2009; Dubois et al., 2010]. Studies in mouse models substantiate implications for a role of c-Rel in immune system-related diseases beyond lymphoma. c-Rel^{-/-} mice are protected from allergen-induced pulmonary inflammation and airway hyperresponsiveness that serves as a mouse model for asthma [Donovan et al., 1999]. With regard to mouse models of arthritis, c-Rel-deficiency can preclude development of collagen-induced arthritis, but c-Rel^{-/-} mice respond comparable to controls in an acute arthritis model [Campbell et al., 2000]. c-Rel also has a central driving function in mouse models of colitis as c-Rel-deficiency can confer protection [Wang et al., 2008; Visekruna et al., 2015]. Moreover, c-Rel^{-/-} mice are resistant to experimental autoimmune encephalomyelitis (EAE), a mouse model for inflammatory diseases of the central nervous system, such as multiple sclerosis [Hilliard et al., 2002]. In addition, combining mutant mice unable to generate membrane-bound Fas ligand (FasL ^{Δ m/ Δ m}) with c-Rel-deficiency can dramatically increase the lifespan and reduce the typical autoimmune pathology that characterizes FasL ^{Δ m/ Δ m} mutant mice [O'Reilly et al., 2015]. Finally, c-Rel plays a crucial role in transplantation immunology as c-Rel-deficiency improves graft tolerance in mice in a diabetes model of pancreatic islet allografts [Yang et al., 2002] or for allograft heart transplants [Finn et al., 2002] and as c-Rel-deficiency alleviates murine graft-versus-host disease (GVHD) after al-

logenic bone marrow transfers [Yu et al., 2013]. The involvement of c-Rel in malignancies beyond the hematopoietic system includes for instance fibrosis and solid tumors [Hunter et al., 2016].

3.5 c-Rel as a therapeutic target

Given the manifold predicted and partially validated involvement of c-Rel in human diseases, the concept of c-Rel as a therapeutic target has been pursued. Specifically targeting c-Rel could have advantages over general NF- κ B inhibition which acts systemically and has dramatic effects on non-immune cells [Pasparakis, 2009; Gilmore and Garbati, 2011]. The viability of c-Rel^{-/-} mice and their defects primarily affecting the immune system corroborate this strategy. In light of the fact that transcription factors are not regarded as easily targetable [Gilmore and Garbati, 2011], it is especially important to thoroughly elucidate the specific signaling pathways that lead to c-Rel activation.

The NF- κ B inhibitor dehydroxymethylepoxyquinomicin (DHMEQ) has been reported to target conserved cysteine residues and to form adducts with c-Rel as well as other NF- κ B subunits, thus impairing their DNA-binding ability [Yamamoto et al., 2008; Ouk et al., 2009]. The inhibitor CM101 targeting at least c-Rel and RelA has been used in human B cell lymphoma cell lines [Yeo et al., 2015] (see 3.3). In a small molecule screen based on a biochemical assay determining c-Rel DNA binding, Shono et al. identified compounds that inhibit NF- κ B and are claimed to show specificity for c-Rel in particular. Subsequently, derivatives of these compounds, namely the thiohydantoin IT-603 and the naphthalenethiobarbiturate IT-901, have been demonstrated to ameliorate GVHD in mouse models and compromise growth of human B cell lymphoma cell lines [Shono et al., 2014, 2016]. In addition, treatment with siRNA targeting c-Rel delivered in micelles via intraperitoneal (i.p.) injection in a mouse model of imiquimod (IMQ)-induced psoriasis has been shown to prevent or mitigate disease symptoms [Fan et al., 2016].

In conclusion, it is evident that c-Rel not only plays a particular role in B cell development and function, but this NF- κ B transcription factor is also implicated in human lymphoma and autoimmunity, in which B cells are the malignant cell type or are major disease drivers or contributors, respectively. The genetic basis of this association lies within the frequent observation of amplifications of the *REL* locus and the identification of SNPs within the *REL* locus potentially connected to higher susceptibility for autoimmune diseases.

Part II

Aim of the thesis

Although the question whether c-Rel can drive malignant transformation has been posed many years ago [Gilmore et al., 2001], there is still no conclusive answer to this subject in an *in vivo* setting. In light of the numerous studies identifying frequent *REL* gene locus amplifications in human B cell lymphomas and associations of SNPs within the *REL* locus with human autoimmune diseases, this puzzling question is more relevant than ever. To date, studies of c-Rel function *in vivo* primarily rely on c-Rel knockout mouse models. In this context, it appears almost surprising that no c-Rel transgenic mouse model for gain-of-function analysis of c-Rel in B cells exists until present. Remarkably, unsuccessful attempts as stated by Gerondakis et al., 2006, do not only emphasize the urgent need for such a model but also prove that this is not a trivial task.

The central objective of this thesis is the generation of novel conditional c-Rel transgenic mouse models that allow investigation of c-Rel gain-of-function in B cells and germinal center B cells *in vivo*. This research project is complemented with a c-Rel loss-of-function approach in human B cell lymphoma cell lines *in vitro*. The combination of these strategies establishes the fundament for unraveling the precise role of c-Rel overexpression in activated and terminally differentiated B cells, which constitutes the central aim of this thesis. In order to achieve this aim, I defined the following pivotal research milestones that are addressed in the indicated sections of the results part (part IV) in this thesis.

- Generation and characterization of novel c-Rel transgenic mouse models (section 1)
- Analyses of consequences of c-Rel overexpression in B cells (subsection 1.2 and 1.3) and germinal center B cells (subsection 1.5) as well as elucidation of the mechanism underlying the ensuing phenotypes (subsection 1.7.4 and 1.7.5)
- Quantification of c-Rel protein levels and identification of regulatory mechanisms of c-Rel expression in B cell subsets (subsection 1.7 and 1.8)
- Investigation of effects of c-Rel downregulation in human B cell lymphoma cell lines (section 2)

Part III

Materials and Methods

1 Standard materials and methods

Standard essential methods of extraction, purification, quantification, analysis and manipulation of DNA, RNA and proteins were performed according to Sambrook et al. [1989] and Sambrook and Russell [2001] unless otherwise specified in the following sections.

Plasmid DNA isolation and gel extraction was based on kits (Qiagen, Macherey-Nagel). Reagents and materials for methods of molecular biology were purchased from New England Biolabs, Promega, Metabion, Eurofins, GenScript and Thermo Fischer Scientific.

Chemicals were purchased from the following manufacturers: Applichem, Calbiochem, Fluka, Merck, Roth and Sigma-Aldrich. Consumables were obtained from companies including Corning, Costar, Braun, Eppendorf, Greiner bio-one, Sarstedt and TPP. Companies of general lab equipment included Bio-Rad, Bosch, Eppendorf, Gilson, Heraeus, Liebherr, Thermo Fisher Scientific and Zeiss.

2 Generation and characterization of mouse lines

2.1 Mouse generation

2.1.1 BAC transgenesis and construct verification

Several modifications of a bacterial artificial chromosome (BAC) containing the endogenous mouse *REL* genetic locus but no other genes (BAC RP23-259L5) were performed in SW102 bacteria: (1) insertion of flippase (Flp) recognition target (Frt) sites flanking exon 9 by galactokinase (*galK*) selection; (2) insertion of a 3xflag-IRES(internal ribosomal entry site)-hygromycin B-resistance cassette at the *REL* carboxy-terminus; (3) addition of a CAG(CMV early enhancer/chicken β actin promoter)-loxP-Stop-neomycin/kanamycin-resistance-loxP cassette combined with an HA-tag or GFP-tag to the first translated *REL* exon.

Plasmid-based fragments were inserted by BAC recombination-mediated genetic engineering (recombineering). Electrocompetent SW102 bacteria were transformed with the

required BAC by electroporation (Bio-Rad GenePulser XCell, pre-set bacterial protocol, 0.2 cm cuvette, 25 μ F, 200 Ω , 2500 V) and subsequently plated on lysogeny broth (LB) agar under selection with chloramphenicol. BAC-carrying bacteria were maintained at 30 °C and stored in glycerol stocks at -80 °C. For recombineering BAC-containing SW102 bacteria were grown up to an OD₆₀₀ of 0.5-0.6. The bacterial suspension was heat-shocked for 15 min at 42 °C and subsequently cooled down on icy water of 4 °C for 5 min. Bacterial cells were washed twice in double-distilled water (H₂O_{dd}) with centrifugation steps at 3200 xg, 4 °C, for 5 min. The cell pellet was resuspended in H₂O_{dd} and used for electroporation with 200 ng of linearized gel-purified plasmid DNA (Bio-Rad GenePulser XCell, pre-set bacterial protocol, 0.2 cm cuvette, 25 μ F, 200 Ω , 2500 V). Electroporated bacterial cells were recovered in LB medium under shaking for 60 min at 30 °C and then plated on LB agar with appropriate selection antibiotics and grown for 24-30 h at 30 °C.

BAC colonies were screened by polymerase chain reaction (PCR) (2.1.4). BAC DNA was prepared using plasmid purification kit buffers (Qiagen) for small scale preparations or the NucleoBond BAC100 kit (Macherey-Nagel) for large scale preparations.

To initially test the functionality of the BAC construct, mouse embryonic fibroblasts (MEF) prepared from *c-Rel*^{-/-} mice were complemented with the BAC construct (Invitrogen Lipofectamine) and essentially the same analysis methods were applied as described in the following for embryonic stem (ES) cell screening and verification, including Cre transduction (1 μ M TAT-Cre/HTNC (Protein core facility Max Planck Institute of Biochemistry) in 1:1 PBS:serum-free culture medium (Gibco), 12 h), antibiotic selection and adenoviral-based Flp expression followed by (GFP)-*c-Rel* protein expression analysis by flow cytometry (2.3) and Western blot (3.3).

2.1.2 Embryonic stem cell culture

Selection, isolation, expansion and storage of ES cells was performed essentially as published [Schmidt-Supprian et al., 2000]. C57BL/6 ES cells (Artemis Pharmaceuticals) were grown on embryonic feeder (EF) cell layers that were pre-treated for mitotic inactivation with mitomycin C (MMC, Sigma-Aldrich) and plated on gelatinized (gelatine solution, Sigma-Aldrich) plates. ES cells were cultured in KnockOut DMEM (Gibco) supplemented with serum (FBS special designed for embryonal stem cells, PAN), L-glutamine (Gibco), non-essential amino acids (NEAA, Gibco), β -mercaptoethanol (Sigma-Aldrich), leukemia inhibitory factor (LIF, culture supernatant) and GSK3 inhibitor (BIO/GSK3 IX, Bio-

zol/Cayman chemical, or SB216763, Selleckchem). Trypsinization solution (Gibco) was supplemented with chicken serum (Sigma-Aldrich).

20 μ g BAC DNA and 5 μ g CAG-IsceI plasmid DNA were introduced into C57BL/6 ES cells for each BAC construct by electroporation (Bio-Rad Gene Pulser XCell, 240 V, 500 μ F). Transfected ES cells were kept under selection with G418 (Sigma-Aldrich) and single clones were subjected to further verification. ES cell clones were first screened by PCR (2.1.4) and Southern blot (2.1.3). Selected clones were Cre-transduced (1 μ M TAT-Cre/HTNC (Protein core facility Max Planck Institute of Biochemistry) in ADCF-MAB without L-glutamine (HyClone, Thermo Scientific), 4-5 h) and functionally validated by hygromycin B (Sigma-Aldrich) selection and (GFP-)c-Rel protein expression was assessed by flow cytometry (2.3) and Western blot (3.3).

Following blastocyst injection of extensively validated ES cell clones at the transgenic core facility of the Max Planck Institute of Biochemistry, germline transmission of the BAC transgenic loci was achieved.

2.1.3 Southern blot

Genomic DNA was digested with BamHI (NEB). DNA fragments were separated by agarose gel electrophoresis and transferred to Amersham Hybond-XL membranes (GE Healthcare Life Sciences) by alkaline capillary transfer. DNA fixation was performed by UV-crosslinking. Southern blot probes were radioactively labelled based on random primer labeling (Prime-it II Random Primer Labeling Kit, Agilent technologies) and filtered to remove unincorporated nucleotides (Whatman Grade GF/C Glass Microfiber Filter, GE Healthcare Life Sciences). Hybridization with the labeled probe was performed over night in Church hybridization buffer (0.17% phosphoric acid, 0.25 M Na₂HPO₄, 1% BSA, 7% SDS, 1 mM EDTA, 100 μ g/ml salmon sperm ssDNA). Following stringency washes (2x SSC, 0.1% SDS; 1x SSC, 0.1% SDS; 0.5x SSC, 0.1% SDS and further dilutions of SSC if required), signals were detected using a phosphorimager (FLA 7000, GE Healthcare Life Sciences). Southern blot probes detecting the neomycin (673 bp; BamHI, PstI fragment from pMMneoflox-8 [Kraus et al., 2001]) or hygromycin B (900 bp; HincII fragment of the EM7-hygromycin-resistance locus) resistance cassette were applied. The probe for BAC locus integration quantification (359 bp) was amplified by PCR from the endogenous *REL* locus using a forward 5'-AAAAGAGCACCTCCCTCGTG-3' and reverse 5'-ATATGTTTCACCTGCCCTCAG-3' primer [Heise et al., 2014].

2.1.4 PCR for ES cell screening and genotyping

The primers used for screening of ES cell clones and for mouse genotyping are listed in Table 2. PCRs for screening covered both the amino-terminal CAG promoter as well as the carboxy-terminal hygromycin B resistance locus. The newly established genotyping PCRs detect not only the transgenic loci but also the endogenous *REL* locus. DNA for genotyping was prepared from mouse earclip biopsies.

Table 2: Primers. Primers used for ES cell screening (S) or genotyping (G) are specified. Sequences are displayed in 5' to 3' orientation. for, forward; rev, reverse.

Designation	Purpose	Direction	Sequence
Exon9firt	G, S	for	CTGCTGCAAGATTGTGGTAAGA
		rev	AATAGTGAGAGTGTGCCGGA
c-Rel/GFP-c-Rel	G	for	CACTGCATTCTAGTTGTGGTTT
		for	CTCTCAGCAAGGACCCCAAC
		for	TGACGTAAGCAGCGGAAAT
		rev	TGAAAGGCAGACCGTCCTAAC
CAG promoter	S	for	ACCGGAGCGCGAAGAT
		rev	GAAAGGTATTGCAACACTCCCCT
		rev	ACTTGAAAGGCAGACCGTCC
Hygromycin B resistance	S	for	TTGTATGGAGCAGCAGACGC
		rev	AGCAAGCACGTGGACTTTAG

2.2 Genetically modified mice

All mouse lines described in this work were maintained on a C57BL/6 background. Mice were housed in specific pathogen-free animal facilities of the Max Planck Institute of Biochemistry and the Klinikum rechts der Isar of the Technische Universität München. All animal procedures were approved by the Regierung of Oberbayern.

The Frt-flanked exon 9 was removed to generate c-Rel Δ Ex9 mice by crossing the c-Rel BAC transgenic mice to an FLPe-deleter strain [Rodríguez et al., 2000]. The CD19Cre and C γ 1Cre mouse lines used in this work have been described previously [Rickert et al., 1997; Casola et al., 2006].

Young mice were sacrificed for experiments at 8 weeks to a maximum of 16 weeks of age. Aged mice ranged between 409 and 571 days of age at day of analysis, with a median age of 511 or 521 days for c-Rel CD19Cre^{I/+} experimental and CD19Cre^{I/+} control mice, respectively.

2.3 Flow cytometry and imaging flow cytometry

Single cell suspensions were prepared from mouse lymphoid organs and red blood cell (RBC) lysis was performed using Gey's solution. Blocking of Fc receptors to minimize non-specific antibody binding was achieved by incubation with anti-mouse CD16/CD32 (93, eBioscience) preceding extra- or intracellular stainings of single cell suspensions with antibodies listed in Table 3 or with peanut agglutinin (PNA, Vector Laboratories). Biotinylated primary antibodies were visualized using streptavidin fluorochrome conjugates (eBioscience, BioLegend). For intracellular stainings the FoxP3/transcription factor staining buffer set (eBioscience) was applied according to the manufacturer's instructions. 7-AAD staining solution (7-amino-actinomycin D, eBioscience) or live/dead fixable near-IR(infrared) dead cell staining kit (Invitrogen) were used for discrimination of viable cells. Doublets were excluded based on FSC-H/A and SSC-W/A characteristics. DNA content visualization for cell cycle analysis or nuclear staining in imaging flow cytometry was based on DRAQ5 (Abcam). For staining of apoptotic cells, the CaspGlow active caspase staining kit (fluorescein, BioVision) was combined with 7-AAD and the Annexin V apoptosis detection kit (APC, eBioscience). Active caspases were labelled *in vitro* according to the CaspGlow kit instructions and the subsequent staining was performed following the Annexin V detection kit procedure.

Samples were acquired on a FACS Canto II (BD Biosciences) flow cytometer or the ImageStream MK II (Amnis Cooperation) imaging flow cytometer. Cell sorting was performed on a FACS Aria II (BD Biosciences).

2.4 Magnetic activated cell sorting (MACS)

Single cell suspensions were pre-stained with monoclonal antibodies anti-IgD-biotin (11-26c, eBioscience) or anti-CD138-PE (281-2, BioLegend) and subsequently labelled with anti-Biotin or anti-PE magnetic microbeads (Miltenyi Biotec), respectively, or directly labelled with anti-CD43 magnetic microbeads (Miltenyi Biotec) according to the manufacturer's instructions. Samples were separated on an autoMACS Pro Separator (Miltenyi Biotec) device using recommended programs for positive enrichment or negative depletion.

Table 3: Flow cytometry antibodies. Antibodies used in flow cytometry are listed including information on clone and manufacturer.

Specificity	clone	Manufacturer	Specificity	clone	Manufacturer
AA4.1/CD93	AA4.1	eBioscience	Bcl-6	K112-91	BD Biosciences
B220	RA3-6B2	eBioscience	Blimp-1	5E7	BD Biosciences
CD1d	1B1	eBioscience	CD95/Fas	Jo2	BD Biosciences
CD4	RM4-5	eBioscience	CXCR4/CD184	2B11	BD Biosciences
CD5	53-7.3	eBioscience	CXCR5	2G8	BD Biosciences
CD8a	53-6.7	eBioscience	CD138	281-2	BD Biosciences
CD11b/Mac1	M1/70	eBioscience	CD21/CD35	7G6	BD Biosciences
CD11c	N418	eBioscience	IgA	C10-1	BD Biosciences
CD19	1D3	eBioscience	IgG1	A85-1	BD Biosciences
CD21/CD35	8D9	eBioscience	IgG3	R40-82	BD Biosciences
CD23/FcεRII	B3B4	eBioscience	Igκ	187.1	BD Biosciences
CD25	3C7, PC61.5	eBioscience	Igλ	R26-46	BD Biosciences
CD38	90	eBioscience	B220	RA3-6B2	BioLegend
CD43	eBioR2/60	eBioscience	CD4	RM4-5	BioLegend
CD44	IM7	eBioscience	CD19	6D5	BioLegend
CD62L	MEL-14	eBioscience	CD38	90	BioLegend
CD69	H1-2F3	eBioscience	CD138	281-2	BioLegend
CD80	16-10A1	eBioscience	Siglec-F	E50-2440	BioLegend
CD86	GL1	eBioscience	TCRβ	H57-597	BioLegend
c-kit	2B8	eBioscience	c-Rel	REA397	Miltenyi Biotec
c-Rel	1RELAH5	eBioscience	CAR	Rmcb	Millipore
GL7	GL7	eBioscience	CAR	sc-56892	Santa-Cruz
Gr1	RB6-8C5	eBioscience	F4/80	CI:A3-1	AbD serotec
ICOS/CD278	7E.17G9	eBioscience	IgM	polyclonal	Dianova
IgD	11-26c	eBioscience			
IgM	II/41	eBioscience			
IRF4	3E4	eBioscience			
Ki-67	SolA15	eBioscience			
MHC-II	M5/114.15.2	eBioscience			
PD-1/CD279	J43	eBioscience			
TCRβ	H57-597	eBioscience			

2.5 Primary mouse cell culture

Splenocytes or MACS-purified B cells – based on CD43⁺ cell depletion with a purity of >85-90% – were cultured in RPMI 1640 medium supplemented with 5% FCS, NEAA, sodium-pyruvate, HEPES, L-glutamine and penicillin/streptomycin (all Gibco). Stimuli were added at the following final concentrations: anti-IgM 10 $\mu\text{g}/\text{ml}$ (Jackson ImmunoResearch Laboratories), anti-CD40 4 $\mu\text{g}/\text{ml}$ (HM40-3, eBioscience), CpG 0.1 μM (InvivoGen), LPS 20 $\mu\text{g}/\text{ml}$ (Sigma-Aldrich). In order to prolong the survival of GC B cells in culture, the pan-caspase inhibitor Q-VD-OPh (R&D Systems) was added to the culture medium if indicated. For inhibition of the proteasome MG-132 (Z-Leu-Leu-Leu-al, Sigma-Aldrich) was applied at indicated concentrations.

2.6 Western blot

Whole cell lysates for protein extracts of defined cell numbers were prepared by incubation of cells for 30 min on ice in high salt whole lysis buffer (20 mM HEPES pH 7.9, 350 mM NaCl, 20% glycerol, 1 mM MgCl_2 , 0.5 mM EDTA pH 8, 1% NP-40) containing 1 mM DTT (dithiothreitol), 1 mM PMSF (phenylmethylsulfonylfluorid), 5 mM NaF (sodium fluoride), 1 mM Na_3VO_4 (sodium orthovanadate), 8 mM β -glycerophosphate, 10 $\mu\text{g}/\mu\text{l}$ leupeptin and 10 $\mu\text{g}/\mu\text{l}$ aprotinin. Protein samples were separated by sodium dodecyl sulfate polyacrylamide gel electrophoresis (SDS-PAGE) and blotted (both Bio-Rad system) to polyvinylidene fluoride (PVDF 0.45 μM , Immobilon-P, Millipore) membranes that were subsequently incubated with primary antibodies against c-Rel (sc-71, Santa-Cruz Biotechnology), PLC γ 2 (sc-407, Santa-Cruz Biotechnology) or flag (M2, HRP(horseradish peroxidase)-conjugated, Sigma-Aldrich) and HRP-conjugated secondary antibodies (Dianova). Blots were developed using a chemiluminescent HRP substrate (Immobilon Western, Millipore) and a digital imager (FLA 4000, GE Healthcare Life Sciences).

2.7 Immunization

Sheep red blood cells (SRBC, Oxoid Limited, Thermo Scientific) were washed three times in PBS, adjusted to 10^9 cells/ml in PBS and 100 μl per mouse were injected intraperitoneally. Mice were analyzed 10-12 days post-immunization.

2.8 ELISA

Enzyme-linked immunosorbent assay (ELISA) to detect IgA, IgG2b, IgG2c and IgG3 mouse serum antibody subclasses was performed using kits (Bethyl Laboratories) according to the manufacturer's instructions. For determination of IgM and IgG1 serum titers 96-well ELISA plates (Nunc MaxiSorp) were coated with anti-mouse λ/κ (goat anti-mouse lambda-UNLB and kappa-UNLB, Southern Biotech) and sample detection was based on anti-mouse IgG1-biotin (biotin rat anti-mouse IgG1, A85-1, BD Pharmingen) or IgM-biotin conjugate (biotin rat anti-mouse IgM, R6-60.2, BD Pharmingen) combined with streptavidin-HRP (Invitrogen). Absolute concentrations were calculated with reference to serial dilutions of mouse IgM κ or IgG κ isotype controls (BD Pharmingen). Assessment of anti-nuclear antibodies (ANA) and cardiolipin antibodies was based on kits (Varelisa Phadia) combined with anti-mouse IgG-HRP conjugate (goat anti-mouse IgG-HRP, Southern Biotech) for detection. For quantification of rheumatoid factor 96-well ELISA plates (Nunc MaxiSorp) were coated with rabbit IgG (Jackson ImmunoResearch Laboratories) and mouse serum Igs were detected applying IgG kit components (Bethyl Laboratories) or as described for IgM above. Tetramethylbenzidine (TMB) served as an HRP-substrate (BD OptEIA, BD Biosciences).

2.9 Data analysis, statistical evaluation and visualization

Flow cytometry data were analyzed with FlowJo (Treestar). For cell cycle analysis the FlowJo cell cycle platform selecting the Watson pragmatic model was applied. IDEAS (Amnis Cooperation) software was used for analysis of imaging flow cytometry data. In order to quantify nuclear translocation, data analysis was performed applying the nuclear translocation wizard of the IDEAS software. ImageJ [Schneider et al., 2012] was used for quantification of Western blot images. Calculations were performed in Excel (Microsoft). GraphPad Prism (GraphPad Software) and R [Raschka, 2013; R Core Team, 2016] were applied for graphical representation and statistical analysis. Where statistically significant results are indicated, p values are provided in figure legends. Adobe Illustrator (Adobe Systems) was employed for data presentation and figure preparation. This thesis was typeset with L^AT_EX.

3 Manipulation of human B cell lymphoma cell lines

3.1 Generation of shRNA constructs by Golden Gate cloning

In the present thesis, transposon-based expression constructs that allow the induction of shRNAs by the tetracycline repressor (tetR)/doxycycline system were applied [Kleinhammer et al., 2011]. For this approach, constitutive expression of the tetR by a CAG promoter and inducible shRNA expression under the control of an H1 promoter containing a tet operator (tetO) sequence were combined on the same DNA construct. Additionally, these constructs carry a puromycin-resistance-2A-Thy1.1-cassette linked to CAG-controlled tetR expression by an IRES sequence which allows stable selection and expression of the surface marker Thy1.1 connected via a self-cleaving 2A site [Szymczak et al., 2004; Kim et al., 2011]. The transposases hyperactive piggyBac (hyPB) and sleeping beauty (sb100x) were used to facilitate stable genomic integration of the shRNA constructs [Mátés et al., 2009; Yusa et al., 2011]. In order to enable highly efficient insertion of shRNAs using Golden Gate cloning that is based on a single restriction-ligation reaction [Engler et al., 2008, 2009; Engler and Marillonnet, 2011], modifications of the knockdown construct were introduced by CloneEZ PCR Cloning Kit (GenScript) and Golden Gate cloning techniques. Sequences of shRNAs used in the present study are listed in Table 4.

Table 4: shRNA knockdown sequences. Sequences of shRNAs used for knockdown in this thesis are listed. shRNAs targeting c-Rel [Barbie et al., 2009; Meylan et al., 2009] and controls [Barbie et al., 2009; Cheung et al., 2011] have been published previously.

Designation	Sequence
shcRel 1	GCCTCATCCTCATGATTTA
shcRel 2	CCAGGAAGTTAGTGAATCTAT
shcRel 3	CTTCAGTTGTGCAGATAACAG
shGFP 1	AAGCTGGAGTACAACTACAT
shGFP 2	ACAACAGCCACAACGTCTATA
shLacZ	TCGTATTACAACGTCGTGACT

3.2 Cell culture: transfection, selection and induction

The PMBCL cell lines MedB-1 and Karpas1106 as well as the cHL cell lines L-428 and U-HO1 were maintained in RPMI 1640 medium (Gibco) supplemented with 20% FCS, sodium-pyruvate, HEPES, L-glutamine and penicillin/streptomycin (all Gibco) at 37 °C,

5% CO₂.

For the generation of stable cell pools carrying the shRNA knockdown constructs, cell lines were transfected and subsequently subjected to antibiotic selection. The cHL lymphoma cell lines were transfected using Amaxa Nucleofector technology (Lonza), while for the PMBCL cell lines suitable transfection conditions were established using the Neon transfection system (Invitrogen, Thermo Fisher Scientific). Detailed information is provided in Table 5.

Knockdown constructs were co-transfected with PGK(phosphoglycerate kinase)-sb100x or CMV(cytomegalovirus)-hyPB transposase expression plasmids at ratios of 1:10 or 1:3. Stable cell pools were selected using appropriate puromycin (InvivoGen) concentrations. In part, independent cell pools were generated for the same knockdown construct. For induction of shRNA expression, cells were counted and seeded in medium containing doxycycline (Sigma-Aldrich) at indicated concentrations.

Table 5: Transfection. Transfection methods for human lymphoma cell lines.

Cell line	System	cell number	DNA	Parameters
MedB-1	Neon	2.5x10 ⁶	10 μ g	100 μ l buffer R, pulse: 1400 V, width 10 ms, # 3
Karpas1106P	Neon	2.5x10 ⁶	10 μ g	100 μ l buffer R, pulse: 1500 V, width 10 ms, # 3
L-428	Amaxa	2x10 ⁶	5 μ g	100 μ l buffer V, T13
U-HO1	Amaxa	2x10 ⁶	5 μ g	100 μ l buffer V, X-001

3.3 Western blot

Whole cell lysates for protein extracts were prepared by incubation of cells for 30 min on ice in RIPA buffer (50 mM Tris pH 7.5, 0.25% sodium deoxycholate, 150 mM NaCl, 1% NP-40) containing 1 mM DTT, 1 mM PMSF, 5 mM NaF, 1 mM Na₃VO₄, 8 mM β -glycerophosphate, 10 μ g/ μ l leupeptin and 10 μ g/ μ l aprotinin. Protein concentrations were determined using the Pierce BCA (bicinchoninic acid assay) protein assay kit (Thermo Fisher Scientific) according to the manufacturer’s instructions. Protein samples of defined amounts were separated by SDS-PAGE and blotted (both Bio-Rad system) to PVDF (0.45 μ M, Immobilon-P, Millipore) membranes that were subsequently incubated with primary antibodies against c-Rel (sc-71, Santa-Cruz Biotechnology) and tubulin (MAB1864, YL1/2, Millipore) and HRP-conjugated secondary antibodies (Dianova). Blots were developed using a chemiluminescent HRP substrate (Immobilon Western, Millipore) and a

digital imager (FLA 4000, GE Healthcare Life Sciences).

3.4 Flow cytometry

Cells were harvested, washed and single cell suspensions were stained using primary antibodies against Thy1.1 (HIS51) and c-Rel (1RELAH5) (eBioscience). For intracellular stainings the FoxP3/transcription factor staining buffer set (eBioscience) was applied according to the manufacturer's instructions. 7-AAD staining solution (eBioscience) or live/dead fixable near-IR dead cell staining kit (Invitrogen) were used for discrimination of viable cells. Doublets were excluded based on FSC-H/A and SSC-W/A characteristics. Samples were acquired on FACS Calibur and FACS Canto II (BD Biosciences) flow cytometers.

3.5 Cell count assay

Cells in medium containing 0.5 or 1 $\mu\text{g}/\text{ml}$ doxycycline or without doxycycline were seeded in triplicates into a 96-well-plate. Assessment of viable cell numbers was performed every day or every second day following treatment start using a Guava ViaCount (Guava Technologies, Merck Millipore). Discrimination of viable cells was based on staining cells with propidium iodide (PI, Sigma-Aldrich) and LDS751 (Invitrogen).

3.6 Competitive co-culture assay

Equal numbers of the unmodified original cell line (MedB-1, L-428) and cell pools derived from that original cell line stably expressing knockdown constructs were seeded in medium with 0.5 $\mu\text{g}/\text{ml}$ doxycycline or without doxycycline at day 0 for defined time periods. Ratios of Thy1.1-expressing and non-Thy1.1-expressing cells were assessed by flow cytometry-based surface staining (3.4) starting from day 1 and every second following day until day 11.

3.7 Cell cycle analysis

For cell cycle analysis, cells were treated with 0.5 $\mu\text{g}/\text{ml}$ doxycycline or left untreated for defined time periods. After harvesting and washing cells in PBS, cells were resuspended in 300 μl PBS and 700 μl ethanol were added dropwise while slowly vortexing the cell

suspension to achieve a final concentration of 70% ethanol. Samples were placed at 4 °C for 60 min or overnight. For longer storage periods, the cell suspension was stored at -20 °C. After incubation, cells were pulse centrifuged followed by regular centrifugation, washed in PBS and resuspended in staining solution containing 50 $\mu\text{g}/\text{ml}$ PI (Sigma-Aldrich) and 100 $\mu\text{g}/\text{ml}$ ribonuclease A (RNase A, Sigma-Aldrich). After incubation for 30 min at 37 °C, cells were directly acquired on a FACS Canto II (BD Biosciences) flow cytometer.

3.8 Active caspase assay

For assessing apoptotic cell death, the CaspGlow active caspase staining kit (fluorescein, BioVision) was applied. Cells were treated for 4 d with 0.5 $\mu\text{g}/\text{ml}$ doxycycline or left untreated. For active caspase detection, cells were stained with FITC-VAD-FMK in RPMI supplemented with 1% FCS (Gibco) for 60 min at 37 °C. Cells were washed twice in wash buffer provided in the kit and the procedure was continued as described for flow cytometry (3.4).

3.9 Data analysis and visualization

Data analysis and representation was performed using the same software as listed for methods of generation and characterization of mouse lines (2.9).

Part IV

Results

1 The first conditional c-Rel transgenic mouse models to investigate enhanced c-Rel function in B cells

1.1 Generation of novel c-Rel transgenic mouse lines

I used bacterial artificial chromosome (BAC) transgenesis for generation of conditional c-Rel transgenic mouse lines. Several modifications of a BAC lacking other genes than the endogenous mouse *REL* genetic locus were performed (Figure 5A). To drive strong transgene expression on a conditional Cre recombinase-mediated basis, a CMV early enhancer/chicken β actin (CAG)-promoter followed by a loxP-site-flanked neomycin/kanamycin-resistance stop cassette was inserted upstream of an HA-tag added to the first translated *REL* exon. Exon 9 was flanked with Flp recombinase-recognizable Frt sites. At the carboxy-terminal part of *REL*, a 3xflag-IRES-hygromycin-resistance cassette was inserted to enable selection of the intact modified locus. In addition, a second version based on the same construct allowing expression of a GFP-c-Rel fusion protein was generated. The BAC constructs were electroporated into C57BL/6 ES cells and neomycin resistant clones were selected, isolated, expanded and stored essentially as published [Schmidt-Supprian et al., 2000]. ES cell clones were verified for functional c-Rel or GFP-c-Rel protein expression upon Cre-transduction and for carrying single BAC integrants quantified by Southern blot (Figure 5B-D). Suitable ES cell clones were injected into blastocysts for chimera generation and germline transmission was obtained resulting in 3 transgenic mouse strains: 2 c-Rel and 1 GFP-c-Rel mouse line. Conditional GFP-c-Rel transgenic mice were crossed to the CD19Cre mouse line [Rickert et al., 1997] for B cell-specific GFP-c-Rel transgene expression and further functional validation. As expected [Schmidt-Supprian et al., 2007], transgenic GFP-c-Rel expression is induced with B cell maturation in the bone marrow and spleen of GFP-c-Rel CD19Cre^{I/+} (I, insertion; +, wild-type) mice, but GFP-c-Rel is not expressed in T cells (Figure 6A and 6B) or other cell types. GFP-c-Rel is expressed in mature B cell subtypes in immune organs, including spleen, lymph nodes, mesenteric lymph nodes, Peyer's patches, peritoneal cavity as well as thymus (Figure 6C).

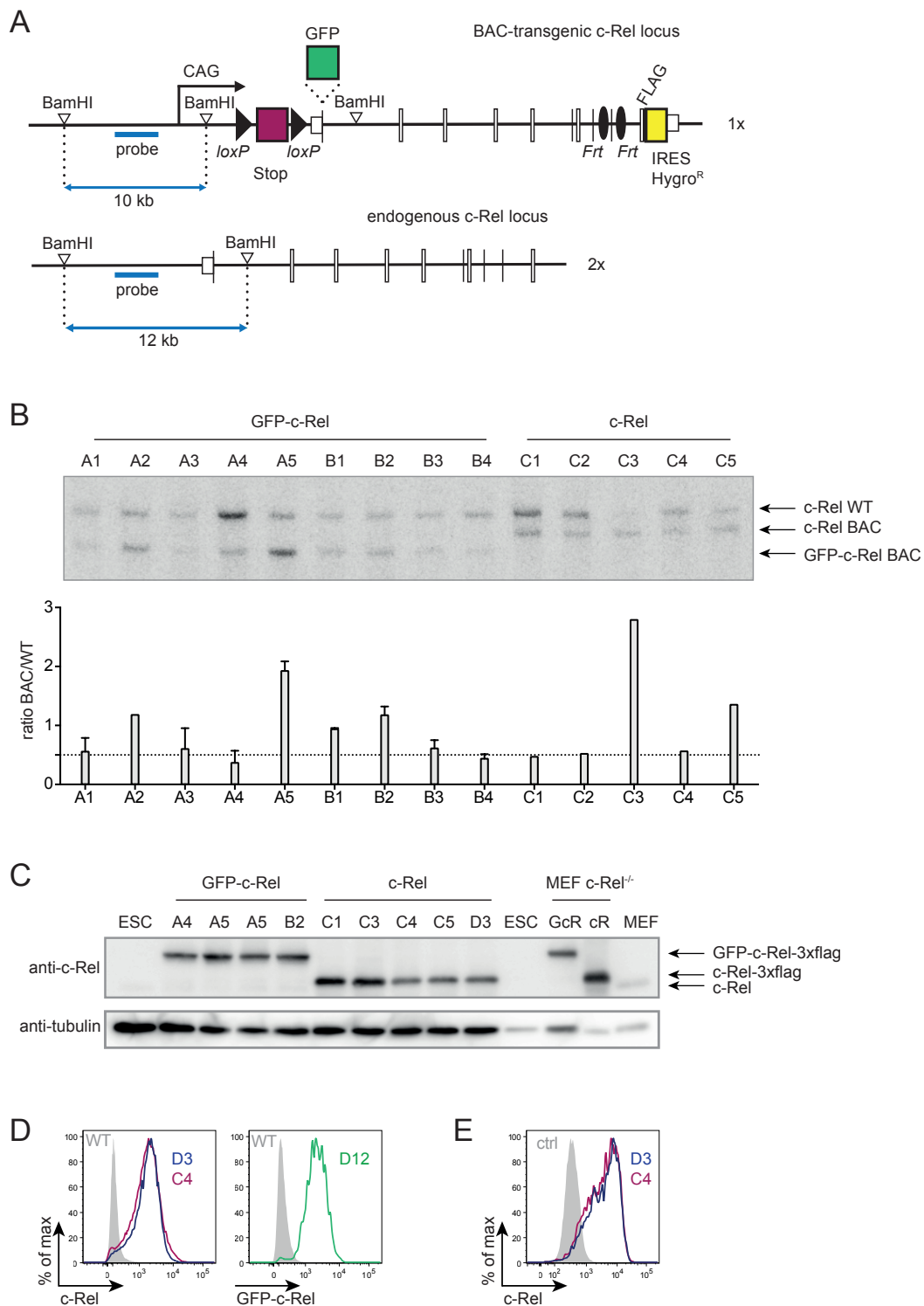


Figure 5: Strategy and generation of novel *c-Rel* transgenic mouse models. (A) The endogenous and transgenic *REL* loci are depicted. The highlighted *c-Rel* Southern blot probe (blue) recognizes differentially sized fragments within the endogenous locus and the BAC-transgenic locus upon BamHI digest of genomic DNA. (B) Representative Southern blot image and quantification of integrations for the depicted clones. For single integration of the BAC transgenic locus, a ratio of BAC to wild-type (WT) fragment of 0.5 is expected. (C) Western blot and (D) flow cytometry analyses of transgenic *c-Rel* and GFP-*c-Rel* in representative ES cell clones. ES cell clones were transduced with Cre recombinase and subsequently selected with hygromycin B. For comparison, BAC-transfected MEF *c-Rel*^{-/-} cells and wild-type (WT) MEFs were loaded on the SDS-PAGE gel for Western blot. (E) Flow cytometry analysis of *c-Rel* expression in *in vitro* Cre recombinase-transduced and hygromycin B-selected mouse tail tip fibroblasts of the two germline transmitted *c-Rel* clones and untransduced control mouse tail tip fibroblasts. GcR, GFP-*c-Rel*; cR, *c-Rel*; ESC, embryonic stem cell; MEF, mouse embryonic fibroblast; ctrl, control.

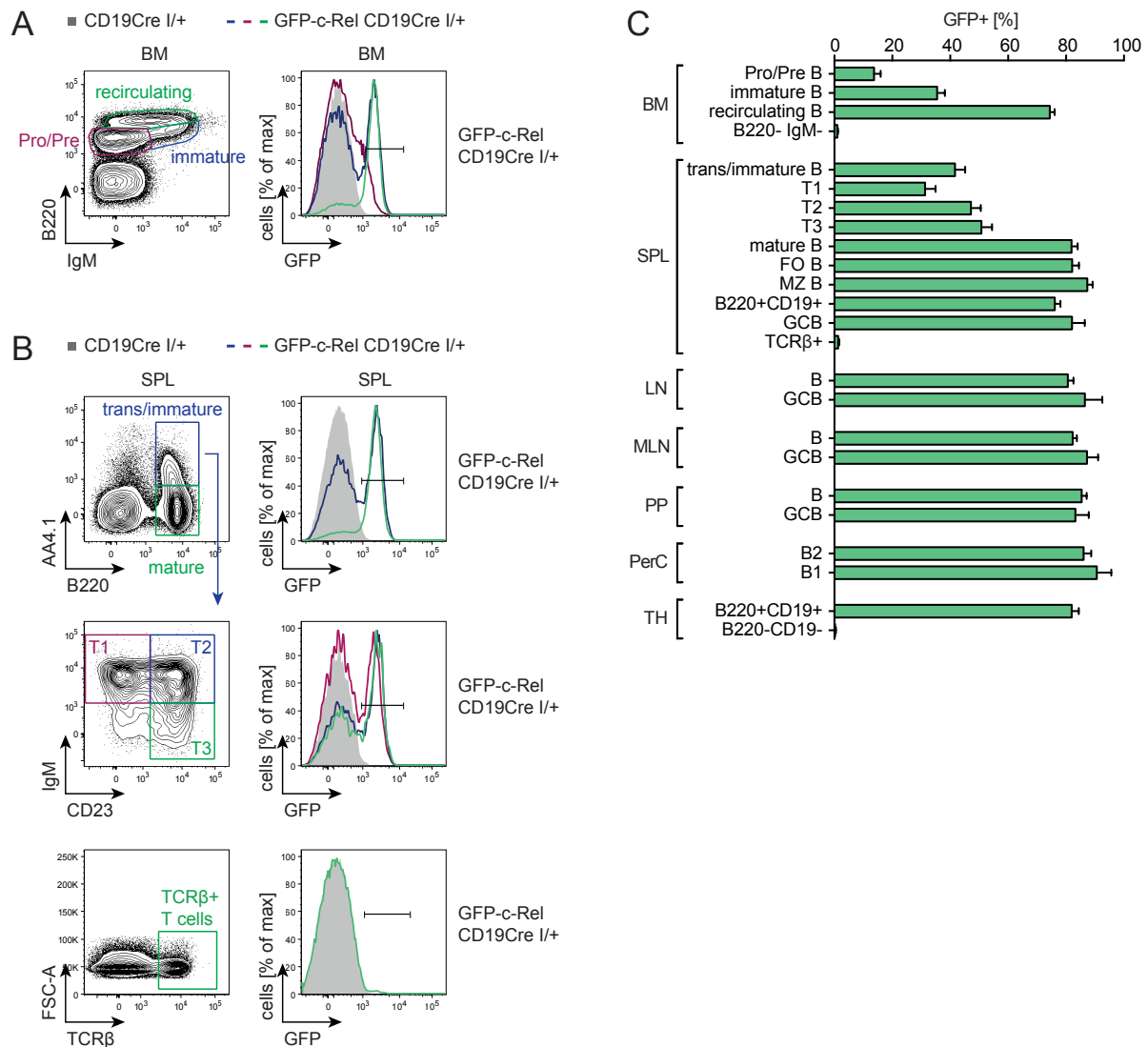


Figure 6: GFP-c-Rel is expressed in B cells upon CD19Cre-mediated stop cassette excision.

Representative flow cytometry plots and histograms for GFP-c-Rel expression in (A) bone marrow and (B) spleen. The color code of the flow cytometry plots gating strategy corresponds to colored lines in the respective histograms. (C) GFP-c-Rel expression in different B cell subsets and mouse organs. Bone marrow (BM): Pro/Pre B220⁺IgM⁻; immature B220^{low}IgM⁺; recirculating/mature B220^{high}IgM⁺. Spleen (SPL): transitional/immature B cells B220⁺AA4.1⁺; transitional 1 (T1) B220⁺AA4.1⁺IgM^{high}CD23⁻; transitional 2 (T2) B220⁺AA4.1⁺IgM^{high}CD23⁺; transitional 3 (T3) B220⁺AA4.1⁺IgM^{low}CD23⁺; mature B cells B220⁺AA4.1⁻; follicular (FO) B220⁺AA4.1⁻CD1d^{int}CD21^{int}; marginal zone (MZ) B220⁺AA4.1⁻CD1d^{high}CD21^{high}; GCB CD19⁺/B220⁺CD95^{high}CD38^{low}. Lymph nodes (LN), mesenteric lymph nodes (MLN), Peyer's patches (PP): B CD19⁺/B220⁺; GCB CD19⁺/B220⁺CD95^{high}CD38^{low}. Peritoneal cavity (PerC): B2 CD19⁺B220^{high}; B1 CD19⁺B220^{low}. TH, thymus; FSC-A, forward scatter area.

1.2 Developmental and naive mature B cell physiology is largely unaltered

Initial analyses of conditional *c-Rel* transgenic mice of the 3 germline-transmitted clones crossed to the CD19Cre mouse line showed that in the B lineage *c-Rel* protein expression levels slightly differ for these clones, despite comparable *c-Rel* levels in ES cells and tail-tip fibroblasts (Figure 5D-E). While the two *c-Rel* clones are characterized on average by a high or intermediate *c-Rel* protein level, respectively, mice of the GFP-*c-Rel* line express total *c-Rel* levels comparable with the intermediate *c-Rel* line. The extent of *c-Rel* expression is discussed in detail in subsection 1.7. To investigate the consequences of *c-Rel* overexpression, I focused on analyzing conditional *c-Rel* transgenic mice of the high *c-Rel* level-expressing clone in this thesis. These *c-Rel* CD19Cre^{I/+} mice are compared to heterozygous CD19Cre^{I/+} littermate controls for all subsequent analyses.

Young mice develop normal and do not show alteration in weight when sacrificed for analysis of general immune organs by flow cytometric characterization at an age of 8-16 weeks (Figure S1). B cell lymphopoiesis in the bone marrow of *c-Rel*CD19Cre^{I/+} mice is unaltered (Figure S2A). No significant difference in spleen weight was observed and immature and mature splenic B cell numbers are not changed. However, within the immature transitional B cell subsets there is a trend for a lower percentage and cell number of transitional 1 (T1) B cells accompanied by slightly higher percentages and cell numbers of T2 and T3 subsets (Figure 7A). There is no difference with regard to mature follicular (FO) or marginal zone (MZ) B cells (Figure 7B). Within the marginal zone subset of B cells one can distinguish CD23^{high} MZ precursor cells. There is a trend for a higher frequency and cell number of these MZ precursor cells in *c-Rel*CD19Cre^{I/+} mice. Both transitional as well as MZ precursor B cell subsets rely on gating on CD23. Quantification of CD23 surface expression demonstrates that CD23 levels are in general enhanced in both immature and mature B cells of *c-Rel*CD19Cre^{I/+} mice (Figure 7). Accordingly, the observed trends in transitional and MZ B cell subsets could be a consequence of differential CD23 expression. In addition, no significant changes were observed in B cells of the peritoneal cavity (Figure S2B) or thymic B cells (Figure S3).

Interestingly, while splenic lymphocyte and B cell numbers are equal, there is a trend for higher lymphocyte and B cell numbers in lymph nodes and gut-associated mesenteric lymph nodes and the lymphoid follicle structures known as Peyer's patches (Figure 9).

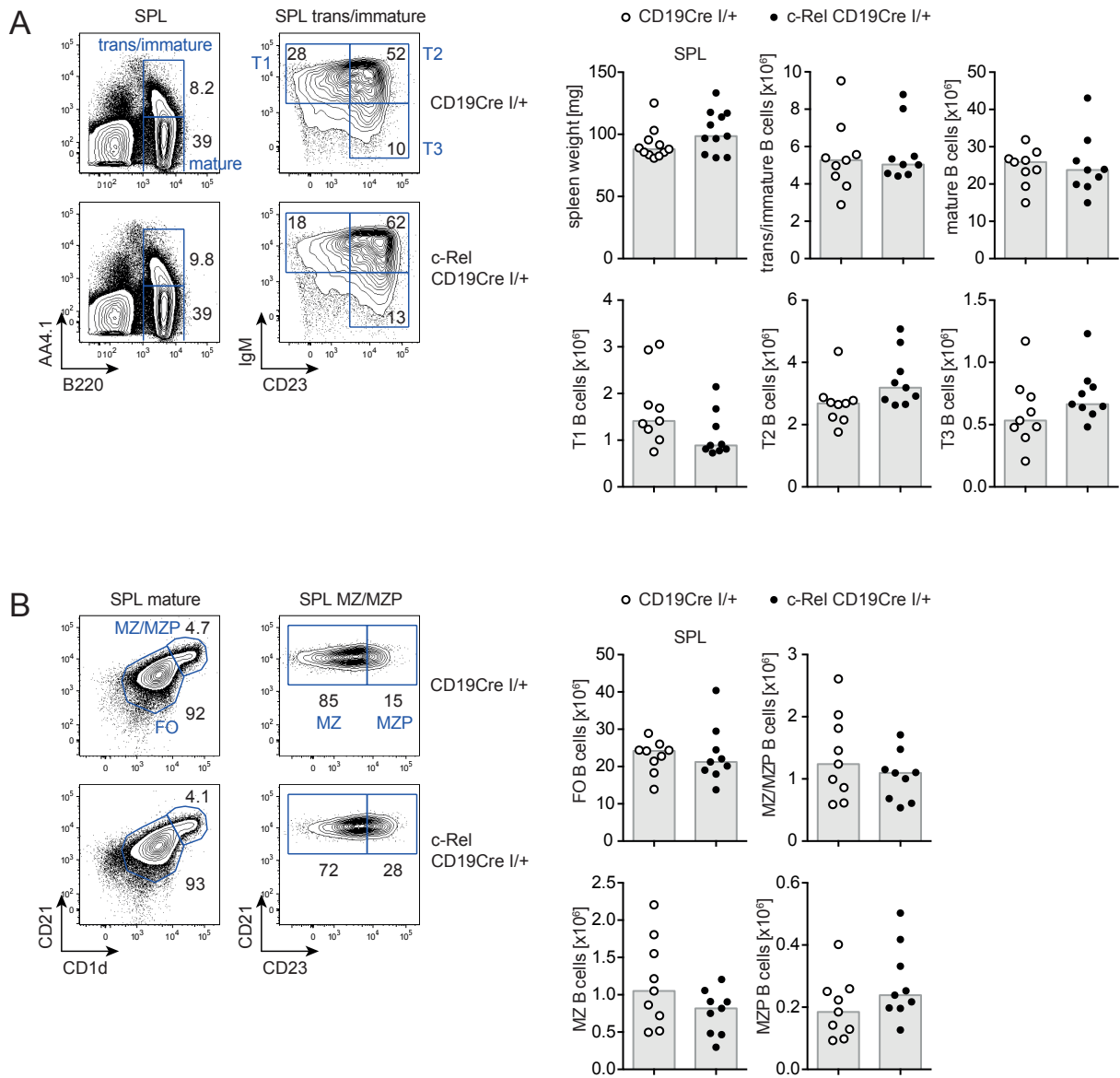


Figure 7: Splenic B cells of *c-Rel CD19Cre^{I/+}* mice. (A, B) Representative flow cytometry plots illustrating the gating strategy for immature and mature splenic (SPL) B cell subsets. Numbers within plots are median percentages calculated from the same dataset considered for bar graph representation of cell numbers for the respective B cell subsets where individual data points are plotted and bars are median values. Data were obtained in ≥ 3 independent experiments. B cell subsets: transitional/immature $B220^+AA4.1^+$; mature $B220^+AA4.1^-$; transitional 1 (T1) $B220^+AA4.1^+IgM^{high}CD23^-$; transitional 2 (T2) $B220^+AA4.1^+IgM^{high}CD23^+$; transitional 3 (T3) $B220^+AA4.1^+IgM^{low}CD23^+$; follicular (FO) $B220^+AA4.1^-CD1d^{int}CD21^{int}$; marginal zone (MZ/MZP) $B220^+AA4.1^-CD1d^{high}CD21^{high}$; MZ precursor (MZP) $B220^+AA4.1^-CD1d^{high}CD21^{high}CD23^{high}$; MZ $B220^+AA4.1^-CD1d^{high}CD21^{high}CD23^{low}$.

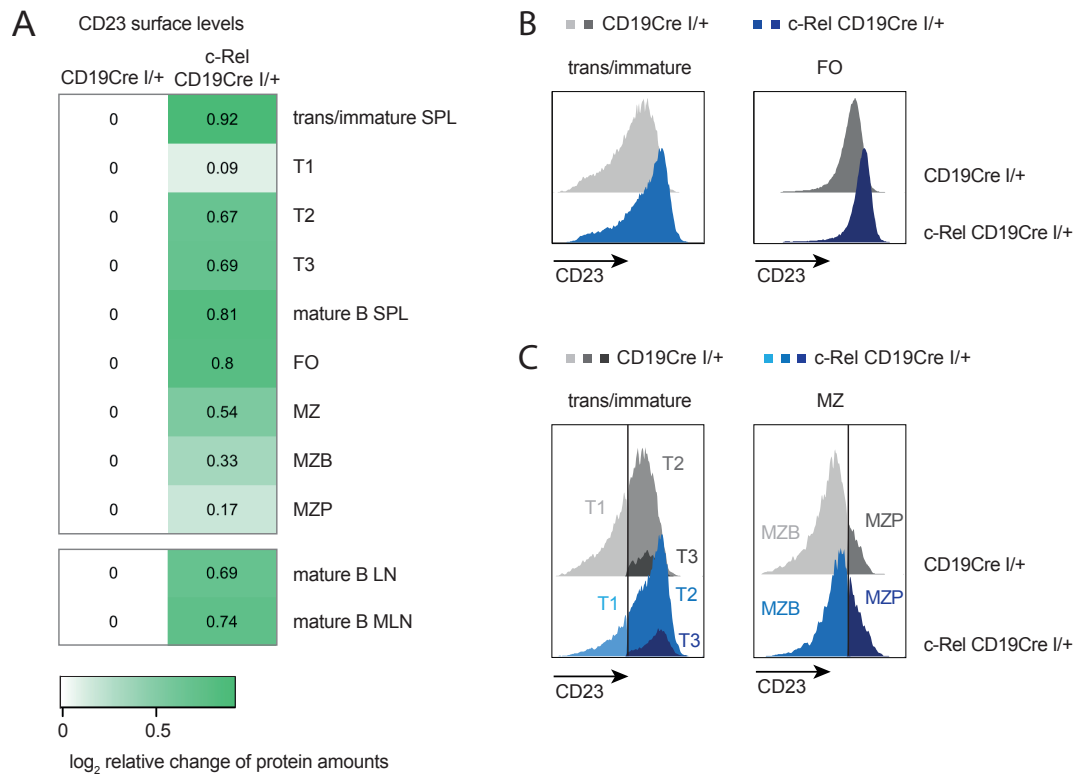


Figure 8: Enhanced CD23 expression in c-Rel CD19Cre^{I/+} mice. (A) Heatmap representation of CD23 surface expression in indicated B cells subsets of spleen (upper part) and lymph nodes and mesenteric lymph nodes (lower part). The log₂ relative change values of geometric means normalized to CD19Cre^{I/+} controls are represented according to the displayed color scale. (B, C) Representative flow cytometry histograms illustrating CD23 expression in indicated splenic B cell populations. The black vertical line in (C) represents the flow cytometry gate for immature or marginal zone B cell subpopulations. Data were obtained in ≥ 3 independent experiments and are representative for 5 (LN, MLN) to 9 (SPL) mice per genotype. Gating and abbreviations of subpopulations as listed in Figure 7. SPL, spleen; LN, lymph nodes; MLN, mesenteric lymph nodes.

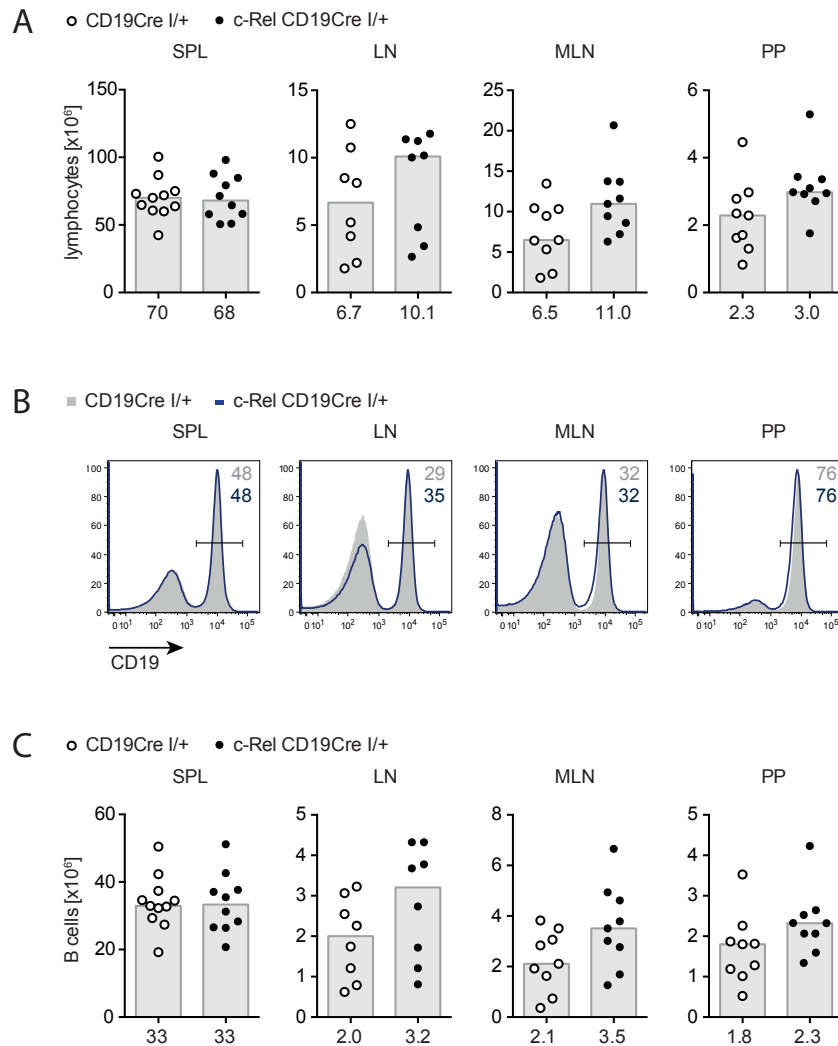


Figure 9: B cells in peripheral mouse immune organs. (A) Total lymphocyte cell numbers for indicated immune organs. Flow cytometry-based analysis of (B) B cell percentages displayed in representative histograms and (C) B cell numbers in bar graphs. Individual data points obtained in ≥ 3 independent experiments are plotted. Bars and numbers below graphs are median values. SPL, spleen; LN, lymph nodes; MLN, mesenteric lymph nodes; PP, Peyer's patches.

1.3 c-Rel overexpression causes expansion of GC B cells and plasma cells

1.3.1 Expansion of germinal center B cells

As the developmental and naive mature B cell physiology is largely unaltered in c-Rel CD19Cre^{I/+} mice, I further investigated post-activation and terminal differentiated B cell stages. Remarkably, spontaneous germinal center (GC) B cells are substantially expanded in young, naive c-Rel CD19Cre^{I/+} mice. Both GC B cell percentages and numbers are significantly higher in peripheral immune organs, including spleen, lymph nodes, mesenteric lymph nodes and Peyer's patches (Figure 10A-C). For these central experiments c-Rel mice not carrying the CD19Cre allele were included as additional controls to exclude an influence of BAC locus integration site.

To further characterize the c-Rel transgenic GC B cells, I quantified intracellular expression of the pivotal GC B cell transcription factor Bcl-6 [Victora and Nussenzweig, 2012]. Bcl-6 protein levels are indistinguishable in c-Rel CD19Cre^{I/+} and CD19Cre^{I/+} control mice, demonstrating that these cells are valid GC B cells (Figure 10D). Moreover, these c-Rel CD19Cre^{I/+} GC B cells are positive for stainings with the GC B cell markers GL7 and PNA as expected (Figure S4). GC B cells are polarized into dark zone (DZ) centroblasts and light zone (LZ) centrocytes that can be distinguished by surface expression of CXCR4 and CD86. DZ GC B cells are CXCR4^{high}CD86^{low}, while LZ GC B cells are CXCR4^{low}CD86^{high} [Victora et al., 2010]. c-Rel CD19Cre^{I/+} GC B cells show a DZ/LZ marker expression pattern comparable to CD19Cre^{I/+} controls, albeit with a trend for a higher proportion of LZ GC B cells in c-Rel transgenic GCs resulting in a lower DZ/LZ ratio (Figure 11).

Analysis of various cell surface activation markers on directly *ex vivo* isolated B cells did not reveal significant differences between c-Rel CD19Cre^{I/+} and CD19Cre^{I/+} controls (Figure S5A). Also upon over night stimulation with anti-IgM, anti-CD40, CpG or LPS, activation markers are comparably upregulated on purified B cells isolated from c-Rel CD19Cre^{I/+} and CD19Cre^{I/+} control mice. Only MHC-II levels are marginally higher in c-Rel CD19Cre^{I/+} mice (Figure S5B). The similar activation marker expression provides evidence that B cells in c-Rel CD19Cre^{I/+} mice are not generally hyperactivated, but that the observed phenotype selectively affects GC B cells.

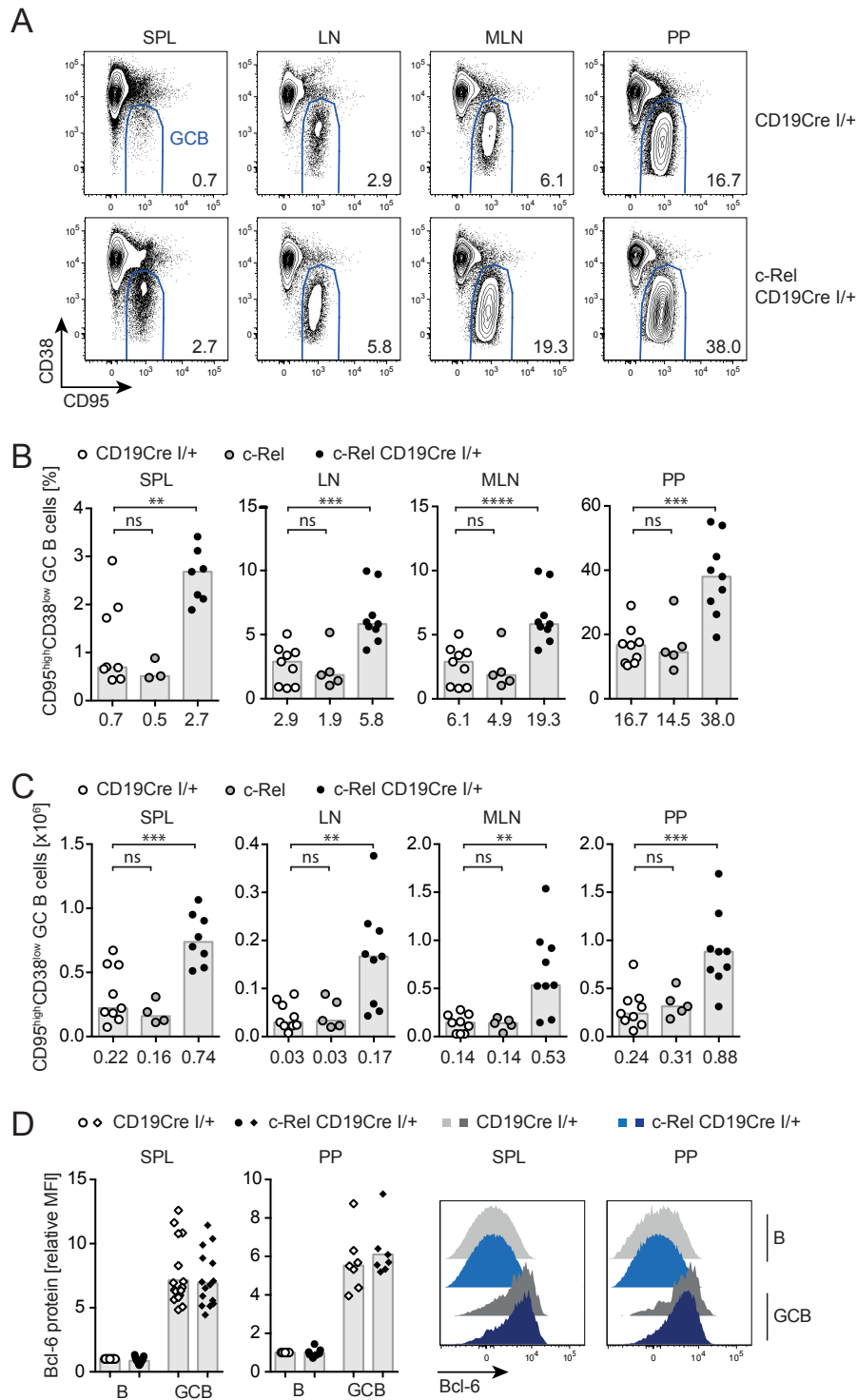


Figure 10: Expansion of GC B cells in c-Rel CD19Cre^{I/+} mice. (A) Representative flow cytometry plots of GC B cells. Numbers are median percentages of GC B cells of total B cells. (B) Percentages of GC B cells of total B cells and (C) GC B cell numbers. Individual data points obtained in ≥ 3 independent experiments are plotted. Bars and numbers below graphs are median values. (D) Intracellular flow cytometry data of Bcl-6 protein levels in GC B cells normalized to the non-GC B cell population of CD19Cre^{I/+} controls. Representative histograms illustrate the bar graphs for which the geometric mean and individual data points obtained in ≥ 3 independent experiments are plotted. not significant (ns) $p > 0.05$, ** $p \leq 0.01$, *** $p \leq 0.001$, **** $p \leq 0.0001$, one-way ANOVA. GCB CD19⁺/B220⁺CD95^{high}CD38^{low}; B (non-GCB) CD19⁺/B220⁺CD95^{high}CD38^{high}; SPL, spleen; LN, lymph nodes; MLN, mesenteric lymph nodes; PP, Peyer's patches.

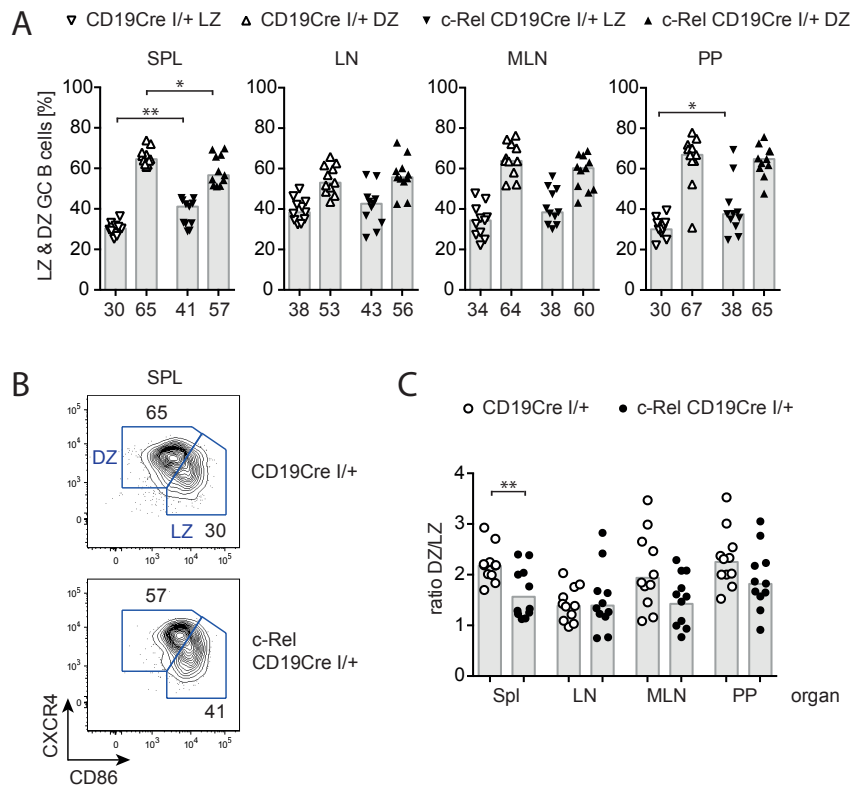


Figure 11: Frequencies of dark zone and light zone GC B cells. (A) Frequencies of dark zone (DZ) and light zone (LZ) GC B cells. Individual data points obtained in 4 independent experiments are plotted. Bars and numbers below graphs are median values. (B) Representative flow cytometry plots of LZ and DZ GC B cells in spleen. Numbers are median percentages. (C) Ratio of DZ and LZ GC B cell frequencies of data set displayed in (A). Individual data points and bars representing geometric means are plotted. * $p < 0.05$, ** $p < 0.01$, unpaired t test. GCB $CD19^+/B220^+CD95^{high}CD38^{low}$; DZ $CXCR4^{high}CD86^{low}$; LZ $CXCR4^{low}CD86^{high}$; SPL, spleen; LN, lymph nodes; MLN, mesenteric lymph nodes; PP, Peyer's patches.

1.3.2 Activated T cells

I found that B cell-specific c-Rel transgene expression has small effects on distinct T cell subpopulations *in vivo*. While frequencies of CD4⁺ and CD8⁺ T cell populations are largely unaltered in c-Rel CD19Cre^{I/+} mice, there is a trend for a lower proportion of central memory like (CML) and higher percentages of effector memory like (EML) T cells within the CD4⁺ and CD8⁺ T cell subsets (Figure 12A and 12B and Figure S6-S10). This trend also translates into elevated effector memory like T cell numbers (Figure 12C and Figure S6C, S8 and S10). In lymph nodes and mesenteric lymph nodes, numbers of CD4⁺CD25⁻ and CD8⁺ as well as CD4⁺CD25⁺ T cells including the regulatory T cell (T_{reg}) pool are generally increased (Figure S7 and S9) reflecting the trend for higher total lymphocyte cell numbers observed in c-Rel CD19Cre^{I/+} mice (Figure 9).

Moreover, specialized follicular helper T cells (T_{fh}) of the GC are consistently expanded in c-Rel CD19Cre^{I/+} mice, although reaching a statistical significant extent only in lymph nodes (Figure 13A and 13B). T_{fh} cells are characterized by high expression of ICOS that is slightly augmented in T_{fh} cells of c-Rel CD19Cre^{I/+} mice (Figure 13C and 13D). A similar tendency is in part observed for the activation marker CD69 (Figure S11). These findings indicate that T cells are not strongly activated in c-Rel CD19Cre^{I/+} mice in general, while the moderately elevated T_{fh} cell population could be secondary to the significantly expanded GC B cell phenotype in particular.

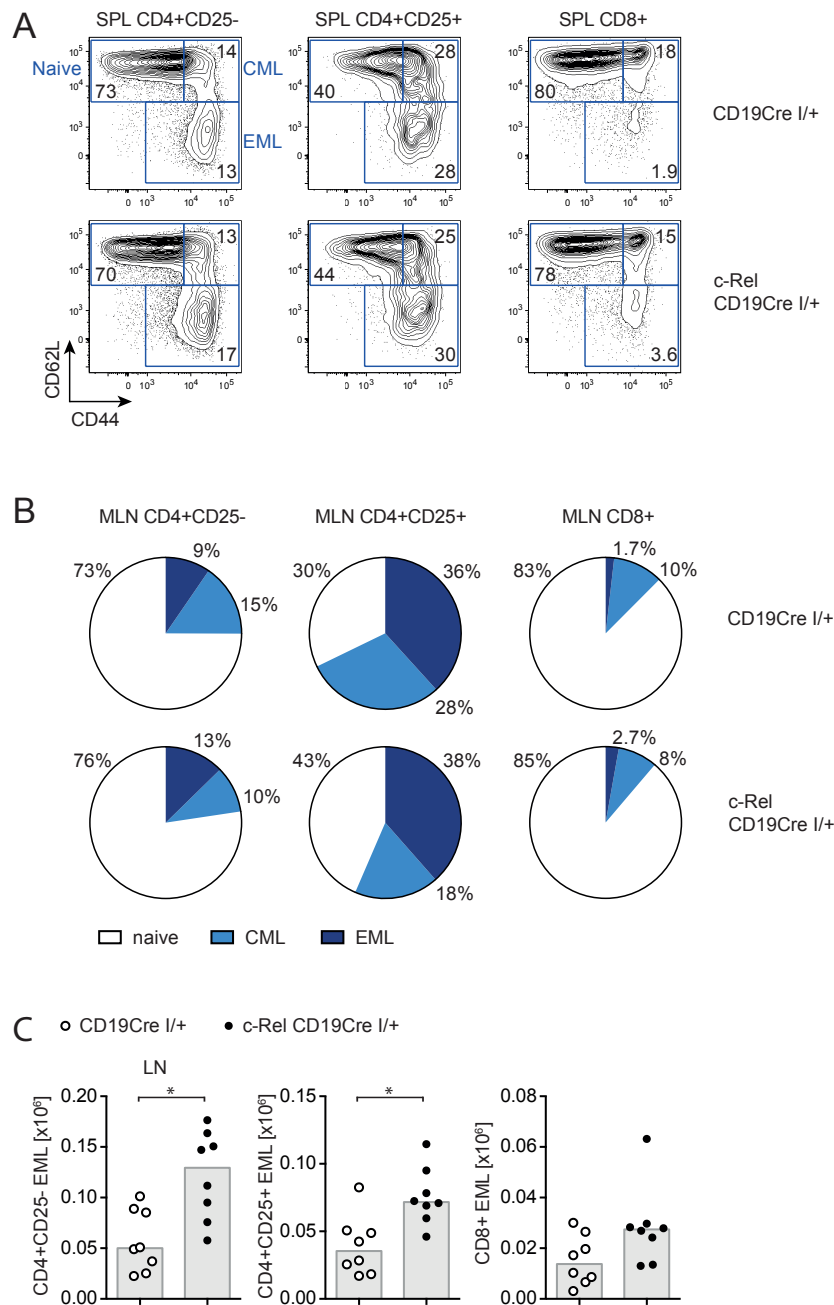


Figure 12: T cell subsets in c-Rel CD19Cre^{I/+} mice. (A) Representative flow cytometry plots illustrating CD44 and CD62L expression of splenic T cell subsets (all pre-gated on TCR β^+ and CD8/CD4 or CD4/CD25 as indicated) representing naive (CD44^{int}CD62L^{high}), central memory like (CML, CD44^{high}CD62L^{high}) and effector memory like (EML, CD44^{high}CD62L^{low}) T cells. Numbers are median percentages. (B) Median frequencies of naive, CML and EML T cells within T cell subsets in mesenteric lymph nodes. (C) Lymph node EML T cell numbers within indicated T cell subsets. Individual data points obtained in 3 independent experiments are plotted. Bars represent median values. * $p \leq 0.05$, unpaired t test. SPL, spleen; LN, lymph nodes; MLN, mesenteric lymph nodes.

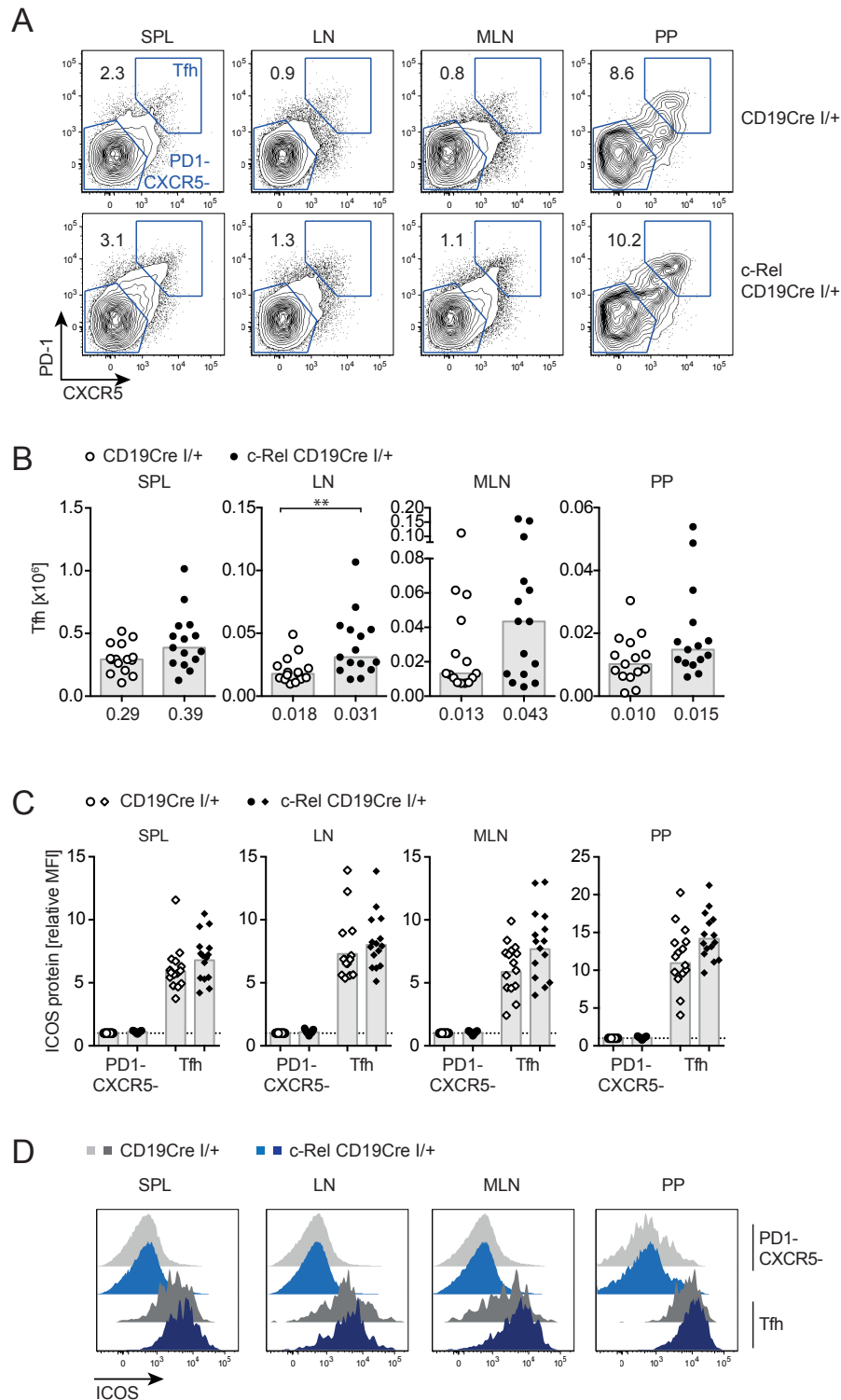


Figure 13: Expansion of T_{fh} cells in $c\text{-Rel CD19Cre}^{I/+}$ mice. (A) Representative flow cytometry plots of follicular helper T cells (T_{fh}). Numbers are median percentages of $PD-1^{\text{high}}CXCR5^{\text{high}}$ T_{fh} cells of $TCR\beta^+CD4^+$ T cells. (B) T_{fh} cell numbers. Individual data points obtained in 6 independent experiments are plotted. Bars and numbers below graphs are median values. (C) Flow cytometry data of ICOS protein levels in T_{fh} cells normalized to the non- T_{fh} cell population of $CD19Cre^{I/+}$ controls. Geometric mean and individual data points obtained in 6 independent experiments are plotted. (D) Representative histograms illustrate the bar graphs shown in (C). ** $p \leq 0.01$, unpaired t test. T_{fh} $TCR\beta^+CD4^+PD-1^{\text{high}}CXCR5^{\text{high}}$, non- T_{fh} $TCR\beta^+CD4^+PD-1^{\text{high}}CXCR5^{\text{low}}$; SPL, spleen; LN, lymph nodes; MLN, mesenteric lymph nodes; PP, Peyer's patches.

1.3.3 Expansion of class-switched plasma cells

During B cell terminal differentiation, GC B cells can give rise to plasma cells [Nutt et al., 2015]. Remarkably, plasmablasts or plasma cells are expanded two-fold in both spleen and bone marrow of *c-Rel* CD19Cre^{I/+} mice (Figure 14A and 14B). The protein expression level of two central mediators of plasma cell fate, IRF4 and Blimp-1, is comparable in *c-Rel* CD19Cre^{I/+} and CD19Cre^{I/+} control mice, thus validating the plasma cell identity of this expanded population (Figure 14C and 14D).

Analysis of plasma cell immunoglobulin (Ig) subtypes revealed that *c-Rel* transgenic plasma cells are largely class-switched. The proportion of unswitched IgM-expressing plasma cells is significantly lower than in controls, whereas the frequency of switched IgA- and IgG1-positive plasma cells is dramatically increased. Especially IgG1-expressing plasma cells are almost not detectable in CD19Cre^{I/+} control mice ($\leq 0.5\%$), but reach 7.4% and 10% in spleen and bone marrow of naive *c-Rel* CD19Cre^{I/+} mice, respectively. In contrast, the percentage of the plasma cell population expressing IgG3 is reduced in *c-Rel* CD19Cre^{I/+} mice (Figure 15A and 15B). The higher percentage of class-switched plasma cells corresponds to increased serum Ig titers of IgG1, IgG2c, IgG2b and to a lesser extent IgA coinciding with a decrease in IgM serum titer in naive *c-Rel* CD19Cre^{I/+} mice. Serum IgG3 titers are not significantly changed (Figure 15C). The class-switched phenotype of *c-Rel* transgenic plasma cells suggests that this population is of GC origin. Interestingly, there is a trend for detectable serum levels of anti-nuclear antibodies (ANA) and antibodies against cardiolipin in young (age range 8-13 weeks) *c-Rel* CD19Cre^{I/+} mice (Figure 15D).

In order to evaluate whether the plasma cell expansion driven by *c-Rel* *in vivo* can be recapitulated *in vitro*, I performed an *in vitro* assay of plasmablast differentiation. In the presence of LPS, *c-Rel* CD19Cre^{I/+} splenocytes display a slight trend for stronger plasmablast differentiation than CD19Cre^{I/+} controls (Figure S12). This indicates that the enlarged plasma cell population *in vivo* is most likely related to the expanded spontaneous GCs.

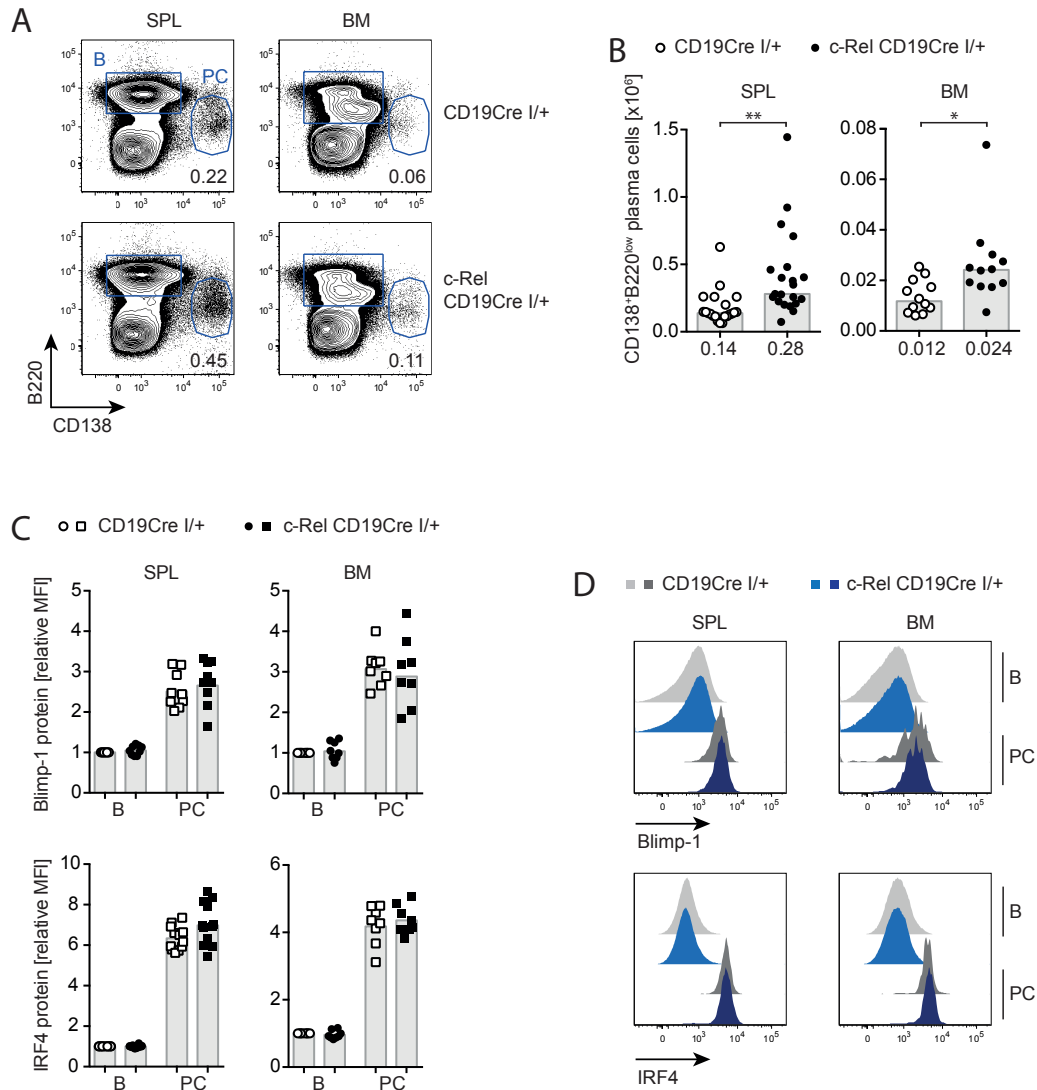


Figure 14: Expansion of plasma cells in *c-Rel*CD19Cre^{I/+} mice. (A) Representative flow cytometry plots of plasma cells. Numbers are median percentages. (B) Plasma cell numbers. Individual data points obtained in ≥ 6 independent experiments are plotted. Bars and numbers below graphs are median values. (C) Intracellular flow cytometry data of IRF4 and Blimp-1 protein levels in plasma cells normalized to the non-plasma cell B cell population of CD19Cre^{I/+} controls. Individual data points obtained in ≥ 3 independent experiments and the geometric mean represented as a bar are plotted. (D) Representative histograms illustrate the bar graphs shown in (C). * $p \leq 0.05$, ** $p \leq 0.01$, unpaired t test. plasma cells (PC) B220^{low}CD138⁺; B (non-PC) B220⁺CD138⁻; SPL, spleen; BM, bone marrow.

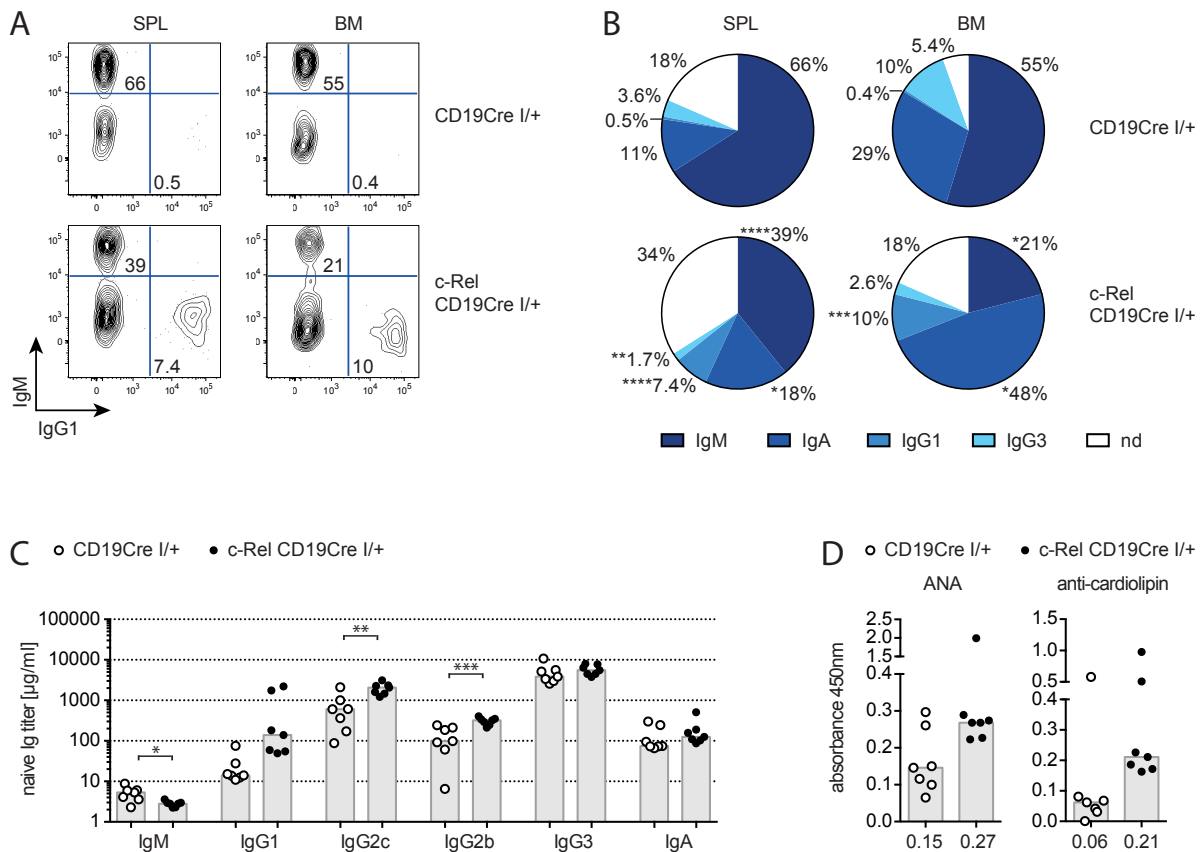


Figure 15: Plasma cells in *c-Rel* CD19Cre^{I/+} mice are class-switched. (A) Representative flow cytometry plots of intracellular IgM- or IgG1-expressing plasma cells. Numbers are median percentages. (B) Percentages of IgM-, IgA-, IgG1- and IgG3-expressing plasma cells determined by intracellular flow cytometry. Data are representative for 8-14 mice analyzed in ≥ 5 independent experiments. Percentage values with stars indicate significant differences with respect to CD19Cre^{I/+} control mice. Naive serum (C) Ig titer and (D) IgG anti-nuclear antibodies (ANA) and anti-cardiolipin antibodies determined by ELISA. Individual data points are plotted. Serum was collected in independent experiments from mice aged 8-13 weeks. * $p \leq 0.05$, ** $p \leq 0.01$, *** $p \leq 0.001$, **** $p \leq 0.0001$, unpaired t test. SPL, spleen; BM, bone marrow; nd, not determined.

1.4 Validation of phenotype in GFP-c-Rel CD19Cre^{I/+} mice

Detailed analyses of GFP-c-Rel CD19Cre^{I/+} mice further corroborate the phenotypes caused by c-Rel overexpression. As in c-Rel CD19Cre^{I/+} mice, B cell development and maturation as well as activation status is largely unaltered in GFP-c-Rel CD19Cre^{I/+} mice (Figure S13-S16); while B cell-specific GFP-c-Rel expression leads to an expansion of GC B cells (Figure 16 and Figure S17), T_{fh} cells (Figure S18) and plasma cells (Figure S19 and S20) that is comparable to the consequences of c-Rel overexpression in B cells. These results not only validate the observed phenotypes in an independently generated c-Rel transgenic mouse line but also substantiate that the GFP-c-Rel fusion does not impair c-Rel function *in vivo*. Accordingly, this novel GFP-c-Rel transgenic mouse line constitutes a useful tool for investigating c-Rel function.

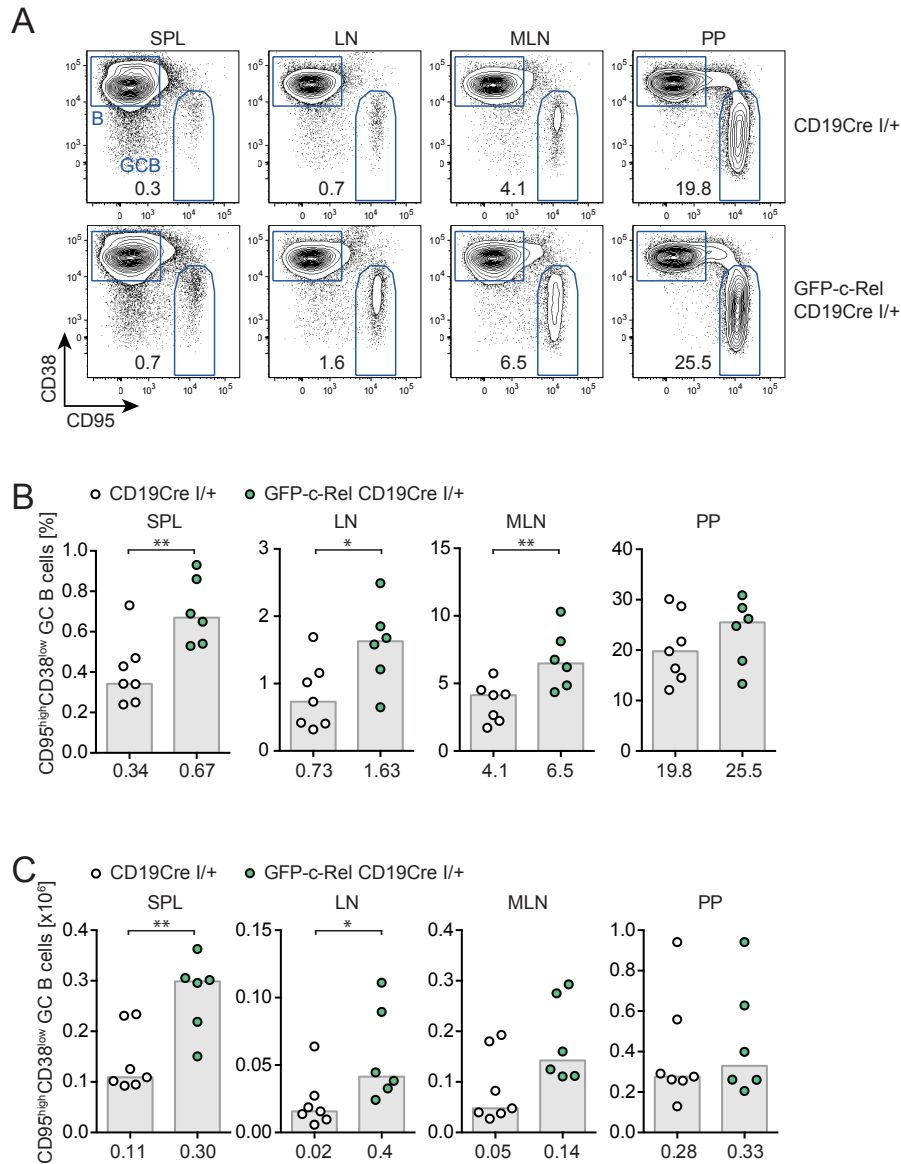


Figure 16: Expansion of GC B cells in GFP-c-Rel CD19Cre^{I/+} mice. (A) Representative flow cytometry plots of GC B cells. Numbers are median percentages of GC B cells of total B cells. (B) Percentages of GC B cells of total B cells and (C) GC B cell numbers. Individual data points obtained in 2 independent experiments are plotted. Bars and numbers below graphs are median values. * $p \leq 0.05$, ** $p \leq 0.01$, unpaired t test. GCB CD19⁺/B220⁺CD95^{high}CD38^{low}; SPL, spleen; LN, lymph nodes; MLN, mesenteric lymph nodes; PP, Peyer's patches.

1.5 Induced GC reactions and acute expression of c-Rel at the GC B cell stage

1.5.1 Expansion of GC B and plasma cells upon immunization

As delineated above, c-Rel transgene expression in B cells enhances spontaneous GC formation and plasma cell numbers. In order to investigate the effects on GC B cells and plasma cells in the context of induced immune reactions, I immunized c-Rel CD19Cre^{I/+} mice intraperitoneally with sheep red blood cells (SRBC) and analyzed spleens of these mice 10-12 days post-immunization. Although spleen weight and total B cell numbers are unchanged, GC B cells are increased in spleens of c-Rel CD19Cre^{I/+} mice also upon immunization (Figure 17A). These GC B cells express high levels of Bcl-6 as expected (Figure 17B) and the polarization into LZ and DZ GC B cells is consistent with the distribution in spontaneous GCs (Figure S21A). This phenotype is again accompanied by a trend for higher T_{fh} cell numbers (Figure S21B).

Plasma cells strikingly accumulate in spleens of c-Rel CD19Cre^{I/+} mice also upon immunization (Figure 17C). This plasma cell population is composed of a significantly lower proportion of unswitched IgM-expressing cells and a higher frequency of IgG1- and IgA-class-switched plasma cells (Figure 17D).

These results demonstrate that also during induced GC reactions transgenic c-Rel expression results in elevated GC B cell and plasma cell numbers resembling the phenotype in naive mice. Intriguingly, although the extent of enhanced GC formation upon immunization is slightly lower than in spontaneous GC reactions, the significant expansion of plasma cells is at least of equivalent magnitude. This finding indicates that c-Rel indeed could have an independent role in driving plasma cell generation or maintenance and that the accumulated plasma cell population might not merely be due to excessive GCs.

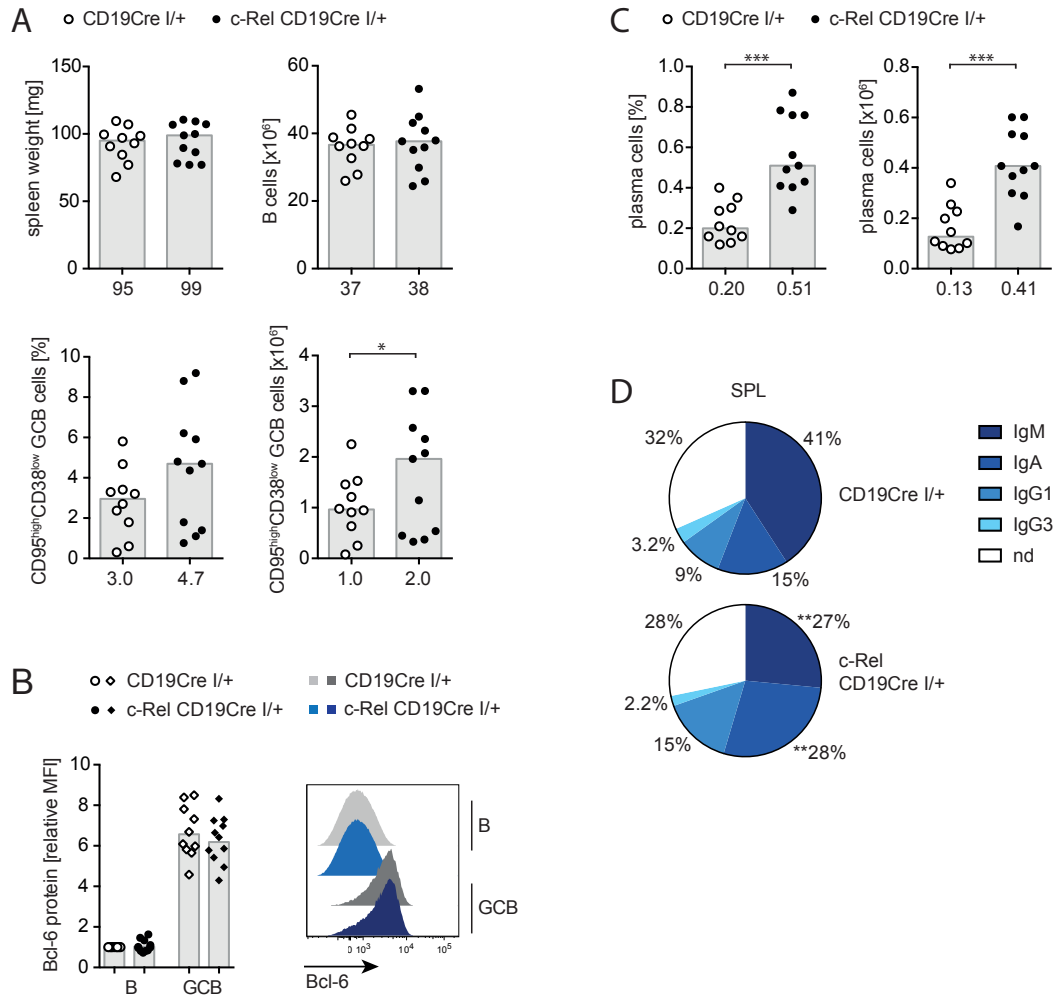


Figure 17: Expansion of splenic GC B cells and plasma cells in SRBC-immunized $c\text{-Rel}CD19Cre^{I/+}$ mice. Mice were immunized with SRBC and spleens were analyzed 10-12 days post-immunization. (A) Spleen weight, total B cell numbers and GC B cell percentages and cell numbers. Bars and numbers below graphs are median values. (B) Intracellular flow cytometry data of Bcl-6 protein levels in GC B cells normalized to the non-GC B cell population of $CD19Cre^{I/+}$ controls. Representative histograms illustrate the bar graphs for which individual data points and the geometric mean are plotted. (C) Plasma cell percentages and cell numbers. Bars and numbers below graphs are median values. Data presented in (A), (B) and (C) were obtained in 4 independent experiments for which individual data points are plotted. (D) Percentages of IgM-, IgA-, IgG1- and IgG3-expressing plasma cells determined by intracellular flow cytometry. Data are representative for 6 mice analyzed in 2 independent experiments. Percentage values with stars indicate significant differences with respect to $CD19Cre^{I/+}$ control mice. * $p \leq 0.05$, ** $p \leq 0.01$, *** $p \leq 0.001$, paired t test. GCB $CD19^+/B220^+CD95^{\text{high}}CD38^{\text{low}}$; B (non-GCB) $CD19^+/B220^+CD95^-CD38^{\text{high}}$; plasma cells (PC) $B220^{\text{low}}CD138^+$; nd, not determined.

1.5.2 c-Rel C γ 1Cre^{I/+} mice phenocopy c-Rel CD19Cre^{I/+} mice

I next asked the question whether developmental timing of c-Rel overexpression is a relevant factor for the observed phenotype. Crossing c-Rel transgenic mice to the C γ 1Cre mouse line allows Cre recombinase expression and, thus, acute c-Rel transgene induction specifically in GC B cells [Casola et al., 2006].

Remarkably, GC B cells are expanded in spontaneous GCs in spleen, lymph nodes, mesenteric lymph nodes and Peyer's patches of c-Rel C γ 1Cre^{I/+} mice (Figure 18). Consistent with findings presented above, there is a trend for a higher proportion of LZ GC B cells in c-Rel C γ 1Cre^{I/+} mice (Figure S22). This phenotype coincides with higher cell numbers of T_{fh} cells (Figure S23 and S24). As in c-Rel CD19Cre^{I/+} mice, plasma cell percentages and cell numbers are significantly higher in c-Rel C γ 1Cre^{I/+} mice compared to controls (Figure 19). Furthermore, SRBC-immunization of c-Rel C γ 1Cre^{I/+} mice shows a comparable trend (Figure S25).

In conclusion, c-Rel C γ 1Cre^{I/+} mice substantially phenocopy c-Rel CD19Cre^{I/+} mice. The characteristic properties of the present conditional c-Rel transgenic mouse model appear to be independent of c-Rel transgene induction before or during GC reactions. These findings indicate that the phenotype is not caused by alterations during initial GC formation but rather originates from effects influencing the maintenance of ongoing GC reactions.

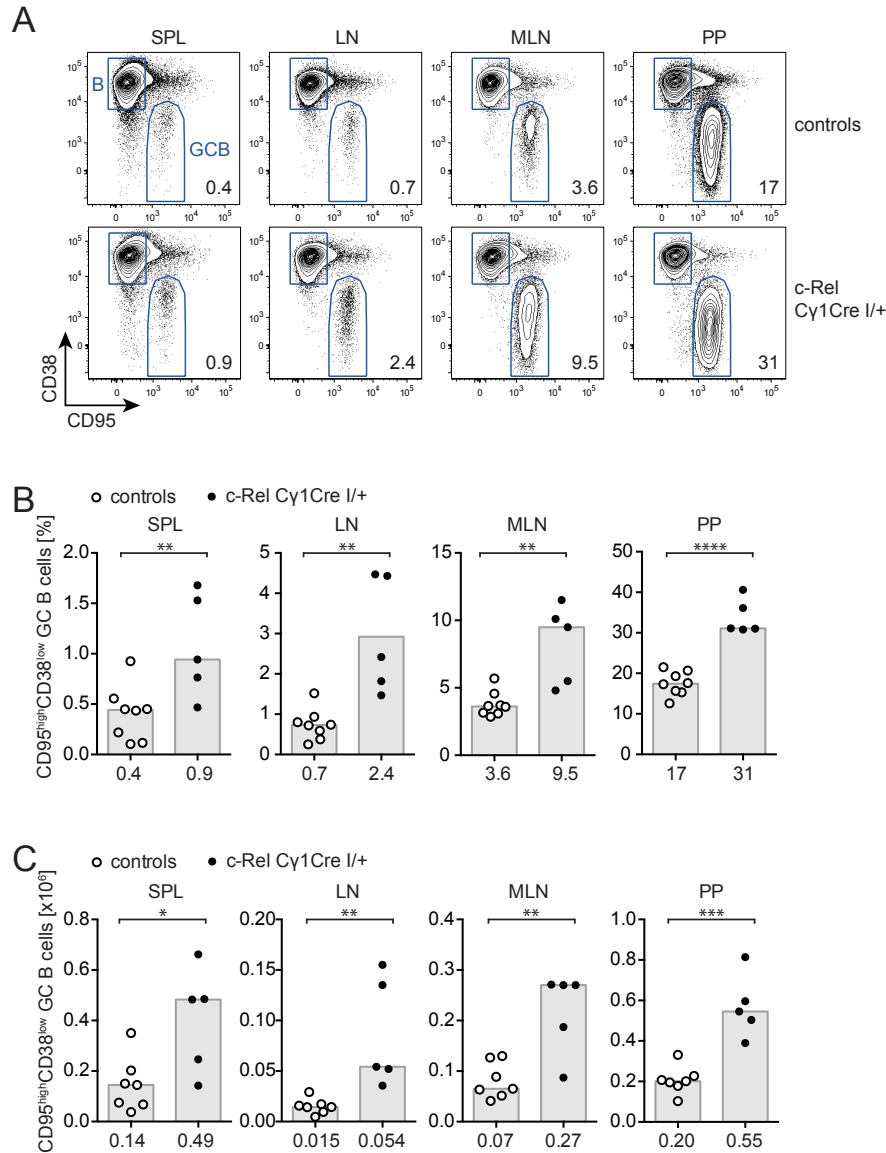


Figure 18: Expansion of GC B cells in c-Rel $C\gamma 1Cre^{I/+}$ mice. (A) Representative flow cytometry plots of GC B cells. Numbers are median percentages of GC B cells of total B cells. (B) Percentages of GC B cells of total B cells and (C) GC B cell numbers. Individual data points obtained in 2 independent experiments are plotted. Bars and numbers below graphs are median values. Controls include c-Rel and $C\gamma 1Cre^{I/+}$ mice. * $p \leq 0.05$, ** $p \leq 0.01$, *** $p \leq 0.001$, **** $p \leq 0.0001$, unpaired t test. GCB $CD19^+/B220^+CD95^{high}CD38^{low}$; SPL, spleen; LN, lymph nodes; MLN, mesenteric lymph nodes; PP, Peyer's patches.

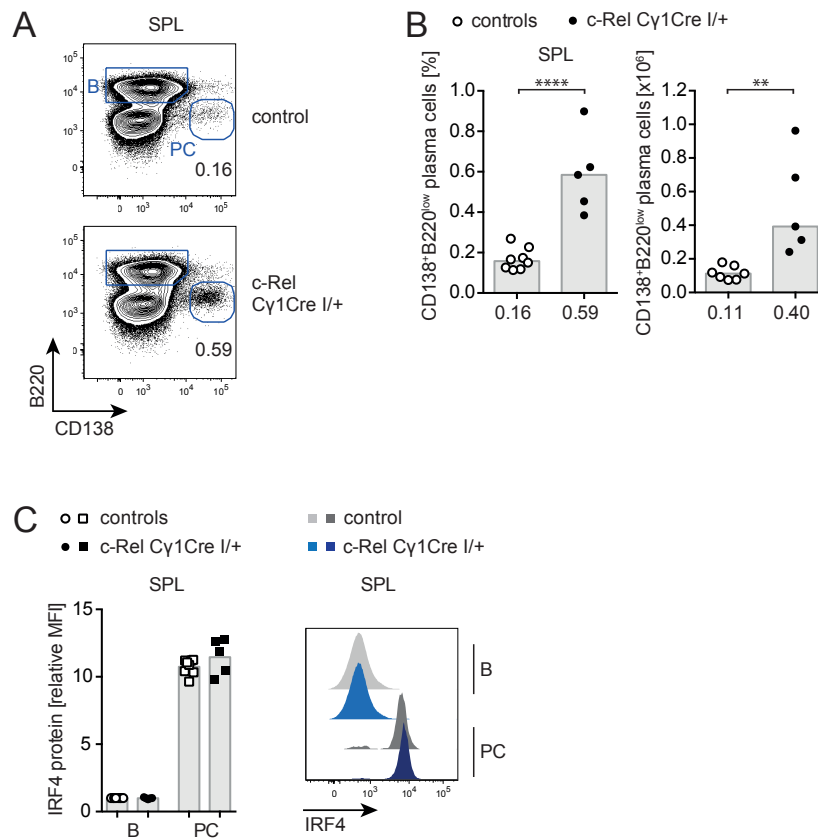


Figure 19: Expansion of plasma cells in c-Rel C γ 1Cre^{I/+} mice. (A) Representative flow cytometry plots of plasma cells. Numbers are median percentages. (B) Plasma cell percentage and cell numbers. Individual data points are plotted. Bars and numbers below graphs are median values. Data were obtained in 2 independent experiments. (C) Intracellular flow cytometry data of IRF4 protein levels in plasma cells normalized to the non-plasma cell B cell population of controls. Representative histograms illustrate the bar graphs for which the geometric mean and individual data points are plotted. Data were obtained in 2 independent experiments. Controls include c-Rel and C γ 1Cre^{I/+} mice. ** $p \leq 0.01$, **** $p \leq 0.0001$, unpaired t test. plasma cells (PC) B220^{low}CD138⁺; B (non-PC) B220⁺CD138⁻; SPL, spleen.

1.6 Aged c-Rel CD19Cre^{I/+} mice

Given the high frequency of *REL* gene locus amplifications in human B cell lymphomas of GC origin (see introduction subsection 3.2) and the expansion of GC B cells and plasma cells in young c-Rel CD19Cre^{I/+} mice, I monitored aged mice in order to investigate whether c-Rel overexpression could act as a potential driver of lymphomagenesis or autoimmunity. c-Rel CD19Cre^{I/+} and CD19Cre^{I/+} control mice were analyzed at a median age of 511 or 521 days, respectively (age range 409-571 days).

There was no visible difference between c-Rel CD19Cre^{I/+} and CD19Cre^{I/+} control mice with regard to general appearance of organs. Spleen weight and total cell numbers of analyzed organs are largely unaltered in aged c-Rel CD19Cre^{I/+} mice compared to controls, except for a trend for higher cell numbers in thymi of c-Rel CD19Cre^{I/+} mice (Figure S26). B cell populations in spleens, lymph nodes and mesenteric lymph nodes are not significantly changed (Figure S27). Both GC B cell and plasma cell populations of aged c-Rel CD19Cre^{I/+} mice still show a trend for enhanced cell numbers in spleen, lymph nodes and mesenteric lymph nodes or spleen and bone marrow, respectively (Figure S28), albeit not to the significant extent that characterizes young animals.

Comparable to findings in young mice, the proportion of class-switched IgG1-expressing plasma cells is substantially increased in aged c-Rel CD19Cre^{I/+} mice, which is accompanied by lower percentages of unswitched IgM-expressing plasma cells (Figure 20A). In accordance with this observation, IgG1 serum titers are significantly higher in aged c-Rel CD19Cre^{I/+} mice and there is a trend for elevated serum Ig titers of IgG2c, IgG2b and IgA, while IgM and IgG3 are slightly lower (Figure 20B). Interestingly, analyses of autoantibodies demonstrate that the trend for detectable ANA titers in young mice is established as significantly augmented ANA titers in aged mice, while anti-cardiolipin antibodies are not significantly different from controls. In addition, rheumatoid factor (RF) of the IgG subtype but not the IgM subtype is detectable in c-Rel CD19Cre^{I/+} mice (Figure 20C). These signs of class-switched autoantibody production suggest that the spontaneous GCs in c-Rel CD19Cre^{I/+} mice are driven at least in part by self-antigens.

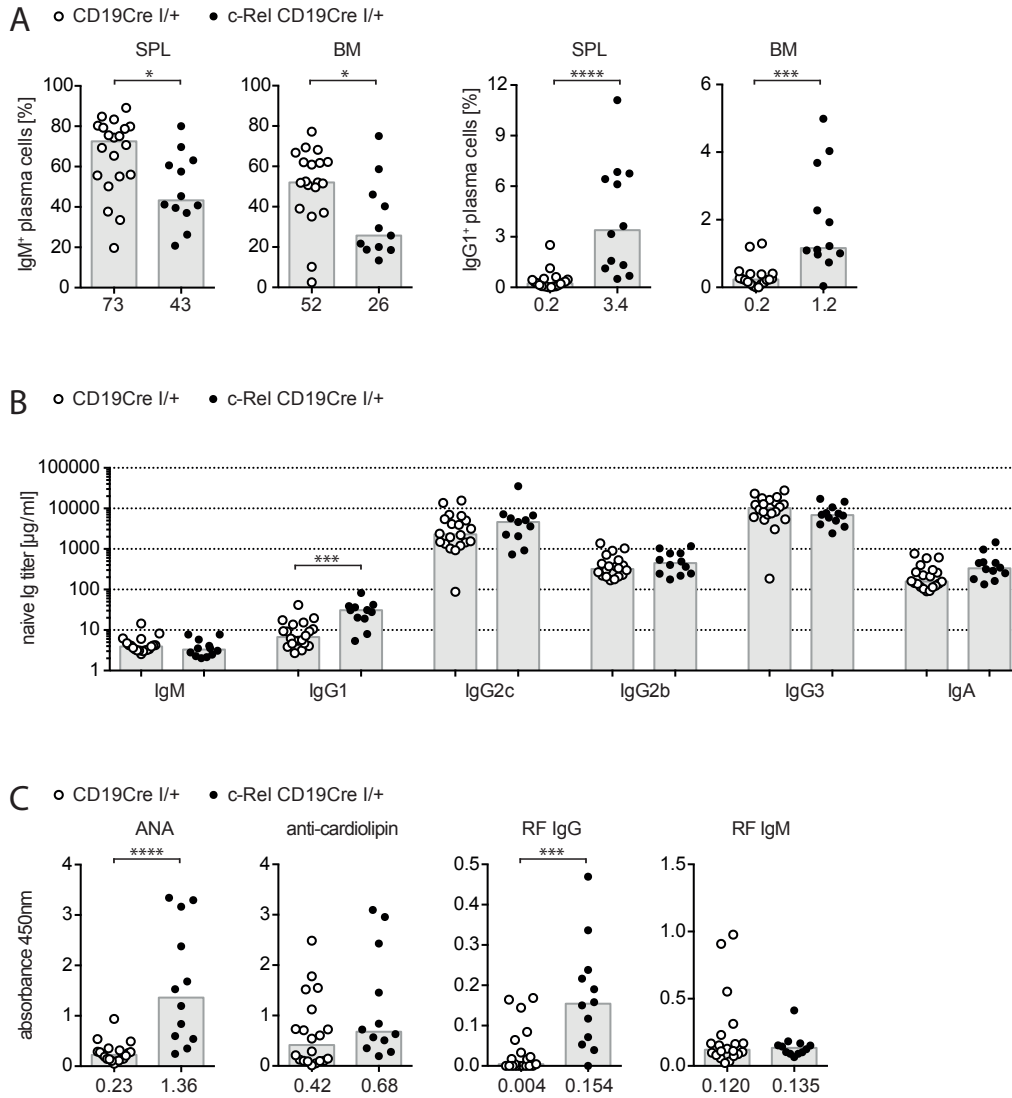


Figure 20: Class-switched autoantibody production in aged c-Rel CD19Cre^{I/+} mice. (A) Percentages of IgM- and IgG1-expressing plasma cells determined by intracellular flow cytometry. Individual data points and bars representing median values are plotted. Data were obtained in 8 independent experiments. Serum (B) Ig titer and (C) IgG anti-nuclear antibodies (ANA) and anti-cardiolipin antibodies as well as rheumatoid factor (RF) of the IgG and IgM isotype determined by ELISA. Individual data points and median values are plotted. Serum was collected in 8 independent experiments. Aged c-Rel CD19Cre^{I/+} and CD19Cre^{I/+} mice were analyzed at a median age of 511 or 521 days, respectively (age range 409-571 days). * $p \leq 0.05$, *** $p \leq 0.001$, **** $p \leq 0.0001$, unpaired t test. SPL, spleen; BM, bone marrow.

1.7 c-Rel levels are B cell subtype-dependent and correlate with cellular expansion

1.7.1 c-Rel is upregulated in GC B cells and decreased in plasma cells

In order to comprehensively characterize the novel conditional c-Rel transgenic mouse model and to elucidate the mechanisms underlying the selective impact on terminally differentiated B cell subsets, I performed detailed analyses of c-Rel protein levels.

To calculate the proportion of transgenic c-Rel of total c-Rel, Western blot was applied as it allows size-dependent resolution and hence distinction of endogenous c-Rel from the 3xflag-tag-containing c-Rel transgene. Quantitative Western blot analysis demonstrates that endogenous c-Rel levels are on average comparable in splenic B cells or total cellular populations of lymph nodes, mesenteric lymph nodes or Peyer's patches isolated from CD19Cre^{I/+} or c-Rel CD19Cre^{I/+} mice (Figure 21A and 21B). Transgenic c-Rel accounts for 24% of total c-Rel in splenic B cells. With regard to the organs for which total cells were analyzed, the proportion of c-Rel transgene increases from 27% in lymph nodes and 31% in mesenteric lymph nodes to 42% in Peyer's patches corresponding to the increase of GC B cell percentages in these organs (Figure 21C, compare to Figure 10 for percentage of GC B cells).

Given the higher contribution of transgenic c-Rel to the total c-Rel pool in organs with higher proportions of GC B cells, I quantified c-Rel protein expression at single cell level by intracellular flow cytometry. Intriguingly, c-Rel levels are highly upregulated in GC B cells in comparison to naive B cells in spleen and lymph nodes as well as gut-associated mesenteric lymph nodes and Peyer's patches. In sharp contrast, c-Rel levels are dramatically decreased in plasma cells. These marked B cell subtype-dependent switches in c-Rel protein levels affect both CD19Cre^{I/+} control and c-Rel CD19Cre^{I/+} transgene-expressing mice (Figure 22). Consistent with the total c-Rel level in isolated splenic B cells quantified by Western blot, B cell-specific c-Rel transgene expression leads to only marginally higher total c-Rel levels in naive B cells (≤ 1.3 -fold), whereas total c-Rel levels are 2-3-fold higher in transgenic GC B cells compared to control GC B cells (Figure 22A and 22B). The c-Rel level in transgenic plasma cells is on average 1.6-fold higher and reaches roughly the level observed in naive control B cells (Figure 22C). Interestingly, within the population of GC B cells c-Rel levels are generally higher in LZ than in DZ GC B cells irrespective of the genotypes (Figure 22B).

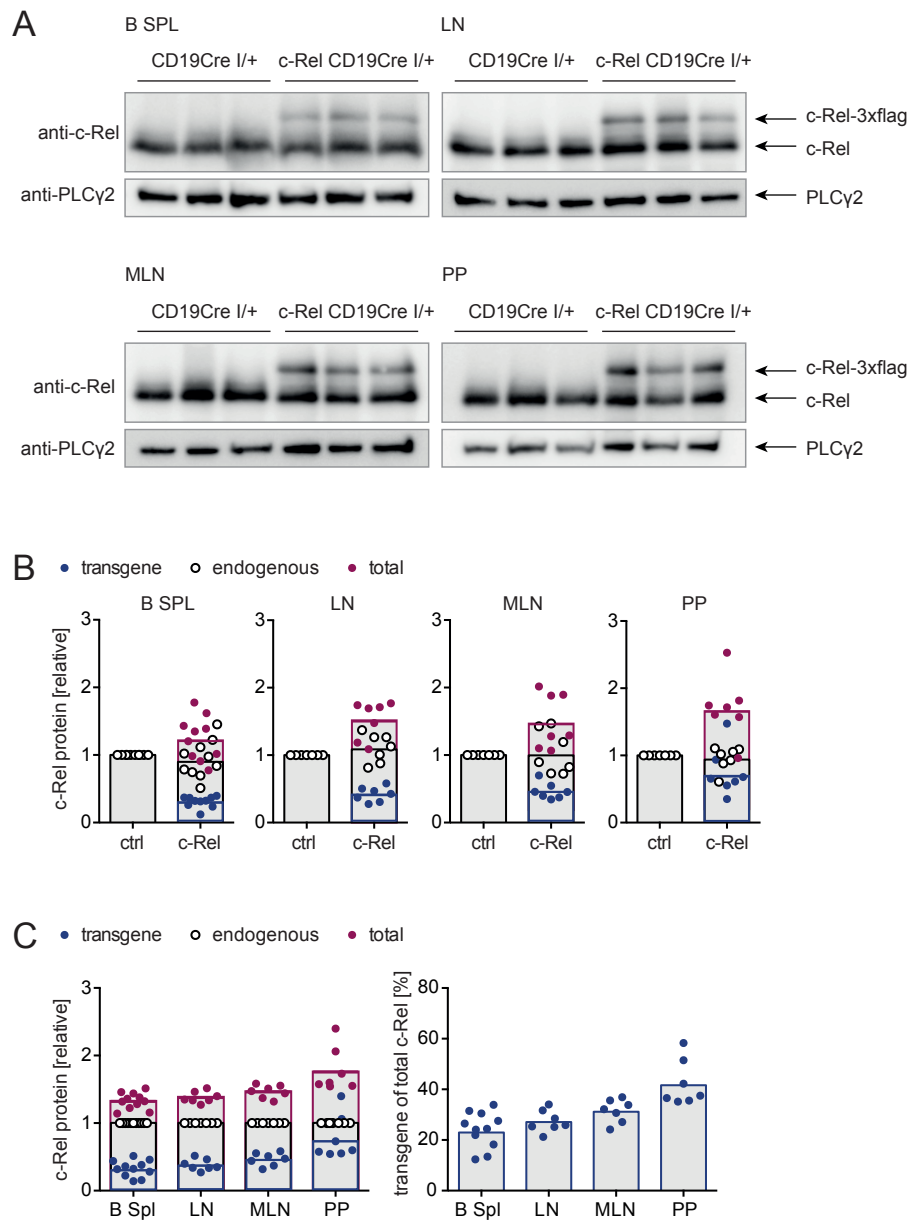


Figure 21: Quantification of c-Rel transgene levels. (A) Representative Western blot images and (B) and (C) quantification of Western blot data. Splenic B cells (B SPL) isolated by MACS-separation or total cellular populations of lymph nodes (LN), mesenteric lymph nodes (MLN) or Peyer's patches (PP) were analyzed. Equal cell numbers were loaded. Due to the 3x-flag tag transgenic c-Rel can be distinguished from endogenous c-Rel according to size. Individual data points obtained in ≥ 3 independent experiments are plotted and bars represent geometric means. (B) Normalization of c-Rel levels in c-Rel CD19Cre^{I/+} (c-Rel) mice to CD19Cre^{I/+} controls (ctrl). (C) Normalization of transgenic c-Rel levels to endogenous c-Rel levels within c-Rel CD19Cre^{I/+} mice and calculation of proportion of transgenic c-Rel of total c-Rel. Each dot in (B) and (C) represents the endogenous (white) or transgenic (blue) fraction or the total (red) amount of quantified c-Rel protein within one sample.

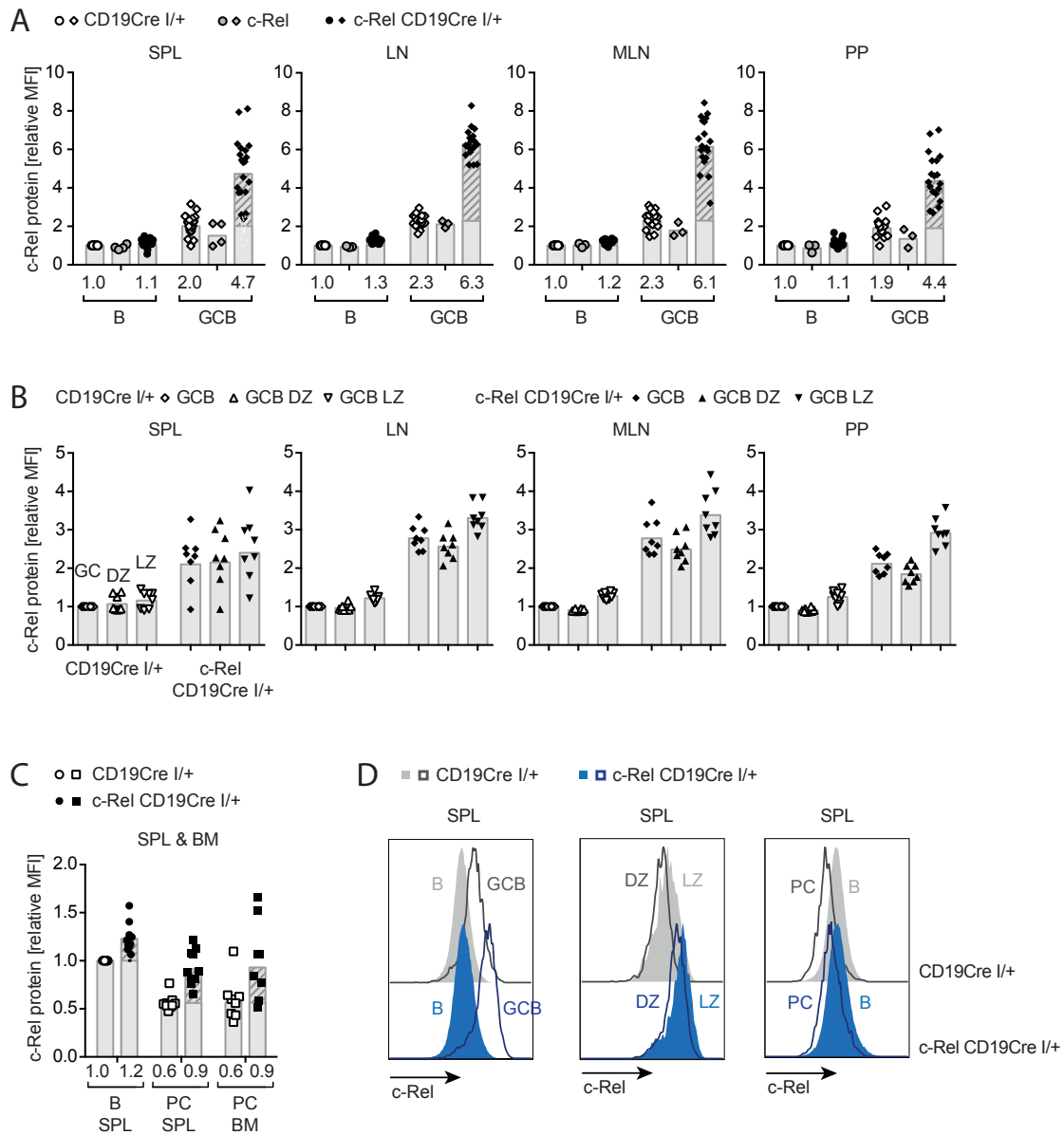


Figure 22: c-Rel levels are highly upregulated in GC B cells and decreased in plasma cells. Intracellular flow cytometry data of c-Rel protein levels in B cell subpopulations. Median fluorescence intensities (MFI) were normalized to CD19Cre^{I/+} controls. Individual data points obtained in ≥ 3 independent experiments and bars representing geometric means are plotted. (A) c-Rel level in B cells and GC B cells. MFIs were normalized to non-GC B cells of CD19Cre^{I/+} controls. Geometric mean values are given for c-Rel CD19Cre^{I/+} and CD19Cre^{I/+} populations below graphs. The shaded part of the bars represents the fraction of total c-Rel that is additionally present in transgene-expressing mice in comparison to the respective control subpopulation. (B) c-Rel level in DZ and LZ of GC B cells. MFIs were normalized to GC B cells of CD19Cre^{I/+} controls. (C) c-Rel level in plasma cells. MFIs were normalized to splenic B cells (non-PC) of CD19Cre^{I/+} controls. Geometric mean values are given below graphs. The shaded part of the bars represents the fraction of total c-Rel that is additionally present in transgene-expressing mice in comparison to the respective control subpopulation. (D) Representative histograms illustrate c-Rel levels in indicated B cell subpopulations. GCB CD19⁺/B220⁺CD95^{high}CD38^{low}; B (non-GCB) CD19⁺/B220⁺CD95^{low}CD38^{high}; DZ CXCR4^{high}CD86^{low}; LZ CXCR4^{low}CD86^{high}; plasma cells (PC) B220^{low}CD138⁺; B (non-PC) B220⁺CD138⁻; BM, bone marrow; SPL, spleen; LN, lymph nodes; MLN, mesenteric lymph nodes; PP, Peyer's patches.

Total c-Rel levels in GC B cells and plasma cells of induced GC reactions upon SRBC-immunization or acute c-Rel transgene expression in c-Rel $C\gamma 1\text{Cre}^{I/+}$ mice are equivalent to c-Rel levels of spontaneous GC reactions (Figure S29). Flow cytometric assessment of GFP fluorescence signals in GFP-c-Rel $\text{CD}19\text{Cre}^{I/+}$ mice demonstrates that GFP-c-Rel levels follow the same switches in expression strength as c-Rel levels: intermediate expression of GFP-c-Rel in naive B cells, higher levels in GC B cells and lowest levels in plasma cells. Moreover, GFP fluorescence of GFP-c-Rel protein is of higher intensity in LZ GC B cells than in DZ GC B cells mirroring the general findings of c-Rel levels in these polarized GC B cell states (Figure 23). This pattern is also reproduced by total c-Rel levels in GFP-c-Rel $\text{CD}19\text{Cre}^{I/+}$ mice measured by intracellular flow cytometric c-Rel staining (Figure S30). Furthermore, c-Rel and GFP-c-Rel levels in *in vitro*-differentiated plasmablasts are lower than in non-plasmablast cells, illustrating that the downregulation of c-Rel in plasma cells is a steady feature of this differentiated state that can be recapitulated *in vitro* (Figure S31).

Expression of c-Rel is induced upon stimulation [Grumont and Gerondakis, 1994; Carrasco et al., 1994; Damdinsuren et al., 2010] (see also introduction section 2). Upon treatment for 60 min, c-Rel is upregulated more than 2-fold by selective stimuli in B cells and GC B cells but almost unchanged in plasma cells, except for a marginal responsiveness towards LPS treatment. Although c-Rel levels are still higher in GC B cells and plasma cells of c-Rel $\text{CD}19\text{Cre}^{I/+}$ mice compared to $\text{CD}19\text{Cre}^{I/+}$ controls (Figure S32A), the relative induction compared to unstimulated cells within the control or transgenic genotype are comparable (Figure S32B). Total c-Rel levels are strongly elevated also upon over night treatment with the same stimuli compared to unstimulated controls in isolated B cells of both c-Rel $\text{CD}19\text{Cre}^{I/+}$ and $\text{CD}19\text{Cre}^{I/+}$ mice (Figure S32C). GFP fluorescence signals are to a certain degree enhanced upon over night stimulation compared to the unstimulated control population in GFP-c-Rel $\text{CD}19\text{Cre}^{I/+}$ mice (Figure S32D). However, a partial influence of the increased cell size on the fluorescent signal cannot be excluded. Consequently, stimulation has a strong effect on total c-Rel levels as expected, but no dramatic additional effect with regard to transgenic c-Rel is observed.

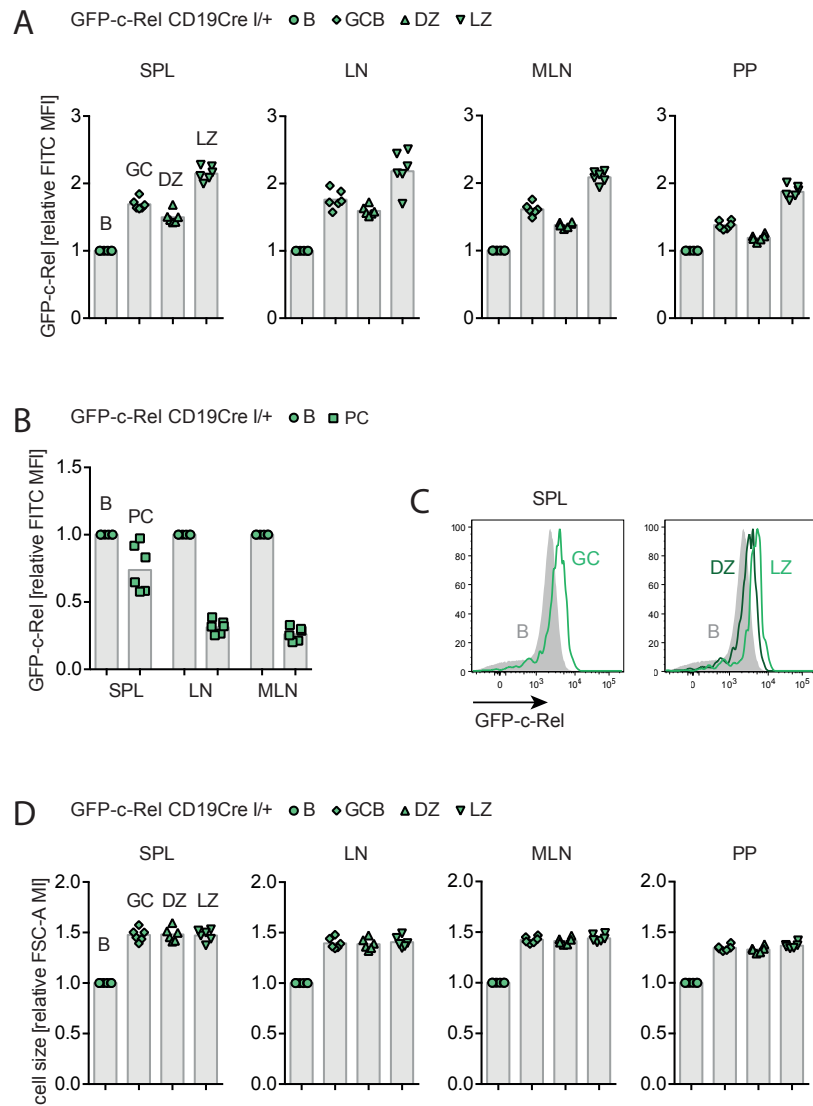


Figure 23: GFP fluorescence signals in GFP-c-Rel CD19Cre^{I/+} mice follow the same expression pattern as c-Rel levels. Flow cytometry data of GFP-c-Rel protein levels assessed by GFP fluorescence signal in B cell subpopulations of GFP-c-Rel CD19Cre^{I/+} mice. Median fluorescence intensities (MFI) were normalized. Individual data points obtained in ≥ 2 independent experiments and bars representing geometric means are plotted. (A) GFP-c-Rel level in B cells and GC B cells including LZ and DZ GC B cells. MFI normalization to non-GC B cells. (B) GFP-c-Rel level in plasma cells. MFI normalization to non-PC B cells. (C) Representative histograms for GFP-c-Rel level in GC B cells of GFP-c-Rel CD19Cre^{I/+} mice. (D) FSC-A median intensities for B cells and GC B cells normalized to non-GC B cells show that changes in cell size cannot be the cause for the differences in GFP-fluorescence observed in GFP-c-Rel CD19Cre^{I/+} transgenic cells. GCB CD19⁺/B220⁺CD95^{high}CD38^{low}; B (non-GCB) CD19⁺/B220⁺CD95⁻CD38^{high}; DZ CXCR4^{high}CD86^{low}; LZ CXCR4^{low}CD86^{high}; plasma cells (PC) B220^{low}CD138⁺; B (non-PC) B220⁺CD138⁻; SPL, spleen; LN, lymph nodes; MLN, mesenteric lymph nodes; PP, Peyer's patches; FSC-A, forward scatter area.

1.7.2 c-Rel level switches are not caused by transgenic promoter regulation

The dramatic alterations in c-Rel level were confirmed by applying an independent c-Rel antibody clone or the same antibody clone coupled to an alternative fluorochrome for intracellular flow cytometry stainings (Figure S33A and data not shown).

The forward scatter area (FSC-A) parameter can serve as a correlate for cell size. GC B cells are greater in size than naive B cells, while plasma cells are even larger than GC B cells. Thus, the largest cell type, namely plasma cells, is characterized by the lowest c-Rel level. Accordingly, the observed c-Rel levels are not correlated to cell size (Figure S33B). Importantly, this also applies to the differences observed in LZ GC B cells and DZ GC B cells, which are comparable in size based on forward scatter area (Figure S34) but express clearly distinguishable c-Rel levels. Likewise, GFP fluorescence signals of GFP-c-Rel CD19Cre^{I/+} mice are not correlated to cell size (Figure 23D).

As in the present mouse model the c-Rel transgene is driven by a CAG promoter, I aimed to exclude the possibility that the differential extent of transgene expression in naive B cells, GC B cells and plasma cells could be a result of potential variations in promoter activation in these subpopulations. For this purpose, I took advantage of a conditional transgenic knock-in mouse line in which transgenic coxsackie/adenovirus receptor (CAR) is driven by a CAG promoter (R26/CAG-CAR Δ 1^{StopF}) [Heger et al., 2015]. R26/CAG-CAR Δ 1^{StopF} VavCre^{I/+} mice, in which CAR is expressed within the hematopoietic lineage [de Boer et al., 2003], show equal levels of intracellular CAR expression in naive B cells and GC B cells. Expression of CAR in plasma cells is even enhanced but certainly not reduced (Figure 24). In conclusion, the unequal strength of transgene expression in B cell subpopulations of c-Rel transgenic mice are not a property of developmental CAG promoter regulation. This validation rather suggests B cell subtype-dependent post-transcriptional c-Rel regulation that affects both endogenous c-Rel and transgenic c-Rel.

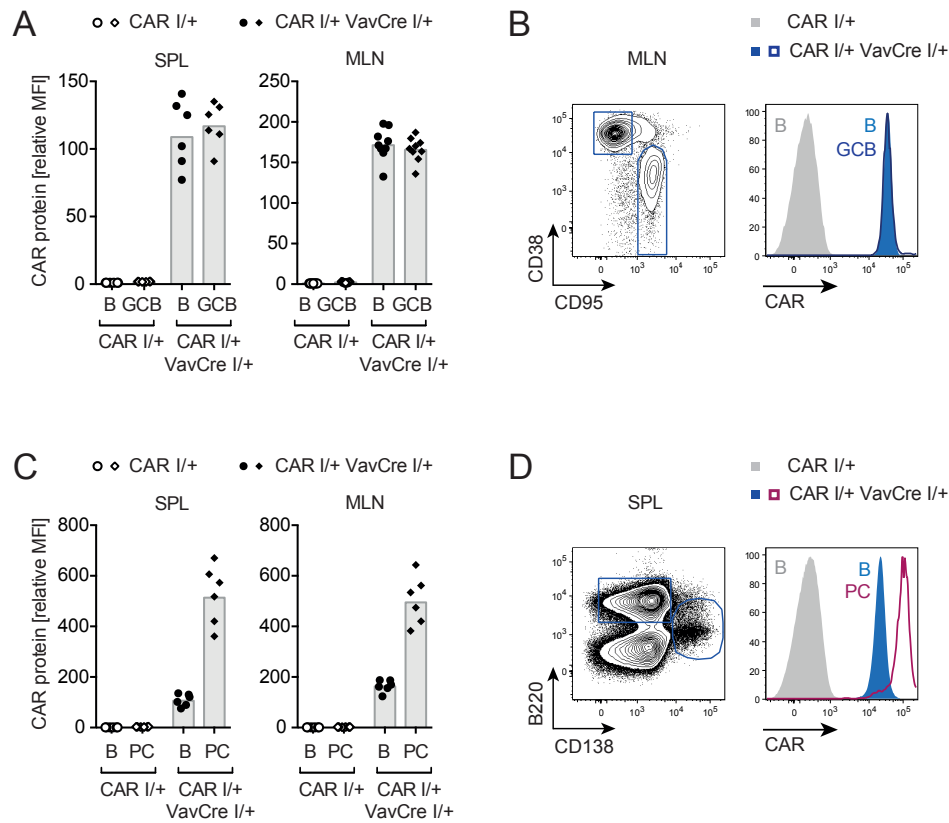


Figure 24: Differential extent of transgene expression in B cell populations is independent of CAG promoter strength. Intracellular flow cytometry stainings of CAG promoter-driven CAR transgene expression in R26/CAG-CAR $\Delta 1^{\text{StopF}}$ VavCre $^{I/+}$ and R26/CAG-CAR $\Delta 1^{\text{StopF}}$ control mice. Median fluorescent intensities (MFI) were normalized to (A) non-GCB or (C) non-plasma cell B cell population of R26/CAG-CAR $\Delta 1^{\text{StopF}}$ control mice. Individual data points obtained in ≥ 2 independent experiments and geometric means are plotted. (A) CAR transgene expression in B cells and GC B cells. (B) Representative flow cytometry plot of GC B cells and representative histogram of CAR expression in B and GC B cells. (C) CAR transgene expression in B cells and plasma cells. (D) Representative flow cytometry plot of plasma cells and representative histogram of CAR expression in B cells and plasma cells. GCB B220 $^{+}$ CD95 $^{\text{high}}$ CD38 $^{\text{low}}$; B (non-GCB) B220 $^{+}$ CD95 $^{-}$ CD38 $^{\text{high}}$; plasma cells (PC) B220 $^{\text{low}}$ CD138 $^{+}$; B (non-PC) B220 $^{+}$ CD138 $^{-}$; SPL, spleen; MLN, mesenteric lymph nodes.

1.7.3 Higher c-Rel nuclear translocation in germinal center B cells

In light of the profound differences in c-Rel levels, I determined the subcellular localization of c-Rel in B cell subpopulations and characterized the properties of transgenic c-Rel in (GFP-)c-Rel CD19Cre^{I/+} mice by imaging flow cytometry. This method constitutes a high throughput approach to quantitatively investigate nuclear translocation in distinct cell populations of a single sample as it allows simultaneous fluorescent parameter and image acquisition of events in single cell suspension. Analysis of nuclear localization is based on a similarity feature that scores the correlation of a nuclear image (DNA stain) and the respective image of a translocation probe. High similarity scores represent high correlation of nuclear image and translocation probe, thus indicating high nuclear translocation. In contrast, low similarity scores are indicative of cytoplasmic localization [George et al., 2006].

As expected, different stimuli, namely anti-CD40, anti-IgM, CpG and LPS, trigger nuclear translocation of c-Rel in splenic B cells of CD19Cre^{I/+} control mice as well as c-Rel CD19Cre^{I/+} transgenic mice (Figure S35). Assessment of GFP fluorescence in GFP-c-Rel CD19Cre^{I/+} mice shows that nuclear translocation of the GFP-c-Rel fusion protein is comparably inducible upon stimulation providing further evidence for the functionality of this fusion protein (Figure S36).

Interestingly, quantification of c-Rel localization in lymph nodes reveals higher c-Rel nuclear translocation scores and percentage of cells showing c-Rel nuclear translocation in GC B cells compared to B cells in unstimulated conditions. Moreover, the present data point towards a trend for slightly enhanced c-Rel nuclear translocation in GC B cells of c-Rel CD19Cre^{I/+} mice compared to CD19Cre^{I/+} controls (Figure 25, Figure 26 and Figure S37). In addition, analyses of stimulatory conditions demonstrate that c-Rel nuclear translocation can be triggered not only in B cells but also in GC B cells from mice of both genotypes. For instance, anti-CD40 treatment results in c-Rel nuclear translocation in almost the entire cellular population of both B cells and GC B cells of lymph nodes with minimally higher nuclear translocation scores obtained for GC B cells (Figure 25, Figure 27 and Figure S38). Similar results were obtained for B cells and GC B cells in mesenteric lymph nodes (Figure S39-S43) and spleen (Figure S35).

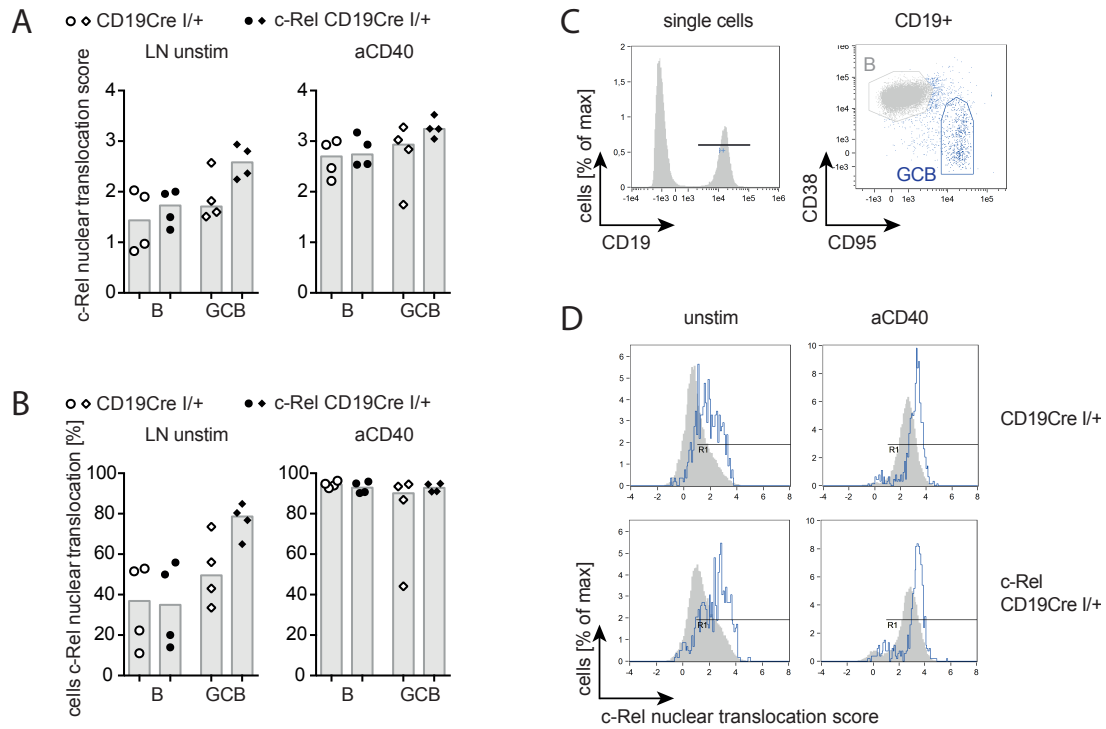


Figure 25: Quantification of c-Rel nuclear localization in B cells and GC B cells by imaging flow cytometry. Cells of lymph nodes (LN) were stimulated with anti-CD40 or left unstimulated (unstim) for 60 min in the presence of 10 μ M Q-VD to prolong the survival of GC B cells in culture. (A) Median c-Rel nuclear localization score and (B) percentage of cells with c-Rel nuclear translocation for B cells and GC B cells of LN from c-RelCD19Cre^{I/+} and CD19Cre^{I/+} mice. Individual data points obtained in 3 independent experiments are plotted. (C) Representative flow cytometry plots illustrating the gating strategy. (D) Representative histograms for c-Rel nuclear translocation score. Example images are provided in Figure 26 and Figure 27. GCB CD19⁺CD95^{high}CD38^{low}; B (non-GCB) CD19⁺CD95⁻CD38^{high}.

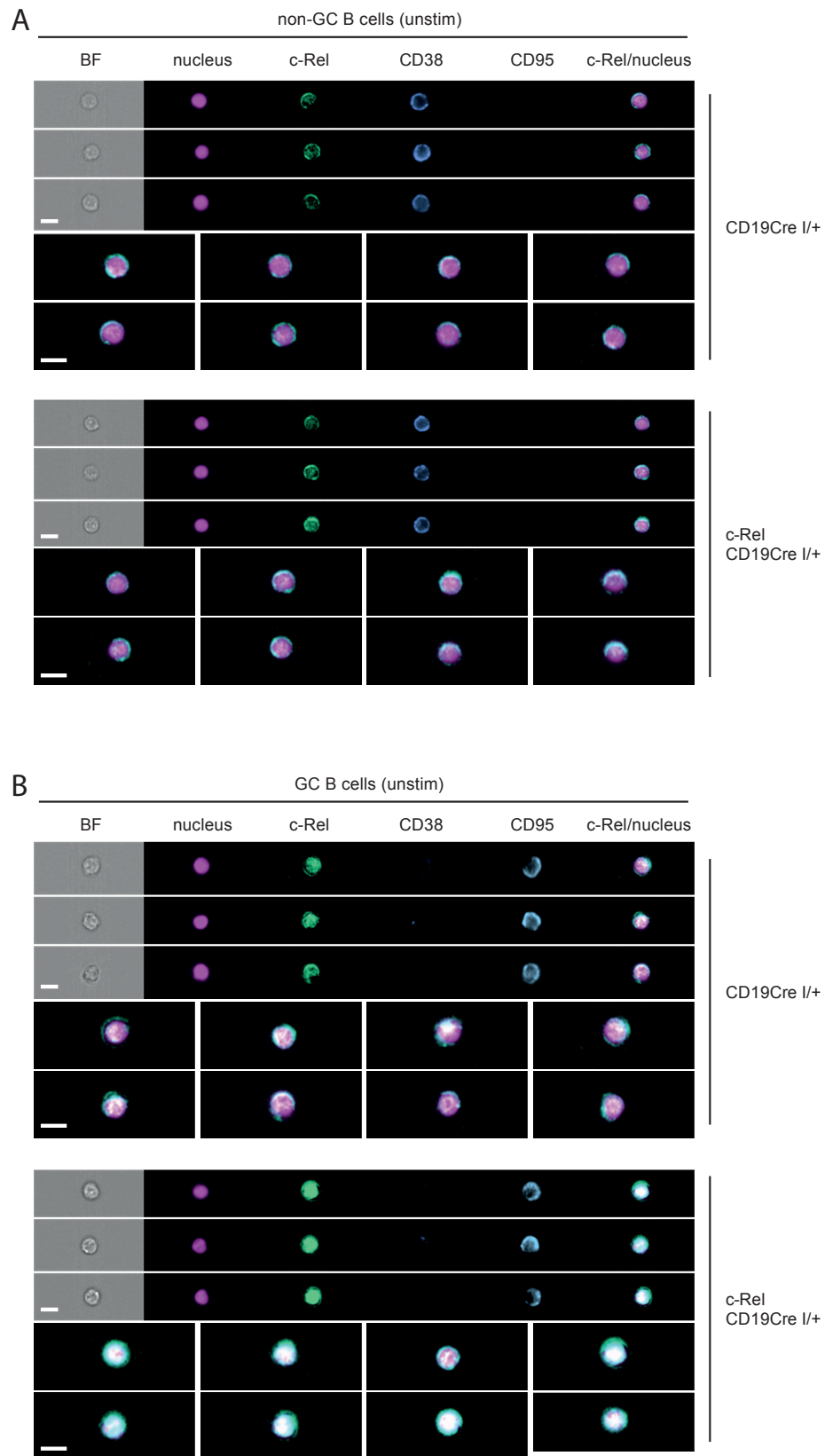


Figure 26: Higher c-Rel nuclear translocation in GC B cells in unstimulated state. Representative images for unstimulated (unstim) (A) non-GC B cells and (B) GC B cells of lymph nodes from CD19Cre^{I/+} controls and c-RelCD19Cre^{I/+} mice. A panel of images for indicated channels as well as magnified images of merged c-Rel/nucleus signals are displayed for each cell type and genotype. Exemplary cells were selected based on average nuclear localization scores. Quantification and gating strategy are displayed in Figure 25. White bar, 10 μ m; BF, bright field.

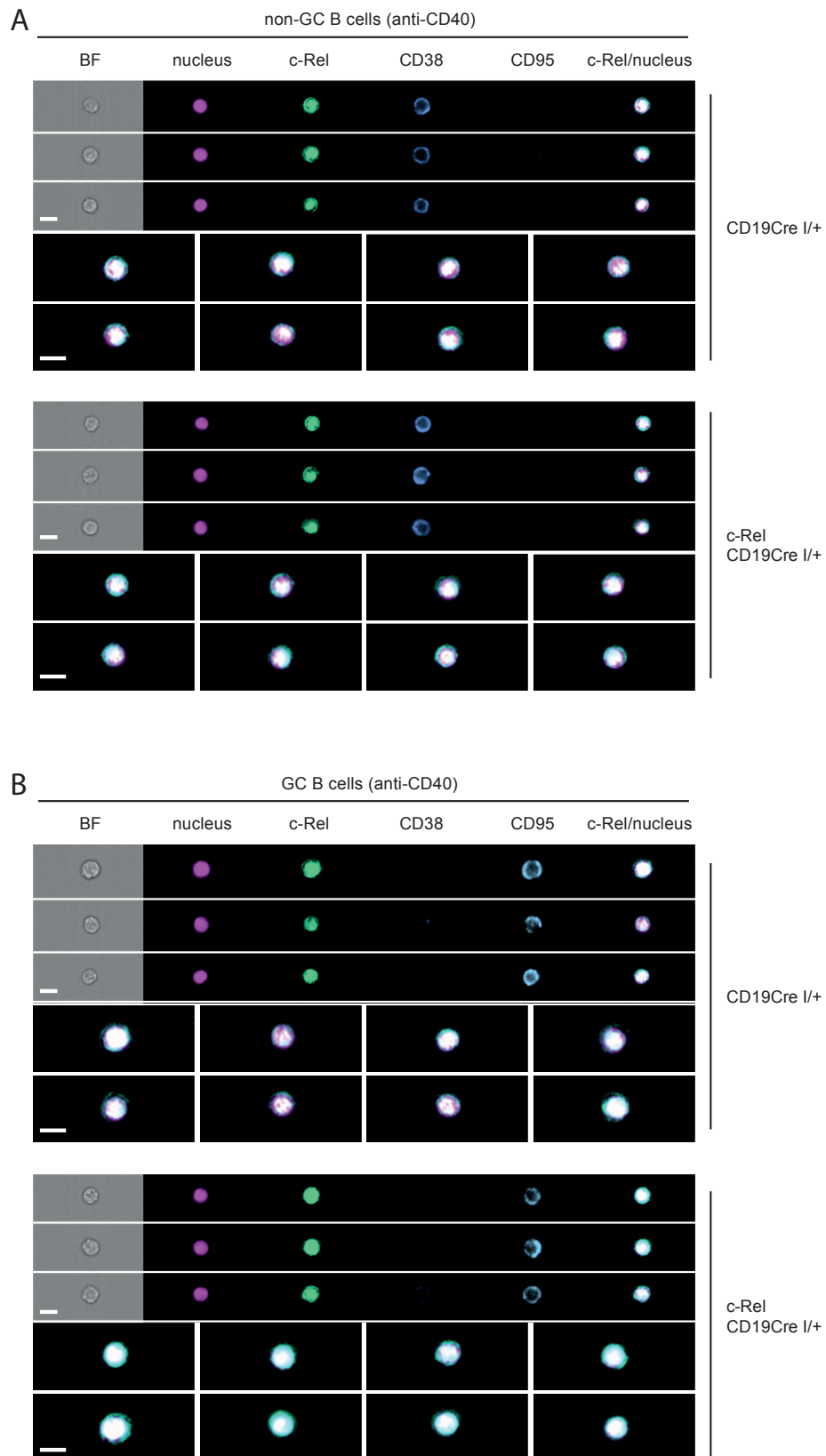


Figure 27: c-Rel nuclear translocation upon stimulation in B cells and GC B cells. Representative images for anti-CD40 stimulated (A) non-GC B cells and (B) GC B cells of lymph nodes from CD19Cre^{I/+} controls and c-RelCD19Cre^{I/+} mice. A panel of images for indicated channels as well as magnified images of merged c-Rel/nucleus signals are displayed for each cell type and genotype. Exemplary cells were selected based on average nuclear localization scores. Quantification and gating strategy are displayed in Figure 25. White bar, 10 μ m; BF, bright field.

Splenic B cells analyzed directly *ex vivo* recapitulate the observation of higher nuclear translocation in the GC B population in general and a trend for elevated nuclear translocation in c-Rel transgenic mice in particular (Figure 28). While an average of around 20% of CD19Cre^{I/+} control B cells show c-Rel nuclear translocation, nuclear c-Rel is observed in 40% of the GC B cell population in these mice. In sharp contrast to B cells and GC B cells, c-Rel is predominantly cytoplasmic in plasma cells with roughly 5% of cells with c-Rel translocation in CD19Cre^{I/+} control mice accompanied by lower nuclear translocation scores in plasma cells than in B cells (Figure 28). Preliminary data obtained for total c-Rel in B cells of GFP-c-Rel CD19Cre^{I/+} mice that were analyzed directly *ex vivo* or following stimulation further support these findings. Of note, this analysis indicates that plasma cells appear to be rather refractory to c-Rel nuclear localization upon stimulation with the tested stimuli (Figure S44).

In summary, c-Rel levels are not only dramatically increased in GC B cells, but also GC B cells are characterized by an enhanced c-Rel nuclear translocation in comparison to non-GC B cells. On the contrary, c-Rel is primarily cytoplasmic in plasma cells.

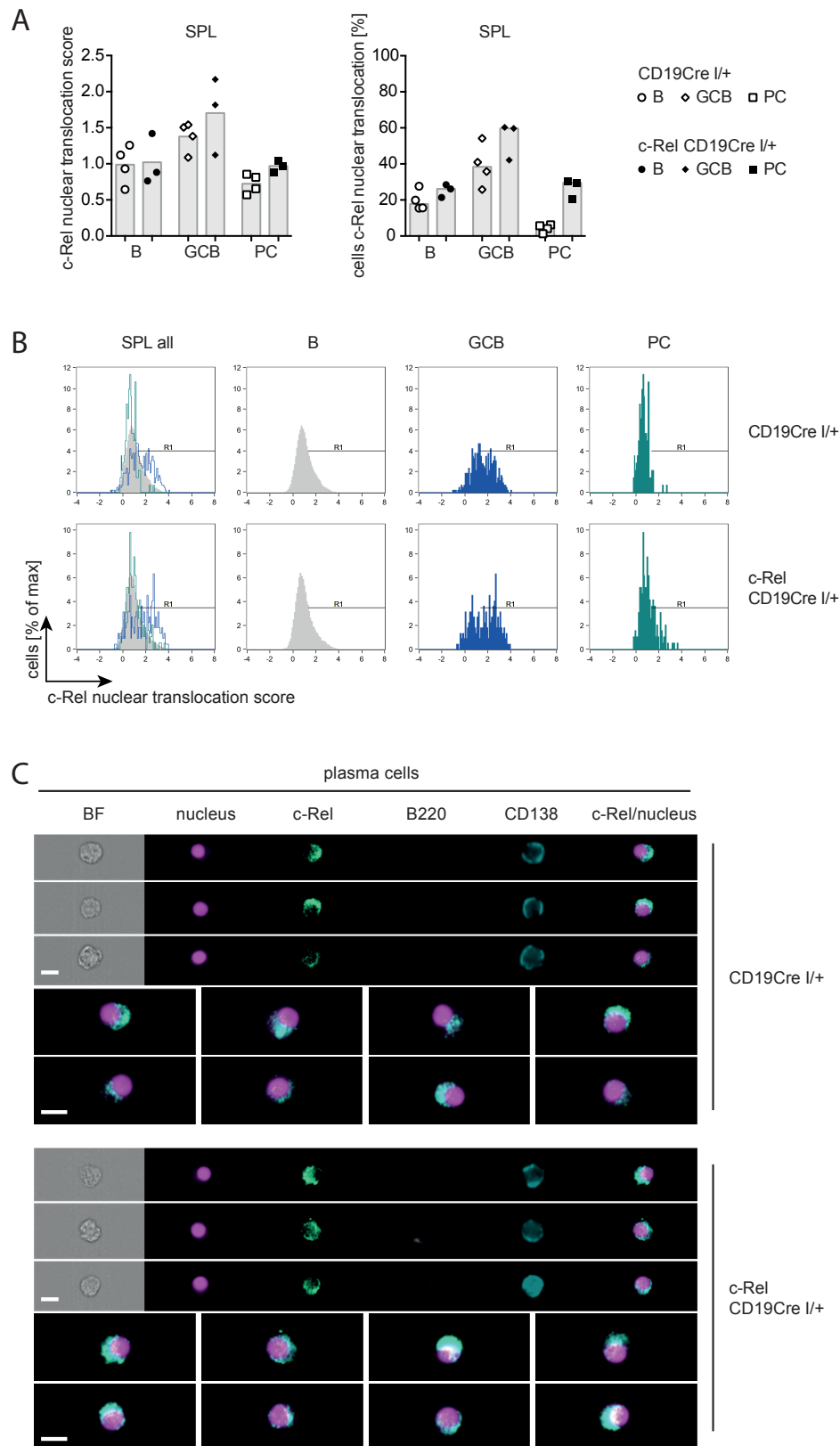


Figure 28: Cytoplasmic c-Rel localization in plasma cells. (A) Median c-Rel nuclear localization score and percentage of cells with c-Rel nuclear translocation for splenic B cells, GC B cells and plasma cells directly analyzed *ex vivo*. Individual data points obtained in 2 independent experiments and bars representing median values are plotted. (B) Representative histograms for c-Rel nuclear translocation score. (C) Representative images for splenic plasma cells. A panel of images for indicated channels as well as magnified images of merged c-Rel/nucleus signals are displayed for each genotype. Exemplary cells were selected based on average nuclear localization scores. GCB B220⁺CD95^{high}CD38^{low}; B (non-GCB) B220⁺CD95⁺CD38^{high}; plasma cells (PC) B220^{low}CD138⁺; white bar, 10 μ m; BF, bright field.

1.7.4 Strong correlation of c-Rel level with GC B cells and plasma cells

Based on the particularly high c-Rel levels observed in transgenic GC B cells combined with an expansion of this cell type, I aimed at analyzing the relation of GC B cell percentages and c-Rel level. For this study, I integrated data obtained for controls and the novel mouse models presented in this thesis. The highest c-Rel expression in GC B cells is observed for the c-Rel transgenic mouse line presented for the major analysis of this work, while GFP-c-Rel transgenic mice express intermediate total c-Rel levels (compare Figure 22 and Figure S30). The elementary endogenous c-Rel level of control mice complements the extensive data set to span a range of different c-Rel levels in GC B cells.

Remarkably, I found a highly significant positive correlation of GC B cell percentage and c-Rel protein expression level in all analyzed organs comprising spleen and lymph nodes as well as the gut-associated mesenteric lymph nodes and Peyer's patches (Figure 29A). Accordingly, c-Rel CD19Cre^{1/+} transgenic mice are not only characterized by the highest c-Rel level in GC B cells but also show the highest accumulation of GC B cells. In addition, a comparable result is obtained for the same analysis of c-Rel levels and percentages of plasma cells (Figure 29B). Consistently, a significant correlation of c-Rel level with the GC B cell and plasma cell gain is determined for cell numbers (Figure S45). These data demonstrate that the expansion of GC B cells and plasma cells as a consequence of c-Rel overexpression in (GFP-)c-Rel CD19Cre^{1/+} mice significantly correlates with the enhanced c-Rel level in these cells.

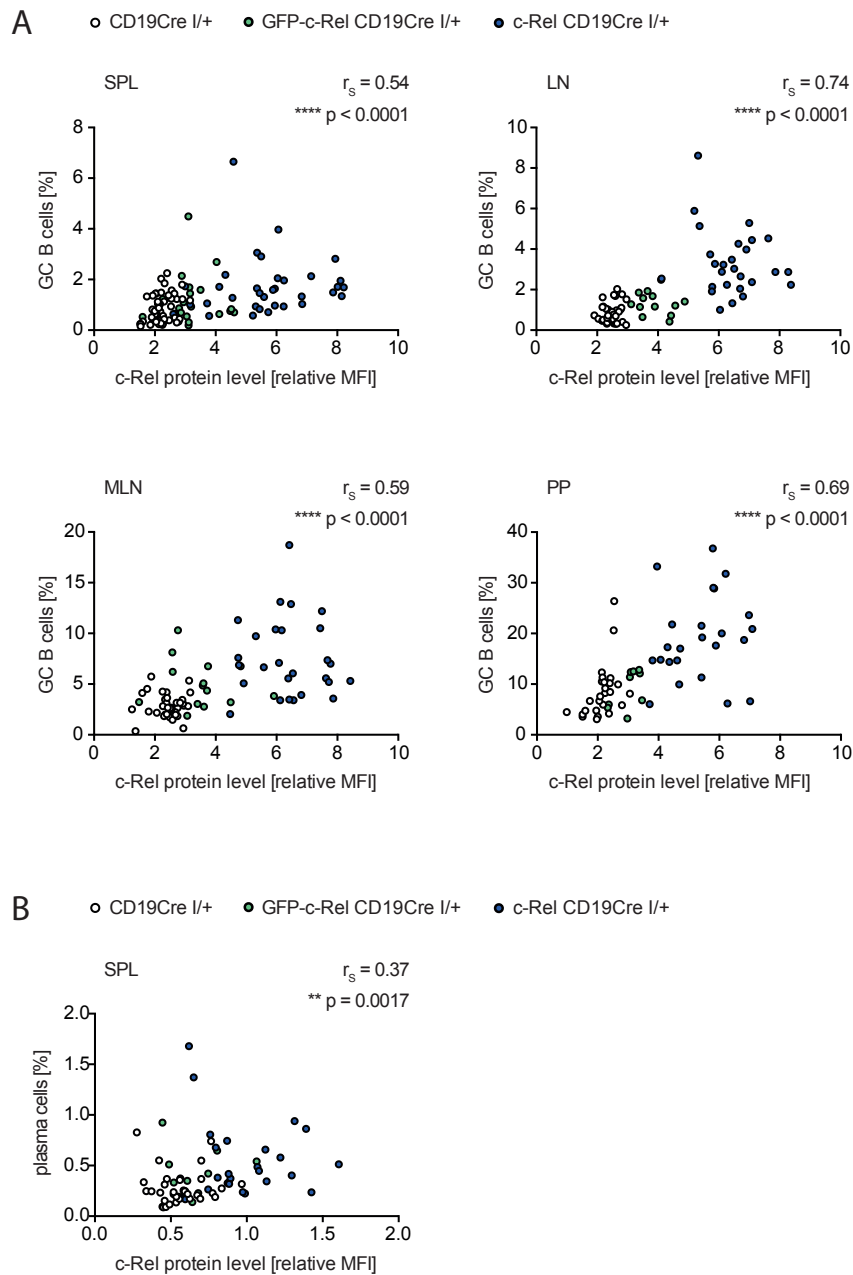


Figure 29: Strong positive correlation of c-Rel levels with cellular expansion of GC B cells and plasma cells. Individual data points for c-Rel level and percentage of (A) GC B cells or (B) plasma cells is plotted. c-Rel levels are relative median fluorescence intensity (MFI) values normalized to the B cell population excluding GC B cells or plasma cells, respectively, of CD19Cre^{I/+} control mice in each experiment. Spearman correlation coefficient (r_s) and respective statistical significance analysis p values (two-tailed) are given for each dataset. GCB: $n_{SPL} = 110$; $n_{LN} = 77$; $n_{MLN} = 78$; $n_{PP} = 59$; PC $n_{SPL} = 70$; GCB CD19⁺/B220⁺CD95^{high}CD38^{low}; plasma cells (PC) B220^{low}CD138⁺; SPL, spleen; LN, lymph nodes; MLN, mesenteric lymph nodes; PP, Peyer's patches.

1.7.5 Higher proliferation could contribute to expansion of GC B cells

GC B cells are in principle highly proliferative, but at the same time this post-activated B lineage population is highly prone to apoptotic cell death [Victoria and Nussenzweig, 2012; De Silva and Klein, 2015] (see also introduction subsection 1.2.1). In order to elucidate the mechanism of how higher c-Rel levels in c-Rel CD19Cre^{I/+} transgenic mice lead to an expansion of GC B cells, analysis of apoptosis and cell cycle was performed as alterations in cell death or proliferation could underlie this interesting phenotype. Preliminary quantification of apoptosis indicates that GC B cells of c-Rel CD19Cre^{I/+} mice could be to a certain extent less sensitive to apoptosis *in vitro* based on a lower proportion of apoptotic cells within the GC B cell population (Figure S46B).

Remarkably, *ex vivo* analysis of cell cycle stages of GC B cells in lymph nodes demonstrates that a significantly higher proportion of c-Rel CD19Cre^{I/+} transgenic GC B cells exists in the proliferative G2 and S phase of the cell cycle, while a significantly lower percentage of GC B cells accounts for cells within the G0/G1 stage (Figure 30A). Splenic GC B cells of c-Rel CD19Cre^{I/+} mice are characterized by a comparable shift to a higher proportion in proliferative cell cycle phases (Figure 30B).

Although in mesenteric lymph nodes and Peyer's patches no significant difference within the GC B cell population is observed (Figure S48), the total B cell population shows a significantly higher percentage of G2/S phase proliferative cells accompanied by a reduction of G0/G1 resting cells reflecting the enlarged GC population in c-Rel CD19Cre^{I/+} transgenic mice (Figure S47A).

In conclusion, higher proliferative capacities of c-Rel transgenic GC B cells could contribute to the expansion of this population in c-Rel CD19Cre^{I/+} mice.

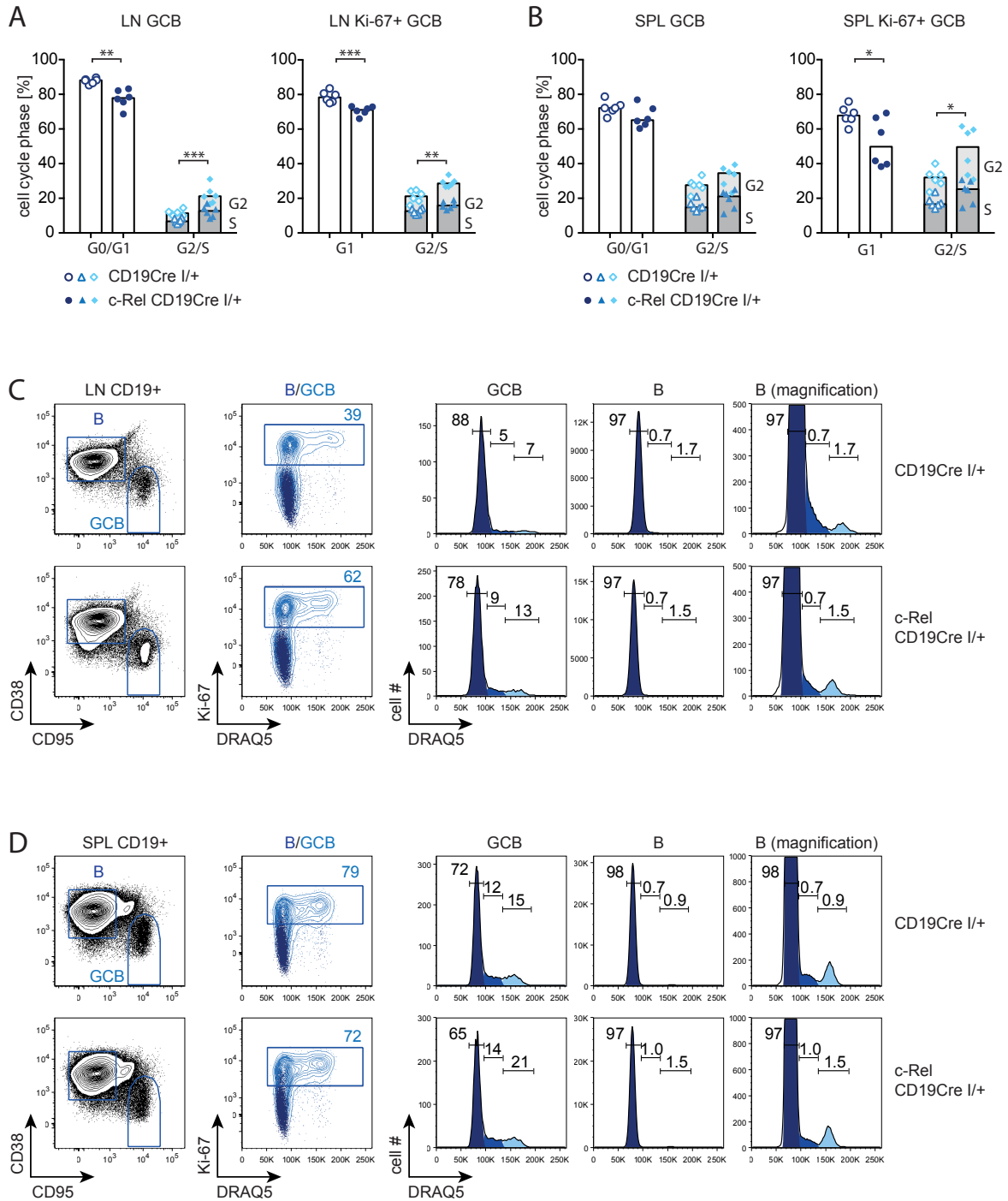


Figure 30: Increased proliferation in GC B cells of c-Rel CD19Cre^{I/+} mice. Percentages of GC B cells in cell cycle phases for (A) lymph nodes and (B) spleen from c-Rel CD19Cre^{I/+} or CD19Cre^{I/+} mice. Percentages of total GC B cells represent cells in G0/G1 and G2/S cell cycle phases, whereas Ki-67-expressing GC B cells include only cells in G1 and G2/S cell cycle phases as the proliferation marker Ki-67 is present in active cell cycle phases but absent in G0 resting cells [Scholzen and Gerdes, 2000]. Individual data points obtained in 3 independent experiments are plotted and bars represent median values. Representative flow cytometry plots and histograms of (C) lymph nodes and (D) spleen illustrating the gating and analysis strategy. In the Ki-67/DRAQ5 staining plot a light blue contour plot of GC B cells is overlaid with a dot plot of the B cell population in dark blue. Numbers in plots represent median percentages. Colors of cell cycle stages in histograms correspond to colors used in bar graphs: G0/G1 dark blue, S medium blue, G2 light blue. * $p \leq 0.05$, ** $p \leq 0.01$, *** $p \leq 0.001$, unpaired t test. GCB CD19⁺CD95^{high}CD38^{low}; B (non-GCB) CD19⁺CD95⁻CD38^{high}; SPL, spleen; LN, lymph nodes.

1.8 c-Rel levels are tightly regulated

1.8.1 c-Rel levels are limited in GC B cells of double transgenic mice

In light of the correlation between c-Rel expression level and the expansion of GC B cells and plasma cells, I crossed the c-Rel and GFP-c-Rel transgenic mouse lines to generate c-Rel/GFP-c-Rel CD19Cre^{I/+} double transgenic mice. Comprehensive comparative analyses of c-Rel CD19Cre^{I/+}, GFP-c-Rel CD19Cre^{I/+} and c-Rel/GFP-c-Rel CD19Cre^{I/+} mice with CD19Cre^{I/+} controls were performed. GC B cell populations are enlarged in all three c-Rel transgenic mouse models as expected. Nevertheless, the extent of GC B cell expansion in c-Rel/GFP-c-Rel CD19Cre^{I/+} double transgenic mice is only slightly higher in lymph nodes and gut-associated lymphoid follicles compared to c-Rel CD19Cre^{I/+} single transgenic mice, but this marginal increase is not significant (Figure S49). Plasma cell numbers in spleen and bone marrow are higher in c-Rel/GFP-c-Rel CD19Cre^{I/+} double transgenic mice compared to c-Rel CD19Cre^{I/+} single transgenic mice, but also not significantly changed (Figure S50).

Quantification of c-Rel protein expression demonstrates that total c-Rel levels in GC B cells and plasma cells are comparable in c-Rel CD19Cre^{I/+} single and c-Rel/GFP-c-Rel CD19Cre^{I/+} double transgenic mice (Figure 31 and Figure S51). Hence, despite the additional c-Rel transgene locus, total c-Rel levels are not further increased. Intriguingly, GFP-c-Rel levels based on GFP fluorescence signals are lower in c-Rel/GFP-c-Rel CD19Cre^{I/+} double transgenic mice compared to GFP-c-Rel CD19Cre^{I/+} single transgenic mice (Figure 32). This decrease of GFP-c-Rel levels in double transgenic mice is independent of cell size (Figure S52). These findings suggest that there is a limit to total c-Rel protein amounts in GC B cells and provides evidence for a tight regulation of c-Rel levels not only in naive B cells but also in GC B cells.

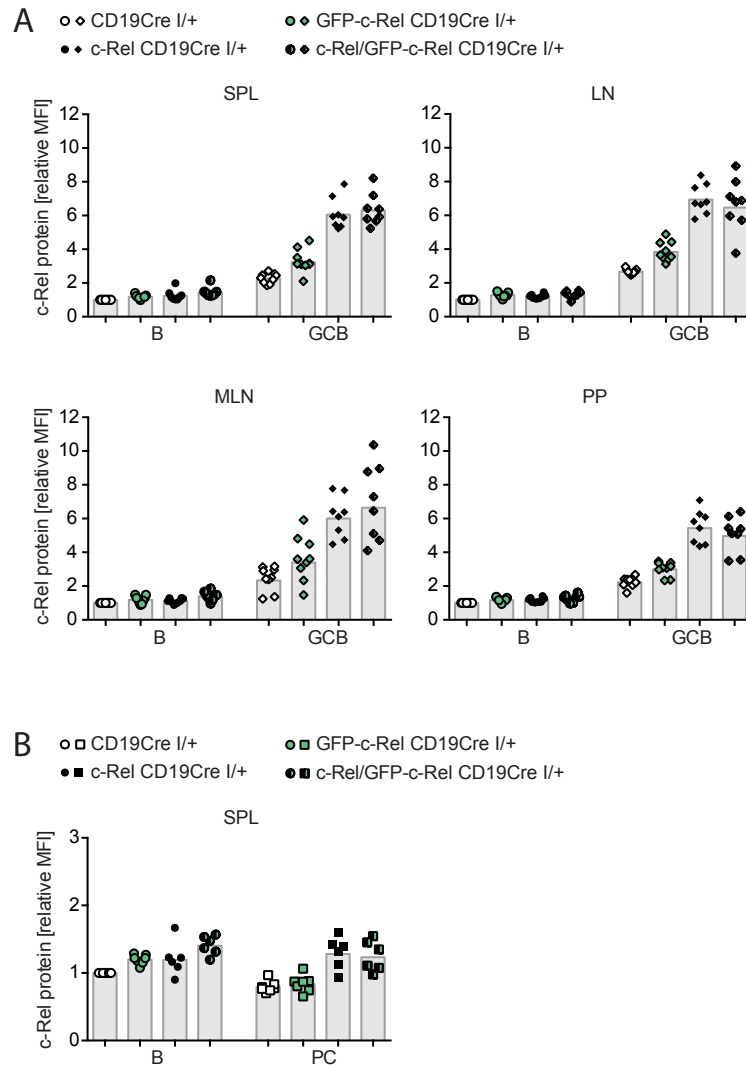


Figure 31: c-Rel levels in c-Rel/GFP-c-Rel CD19Cre^{I/+} double transgenic mice are comparable to c-Rel CD19Cre^{I/+} single transgenic mice. Intracellular flow cytometry data of c-Rel protein levels in B cell subpopulations. Median fluorescence intensities (MFI) were normalized to CD19Cre^{I/+} controls. Individual data points obtained in ≥ 3 independent experiments and bars representing geometric means are plotted. (A) c-Rel level in B cells and GC B cells. MFIs were normalized to non-GC B cells of CD19Cre^{I/+} controls. GCB B220⁺CD95^{high}CD38^{low}; B (non-GCB) B220⁺CD95^{high}CD38^{high}; plasma cells (PC) B220^{low}CD138⁺; B (non-PC) B220⁺CD138⁻; SPL, spleen; LN, lymph nodes; MLN, mesenteric lymph nodes; PP, Peyer's patches.

1.8.2 c-Rel level in B cells is sensitive to proteasomal inhibition

The dramatic switches in c-Rel level in different B lineage subpopulations, which are phenocopied by c-Rel transgenic mice despite the in principle high activity of the CAG promoter in these cell types, prompted me to address the mechanism of this to date unidentified regulation. It has been previously shown that c-Rel can be modified by post-translational modifications (see introduction subsection 2.2.3). In T cells ubiquitination and subsequent proteasomal degradation serves as a regulatory mechanism to control c-Rel levels [Chang et al., 2011].

In light of a possible control of c-Rel protein on a post-translational level, I treated splenocytes with the proteasome inhibitor MG-132 for 6 h or 12 h in culture and subsequently quantified c-Rel levels by intracellular flow cytometry as it allows simultaneous analysis of B cells and GC B cells. As GC B cells are highly prone to cell death, I added the pan-caspase inhibitor Q-VD to prolong the survival of GC B cells *in vitro*. Interestingly, inhibition of the proteasome causes an increase of c-Rel levels relative to untreated cells in B cells but not in GC B cells (Figure 33A). In detail, c-Rel levels in GC B cells remain unchanged after 6 h or 12 h of proteasomal inhibition, whereas c-Rel protein expression in B cells reaches an amount comparable to the elementary level observed in GC B cells (Figure 33B). This sensitivity of c-Rel levels in response to proteasomal inhibition is observed in both CD19Cre^{I/+} control and GFP-c-Rel CD19Cre^{I/+} transgenic mice.

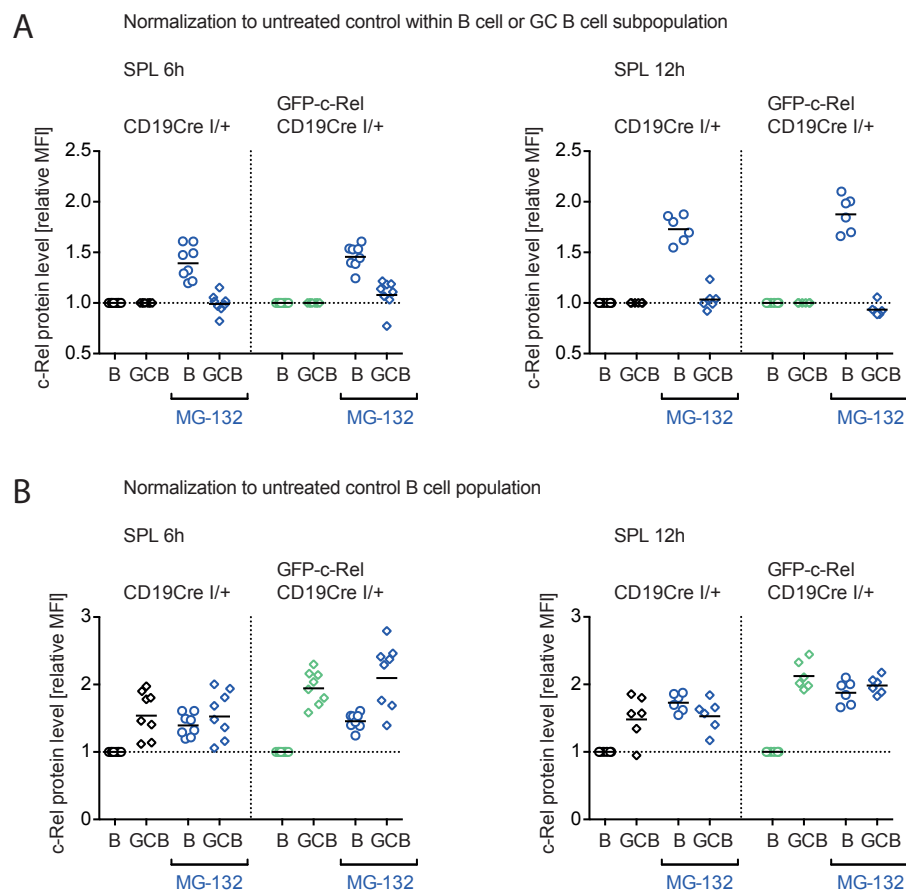


Figure 33: c-Rel level in B cells is sensitive to proteasomal inhibition. Splenocytes were treated or left untreated for indicated time periods with MG-132 in the presence of Q-VD to prolong the survival of GC B cells in culture followed by analysis of total c-Rel levels by intracellular flow cytometry. Individual data points and geometric means of 3 (6 h) or 2 (12 h) independent experiments are plotted. (A) Normalization of c-Rel median fluorescence intensities (MFI) to untreated control within the B cell or GC B cell subpopulation for each genotype. (B) Normalization of c-Rel MFI to untreated control of B cell population for each genotype. MG-132 25 μ M or 50 μ M; Q-VD 10 μ M or 20 μ M; GCB CD19⁺CD95^{high}CD38^{low}; B (non-GCB) CD19⁺CD95^{low}CD38^{high}; SPL, spleen.

1.9 Expression of the novel c-Rel Δ Ex9 splice variant

Alterations of c-Rel protein can impact c-Rel transactivation activity *in vitro* (see introduction subsection 3.2). A c-Rel splice variant lacking exon 9 has been shown to potentiate c-Rel transactivation activity in comparison to full length c-Rel *in vitro*. Intriguingly, this c-Rel Δ Ex9 splice variant was found to be expressed exclusively in DLBCL patients but not in healthy individuals [Leeman et al., 2008]. These data were reproduced in our laboratory [Kumar et al., unpublished].

I crossed my novel c-Rel transgenic mice to the FLPe-deleter strain [Rodríguez et al., 2000], in order to remove the Frt-flanked *REL* exon 9 to obtain c-Rel Δ Ex9 mice that conditionally express the shortened c-Rel protein without exon 9. c-Rel Δ Ex9 CD19Cre^{I/+} mice were compared to full-length transgenic c-Rel-expressing c-Rel CD19Cre^{I/+} mice and CD19Cre^{I/+} control mice (Figure S53-S58 and data not shown).

c-Rel Δ Ex9 CD19Cre^{I/+} mice are characterized by an expansion of GC B cells and plasma cells that is similar to c-Rel CD19Cre^{I/+} mice. Despite a more pronounced elevation of GC B cells in lymph nodes and mesenteric lymph nodes of c-Rel Δ Ex9 CD19Cre^{I/+} mice (Figure S53) and minimally higher plasma cell numbers (Figure S57), I did not encounter significant differences between c-Rel full length and c-Rel Δ Ex9 transgenic mice. Furthermore, total c-Rel protein levels assessed by intracellular flow cytometry are comparable in c-Rel Δ Ex9 CD19Cre^{I/+} and c-Rel CD19Cre^{I/+} transgenic mice (Figure S58).

2 Consequences of c-Rel knockdown in human B cell lymphoma cell lines

In light of the frequent *REL* gene locus amplifications in human B cell lymphomas, I applied a c-Rel loss-of-function approach to address the role of c-Rel in this disease context. Human B cell lymphomas with *REL* amplifications include classical Hodgkin lymphoma (cHL, 39%), diffuse large B cell lymphoma (DLBCL, 17%) and primary mediastinal B cell lymphoma (PMBCL, 28%). Amongst these disease entities, a positive correlation of *REL* gene locus amplification with c-Rel expression levels and nuclear c-Rel localization is predominantly observed in cHL and PMBCL (see introduction subsection 3.2). Accordingly, I chose 2 cHL cell lines, L-428 and U-HO1, and 2 PMBCL cell lines, MedB-1 and Karpas1106P, to investigate the consequences of c-Rel downregulation in human B cell lymphoma cell lines (see introduction subsection 3.3).

2.1 Strategy for c-Rel knockdown

In order to achieve c-Rel downregulation in human B cell lymphoma cell lines, I generated a system for transposon encoded inducible shRNA-mediated c-Rel or control knockdown. Here, shRNA expression is under control of an H1 promoter containing a tet operator (tetO) sequence that is repressed by the tetracycline repressor (tetR) [Kleinhammer et al., 2011]. As tetR is constitutively expressed from the same construct under a strong CAG promoter, this H1^{tetO} promoter is only active in the presence of doxycycline that impedes tetR binding to the promoter. In addition, these constructs contain a puromycin resistance cassette followed by the surface marker Thy1.1 connected by a self-cleaving 2A site [Szymczak et al., 2004; Kim et al., 2011] and linked to CAG-controlled tetR expression by an internal ribosomal entry site (IRES) sequence (Figure 34A). To facilitate stable genomic integration of the shRNA constructs, the transposases hyperactive piggyBac (hyPB) and sleeping beauty (sb100x) were applied as transposase-mediated cut-and-paste integration has the advantage of generating single integrants in diverse loci opposed to bulk copy integration [Izsvák et al., 2009; Mátés et al., 2009; Yusa et al., 2011]. shRNA knockdown sequences used in this thesis for shRNAs targeting c-Rel [Barbie et al., 2009; Meylan et al., 2009] and controls [Barbie et al., 2009; Cheung et al., 2011] have been published previously.

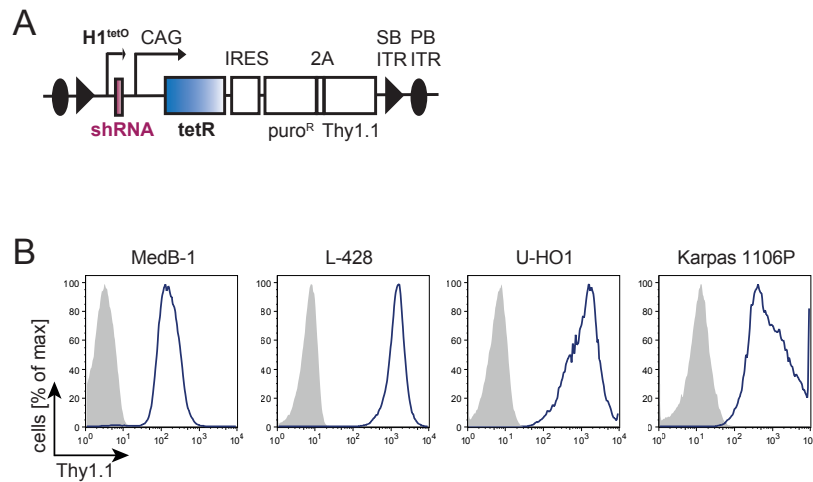


Figure 34: Strategy for c-Rel downregulation in B cell lymphoma cell lines. (A) Schematic representation of shRNA knockdown construct. Expression of an shRNA (red) is controlled by an H1^{tetO} promoter that contains a tet operator (tetO) sequence. Expression of the tetracycline repressor (tetR, blue) followed by an IRES(internal ribosomal entry site)-puromycin-resistance(puro^R)-2A-Thy1.1 cassette is driven by a constitutively active CAG promoter. The construct is flanked by inverted terminal repeat (ITR) recognition sites for the transposases hyperactive piggyBac (PB) and sleeping beauty 100x (SB). (B) Representative histograms displaying Thy1.1 expression in stable cell pools of indicated human B cell lymphoma cell lines carrying shRNA constructs as shown in (A).

Inducible transposon encoded shRNA knockdown constructs were transfected together with plasmids for transient transposase expression into the human B cell lymphoma cell lines by electroporation-based methods and subsequently selected with puromycin to generate stable cell pools. Selected cell pools with stable incorporation of the construct can be identified by expression of the surface marker Thy1.1 as assessed by flow cytometry (Figure 34B).

2.2 Efficient c-Rel knockdown in human lymphoma cell lines

c-Rel knockdown in the generated human lymphoma cell pools was induced by doxycycline and the knockdown efficiency assessed by Western blot quantification. In L-428 cHL cells c-Rel knockdown can be observed already after 1 day of doxycycline treatment and reaches its maximum extent after 3 days as comparable results were obtained for knockdown efficiency after 3 to 5 days of doxycycline treatment (Figure 35). Similarly efficient knockdown is induced by 0.5 or 1 $\mu\text{g}/\text{ml}$ doxycycline (Figure 36A).

The efficiency of c-Rel knockdown in cHL cell lines L-428 and U-HO1 as well as the PMBCL cell lines MedB-1 and Karpas 1106P is summarized in Figure 36B-E. Cell pools for 3 different shRNAs targeting c-Rel and 3 control shRNAs were generated from each cell line. In part, independent cell pools were generated for the same shRNA to verify

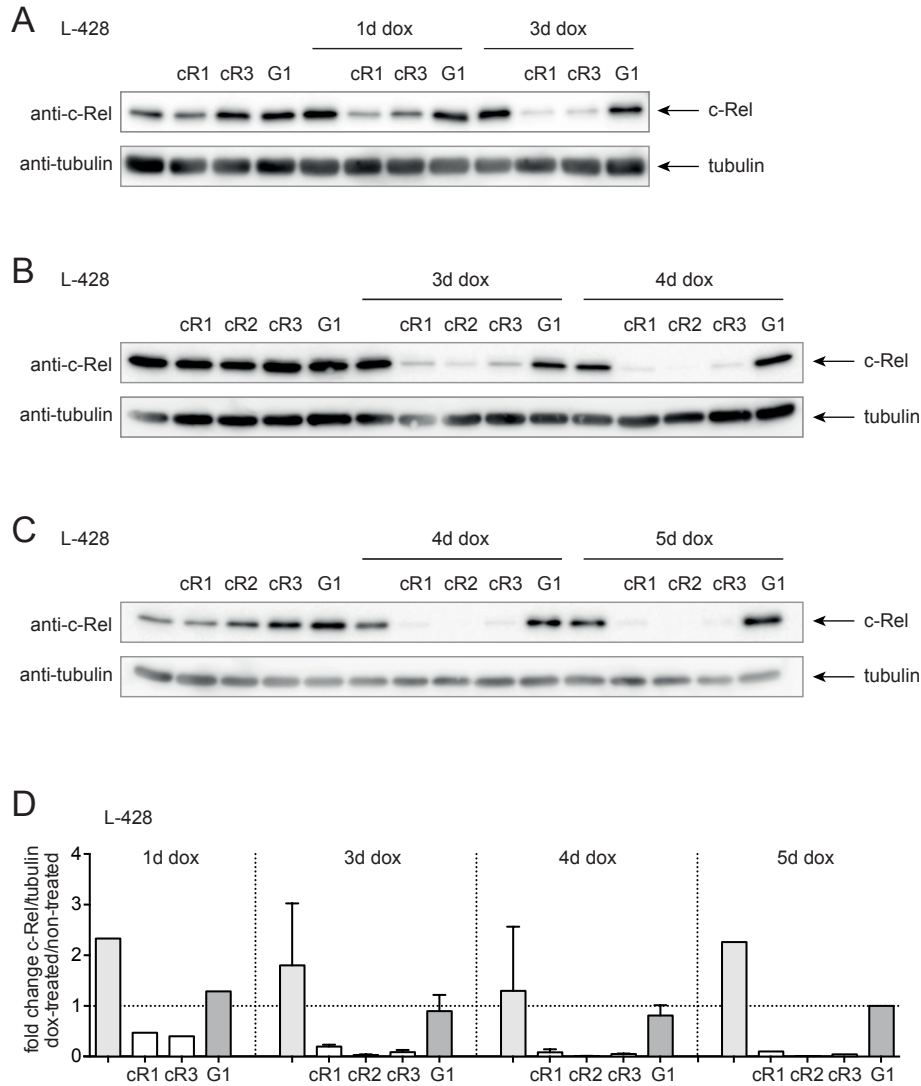


Figure 35: Kinetics of doxycycline-inducible c-Rel knockdown. (A-C) Representative Western blots of shRNA-mediated c-Rel knockdown in L-428 cell pools. Cells were treated with 1 μ g/ml doxycycline or left untreated for the indicated time periods. (D) Quantification of Western blot c-Rel protein levels in L-428 for different doxycycline treatment periods (1 day to 5 days). c-Rel levels are normalized to tubulin and the fold change difference of doxycycline-treated to untreated sample for each cell pool is displayed. Bars represent means and error bars are the standard error of the mean. $n_{1d}=1$, $n_{3d}=3$, $n_{4d}=2$, $n_{5d}=1$. cR1/2/3, shcRel 1/2/3; G1, shGFP 1; dox, doxycycline; d, day.

the results. The highest knockdown efficiency is achieved in MedB-1 and L-428 cell lines reaching efficiencies greater than 90% for all 3 shRNAs targeting c-Rel in MedB-1. In cell pools of U-HO1 and Karpas 1106P knockdown efficiency for the 3 c-Rel-targeting shRNAs varies and is in part only moderate to low.

The c-Rel knockdown was verified by intracellular flow cytometry measurement of c-Rel protein levels in MedB-1 cell pools (Figure 37). The uniform distribution of reduced c-Rel expression in the cell pool visualized by flow cytometry indicates that c-Rel is downregulated to a comparable extent in the entire cellular population (Figure 37B).

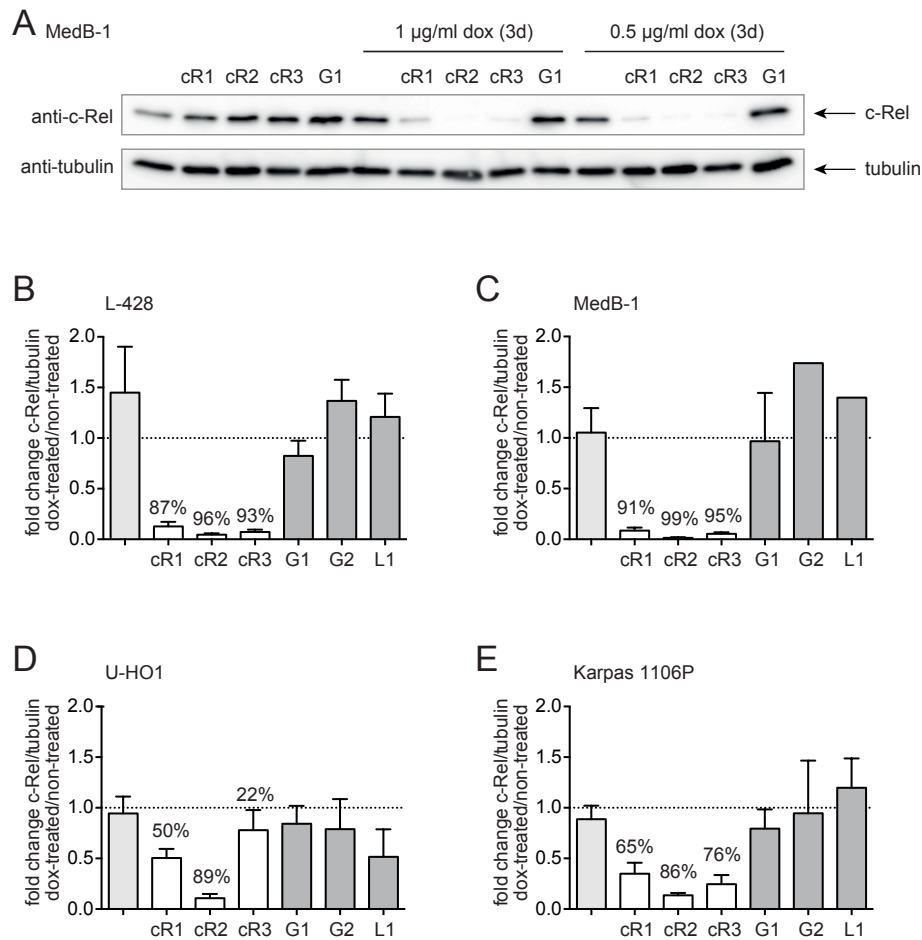


Figure 36: Efficient doxycycline-inducible c-Rel knockdown in MedB-1 and L-428 human B cell lymphoma cell pools. (A) Representative Western blots of shRNA-mediated c-Rel knockdown in MedB-1 cell pools. Cells were treated with 1 $\mu\text{g/ml}$ or 0.5 $\mu\text{g/ml}$ doxycycline or left untreated for 3 days. (B-E) Quantification of Western blot c-Rel protein levels. c-Rel levels are normalized to tubulin and the fold change difference of doxycycline-treated to untreated sample for each cell pool is displayed. Displayed data was obtained in ≥ 2 independent experiments including 1-4 independently generated cell pools for each construct. Bars represent means and error bars are the standard error of the mean. L-428: 3d, 0.5/1 $\mu\text{g/ml}$ dox; MedB-1: 3d, 0.5 $\mu\text{g/ml}$ dox; U-HO1: 3d, 0.5/1 $\mu\text{g/ml}$ dox; Karpas: 3d/5d, 0.5 $\mu\text{g/ml}$ dox. cR1/2/3, shcRel 1/2/3; G1/G2, shGFP 1/2; L1, shLacZ; dox, doxycycline; d, day.

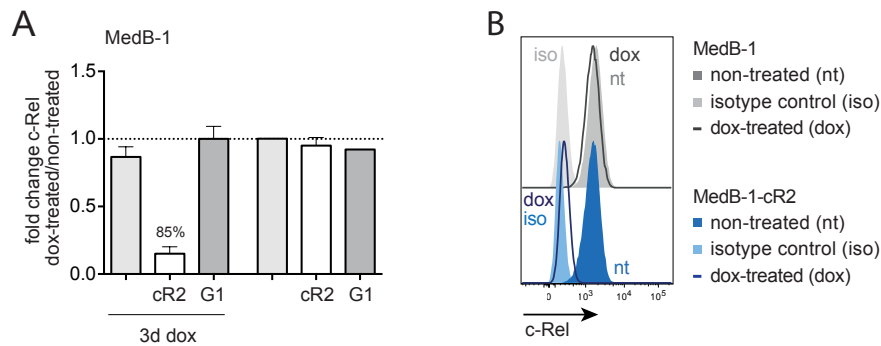


Figure 37: Verification of efficient doxycycline-inducible c-Rel knockdown by flow cytometry. (A) Quantification of c-Rel knockdown of shcRel2 and shGFP 1 control by flow cytometry. Quantification is based on median fluorescence intensity values (MFI) by subtraction of values for isotype control or unstained cells and normalization of all samples to untreated MedB-1 or in case no untreated population was included in the experiment normalization to doxycycline-treated MedB-1 control cell line. Data from 1 (shGFP 1 untreated) to ≥ 3 (all others) independent experiments is shown. Bars represent means and error bars are the standard error of the mean. (B) Representative histograms of intracellular flow cytometry staining of c-Rel upon doxycycline treatment of MedB-1 control cell line and MedB-1 cell pool carrying shcRel2. cR2, shcRel2; G1, shGFP 1; dox, doxycycline; d, day.

2.3 c-Rel knockdown in MedB-1 cells reduces cellular expansion

Activation of c-Rel can contribute to cell survival and proliferation (see introduction section 2). In order to investigate consequences of c-Rel knockdown, I therefore analyzed cell proliferative capacities assessed by cell count upon doxycycline treatment of MedB-1 and L-428 cell pools as I could achieve high knockdown efficiencies of $\geq 85\%$ in these cell pools.

c-Rel knockdown leads to decreased cell numbers in MedB-1 cells (Figure 38A). Reduced cell counts for shcRel 2/3 but not the control shGFP 1/2 and shLacZ appear around 6 days of doxycycline treatment and continue to decline subsequently. In contrast, no difference with regard to cell counts could be observed in L-428 cell pools upon doxycycline treatment to induce c-Rel downregulation (Figure 38C).

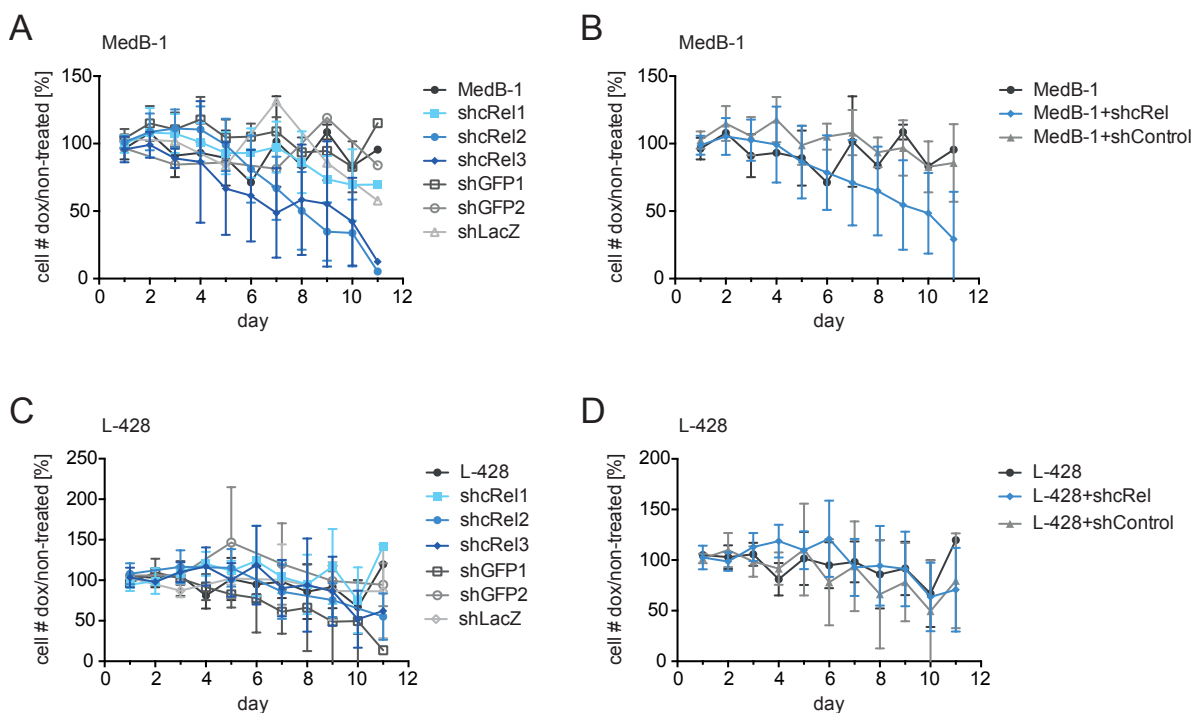


Figure 38: Cell numbers of MedB-1 and L-428 cell pools upon induced c-Rel knockdown. (A, B) MedB-1 or (C, D) L-428 cell pools were treated with doxycycline or left untreated. Viable cell count was assessed starting at day 1 following treatment start. Data are cell numbers of treated normalized to untreated samples for original cell line or each cell pool. Data points and error bars represent mean values and standard deviation, respectively. Data are combined from 3 independent experiments for 1-4 independent cell pools for each construct. While in (A, C) data for each c-Rel knockdown and control cell pool are shown individually, the average of the 3 shcRel or control cell pools based on the same dataset is shown in (B, D). cR1/2/3, shcRel 1/2/3; G1/G2, shGFP 1/2; L1, shLacZ; dox, doxycycline.

2.4 c-Rel knockdown causes a clear disadvantage in competitive co-cultures

Based on the interesting results of the cell count assay, I designed a co-culture assay that allows evaluating the effects of c-Rel knockdown under competitive conditions. For this purpose, cell pools carrying c-Rel or control knockdown constructs were cultured in equal ratios with the unmodified original cell line in the absence or presence of doxycycline to induce shRNA expression in the cell pool. Thy1.1 surface expression on selected cell pools but not the original cell line allows distinction of shRNA construct-expressing cells in the mixed culture (Figure 39A).

Remarkably, MedB-1 cells clearly outcompete MedB-1 cells with c-Rel knockdown but not any of the control shRNAs (Figure 39B). c-Rel knockdown causes a disadvantage in the competitive co-culture as early as day 3 after shRNA induction consistent with the strong knockdown efficiency observed at this timepoint. MedB-1 cell pools carrying shcRel 2/3 disappear within the following days until they are almost extinguished at day 11 after induction of c-Rel knockdown. Despite an efficient c-Rel knockdown observed for all 3 shRNAs targeting c-Rel, the cell pool carrying shcRel 1 does not show a disadvantage in co-culture with the original MedB-1 cell line. This finding corresponds to data obtained in the cell count assay (Figure 38A) and correlates with the lower knockdown efficiency for shcRel 1 in comparison to shcRel 2/3 (Figure 36C).

Preliminary results indicate that under competitive conditions L-428 cells show a trend for a slightly reduced percentage of the population with c-Rel knockdown relative to the respective uninduced cell pool and in comparison to control shRNAs (Figure 39C). However, this tendency is by far not as pronounced as the observed competitive disadvantage in MedB-1 cells upon c-Rel knockdown.

Analysis of cell viability data obtained during the competitive co-culture assays demonstrates that viability is not altered in either the mixed cultures of shRNAs targeting c-Rel or of shRNA controls upon doxycycline-induced shRNA expression (Figure 39D). Accordingly, enhanced cell death is most likely not the reason for the disadvantage of MedB-1 cells with c-Rel downregulation in a competitive setting. In agreement with this finding, analysis of apoptosis by active caspase staining suggests that c-Rel knockdown in MedB-1 cells does not cause apoptotic cell death (Figure 39F).

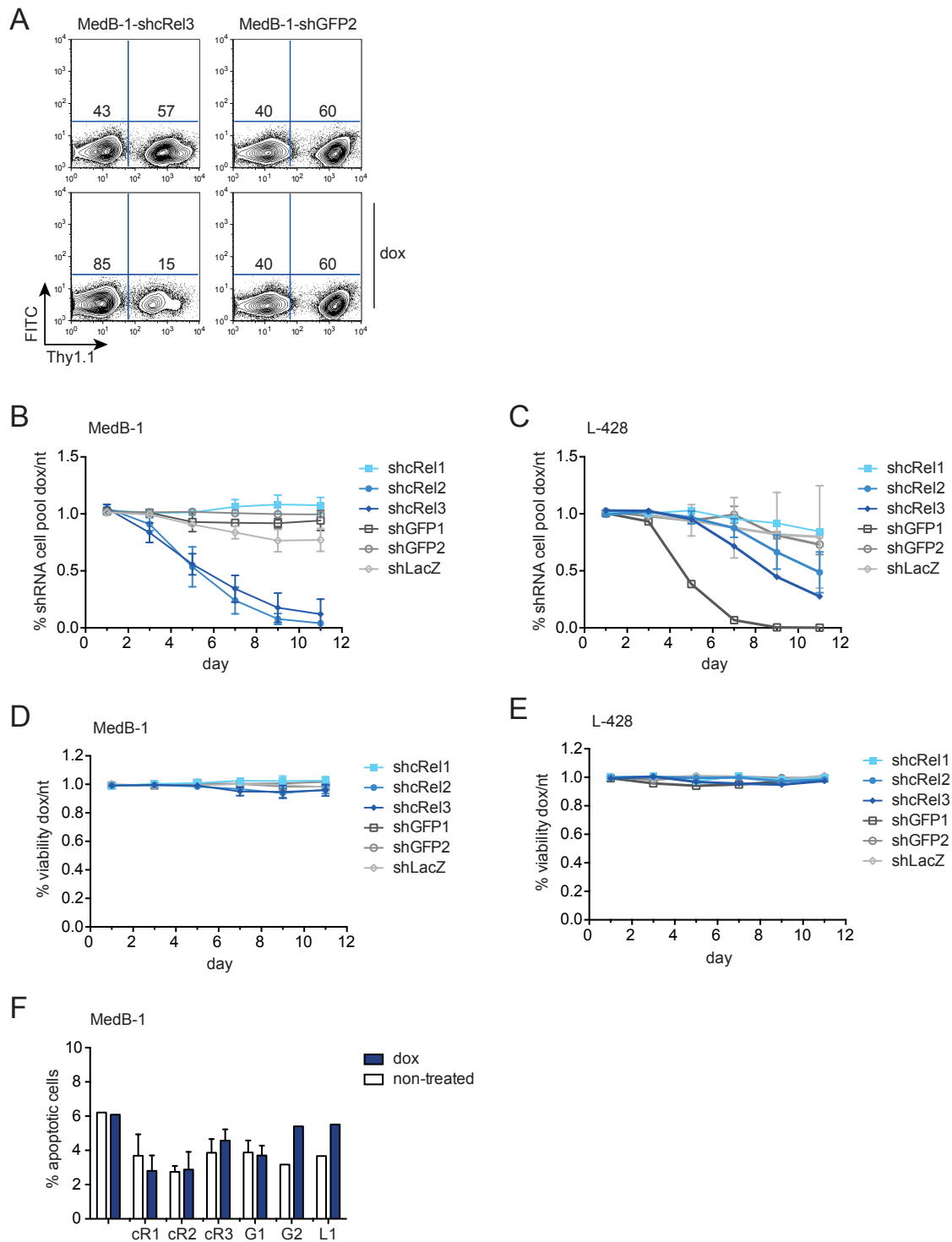


Figure 39: c-Rel knockdown in MedB-1 cells causes competitive disadvantage in co-culture.

Percentages of Thy1.1⁺ cells in doxycycline-treated mixed cultures of a distinct cell pool were normalized to the percentage of Thy1.1⁺ cells in the respective untreated mixed culture. Data points and error bars represent mean values and standard deviation, respectively. (A) Representative flow cytometry plots of competitive co-culture on day 7 of assay. Numbers are percentages of Thy1.1⁺ and Thy1.1⁻ cells for the shown data set. (B) MedB-1. Data are combined from 2 independent experiments for 1-2 independent cell pools for each construct. (C) L-428. Data are from 1 experiments for 1-4 independent cell pools for each construct. Cell viability data for (D) MedB-1 and (E) L-428 of the competitive co-culture assays shown in (B, C). Percentages of viable cells in doxycycline-treated mixed cultures were normalized to respective untreated mixed cultures. (F) MedB-1 cells or MedB-1 cell pools of indicated shRNA constructs were treated with doxycycline or left untreated for 4 days and apoptotic cells were assessed by flow cytometric active caspase staining. Data are from 1 experiment for 1-2 independent cell pools for each construct. cR1/2/3, shcRel 1/2/3; G1/G2, shGFP 1/2; L1, shLacZ; dox, doxycycline; nt, non-treated.

2.5 c-Rel knockdown reduces proliferative cell cycle phases

I next aimed at elucidating the mechanism underlying the observed phenotype upon c-Rel knockdown in MedB-1 cells. c-Rel is involved in cell cycle progression as studies in c-Rel-deficient mouse B cells demonstrate a block in early G1 cell cycle stage and failure to transit to S phase (see introduction subsection 2.2.6).

Interestingly, cell cycle analysis demonstrates that c-Rel knockdown in MedB-1 cells leads to a strong reduction of cells in the proliferative S and G2 phase of the cell cycle in contrast to control cell pools and untreated cell pools (Figure 40). A decrease in proliferative capacities in MedB-1-shcRel 2/3 cell pools can already be observed after 4 days of doxycycline treatment. While in untreated MedB-1 cell pools roughly one third of the population accounts for each of the three determined cell cycle fractions – G0/G1, S and G2 – more than 70% of MedB-1-shcRel 2 cells accumulate in G0/G1 phase upon c-Rel knockdown after 10 days of doxycycline treatment. Again, no alteration in the proliferative population is observed for knockdown mediated by shcRel 1.

In conclusion, c-Rel knockdown in MedB-1 human B cell lymphoma cells reduces the percentage of cells in proliferative S and G2 cell cycle stages and consequently results in decreased proliferation and a clear competitive disadvantage in co-culture with MedB-1 cells that express regular c-Rel protein levels. These strong consequences of c-Rel knockdown are observed for two out of three shRNAs targeting c-Rel. Whether the absence of these deficits for shcRel 1 could be due to a threshold effect based on the lower but still > 90% knockdown efficiency of this shRNA remains to be determined.

The results of this cell line-based study indicate that high c-Rel expression could play a role in maintaining proliferative capacities in human B cell lymphoma cells. While the PMBCL cell line MedB-1 clearly relies on c-Rel expression for sustained proliferation, the cHL lymphoma cell line L-428 seems to be less dependent on c-Rel, although there is a trend for a contribution of c-Rel to proliferation in a competitive scenario.

Figure 40: (figure on following page) MedB-1 cells stably expressing indicated shRNA constructs were treated with doxycycline or left untreated for (A) 4 days, (B) 6 days, (C) 8 days and (D) 10 days followed by flow cytometric cell cycle analysis. Data are combined from 2 independent experiments for 1-2 independent cell pools for each construct. Bars and error bars represent mean values and standard deviation, respectively. (E-H) Representative histograms of cell cycle stages for the data shown in (A-D). Color code for cell cycle stages: G0/G1 white, S grey, G2 dark blue. Percentages of cell cycle stages are mean values of the indicated cell pools. cR1/2/3, shc-Rel 1/2/3; G1/G2, shGFP 1/2; L1, shLacZ; dox, doxycycline; PI, propidium iodide; d, day.

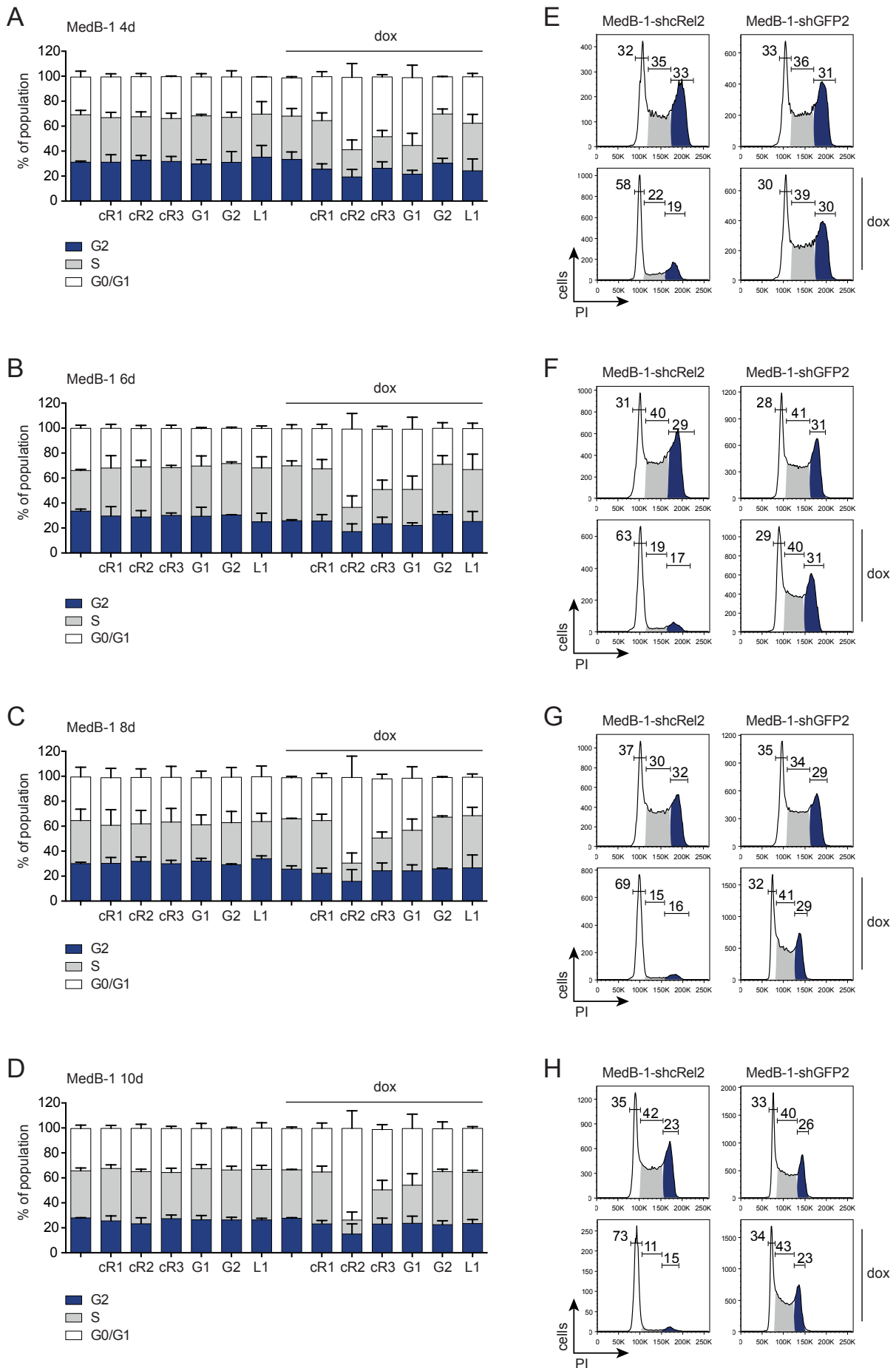


Figure 40: Cell cycle analysis in MedB-1 cell pools upon c-Rel knockdown. For figure legend see previous page.

Part V

Discussion

In this thesis, I present comprehensive analyses of the first mouse models for cell type-specific overexpression of c-Rel. My study established the first *in vivo* data regarding the consequences of enhanced c-Rel expression in B cells, GC B cells and plasma cells. Furthermore, the quantification of general c-Rel expression levels in B cell subpopulations also led to the discovery of fundamental regulatory mechanisms restricting c-Rel expression in B cell subtypes.

1 Generation of the first conditional c-Rel transgenic mouse models

Much that is known about the immune system today has been established in genetically engineered mouse models that can yield invaluable information of systemic cellular functions *in vivo*. In particular lymphocytes are tightly intertwined with their microenvironment composed of both immune and non-immune cells limiting *in vitro* recapitulation and eventually requiring mouse models to precisely delineate lymphocyte function.

Conventional c-Rel knockout mice were established more than 20 years ago [Kontgen et al., 1995] and mice carrying a conditional c-Rel allele were published recently [Heise et al., 2014]. Carrasco et al. generated mice that express the transforming viral gene v-Rel of an oncogenic avian retrovirus in the mouse thymus [Carrasco et al., 1996] and a mouse line that expresses a carboxy-terminal-truncated form of c-Rel lacking the TAD instead of endogenous c-Rel [Carrasco et al., 1998] (see introduction subsection 2.2.6). To my knowledge, beyond these studies only mice with c-Rel cDNA expression under a mouse mammary tumor virus promoter have been published [Romieu-Mourez et al., 2003]. Hence, despite the frequent *REL* locus amplifications in human B cell lymphomas and associations of single nucleotide polymorphisms within the *REL* gene with human autoimmune diseases (see introduction section 3), no mouse model to investigate the consequences of enhanced c-Rel function in a cell type-specific manner existed to date. Remarkably, Gerondakis et al. stated 10 years ago "Of note, my lab has been unable to generate transgenic mice with *c-rel* under the control of a B-cell-specific promoter,

suggesting that overexpression of c-Rel may be toxic at some stage of B-cell development (S Gerondakis, unpublished observations)” [Gerondakis et al., 2006]. This statement emphasizes the long-standing need for a conditional c-Rel gain-of-function mouse model and proves that the generation of such a model is not a trivial task.

The novel c-Rel transgenic mouse models presented in this thesis permit conditional expression of c-Rel/c-Rel Δ Ex9 or GFP-c-Rel from a single BAC-transgenic locus to facilitate dissection of an autonomous cell type-specific role of c-Rel overexpression. These carefully validated mouse models provide versatile tools for exploring c-Rel overexpression and basic function in future studies. Research could be extended from the B lineage as presented in this work to the T lineage, where c-Rel is known to have important functions for instance in T_{reg} cells (see introduction subsection 2.2.4), and other immune cell subsets as well as non-immune cells.

2 c-Rel in terminal B cell differentiation

Studies of c-Rel conventional and conditional knockout mice demonstrated that GC reactions are strikingly impaired or not maintained in the absence of c-Rel [Kontgen et al., 1995; Heise et al., 2014]. Nevertheless, gain-of-function experiments frequently do not inversely correlate with loss-of-function experiments. Here, I demonstrate for the first time that c-Rel overexpression causes an amplification of the GC reaction. This phenotype emerges irrespective of whether conditional c-Rel transgene expression is specifically induced in B cells (CD19Cre) or GC B cells (C γ 1Cre). Therefore, my results suggest that c-Rel overexpression does not drive GC B cell expansion during GC entry or during the very early GC seeding phase. This finding is consistent with Heise et al. who report that GC reactions can initially form in c-Rel^{f/f} C γ 1-Cre mice and conclude that c-Rel is required for GC maintenance [Heise et al., 2014]. C γ 1Cre-mediated recombination has been shown to affect 25-50% of GC B cells already at day 4 post-immunization [Casola et al., 2006], thus preceding vast GC B cell expansion and the fully mature GC state according to current models [Victora, 2014; De Silva and Klein, 2015] at least in a fraction of cells. c-Rel overexpression-mediated effects could influence the GC reaction as early as this phase. Nevertheless, the cell cycle analysis and the accumulation of class-switched plasma cells observed in the present work support the notion that c-Rel exerts its pivotal functions during the proliferative phase and mature stages of GC reactions.

Not only GC B cells are expanded in c-Rel transgenic mice, but also T_{fh} cells are gained to a certain extent although the c-Rel transgene is specifically expressed in B cells. While T_{fh} cells can promote GC B cell survival [Fazilleau et al., 2009; Vinuesa et al., 2010; Crotty, 2011] (see introduction subsection 1.2.1), it has also been shown that GC B cell-mediated signaling is important for T_{fh} cell development [Nurieva et al., 2008] highlighting the interdependent linkage of GC B cells and T_{fh} cells [Linterman et al., 2010]. This mutual impact provides a possible explanation for the observed T_{fh} cell increase.

The essential character of GC B cell- T_{fh} cell interactions is established by long-standing studies demonstrating that CD40 or CD40L deficiency [Xu et al., 1994; Kawabe et al., 1994] or blockade of CD40-CD40L signaling [Han et al., 1995; Foy et al., 1994] causes GC reactions to collapse. I demonstrate that anti-CD40 stimulation can trigger c-Rel nuclear translocation in GC B cells at least *in vitro*. T_{fh} cells have been shown to influence proliferation of GC B cells [Gitlin et al., 2014, 2015] and my data suggests that higher proliferation in c-Rel-overexpressing GC B cells contributes to the observed GC B cell expansion. I therefore hypothesized that c-Rel might be involved in mediating downstream effects of T_{fh} cell signals to GC B cells that culminate in proliferation.

LZ GC B cells expressing c-Myc were proposed to constitute a cellular fraction that re-enters the GC DZ where rapid proliferation occurs [Calado et al., 2012; Dominguez-Sola et al., 2012]. Of note, *Myc* mRNA levels are reduced upon anti-CD40 stimulation in c-Rel^{-/-} compared to wild-type B cells [Zarnegar et al., 2004], suggesting that c-Rel contributes to activation of c-Myc downstream of CD40. It would therefore be of interest to study c-Myc expression and c-Myc-dependent pathways in c-Rel transgenic mice.

Certainly, c-Rel is known to be directly involved in cell cycle control as studies in c-Rel^{-/-} B cells provide substantial evidence that c-Rel deficiency causes a block in G1 to S phase transition (see introduction subsection 2.2.6). Accordingly, it is also a possibility that elevated c-Rel levels independently promote higher proliferation. Only few cells are needed to seed and initiate GC formation [Schwickert et al., 2007] highlighting the massive proliferation that characterizes GC B cells. It can be imagined that also minor acceleration of proliferation or elongation of the proliferative phase driven by higher c-Rel levels in c-Rel transgenic mice could have strong potentiating effects as GC B cells cycle in repetitive rounds between LZ and DZ.

The complementary loss-of-function approach in B cell lymphoma cells lines presented in this thesis shows that c-Rel downregulation reduces the fraction of cells in proliferative

cell cycle stages in the MedB-1 B cell lymphoma cell line corroborating the idea that c-Rel levels influence cell cycle entry or progression to proliferative phases.

Plasma cells in c-Rel transgenic mice are highly class-switched accompanied by elevated serum titers of class-switched antibody isotypes. The opposite effect is observed in mice with c-Rel deficiency that show reduced class-switched serum antibody titers [Kontgen et al., 1995; Harling-McNabb et al., 1999].

The increased proliferation of transgenic c-Rel GC B cells could influence the enhanced isotype class switch as this process is closely linked to proliferation [Hodgkin et al., 1996]. However, a defect to switch to IgG1 in plasmablast cultures [Heise et al., 2014] and to produce $\gamma 1$ germline transcripts [Kaku et al., 2002] as a result of c-Rel-deficiency provides evidence for additional direct involvements of c-Rel in class switch recombination (see introduction subsection 2.2.6). Besides c-Rel also other members of the NF- κ B transcription factor family are known to have an impact on class switch recombination [Snapper et al., 1996a,b; Doi et al., 1997; Xu et al., 2012]. IgG3 is the only analyzed class-switched subtype that is reduced in percent in c-Rel transgenic mice. Amongst the NF- κ B subunits, RelA is implicated in IgG3 class switching and $\gamma 3$ germline transcription [Horwitz et al., 1999]. Therefore, I hypothesize that c-Rel overexpression could indeed actively promote preferential class switch recombination to certain isotypes including IgG1, while switching to IgG3 that is induced by RelA is reduced as a result of a potentially changed NF- κ B subunit balance due to c-Rel transgene overexpression. This hypothesis and a possible influence of cell division on class switching in c-Rel transgenic mice are not mutually exclusive.

The study of c-Rel in plasma cells *in vivo* has been impeded by the crucial role of c-Rel in GC B cells entailing the collapse of GC reactions in studied c-Rel deficient mouse models. Also in the c-Rel transgenic mouse model presented in this thesis, it is likely that higher plasma cell counts are in part a result of enhanced GC reactions. Plasmablast differentiation *in vitro* shows a trend for slightly higher percentage of c-Rel transgenic plasma cells, indicating that c-Rel potentially enhances plasma cell differentiation. In contrast, Heise et al. observed a higher percentage of plasmablasts in *in vitro* differentiation of c-Rel^{-/-} cells [Heise et al., 2014]. However, this *in vitro* differentiation approach is a model for extrafollicular plasma cell generation and does not reflect the follicular GC-dependent plasma cell response. *In vivo* c-Rel transgenic plasma cells are significantly expanded in

both naive and immunized mice, whereas the extent of enhanced GC B cells is slightly less pronounced upon immunization. These findings could hint towards an independent role of elevated c-Rel levels in plasma cell differentiation. However, at this stage the distinct delineation of c-Rel function in plasma cells requires further investigation.

3 c-Rel protein expression and regulation

Based on microarray gene expression studies of immune cells, it was reported that GC B cells lack a typical NF- κ B signature [Shaffer et al., 2001, based on data in Alizadeh et al., 2000]. A reason for the absence of a usual NF- κ B signature in GC B cells could be that in particular c-Rel but not RelA plays a central role in GC reactions [Heise et al., 2014]. Possibly, a general NF- κ B signature does not represent a characteristic c-Rel signature. Indeed, c-Rel is unique amongst the NF- κ B subunits with regard to κ B site sequence recognition as several studies suggest a lower stringency and higher degeneracy for c-Rel binding motifs associated with an increased flexibility for c-Rel target gene sequence binding [Kunsch et al., 1992; Sanjabi, 2005; Siggers et al., 2012; Zhao et al., 2014].

In studies of GC B cells in human lymphoid tissue, c-Rel was found mainly in the cytoplasm and only rarely in the nucleus [Barth et al., 2003; Basso et al., 2004; Saito et al., 2007]. Unfortunately, none of these publications show a quantitative analysis of c-Rel expression. In contrast to these data, as discussed above, c-Rel-deficient mouse models demonstrate that c-Rel certainly plays a crucial role in GC B cells. Moreover, I establish by comprehensive analyses in this work that c-Rel expression is generally higher in GC B cells than in naive B cells. These results are associated with a functional implication as c-Rel expression levels strikingly correlate with cellular expansion of GC B cells and plasma cells. Furthermore, quantitative imaging flow cytometry data of this thesis suggests a higher c-Rel nuclear translocation in around 40% of *ex vivo* analyzed splenic GC B cells compared to roughly 20% of naive B cells. While I am not aware of another study that quantitatively assessed c-Rel nuclear localization in non-malignant primary mouse GC B cells, the nuclear translocation observed in the splenic mature B cell population is in agreement with published quantitative immunofluorescence data [Ferch et al., 2007; Wuerzberger-Davis et al., 2011].

The few GC B cells for which c-Rel nuclear localization is found by Basso et al. and by the same group in the later publication by Saito et al. are centrocytes of the LZ

[Barth et al., 2003; Basso et al., 2004]. In addition, LZ GC B cells were described to be enriched for an NF- κ B signaling signature in comparison to DZ GC B cells [Victora et al., 2010]. Consistently, I demonstrate that the highest levels of c-Rel within the GC B cell population can be detected in LZ GC B cells, while DZ GC B cells express relatively lower c-Rel levels. There is evidence that PI3K activity is involved in maintaining c-Rel levels in mature naive B cells [Suzuki et al., 1999; Yamazaki and Kurosaki, 2003; Matsuda et al., 2008] (see introduction subsection 2.2.2). In this line, it is interesting that recent publications report that PI3K signaling is particularly active in LZ GC B cells [Dominguez-Sola et al., 2015; Sander et al., 2015]. However, at this point in time the connection of high PI3K activity and c-Rel expression levels in LZ GC B cells remains speculative.

The drop of c-Rel protein level that I detect in plasma cells is in agreement with a lowered *REL* mRNA level in plasma cells in a recent publication of transcriptional profiling of plasma cell populations [Shi et al., 2015]. Furthermore, I found that the reduction of c-Rel protein expression is recapitulated in *in vitro* plasmablast differentiation, indicating that the decrease of c-Rel in plasma cells is a central feature of this terminally differentiated cell type. These reduced c-Rel protein levels are in accordance with the observed predominantly cytoplasmic localization of c-Rel in plasma cells.

Transcription factor expression levels in immune cells are pivotal determinants of cell fate decisions. For instance, in GC B cell versus plasmablast fate choice, IRF4 and IRF8 have been described to act in a dose-dependent manner [Klein et al., 2006; Sciammas et al., 2006; Ochiai et al., 2013], which was proposed to be controlled by an antagonistic feedback loop [Xu et al., 2015]. Dose-dependent effects of c-Rel expression level were reported upon heterozygous c-Rel deficiency in lymphocytes or GC B cells that present intermediate phenotypes [Kontgen et al., 1995; Heise et al., 2014]. As mentioned above, I find a highly significant correlation of c-Rel levels with the expansion of both GC B cells and plasma cells. These analyses clearly demonstrate that c-Rel is a potent driver of GC reactions in a dose-dependent manner.

The data presented in this thesis provide evidence for a tight regulation of c-Rel protein levels in B cell subpopulations. Although c-Rel transgene overexpression in the B lineage is induced in the course of development in the bone marrow mediated by CD19Cre, total c-Rel levels are only marginally higher in mature naive B cells but several fold increased

in GC B cells of c-Rel transgenic mice. Analysis of CAG-CAR-reporter mice illustrates that these sharp switches are not a consequence of differential transgenic CAG promoter activity that drives c-Rel transgene expression. I conclude that c-Rel levels are regulated in naive B cells, possibly on the post-transcriptional or post-translational level. Similarly, the limited extent of c-Rel transgene expression in plasma cells, despite strong CAG promoter activity, suggests that also in this terminally differentiated B lineage cell type c-Rel protein expression levels are restricted. With the intention to generate even higher c-Rel overexpression levels, I generated c-Rel/GFP-c-Rel double transgenic mice. Surprisingly, this did not have an additive effect as total c-Rel levels in GC B cells are comparable in double and single transgenic mice. Intriguingly, GFP-c-Rel levels are even reduced in c-Rel/GFP-c-Rel double transgenic mice. This observation indicates that despite the strongly elevated c-Rel transgene levels in GC B cells, there appears to be a limit of c-Rel expression also in this cell type. I therefore postulate that c-Rel protein expression levels are constrained by tight regulation, possibly on multiple molecular layers.

Indeed, I provide first evidence for a molecular mechanism involving proteasomal degradation of c-Rel in naive B cells but not in GC B cells. Proteasomal degradation as a means of c-Rel protein turnover has been reported for other immune cell types (see introduction 2.2.3). In T cells the E3 ubiquitin ligase Peli1 has been identified as a fundamental negative regulator of c-Rel and Peli1-deficient mice develop syndromes of autoimmunity [Chang et al., 2011]. Furthermore, the E3 ubiquitin ligase cIAP has been suggested to be involved in c-Rel proteasomal degradation in macrophages [Jin et al., 2015].

c-Rel has also been shown to be controlled on the post-transcriptional level. The RNA-regulating protein Regnase-1 that acts through cleavage of 3'UTRs of target mRNAs controls *REL* mRNA in T cells. The authors further show that Regnase-1 is cleaved by MALT1 protease downstream of TCR stimulation serving as a mechanism that is suggested to stabilize *REL* mRNA [Uehata et al., 2013]. It is noteworthy that MALT1 is specifically required for c-Rel nuclear translocation downstream of BCR signaling in mature B cells [Ferch et al., 2007] and that c-Rel levels are rapidly upregulated following stimulation. However, Ferch et al. found no difference in total c-Rel amounts in MALT1^{-/-} and control B cells after 4 h of anti-IgM stimulation. In addition, *REL* is a target of the RNA-binding and -regulating Roquin proteins as shown by Roquin-1/2 ablation in T cells [Jeltsch et al., 2014]. As both Regnase-1 [Uehata et al., 2013] and Roquin proteins [Bertossi et al., 2011] are also expressed in B cells, it would be interesting to investigate

the potential relation of c-Rel and these RNA-regulators in activated and terminally differentiated B cells.

4 c-Rel in lymphoma and autoimmunity - a yet unresolved question

The dose-dependent correlation of c-Rel protein with GC B cell and plasma cell expansion provides evidence for a physiological relevance of tight control of c-Rel expression. In light of the frequent *REL* gene locus amplifications in human B cell lymphoma, the interesting finding that c-Rel transgene expression can drive GC reactions and the subsequent appearance of class-switched plasma cells has an implication for the role of c-Rel in B cell lymphomagenesis. This is substantiated by the observation that the vast majority of human B cell lymphomas show indications of GC or post-GC origin [Küppers, 2005]. Yet, aged B cell-specific c-Rel transgenic mice do not spontaneously develop overt lymphoma. Lymphoma development requires not only intrinsic malignant transformation but is also coupled to the microenvironment and its cell types that provide protection by immune surveillance [Küppers, 2005; Schreiber et al., 2011]. In mouse models, T cells were found to control B cell lymphoma development [Zhang et al., 2012; Afshar-Sterle et al., 2014]. However, the B cell-specific phenotype of c-Rel transgenic mice is accompanied by only moderate T cell activation, suggesting that this pathway does not lead to strong cell-extrinsic activation of the immune system.

The findings that enhanced proliferation could contribute to the expansion of the GC B cell population in c-Rel transgenic mice and that c-Rel knockdown in the PMBCL cell line MedB-1 strongly decreases proliferation are of particular interest as unrestrained proliferation is considered one of the hallmarks of lymphoma [Küppers and Dalla-Favera, 2001; Shaffer et al., 2002b]. My findings indicate that high c-Rel expression could play a role in maintaining proliferative capacities in human B cell lymphoma cells. The observation that one out of three c-Rel-targeting shRNAs of my cell line-based loss-of-function approach does not exhibit proliferative defects correlates with the lower but still >90% knockdown efficiency of this shRNA compared to >95% knockdown efficiency for the other two shRNAs. Whether a threshold effect for c-Rel levels or potential off-target effects account for these results remains to be determined. A subsequent attempt to validate the findings

using an inducible strategy mediated by the reverse tetracycline transactivator (rtTA) and the tetracycline-responsive element (TRE) [Zuber et al., 2010] was not successful due to toxicity effects of the induced transactivators. During the course of my studies, the novel CRISPR/Cas9 genome engineering technology emerged as a novel versatile tool for targeted loss-of-function approaches [Jinek et al., 2012; Mali et al., 2013b,a; Doudna and Charpentier, 2014] and represents the method of choice to further investigate the role of c-Rel in human B cell lymphoma cell lines in future studies.

Lymphoma patients clinically present with multiple genetic lesions corroborating the model that multiple oncogenic hits eventually cause malignant transformation [Küppers and Dalla-Favera, 2001; Shaffer et al., 2002b]. In the present mouse model, c-Rel does not act as a sole driver of lymphomagenesis despite conferring enhanced proliferation on GC B cells. It can be speculated that a higher number of GCs that undergo class switch recombination at higher frequency, which mechanistically involves gene rearrangements, might lower the threshold to acquire additional genetic aberrations by increasing the incidence of the processes that constitute the peril of GC reactions. This could especially represent a possible pathway under physiological circumstances outside of the hygienically controlled microenvironment of mouse facilities. Nevertheless, these theoretical possibilities demand practical investigation in future studies.

c-Rel probably acts in cooperation with other proto-oncogenes and several studies provide evidence for possible candidates. First, the negative regulator of NF- κ B signaling A20 is implicated in autoimmune diseases and as a tumor suppressor in human B cell lymphomas, including cHL, PMBCL and DLBCL [Compagno et al., 2009; Kato et al., 2009; Schmitz et al., 2009; Vereecke et al., 2009; Chu et al., 2011]. As published recently, A20 inactivation and *REL* amplification can occur in the same tumor entities: in a cohort of 19 cHL patients, more than half (4/7) of the cases with heterozygous loss of *TNFAIP3*, the gene encoding A20, showed concurrent *REL* copy number gains >4 [Salipante et al., 2016]. Second, although translocations involving *Myc* and Ig loci are best known as a characteristic of virtually all Burkitt lymphoma cases, genetic alterations deregulating c-Myc have for instance also been found in DLBCL [Kramer et al., 1998; Stasik et al., 2010; Ott et al., 2013]. In a cohort of 114 DLBCL cases, Jardin et al. found an association of *REL* and *Myc* gains as 75% (8/12) of cases with *Myc* gain showed concomitant *REL* gains. Third, another possible candidate to be investigated in compound studies is Bcl-11a. The gene locus of *BCL11A* is frequently co-amplified with the *REL* locus and whether

c-Rel, Bcl-11a or both are targets of the locus amplifications remains controversial (see introduction subsection 3.2.5).

In addition, Janus kinase 2 (JAK2) amplifications [Joos et al., 1996, 2000, 2003; Savage, 2006] or loss of its negative regulator, the suppressor of cytokine signaling 1 (SOCS1) [Melzner, 2005; Melzner et al., 2006; Weniger et al., 2006a; Mottok et al., 2007], is frequently found in cHL and PMBCL patient samples and cell lines. Amongst common aberrations in DLBCL, further candidates for compound mouse studies include Bcl-2 translocation [Rosenwald et al., 2002] or amplification of the genomic region containing the microRNA (miRNA) cluster miR-17-92 [Tagawa and Seto, 2005; Xiao et al., 2008]. Accordingly, there are numerous genetic aberrations occurring in human B cell lymphomas that could possibly cooperate with c-Rel and therefore represent interesting candidates for future studies aiming at investigation of potential additive or synergistic effects of c-Rel in combination with these proto-oncogenes or tumor suppressors.

Initial analyses of c-Rel transgenic mice overexpressing the lymphoma-specific aberrant splice version of c-Rel lacking exon 9 (c-Rel Δ Ex9) [Leeman et al., 2008] did not reveal significant differences in comparison to full-length c-Rel overexpression in B cells. Nevertheless, I observed an interesting trend for higher GC B cell numbers in lymph nodes and for higher plasma cell numbers in bone marrow despite similar or only slightly enhanced total c-Rel levels, respectively. In this regard, it would be of particular interest to delineate the specific signals that activate c-Rel in lymph nodes and bone marrow plasma cells as well as to investigate target gene expression to continue the evaluation of this c-Rel splice variant in B cells.

Aberrant GC reactions and plasma cells are also associated with autoimmunity and autoantibodies are a central characteristic for most autoimmune diseases and are commonly used in diagnosis [Vinuesa et al., 2009]. Interestingly, aged c-Rel transgenic mice show signs of class-switched autoantibody production, indicating that the spontaneous GCs are driven by self-antigens. Human disease-associated autoantibodies are often of class-switched isotypes and autoantibody-secreting cells frequently carry somatic mutations in Ig variable gene segments, indicating that they have undergone GC reactions and are antigen-selected [Shlomchik, 2008]. While the extent of somatic hypermutation in terminally differentiated c-Rel transgenic B lineage cells remains to be determined, the anti-nuclear antibodies (ANA) and rheumatoid factor (RF) autoantibodies detectable in

aged c-Rel CD19Cre^{I/+} mice are of the IgG class-switched isotype.

Detection of autoantibodies is not only characteristic for most autoimmune diseases but can precede appearance of clinical symptoms [Arbuckle et al., 2003; Scofield, 2004; Bizzaro, 2007]. Therefore, although no overt signs of disease were visible in aged c-Rel transgenic animals, the appearance of class-switched autoantibodies indicates that enhanced c-Rel activation could indeed contribute to autoimmunity. In this line, it is remarkable that SNPs within the *REL* locus are associated with numerous autoimmune diseases, including rheumatoid arthritis [Gregersen et al., 2009; Eyre et al., 2010], psoriasis [Strange et al., 2010], ulcerative colitis [McGovern et al., 2010] and celiac disease [Trynka et al., 2009; Dubois et al., 2010].

In conclusion, c-Rel overexpression in B cells in the present mouse model does not cause overt lymphoma or autoimmune disease when aging mice up to 1.5 years of age. Nevertheless, the results of this thesis are still in support of a potential disease-promoting role of c-Rel, as I could demonstrate that c-Rel is a potent dose-dependent driver of GC reactions and causes accumulation of class-switched autoantibody-producing plasma cells *in vivo* and confers proliferative capacities to the human B cell lymphoma cell line MedB-1 *in vitro*. However, under which circumstances this might have an impact on severe disease manifestation needs to be addressed in future studies.

5 Concluding remarks and outlook

Despite more than 30 years of research since the discovery of c-Rel as an NF- κ B family transcription factor followed by an enormous progress of delineating c-Rel function in immune cells, still intriguing questions remain unanswered. The significance of elucidating the precise molecular mechanisms and consequences of c-Rel signaling in GC reactions is emphasized by the implication of c-Rel in human B cell lymphoma and autoimmune disease – in particular with regard to paving the way towards development of novel therapeutic approaches (see introduction subsection 3.5).

The first conditional c-Rel overexpression mouse models presented in this thesis did not only reveal that c-Rel is a potent driver of GC reactions and plasma cell expansion and led to the discovery of tight c-Rel protein level regulation, but they also permit to further advance the knowledge of c-Rel function in lymphocytes and beyond.

Supplemental Figures

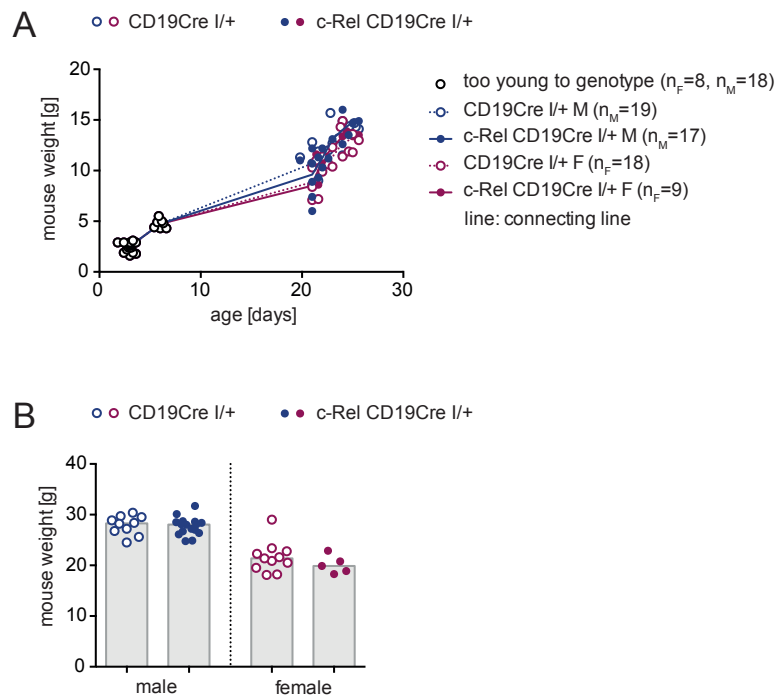
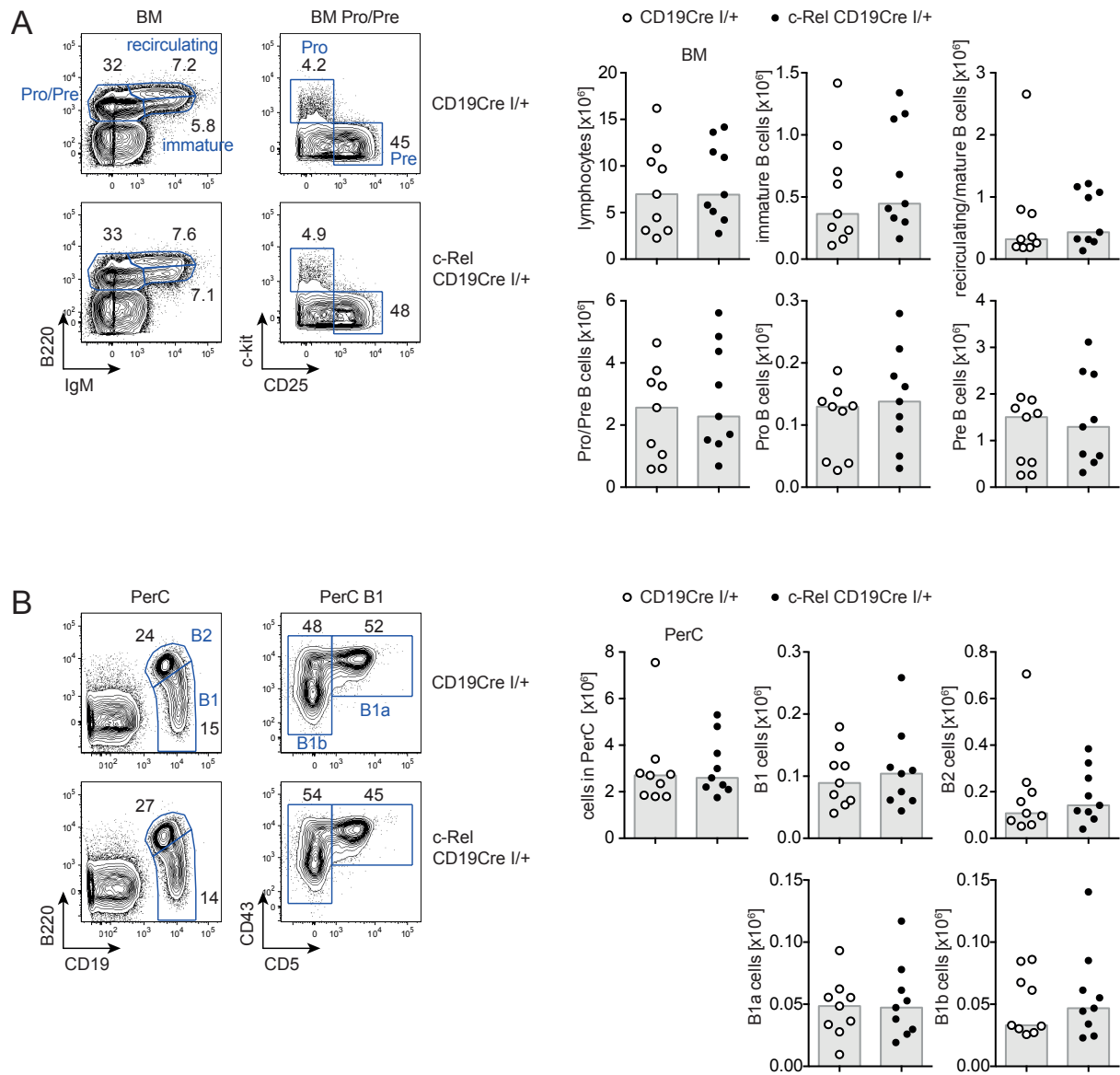


Figure S1: Weight gain of c-Rel CD19Cre^{I/+} mice. (A) Mouse weight at the indicated days after birth. Individual data points are plotted. Lines connect mean values averaged over females or males of each genotype. (B) Mouse weight assessed at day of analysis. Individual data points and bars representing median values are plotted. M, male; F, female.



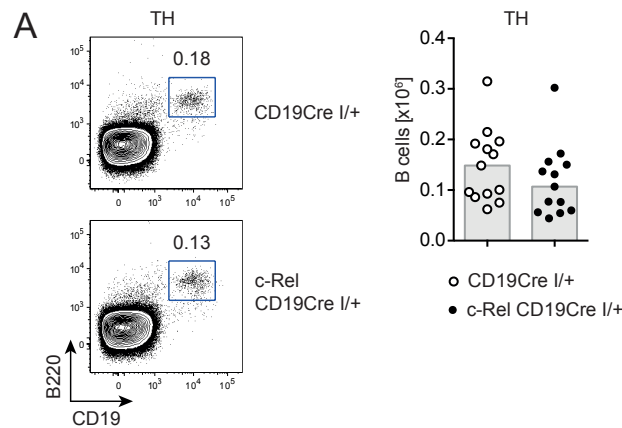


Figure S3: B cells in thymus of $c\text{-Rel}^{\text{CD19Cre}^{\text{I/+}}}$ mice. Representative flow cytometry plots illustrating the gating strategy for B cell subsets in (A) thymus (TH). Numbers within plots are median percentages calculated from the same dataset considered for bar graph representation of cell numbers for the respective B cell subsets where individual data points are plotted and bars are median values. Data were obtained in 5 independent experiments. B cells $\text{B220}^{\text{+}}\text{CD19}^{\text{+}}$.

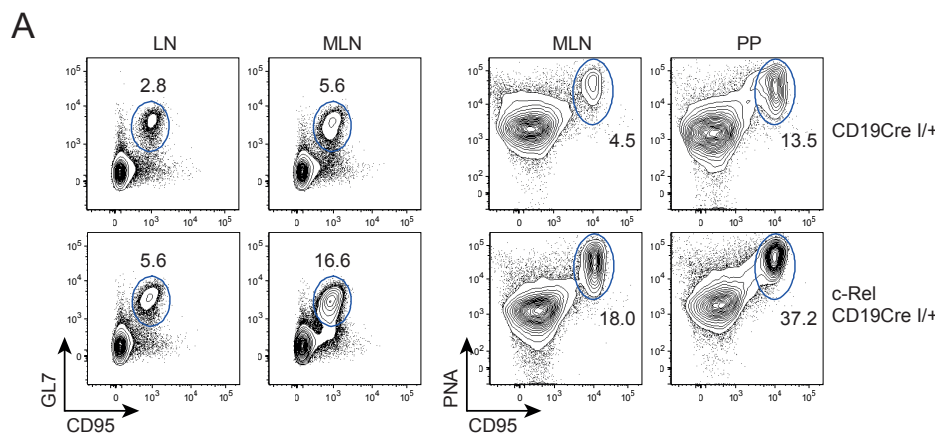


Figure S4: Staining of GC B cells in $c\text{-Rel}^{\text{CD19Cre}^{\text{I/+}}}$ mice with GL7 and PNA. (A) Representative flow cytometry plots of GL7 and PNA stainings for identification of GC B cells within the population of $\text{CD19}^{\text{+}}/\text{B220}^{\text{+}}$ B cells. Numbers are percentages of gated populations for displayed plots. Data are representative for ≥ 2 independent experiments. LN, lymph nodes; MLN, mesenteric lymph nodes; PP, Peyer's patches.

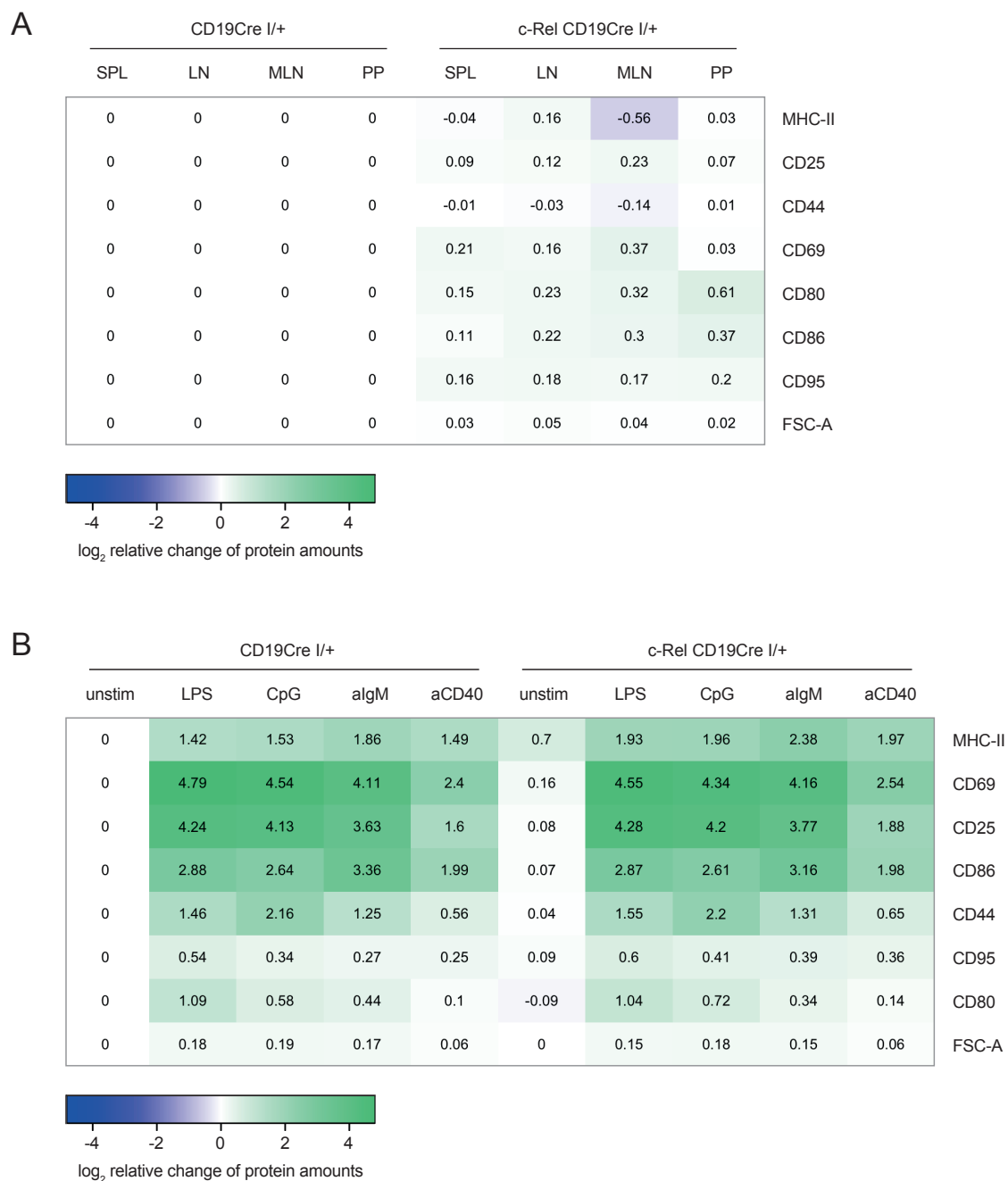


Figure S5: Regulation of B cell activation markers in c-Rel CD19Cre^{I/+} mice. Heatmap representation of \log_2 values of geometric means of relative change of activation marker protein amounts for c-Rel CD19Cre^{I/+} mice and CD19Cre^{I/+} controls. (A) Flow cytometry data of activation markers of CD19⁺ B cells in indicated organs. Activation markers were assessed directly *ex vivo*. Data were normalized to CD19Cre^{I/+} controls for each organ. Data are representative for ≥ 6 mice per genotype and were obtained in ≥ 2 independent experiments. (B) Flow cytometry data of activation markers after over night stimulation of MACS-isolated splenic B cells with indicated stimuli (LPS 20 $\mu\text{g}/\text{ml}$, CpG 0.1 μM , anti-IgM (aIgM) 10 $\mu\text{g}/\text{ml}$, anti-CD40 (aCD40) 4 $\mu\text{g}/\text{ml}$). Data were normalized to unstimulated (unstim) B cells of CD19Cre^{I/+} controls. Data are representative for ≥ 9 mice per genotype and were obtained in 3 independent experiments. FSC-A, forward scatter area;

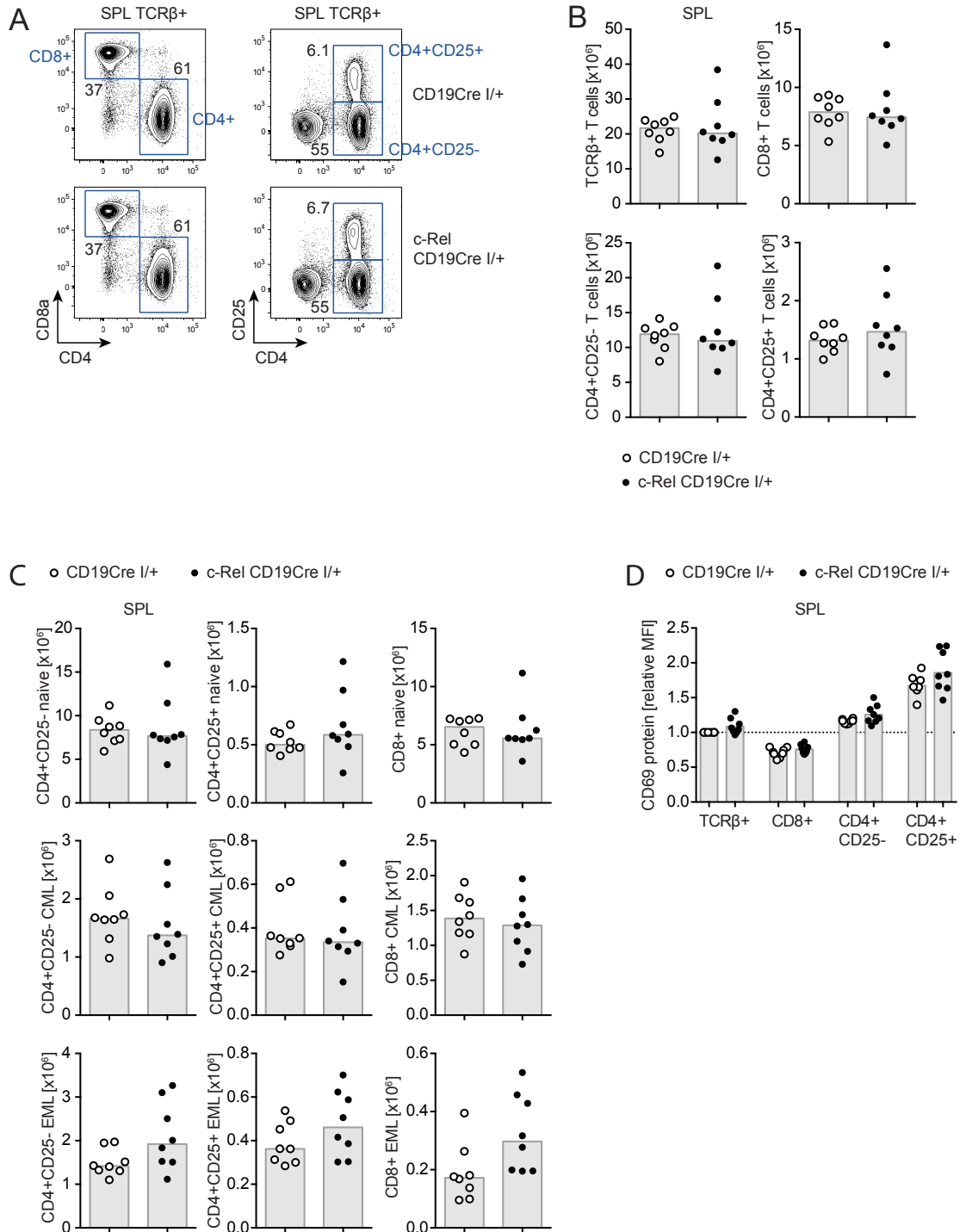


Figure S6: T cell subsets in spleen of c-Rel CD19Cre^{I/+} mice. (A) Representative flow cytometry plots illustrating CD8, CD4 and CD25 expression on splenic TCR β ⁺ T cells. Numbers are median percentages. (B) Cell numbers of splenic T cell subsets. Individual data points obtained in 3 independent experiments are plotted and bars represent median values. (C) Cell numbers of naive (CD44^{int}CD62L^{high}), central memory like (CML, CD44^{high}CD62L^{high}) and effector memory like (EML, CD44^{high}CD62L^{low}) T cells within indicated T cell subsets (all pre-gated on TCR β ⁺ and CD8/CD4 or CD4/CD25 as indicated). Data were obtained in 3 independent experiments. These cell numbers correspond to the percentages shown in Figure 12A. (D) CD69 protein expression on indicated splenic T cell subsets. All data are normalized to TCR β ⁺ T cells of CD19Cre^{I/+} controls. Individual data points obtained in 3 independent experiments are plotted and bars represent geometric means. SPL, spleen.

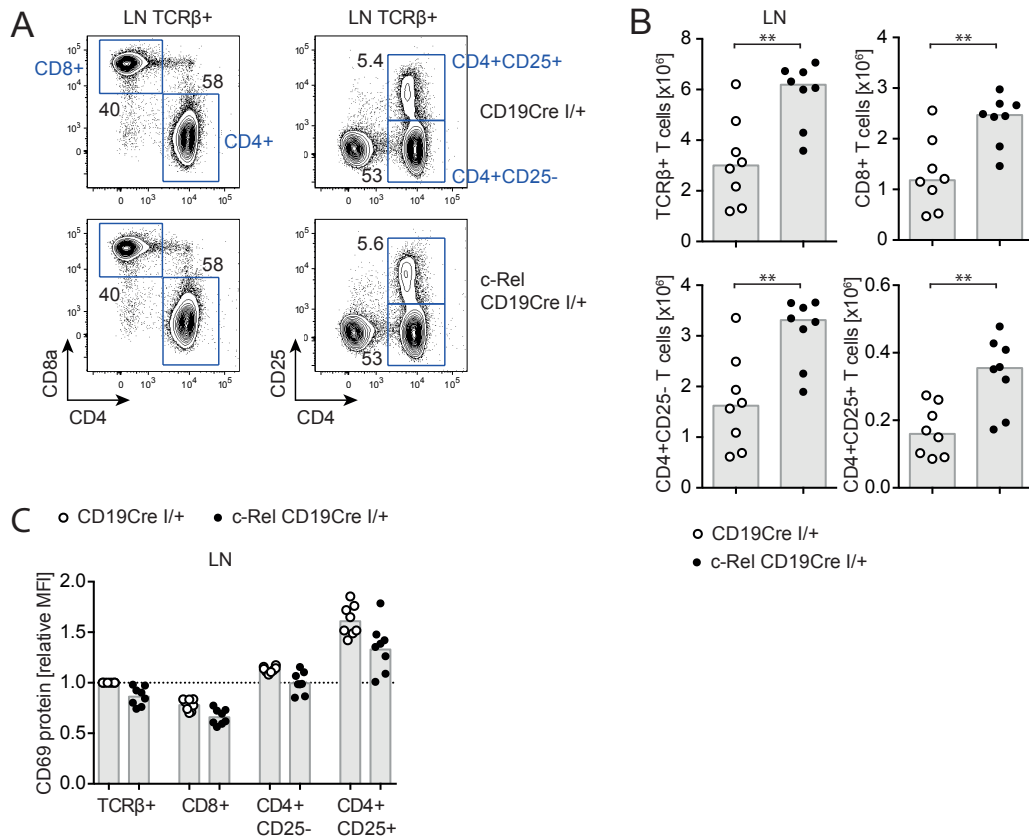


Figure S7: T cell subsets in lymph nodes of c-RelCD19Cre^{I/+} mice. (A) Representative flow cytometry plots illustrating CD8, CD4 and CD25 expression on TCR β^+ T cells in lymph nodes. Numbers are median percentages. (B) Cell numbers of T cell subsets in lymph nodes. Individual data points obtained in 3 independent experiments are plotted and bars represent median values. (C) CD69 protein expression on indicated T cell subsets of lymph nodes. All data are normalized to TCR β^+ T cells of CD19Cre^{I/+} controls. Individual data points obtained in 3 independent experiments are plotted and bars represent geometric means. ** $p \leq 0.01$, unpaired t test. LN, lymph node.

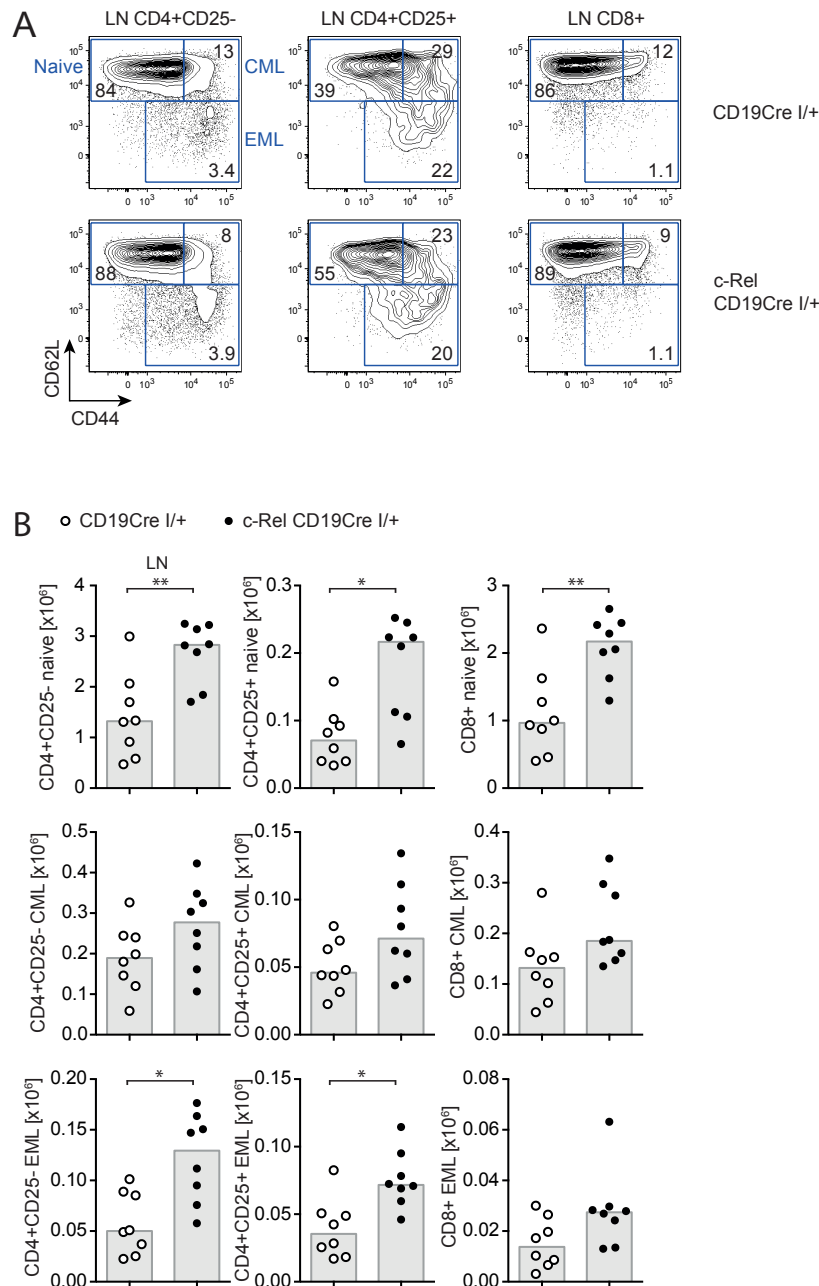


Figure S8: Naive and memory like T cell subsets in lymph nodes of c-RelCD19Cre^{I/+} mice. (A) Representative flow cytometry plots illustrating CD44 and CD62L expression of T cell subsets in lymph nodes (all pre-gated on TCR β^+ and CD8/CD4 or CD4/CD25 as indicated) representing naive (CD44^{int}CD62L^{high}), central memory like (CML, CD44^{high}CD62L^{high}) and effector memory like (EML, CD44^{high}CD62L^{low}) T cells. Numbers are median percentages. (B) Cell numbers of naive, CML and EML T cells within indicated T cell subsets. Individual data points obtained in 3 independent experiments and bars representing median values are plotted. Cell numbers for EML T cell subsets are also shown in Figure 12C. * $p \leq 0.05$, ** $p \leq 0.01$, unpaired t test. LN, lymph node.

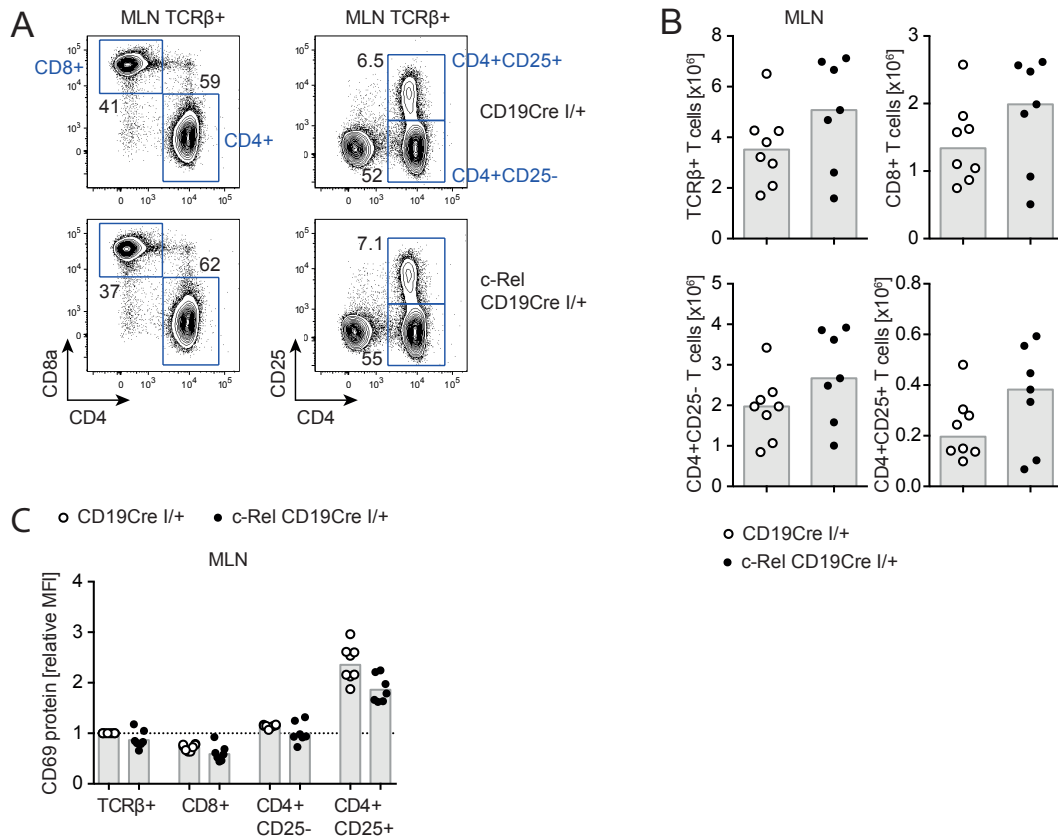


Figure S9: T cell subsets in mesenteric lymph nodes of c-Rel CD19Cre^{1/+} mice. (A) Representative flow cytometry plots illustrating CD8, CD4 and CD25 expression on TCR β ⁺ T cells in mesenteric lymph nodes. Numbers are median percentages. (B) Cell numbers of T cell subsets in mesenteric lymph nodes. Individual data points obtained in 3 independent experiments are plotted and bars represent median values. (C) CD69 protein expression on indicated T cell subsets of mesenteric lymph nodes. All data are normalized to TCR β ⁺ T cells of CD19Cre^{1/+} controls. Individual data points obtained in 3 independent experiments are plotted and bars represent geometric means. MLN, mesenteric lymph node.

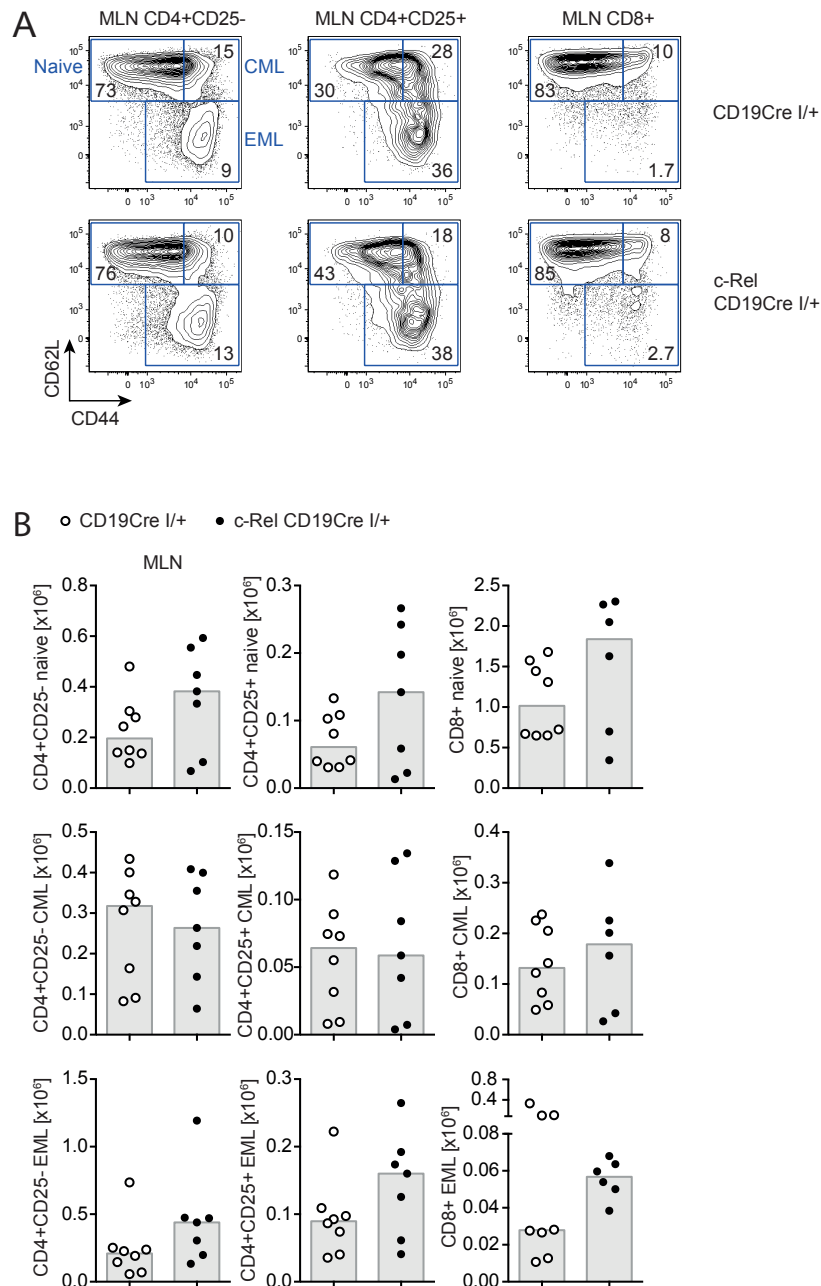


Figure S10: Naive and memory like T cell subsets in mesenteric lymph nodes of c-Rel CD19Cre^{I/+} mice. (A) Representative flow cytometry plots illustrating CD44 and CD62L expression of T cell subsets in mesenteric lymph nodes (all pre-gated on TCR β^+ and CD8/CD4 or CD4/CD25 as indicated) representing naive (CD44^{int}CD62L^{high}), central memory like (CML, CD44^{high}CD62L^{high}) and effector memory like (EML, CD44^{high}CD62L^{low}) T cells. Numbers are median percentages. These percentages correspond to the frequencies shown in Figure 12B. (B) Cell numbers of naive, CML and EML T cells within indicated T cell subsets. Individual data points obtained in 3 independent experiments and bars representing median values are plotted. MLN, mesenteric lymph node.

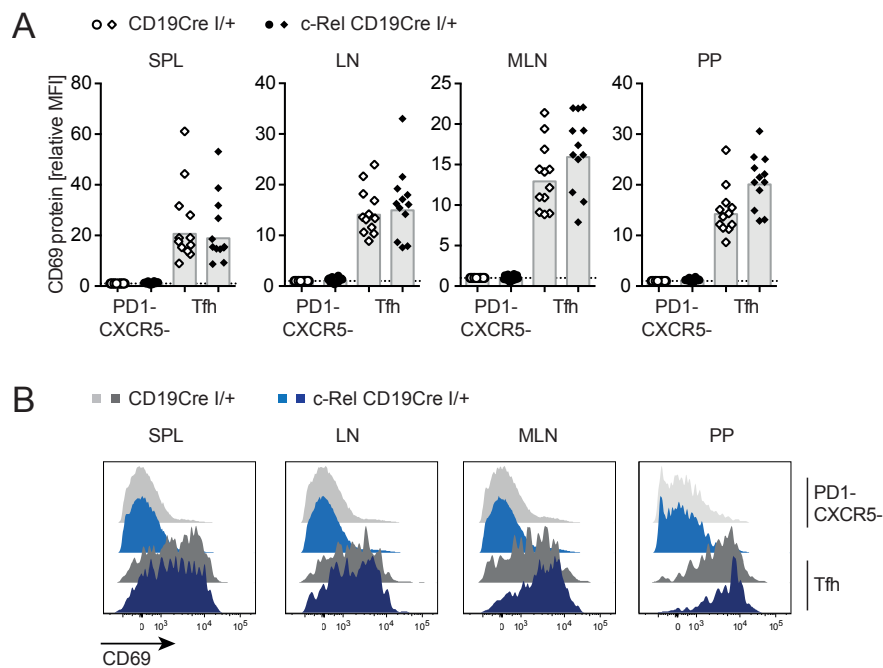


Figure S11: Characteristics of T_{fh} cells of c-Rel CD19Cre^{I/+} mice. (A) Flow cytometry data of CD69 protein levels of T_{fh} cells normalized to the non-T_{fh} cell population of CD19Cre^{I/+} controls. Geometric mean and individual data points obtained in 5 independent experiments are plotted. (B) Representative histograms illustrating the bar graphs shown in (A). T_{fh} TCR β ⁺CD4⁺PD-1^{high}CXCR5^{high}; non-T_{fh} TCR β ⁺CD4⁺PD-1^{low}CXCR5^{low}; SPL, spleen; LN, lymph nodes; MLN, mesenteric lymph nodes; PP, Peyer's patches.

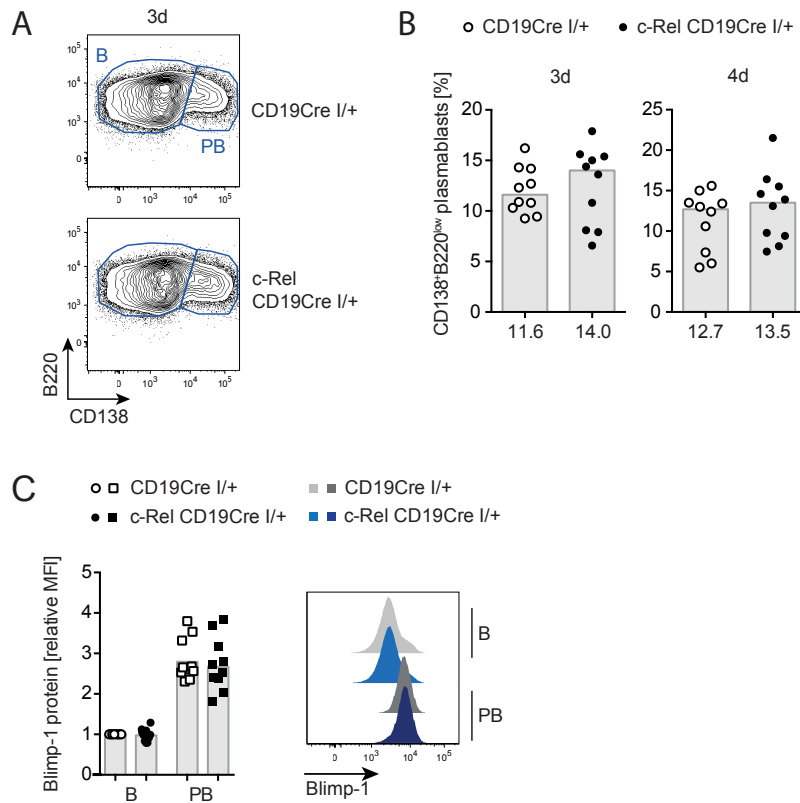


Figure S12: *In vitro* plasmablast differentiation with c-Rel CD19Cre^{I/+} splenocytes. (A) Representative flow cytometry plots of plasmablasts. (B) Percentages of plasmablasts after 3 days or 4 days of LPS treatment *in vitro*. Individual data points obtained in 3 independent experiments and bars representing median values are plotted. (C) Intracellular flow cytometry data of Blimp-1 protein levels in plasmablasts after 3 days of LPS treatment *in vitro* normalized to the non-plasmablast cell population of CD19Cre^{I/+} controls. Representative histograms illustrate the bar graphs for which the geometric mean and individual data points obtained in 3 independent experiments are plotted. Plasmablasts (PB) B220^{low}CD138⁺; B (non-PB) B220⁺CD138⁻.

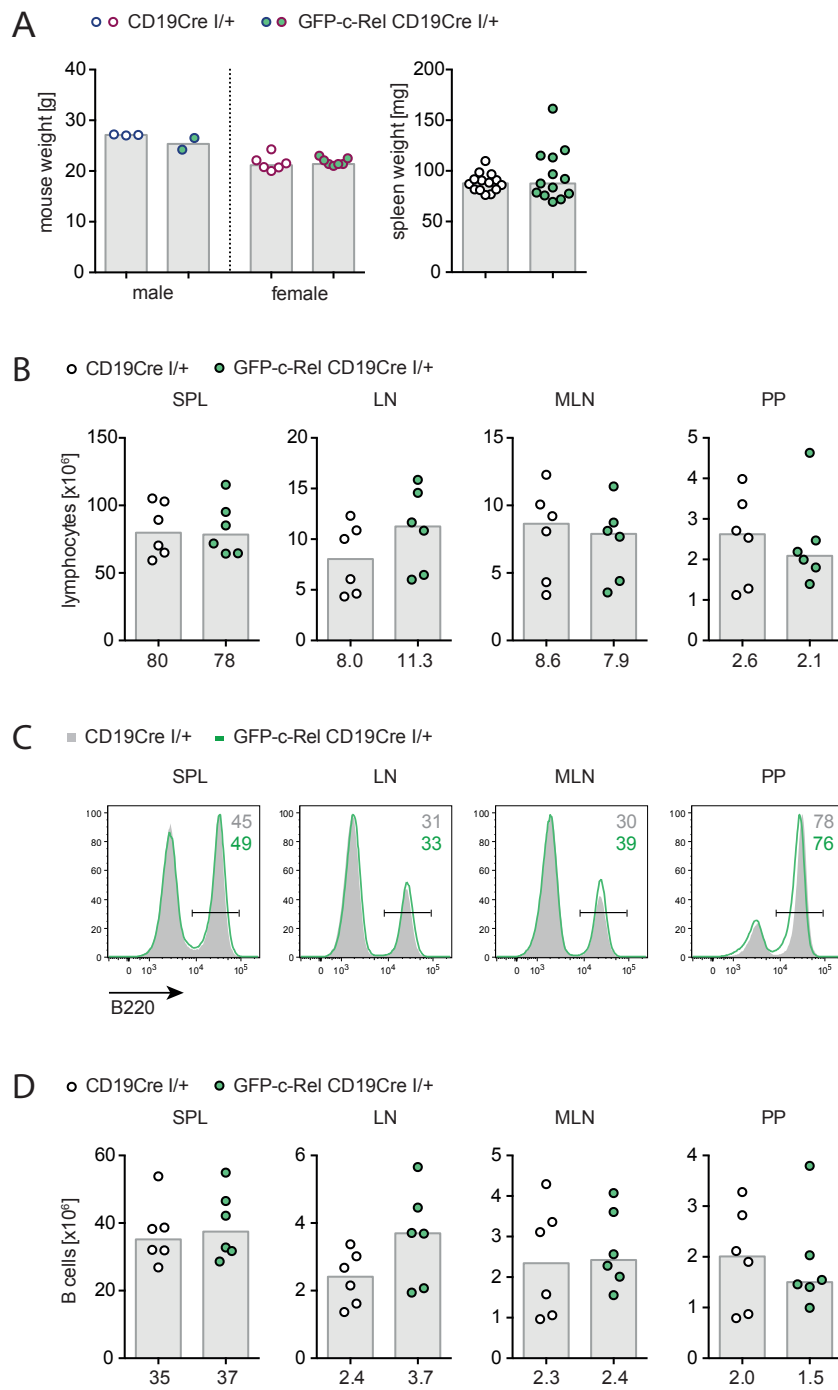
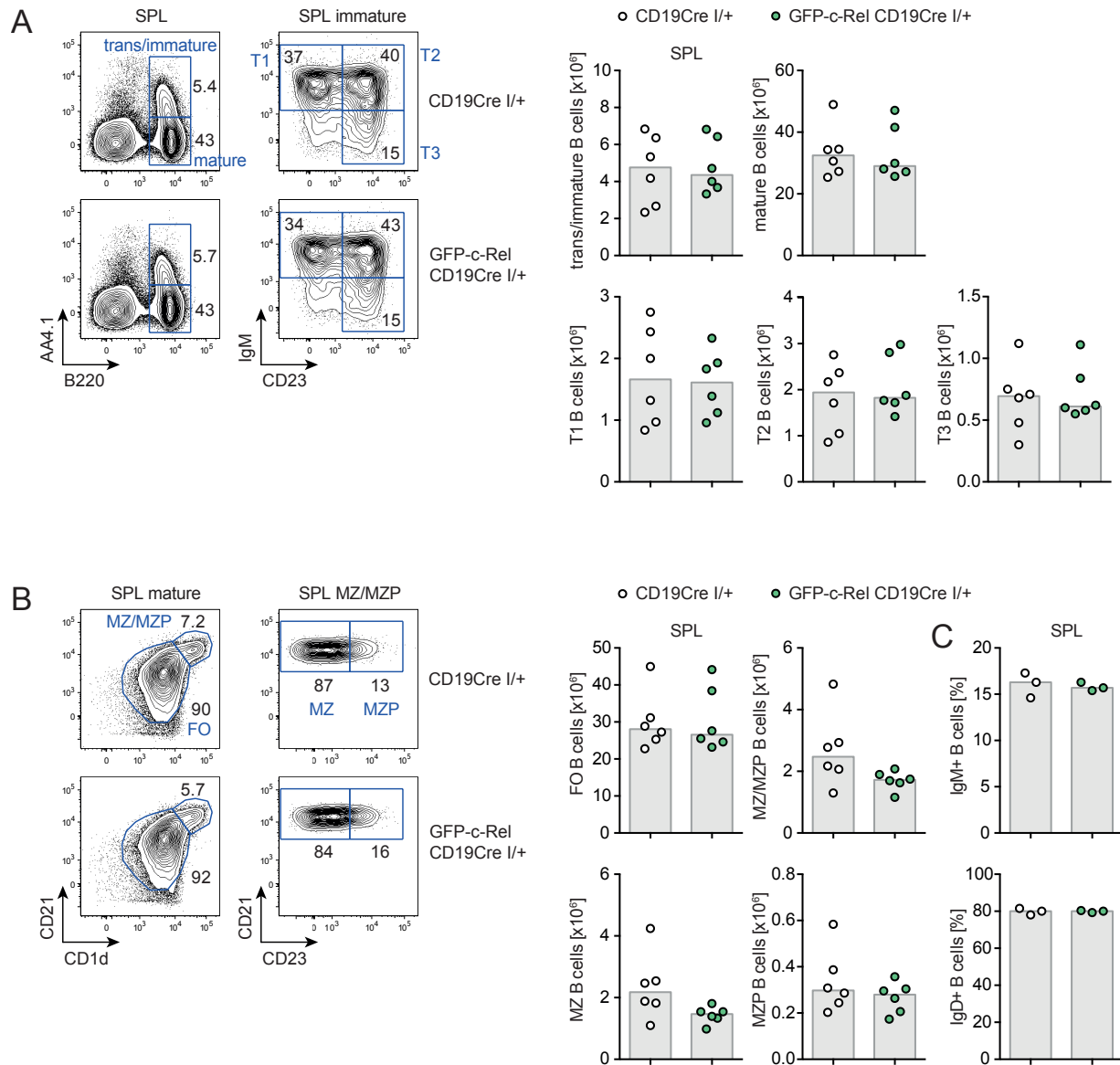
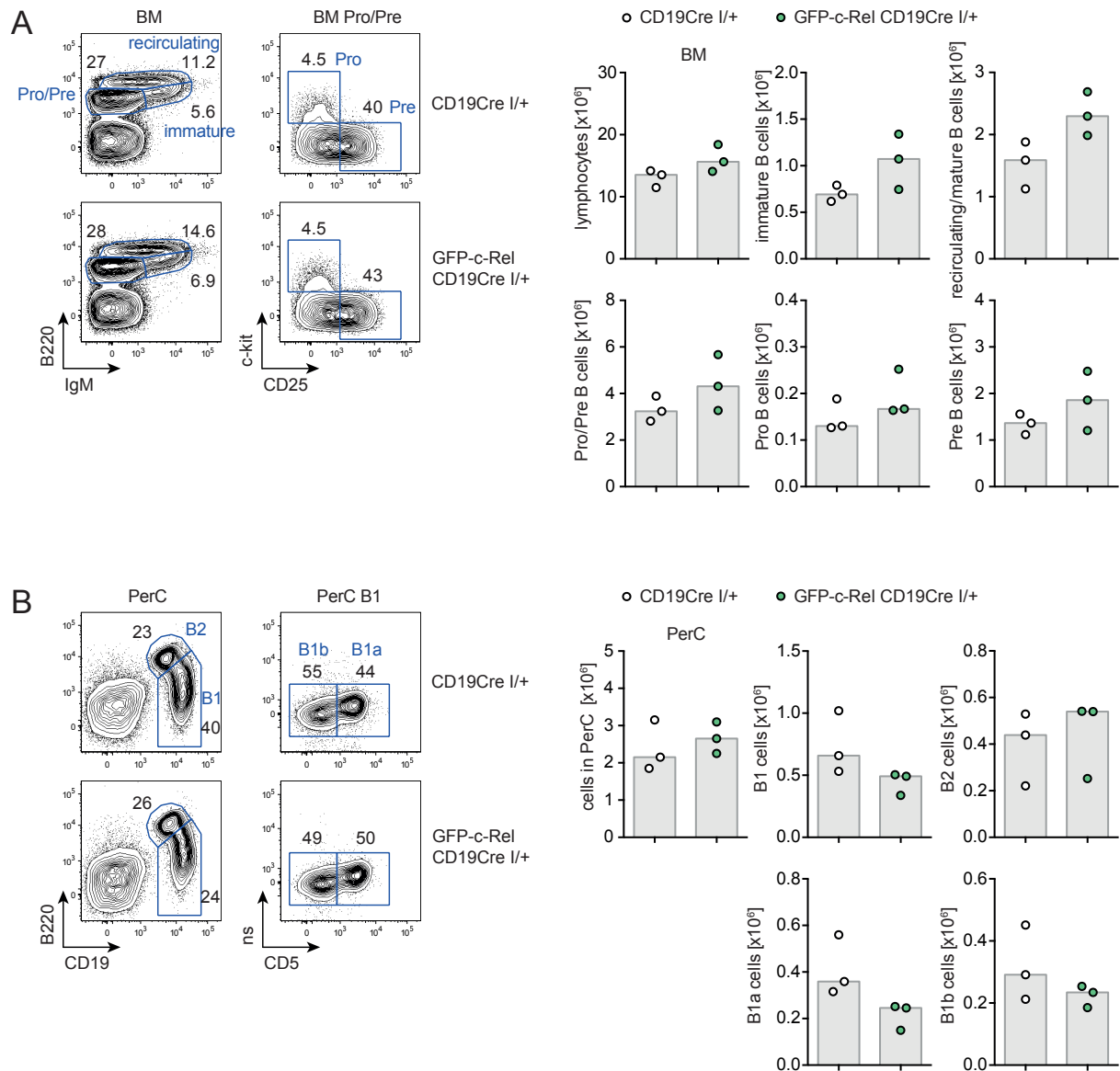


Figure S13: B cells in peripheral mouse immune organs of GFP-c-Rel CD19Cre^{I/+} mice. (A) Mouse weight and spleen weight assessed at day of analysis. (B) Total lymphocyte cell numbers for indicated immune organs. Flow cytometry-based analysis of (C) B cell percentages displayed in representative histograms and (D) B cell numbers in bar graphs. Individual data points obtained in ≥ 2 independent experiments are plotted. Bars and numbers below graphs are median values. SPL, spleen; LN, lymph nodes; MLN, mesenteric lymph nodes; PP, Peyer's patches.





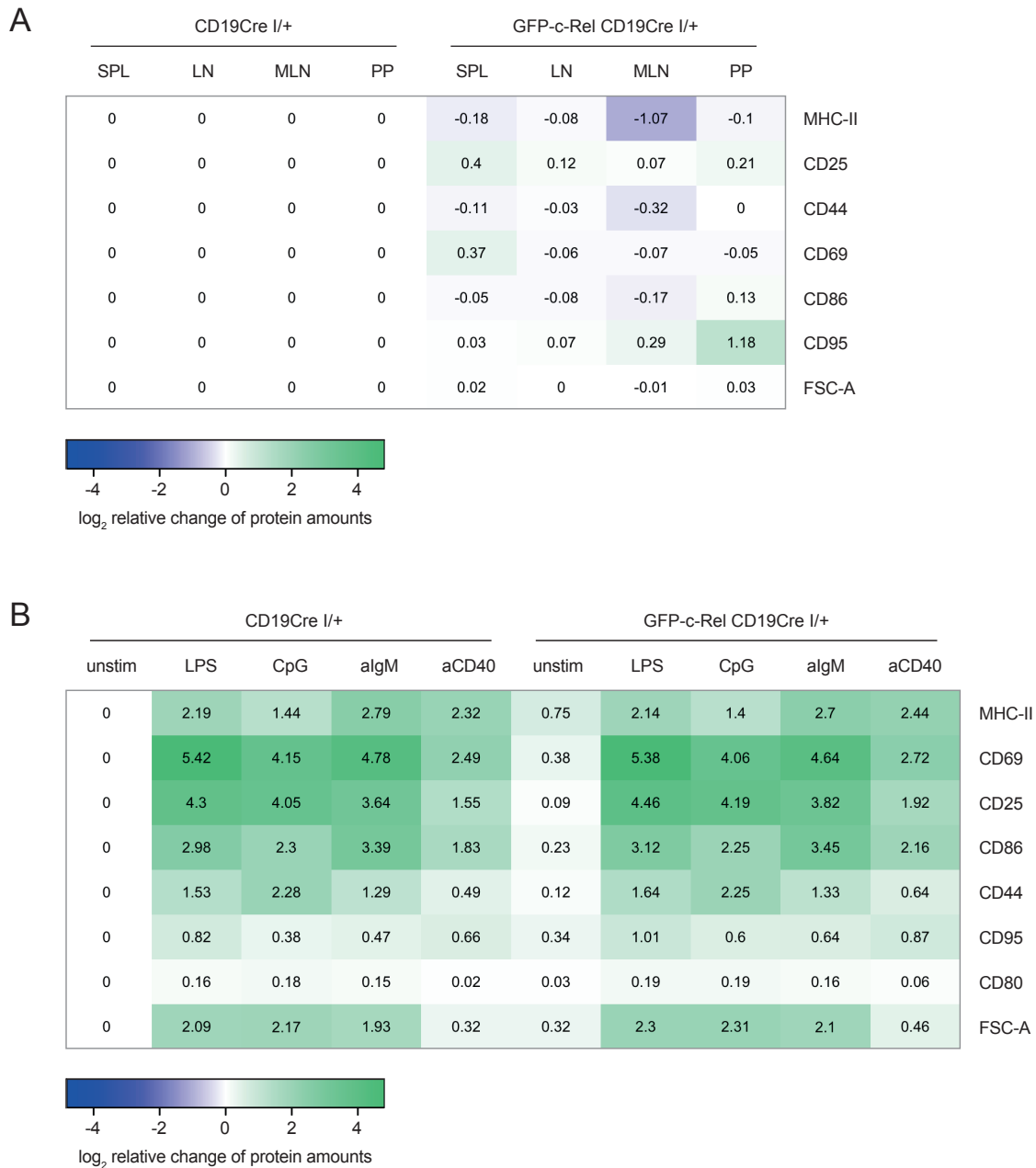


Figure S16: Regulation of B cell activation markers in GFP-c-Rel CD19Cre^{I/+} mice. Heatmap representation of \log_2 values of geometric means of relative change of activation marker protein amounts for GFP-c-Rel CD19Cre^{I/+} mice and CD19Cre^{I/+} controls. (A) Flow cytometry data of activation markers of CD19⁺ B cells in indicated organs. Activation markers were assessed directly *ex vivo*. Data were normalized to CD19Cre^{I/+} controls for each organ. Data are representative for 3 mice per genotype from 1 experiment. (B) Flow cytometry data of activation markers after over night stimulation of MACS-isolated splenic B cells with indicated stimuli (LPS 20 $\mu\text{g}/\text{ml}$, CpG 0.1 μM , anti-IgM (aIgM) 10 $\mu\text{g}/\text{ml}$, anti-CD40 (aCD40) 4 $\mu\text{g}/\text{ml}$). Data were normalized to unstimulated (unstim) B cells of CD19Cre^{I/+} controls. Data are representative for ≥ 4 mice per genotype and were obtained in ≥ 2 independent experiments. FSC-A, forward scatter area.

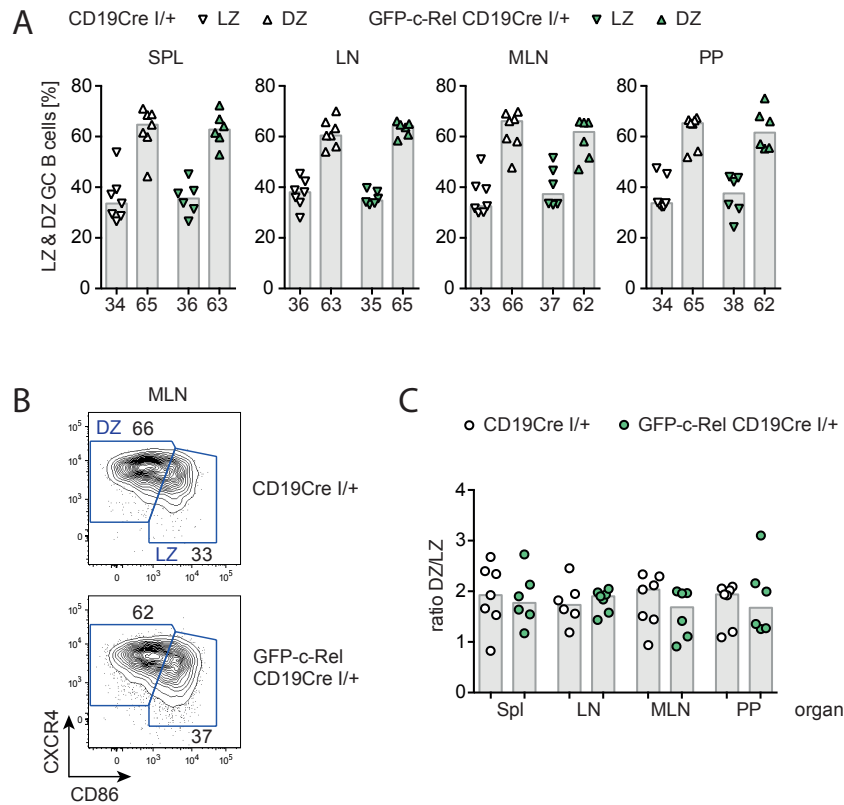


Figure S17: Frequencies of dark zone and light zone GC B cells in GFP-c-Rel CD19Cre^{I/+} mice. (A) Frequencies of dark zone (DZ) and light zone (LZ) GC B cells. Individual data points obtained in 2 independent experiments are plotted. Bars and numbers below graphs are median values. (B) Representative flow cytometry plots of LZ and DZ GC B cells in spleen. Numbers are median percentages. (C) Ratio of DZ and LZ GC B cell frequencies as given in (A). Individual data points are plotted. Bars represent geometric means. DZ CXCR4^{high}CD86^{low}; LZ CXCR4^{low}CD86^{high}; SPL, spleen; LN, lymph nodes; MLN, mesenteric lymph nodes; PP, Peyer's patches.

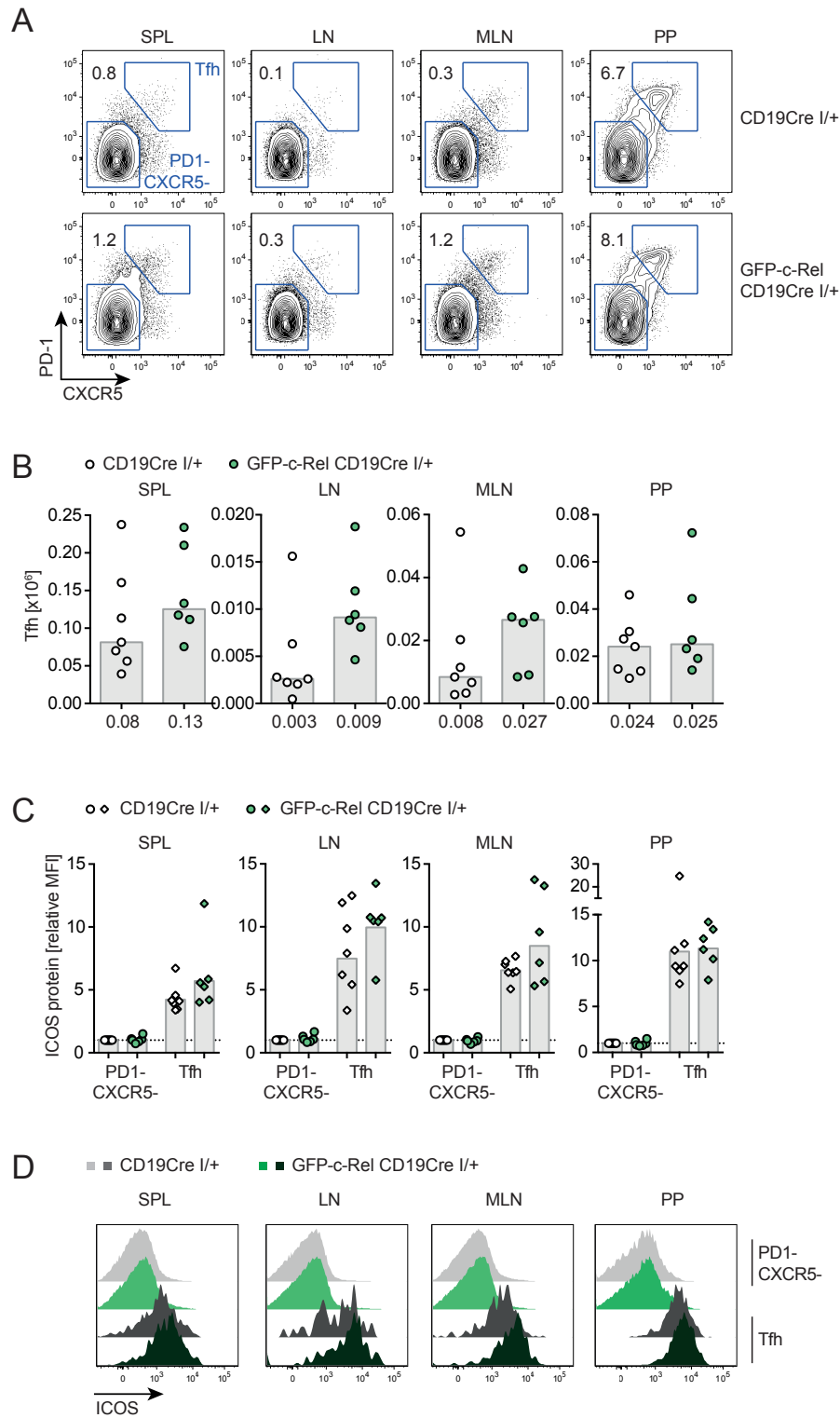


Figure S18: T_{fh} cells in GFP-c-Rel CD19Cre^{I/+} mice. (A) Representative flow cytometry plots of follicular helper T (T_{fh}) cells. Numbers are median percentages of PD-1^{high}CXCR5^{high} T_{fh} cells of TCR β ⁺CD4⁺ T cells. (B) T_{fh} cell numbers. Individual data points obtained in 2 independent experiments are plotted. Bars and numbers below graphs are median values. (C) Flow cytometry data of ICOS protein levels in T_{fh} cells normalized to the non-T_{fh} cell population of CD19Cre^{I/+} controls. Geometric mean and individual data points obtained in 2 independent experiments are plotted. (D) Representative histograms illustrate the bar graphs shown in (C). T_{fh} TCR β ⁺CD4⁺PD-1^{high}CXCR5^{high}; non-T_{fh} TCR β ⁺CD4⁺PD-1⁺CXCR5⁺; SPL, spleen; LN, lymph nodes; MLN, mesenteric lymph nodes; PP, Peyer's patches.

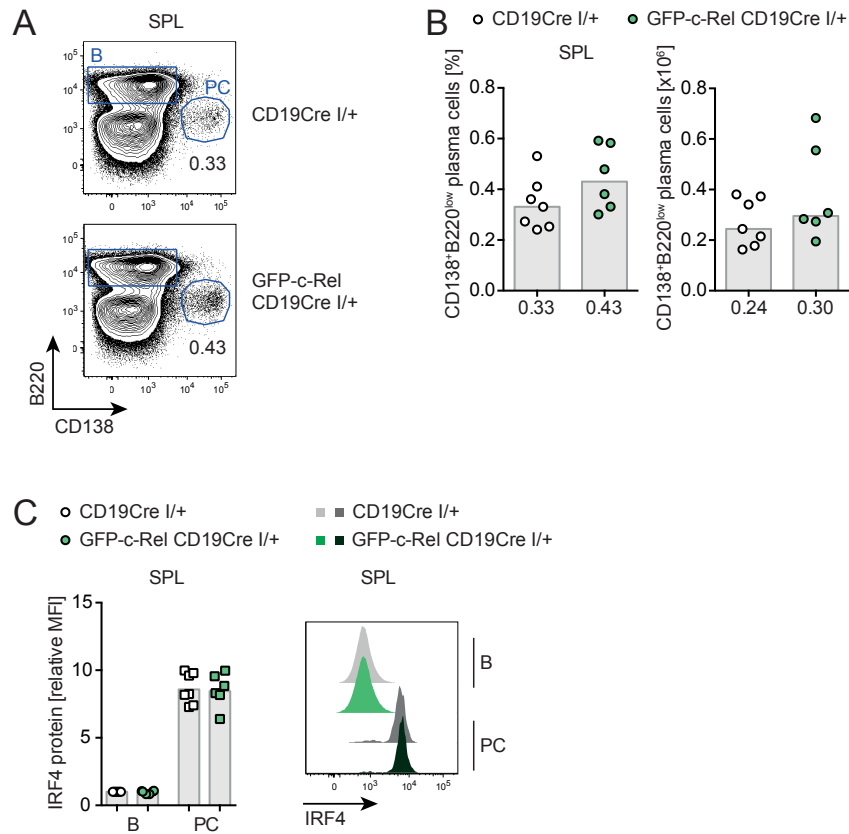


Figure S19: Plasma cells in GFP-c-Rel CD19Cre^{I/+} mice. (A) Representative flow cytometry plots of plasma cells. Numbers are median percentages. (B) Plasma cell percentages and cell numbers. Individual data points obtained in 2 independent experiments are plotted. Bars and numbers below graphs are median values. (C) Intracellular flow cytometry data of IRF4 protein levels in plasma cells normalized to the non-plasma cell B cell population of CD19Cre^{I/+} controls. Representative histograms illustrate the bar graph for which Individual data points obtained in 2 independent experiments and the geometric mean represented as a bar are plotted. plasma cells (PC) B220^{low}CD138⁺; B (non-PC) B220⁺CD138⁻; SPL, spleen; BM, bone marrow.

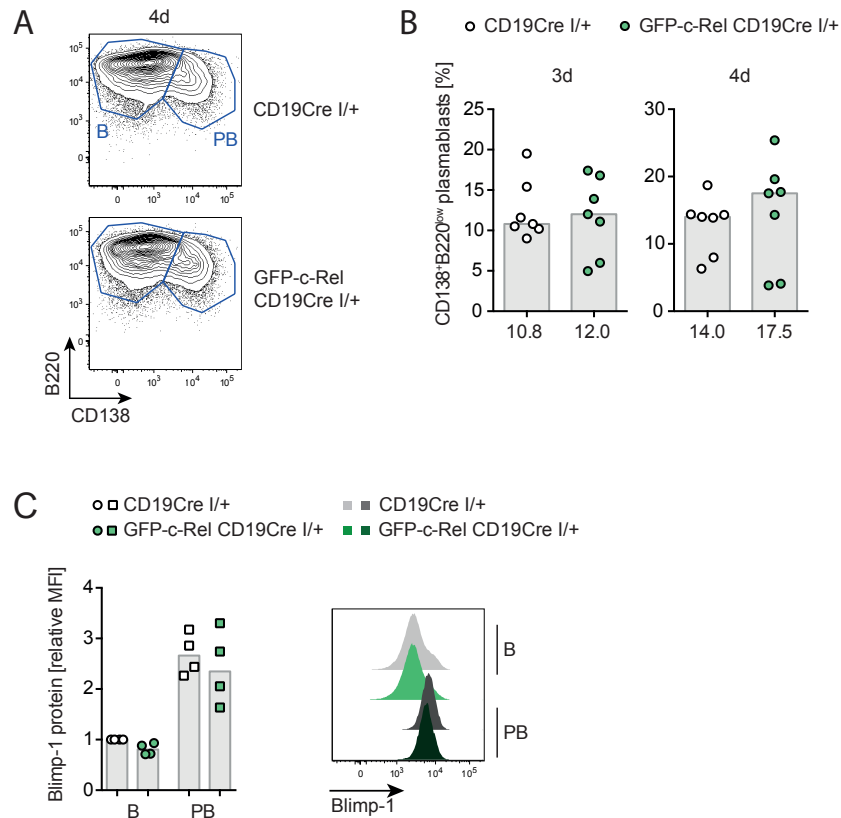


Figure S20: *In vitro* plasmablast differentiation with GFP-c-Rel CD19Cre^{I/+} splenocytes. (A) Representative flow cytometry plots of plasmablasts. (B) Percentages of plasmablasts after 3 days or 4 days of LPS treatment *in vitro*. Individual data points obtained in 3 independent experiments are plotted. Bars represent median values. (C) Intracellular flow cytometry data of Blimp-1 protein levels in plasmablasts after 3 days of LPS treatment *in vitro* normalized to the non-plasmablast cell population of CD19Cre^{I/+} controls. Representative histograms illustrate the bar graphs for which the geometric mean and individual data points obtained in 2 independent experiments are plotted. Plasmablasts (PB) B220^{low}CD138⁺; B (non-PB) B220⁺CD138⁻.

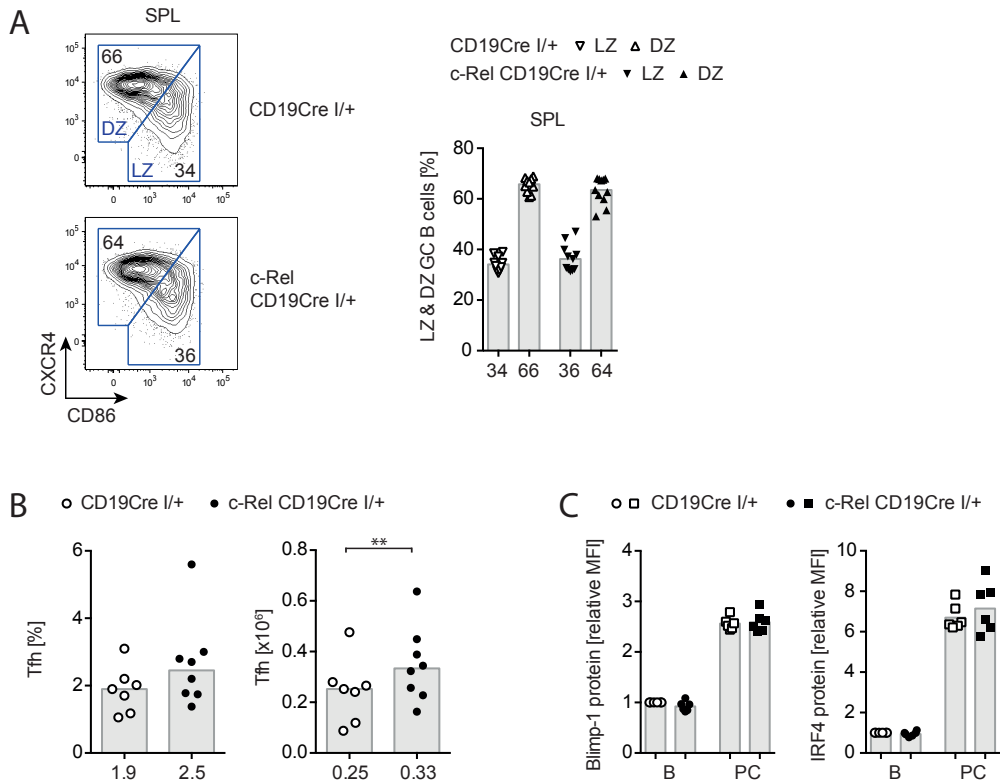


Figure S21: SRBC-immunized c-Rel CD19Cre^{I/+} mice. Mice were immunized with SRBC and spleens were analyzed 10-12 days post-immunization. (A) Representative flow cytometry plots and median percentages of light zone (LZ) and dark zone (DZ) splenic GC B cells. Individual data points obtained in 4 independent experiments are plotted. Bars and numbers below graphs are median values. (B) Percentages and cell numbers of splenic T_{fh} cells. Individual data points obtained in 3 independent experiments are plotted. Bars and numbers below graphs are median values. (C) Intracellular flow cytometry data of Blimp-1 and IRF4 protein levels in splenic plasma cells normalized to the non-PC population of CD19Cre^{I/+} controls. Individual data points obtained in 2 independent experiments and the geometric mean are plotted. ** $p \leq 0.01$, paired t test. GCB CD19⁺/B220⁺CD95^{high}CD38^{low}; DZ CXCR4^{high}CD86^{low}; LZ CXCR4^{low}CD86^{high}; T_{fh} TCR β ⁺CD4⁺PD-1^{high}CXCR5^{high}; plasma cells (PC) B220^{low}CD138⁺; B (non-PC) B220⁺CD138⁺;

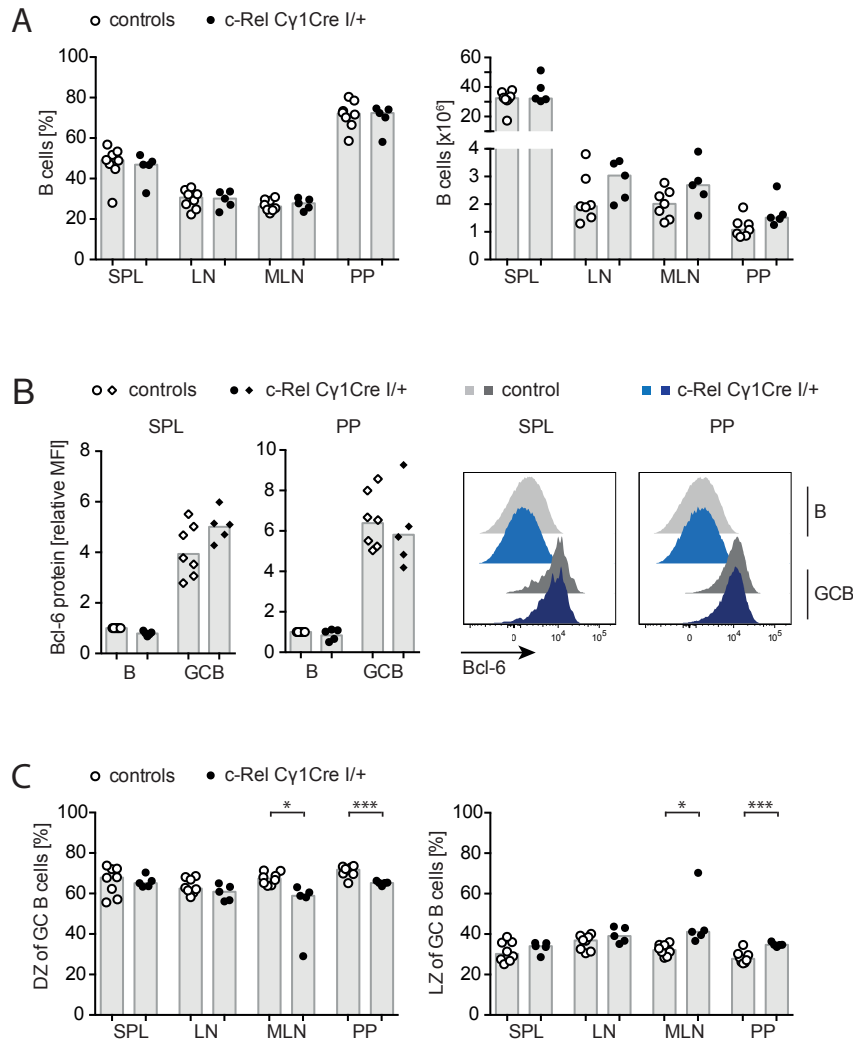


Figure S22: B cells and GC B cells in $c\text{-Rel } C\gamma 1Cre^{I/+}$ mice. (A) Percentages and cell numbers of B cells. Individual data points and medians represented as bars are plotted. (B) Intracellular flow cytometry data of Bcl-6 protein levels in GC B cells normalized to the non-GC B cell population of controls. Representative histograms illustrate the bar graphs for which the geometric mean and individual data points are plotted. (C) Frequencies of dark zone (DZ) and light zone (LZ) GC B cells. Individual data points are plotted and bars represent median values. Controls include $c\text{-Rel}$ and $C\gamma 1Cre^{I/+}$ mice. Data were obtained in 2 independent experiments. * $p \leq 0.05$, ** $p \leq 0.01$, *** $p \leq 0.001$, unpaired t test. B $CD19^+/B220^+$ in (A); GCB $CD19^+/B220^+CD95^{\text{high}}CD38^{\text{low}}$; B (non-GCB) $CD19^+/B220^+CD95^{\text{low}}CD38^{\text{high}}$ in (B); DZ $CXCR4^{\text{high}}CD86^{\text{low}}$; LZ $CXCR4^{\text{low}}CD86^{\text{high}}$; SPL, spleen; LN, lymph nodes; MLN, mesenteric lymph nodes; PP, Peyer's patches.

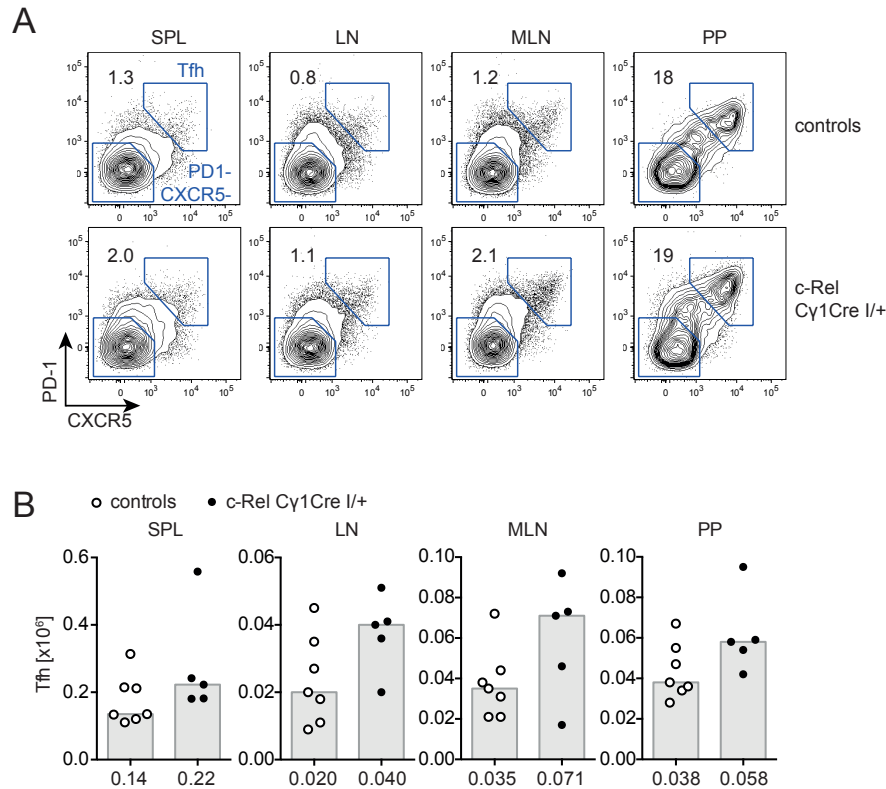


Figure S23: Expansion of T_{fh} cells in c-Rel C γ 1Cre^{I/+} mice. (A) Representative flow cytometry plots of follicular helper T (T_{fh}) cells. Numbers are median percentages of PD-1^{high}CXCR5^{high} T_{fh} cells of TCR β ⁺CD4⁺ T cells. (B) T_{fh} cell numbers. Individual data points obtained in 2 independent experiments are plotted. Bars and numbers below graphs are median values. Controls include c-Rel and C γ 1Cre^{I/+} mice. T_{fh} TCR β ⁺CD4⁺PD-1^{high}CXCR5^{high}; SPL, spleen; LN, lymph nodes; MLN, mesenteric lymph nodes; PP, Peyer's patches.

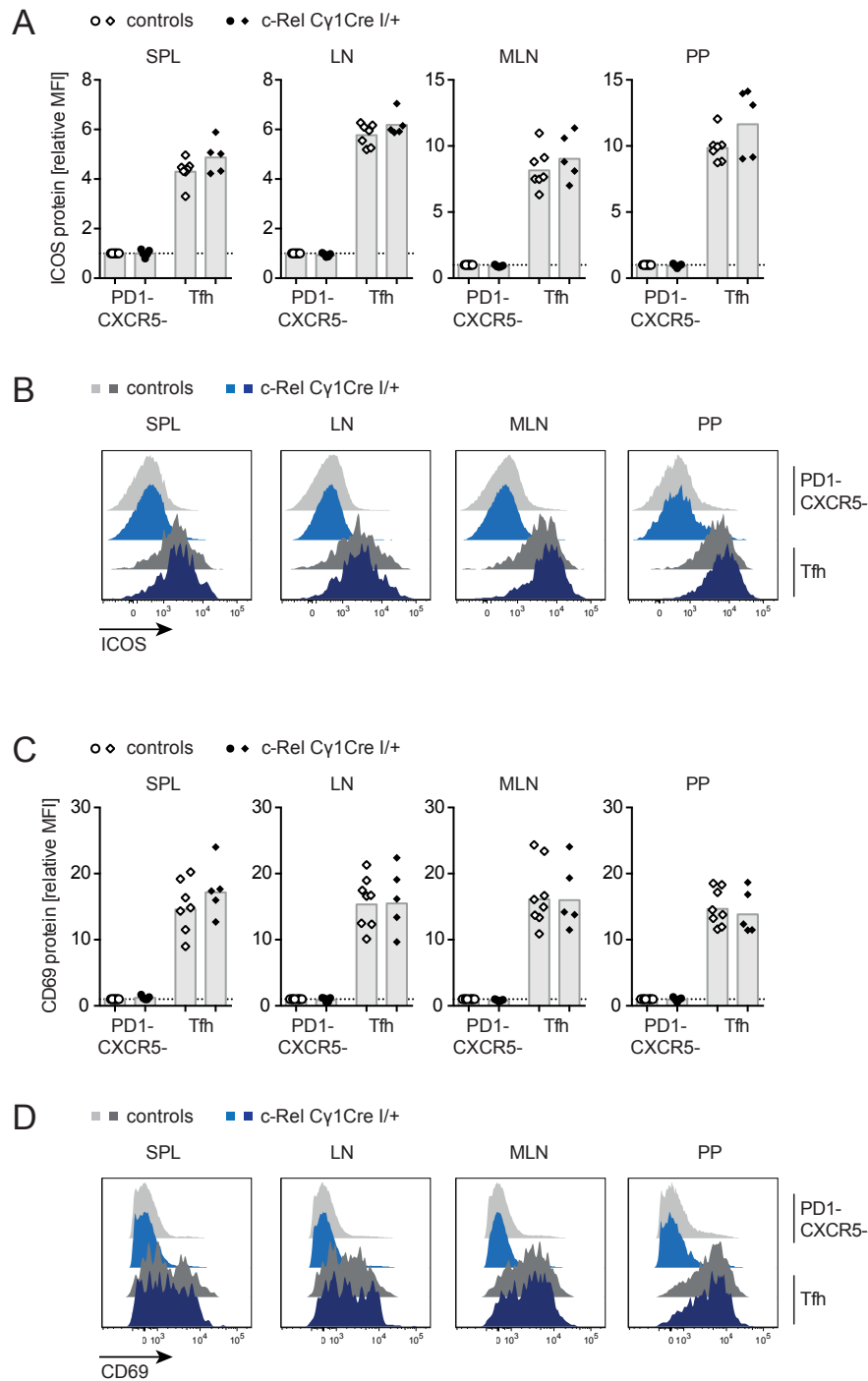


Figure S24: Characteristics of T_{fh} cells in $c\text{-Rel } \text{C}\gamma\text{1Cre}^{\text{I/+}}$ mice. Flow cytometry data of (A) ICOS or (C) CD69 protein levels of T_{fh} cells normalized to the non- T_{fh} cell population of controls. Geometric mean and individual data points obtained in 2 independent experiments are plotted. (B) and (D) show representative histograms illustrating the bar graphs shown in (A) and (C), respectively. Controls include $c\text{-Rel}$ and $\text{C}\gamma\text{1Cre}^{\text{I/+}}$ mice. T_{fh} $\text{TCR}\beta^+\text{CD4}^+\text{PD-1}^{\text{high}}\text{CXCR5}^{\text{high}}$; non- T_{fh} $\text{TCR}\beta^+\text{CD4}^+\text{PD-1}^{\text{low}}\text{CXCR5}^{\text{low}}$; SPL, spleen; LN, lymph nodes; MLN, mesenteric lymph nodes; PP, Peyer's patches.

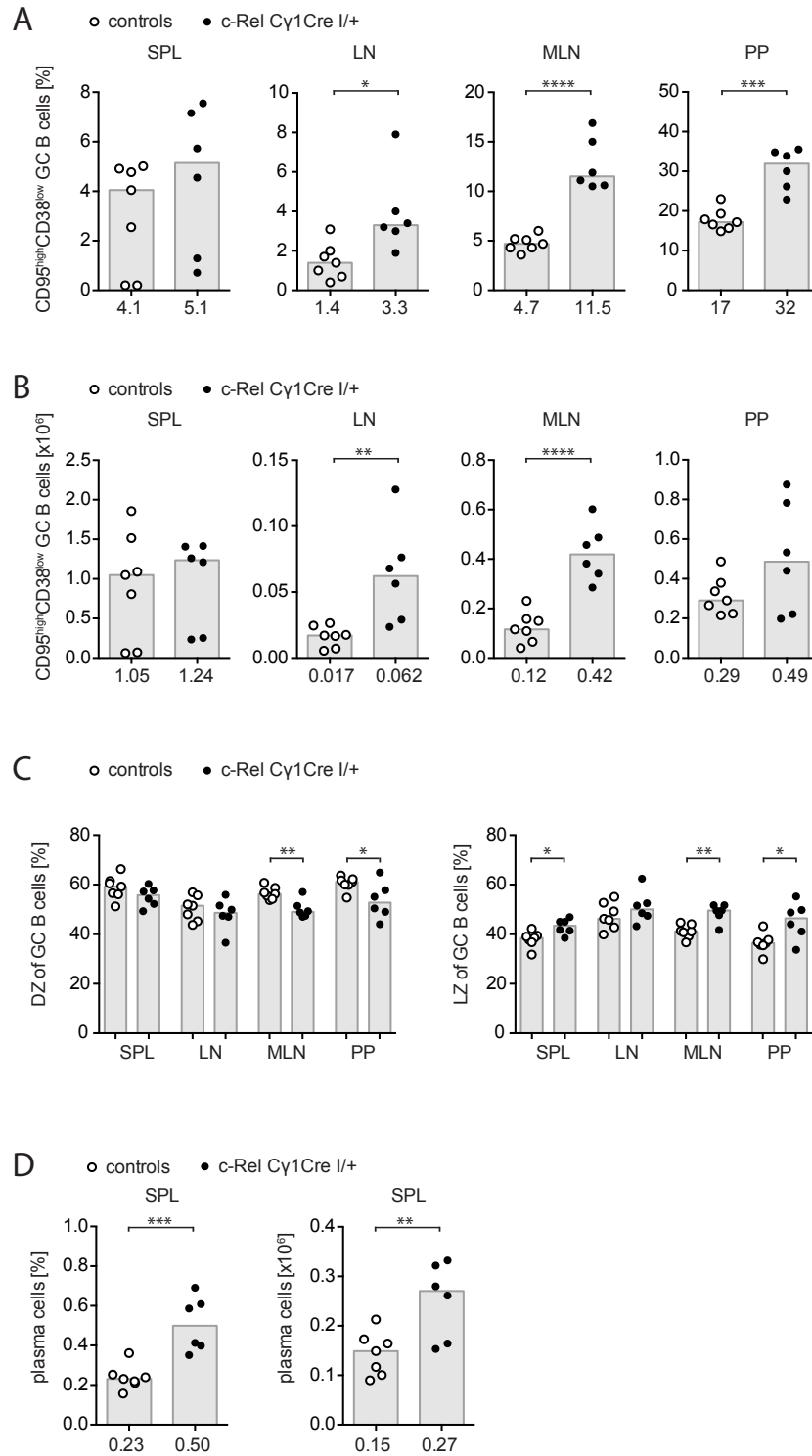


Figure S25: GC B cells and plasma cells in SRBC-immunized c-Rel $C\gamma 1Cre^{I/+}$ mice. Mice were immunized with SRBC and organs were analyzed 10-12 days post-immunization. GC B cell (A) percentages of total B cells and (B) cell numbers. (C) Frequencies of dark zone (DZ) and light zone (LZ) GC B cells. (D) Plasma cell percentages and cell numbers. Individual data points obtained in 2 independent experiments are plotted. Bars and numbers below graphs are median values. Controls include c-Rel and $C\gamma 1Cre^{I/+}$ mice. * $p \leq 0.05$, ** $p \leq 0.01$, *** $p \leq 0.001$, **** $p \leq 0.0001$, unpaired t test. GCB $CD19^+/B220^+CD95^{\text{high}}CD38^{\text{low}}$; DZ $CXCR4^{\text{high}}CD86^{\text{low}}$; LZ $CXCR4^{\text{low}}CD86^{\text{high}}$; plasma cells (PC) $B220^{\text{low}}CD138^+$; SPL, spleen; LN, lymph nodes; MLN, mesenteric lymph nodes; PP, Peyer's patches.

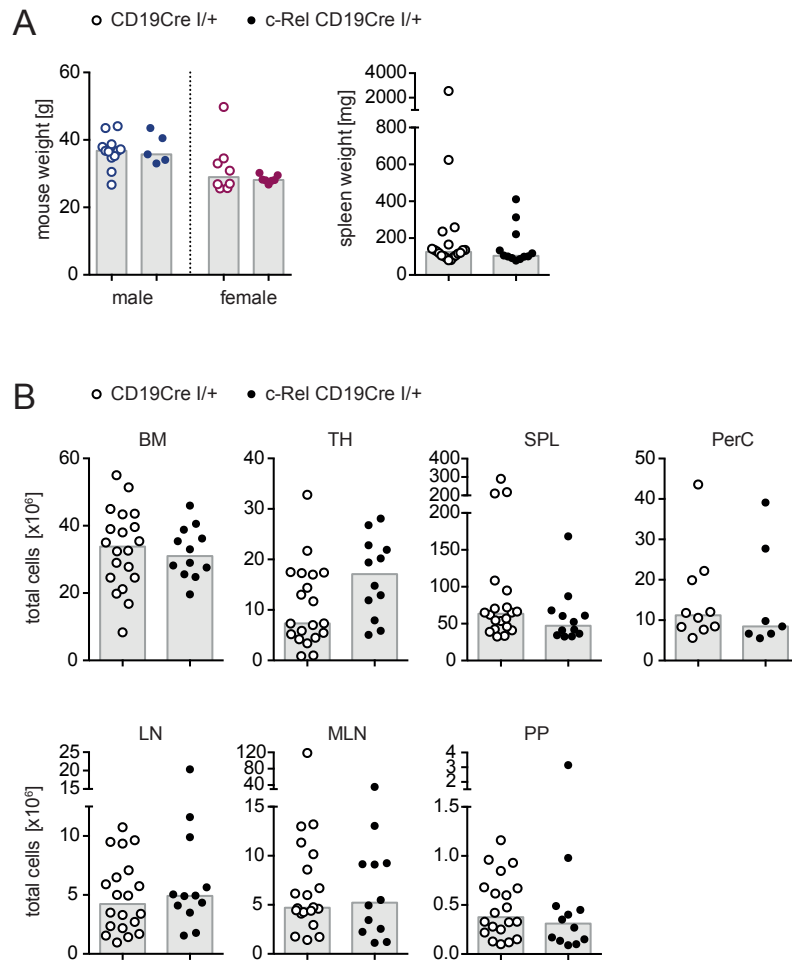


Figure S26: Immune organ cell numbers in aged c-Rel CD19Cre^{I/+} mice. (A) Mouse weight and spleen weight of aged c-Rel CD19Cre^{I/+} mice and CD19Cre^{I/+} control mice. (B) Total cell numbers for indicated immune organs. Individual data points and bars representing median values are plotted. Data were obtained in 4-8 independent experiments. BM, bone marrow; TH, thymus; SPL, spleen; PerC, peritoneal cavity; LN, lymph nodes; MLN, mesenteric lymph nodes; PP, Peyer's patches.

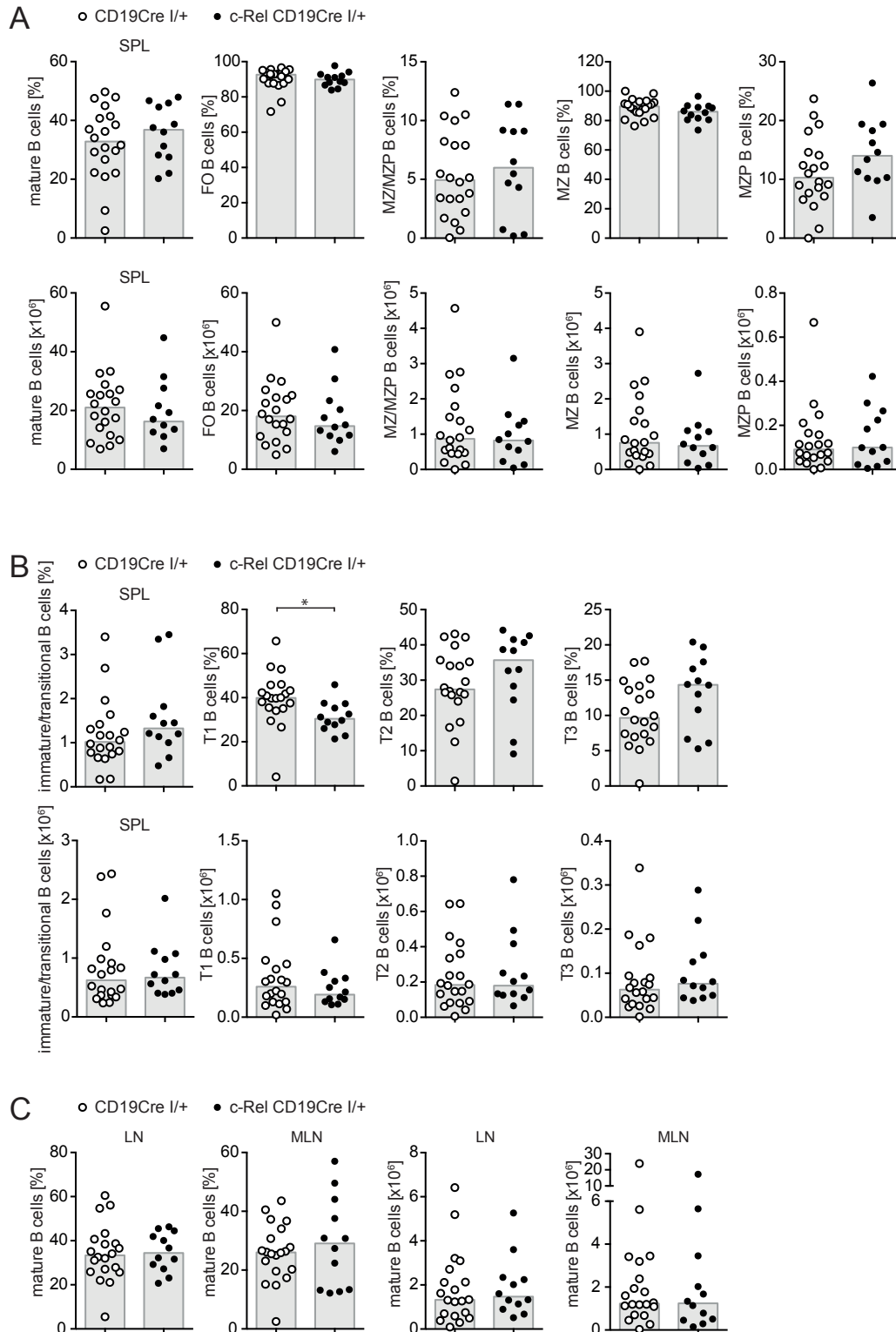


Figure S27: B cells in aged c-Rel CD19Cre^{I/+} mice. Percentages and cell numbers of (A) mature and (B) immature B cell subpopulations in spleens of c-Rel CD19Cre^{I/+} and CD19Cre^{I/+} control mice. (C) Mature B cell percentages and cell numbers in lymph nodes and mesenteric lymph nodes. Individual data points obtained in 8 independent experiments and bars representing median values are plotted. For gating strategy of indicated B cell populations see Figure 7. * $p \leq 0.05$, unpaired t test. SPL, spleen; LN, lymph nodes; MLN, mesenteric lymph nodes.

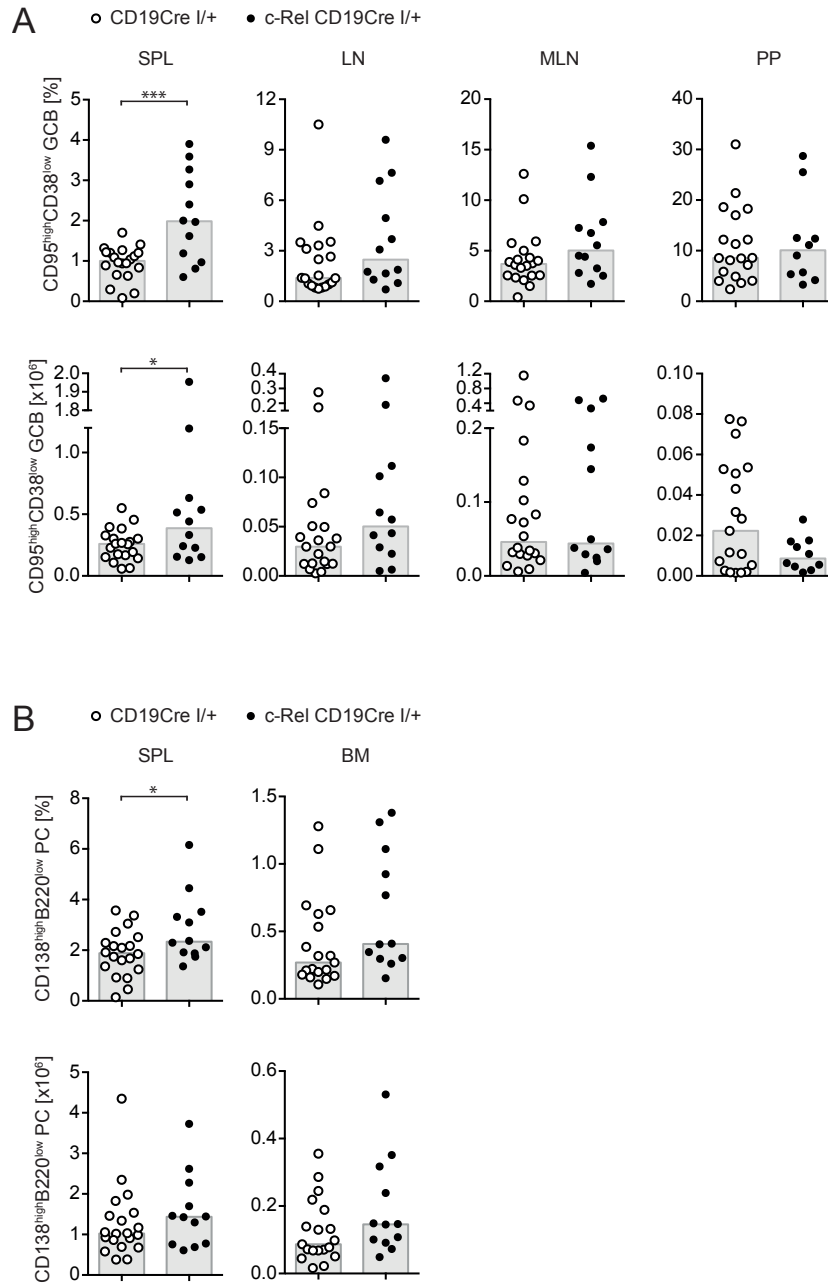


Figure S28: GC B cells and plasma cells in aged c-Rel CD19Cre^{I/+} mice. Percentages and cell numbers of (A) GC B cells and (B) plasma cells of aged c-Rel CD19Cre^{I/+} and CD19Cre^{I/+} control mice. Individual data points obtained in 8 independent experiments and medians represented as bars are plotted. ** $p \leq 0.01$, unpaired t test. GCB CD19⁺CD95^{high}CD38^{low}; plasma cells (PC) B220^{low}CD138⁺; BM, bone marrow; SPL, spleen; LN, lymph nodes; MLN, mesenteric lymph nodes; PP, Peyer's patches.

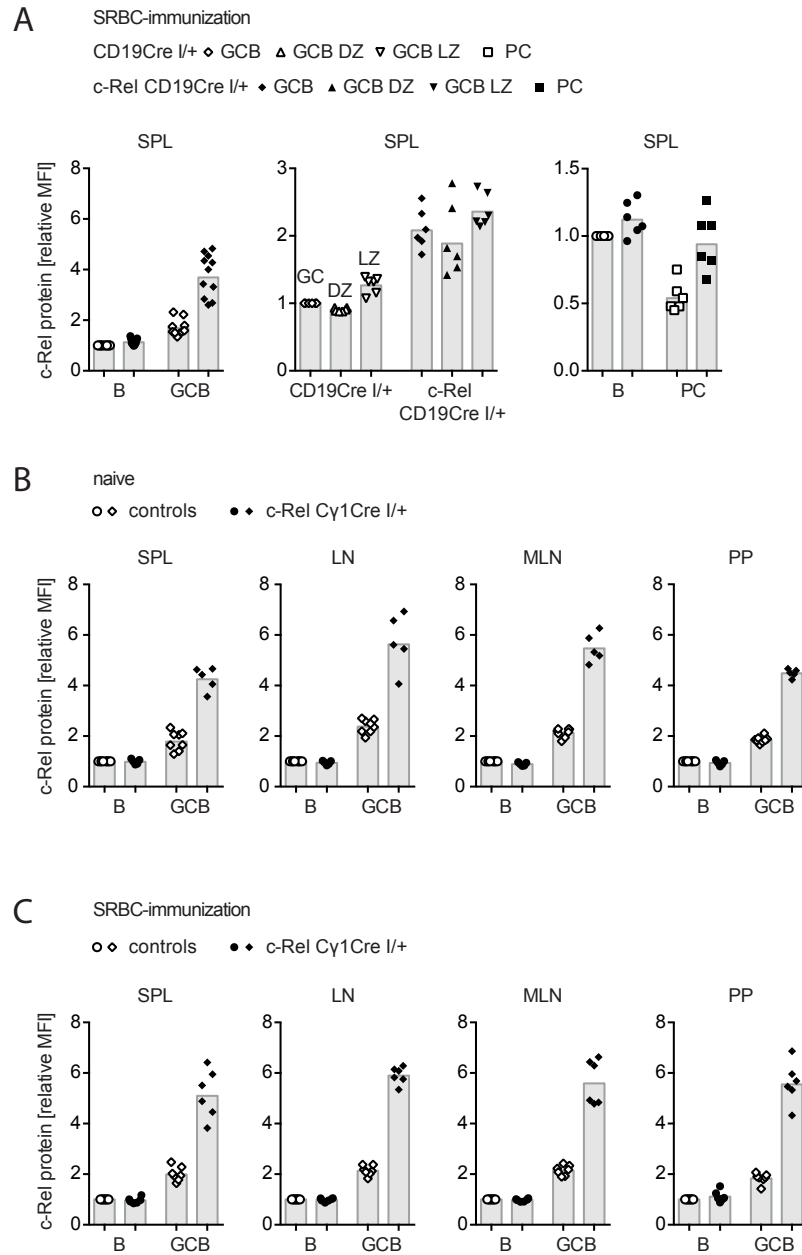


Figure S29: c-Rel levels are highly upregulated in GC B cells and decreased in plasma cells. Intracellular flow cytometry data of c-Rel protein levels in B cell subpopulations. Median fluorescence intensities (MFI) were normalized to (A) CD19Cre^{I/+} controls or to (B) and (C) controls (for more information on normalization for individual populations see Figure 22). Individual data points obtained in ≥ 2 independent experiments and bars representing geometric means are plotted. Controls in C γ 1Cre^{I/+} experiments include c-Rel and C γ 1Cre^{I/+} mice. (A) c-Rel level in B cells, GC B cells and plasma cells of SRBC-immunized c-Rel CD19Cre^{I/+} mice. (B) c-Rel level in GC B cells of naive c-Rel C γ 1Cre^{I/+} mice. (C) c-Rel level in GC B cells of SRBC-immunized c-Rel C γ 1Cre^{I/+} mice. GCB CD19⁺/B220⁺CD95^{high}CD38^{low}; B (non-GCB) CD19⁺/B220⁺CD95⁻CD38^{high}; DZ CXCR4^{high}CD86^{low}; LZ CXCR4^{low}CD86^{high}; plasma cells (PC) B220^{low}CD138⁺; B (non-PC) B220⁺CD138⁻; SPL, spleen; LN, lymph nodes; MLN, mesenteric lymph nodes; PP, Peyer's patches.

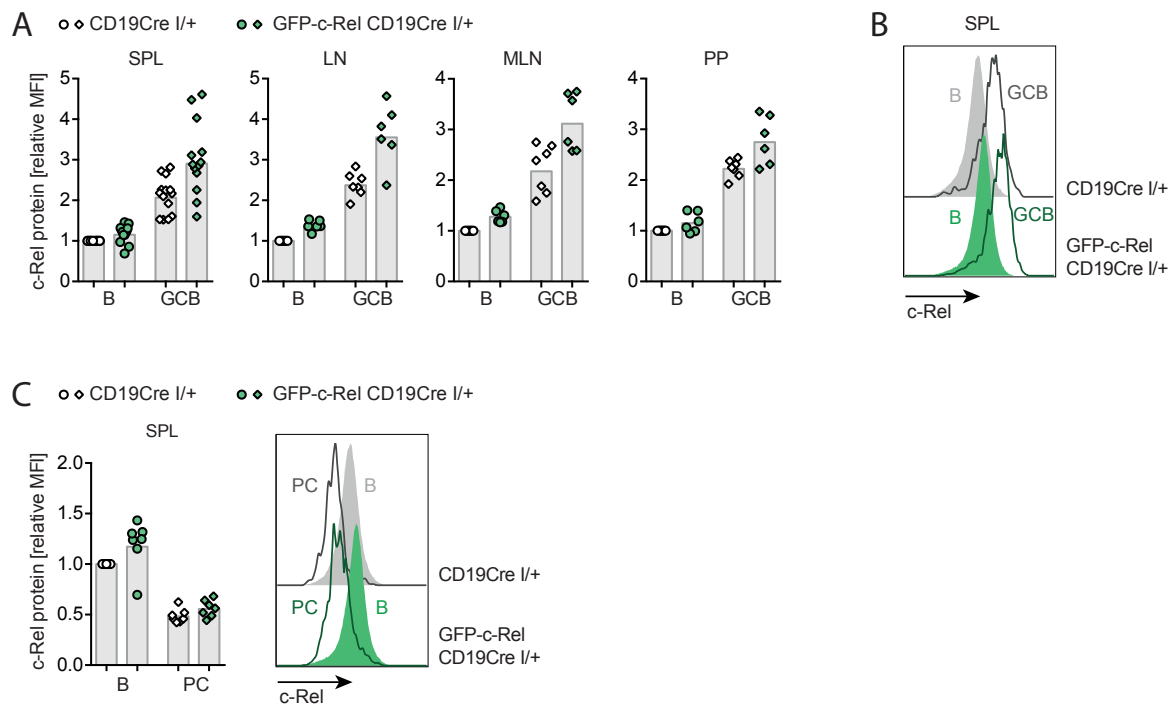


Figure S30: Total c-Rel levels in GFP-c-Rel CD19Cre^{I/+} mice. Intracellular flow cytometry data of c-Rel protein levels in B cell subpopulations. Median fluorescence intensities (MFI) were normalized to CD19Cre^{I/+} controls. Individual data points obtained in ≥ 2 independent experiments and bars representing geometric means are plotted. (A) c-Rel level in B cells and GC B cells. MFIs were normalized to non-GCB of CD19Cre^{I/+} controls. (B) Representative histograms illustrate c-Rel level in B and GC B cells. (C) c-Rel level in plasma cells. MFIs were normalized to splenic B cells (non-PC) of CD19Cre^{I/+} controls. GCB CD19⁺/B220⁺CD95^{high}CD38^{low}; B (non-GCB) CD19⁺/B220⁺CD95⁻CD38^{high}; plasma cells (PC) B220^{low}CD138⁺; B (non-PC) B220⁺CD138⁻; SPL, spleen; LN, lymph nodes; MLN, mesenteric lymph nodes; PP, Peyer's patches.

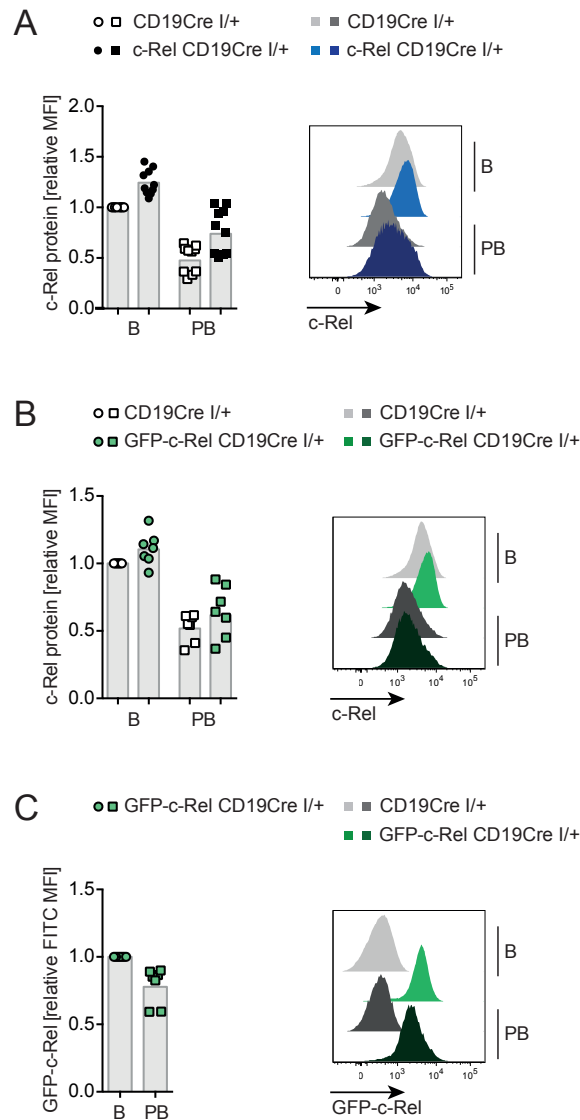


Figure S31: c-Rel and GFP-c-Rel levels in *in vitro*-differentiated plasmablasts. Displayed data were obtained after LPS treatment of splenocytes for 3 days *in vitro* in 3 independent experiments. Representative histograms illustrate the bar graphs for which the geometric mean and individual data points are plotted. Median fluorescence intensity (MFI) values were normalized to non-plasmablasts of CD19Cre^{I/+} controls. c-Rel level in plasmablasts of (A) c-Rel CD19Cre^{I/+} and (B) GFP-c-Rel CD19Cre^{I/+} mice and (C) GFP-c-Rel level in plasmablasts of GFP-c-Rel CD19Cre^{I/+} mice. Plasmablasts (PB) B220^{low}CD138⁺; B (non-PB) B220⁺CD138⁻.

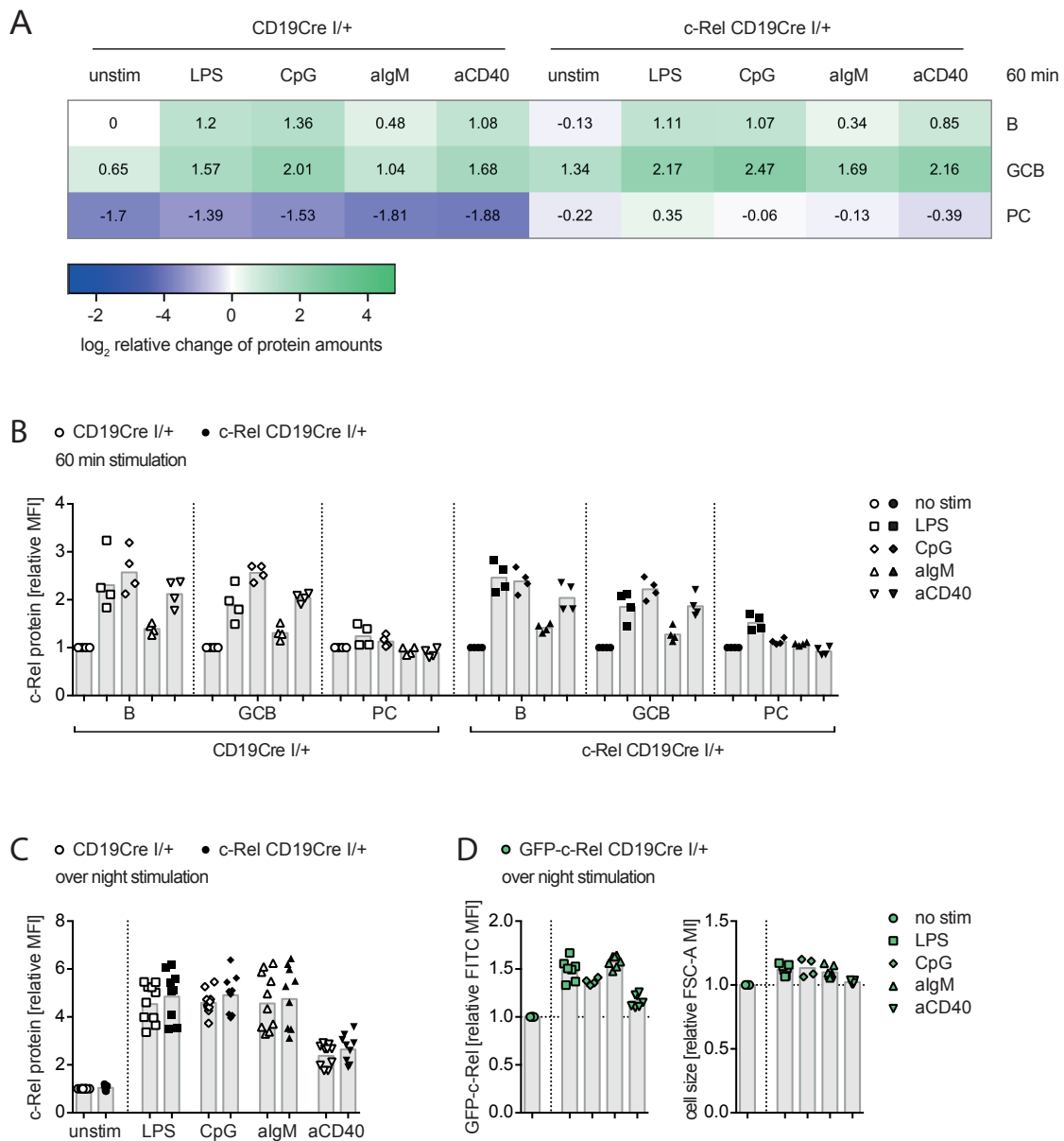


Figure S32: Induction of c-Rel following stimulation. c-Rel levels after (A, B) stimulation of splenocytes for 60 min or (C, D) stimulation of MACS-isolated B cells over night with the indicated stimuli (LPS 20 $\mu\text{g}/\text{ml}$, CpG 0.1 μM , anti-IgM (aIgM) 10 $\mu\text{g}/\text{ml}$, anti-CD40 (aCD40) 4 $\mu\text{g}/\text{ml}$). (A) Heatmap representation of \log_2 values of geometric means of relative change of c-Rel protein amounts. All data were normalized to unstimulated (unstim) B cells of CD19Cre^{I/+} controls. (B) Individual data points with geometric mean bar graph representation for the same dataset presented in (A) but with data normalization to unstimulated cells within each subpopulation separately for each genotype. For (A, B) data are representative for 4 mice per genotype from 2 independent experiments. (C) c-Rel level in c-Rel CD19Cre^{I/+} B cells normalized to unstimulated B cells of CD19Cre^{I/+} controls. (D) GFP-c-Rel level and FSC-A in GFP-c-Rel CD19Cre^{I/+} B cells normalized to unstimulated B cells. For (C, D) individual data points obtained in 3 independent experiments and bar graphs representing geometric means are plotted. GCB CD19⁺CD95^{high}CD38^{low}; B (non-GCB) CD19⁺CD95^{high}CD38^{high}; plasma cells (PC) B220^{low}CD138⁺; FSC-A, forward scatter area.

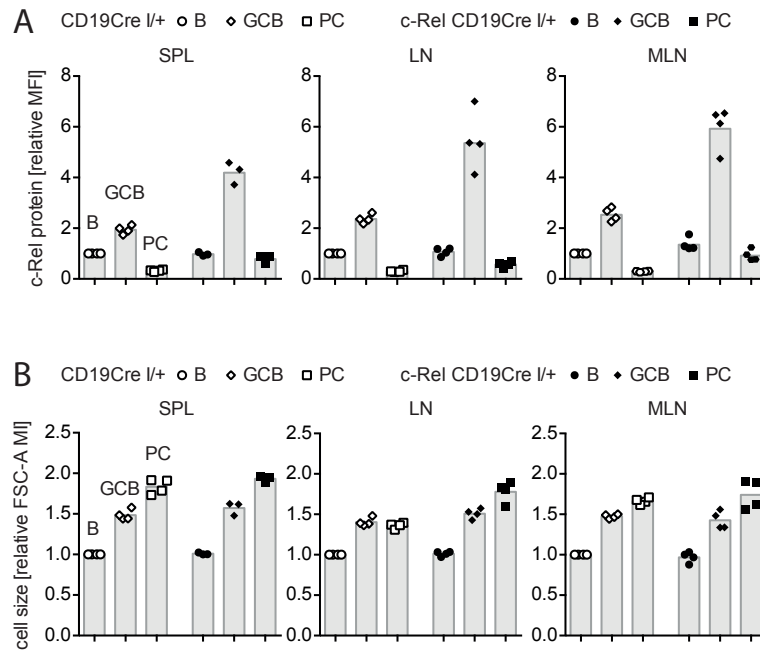


Figure S33: Verification of c-Rel level switches in B cell subpopulations by use of a different antibody clone. Intracellular flow cytometry data of (A) c-Rel protein levels or (B) FSC-A levels in B cells, GC B cells and plasma cells. Median fluorescence intensities (MFI) were normalized to non-GC B cells of CD19Cre^{I/+} controls. Individual data points obtained in 2 independent experiments and bars representing geometric means are plotted. GCB CD19⁺CD95^{high}CD38^{low}; B (non-GCB) CD19⁺CD95⁻CD38^{high}; plasma cells (PC) B220^{low}CD138⁺; SPL, spleen; LN, lymph nodes; MLN, mesenteric lymph nodes; FSC-A, forward scatter area.

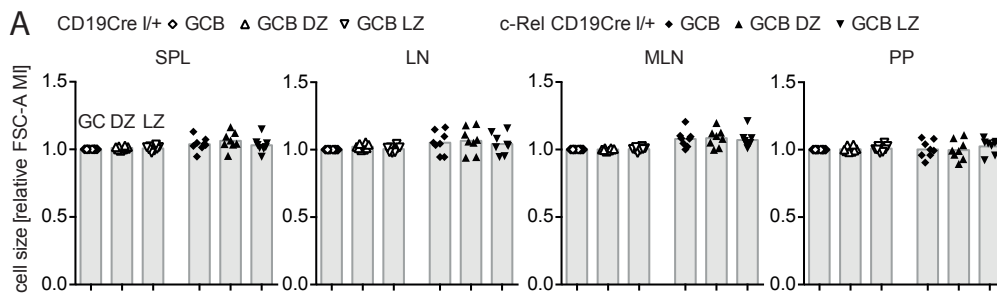


Figure S34: Cell size of DZ and LZ GC B cells. (A) FSC-A level in LZ and DZ of GC B cells. Data were normalized to GC B cells of CD19Cre^{I/+} controls. Individual data points obtained in 3 independent experiments and bars representing geometric means are plotted. GC B CD19⁺/B220⁺CD95^{high}CD38^{low}; DZ CXCR4^{high}CD86^{low}; LZ CXCR4^{low}CD86^{high}; SPL, spleen; LN, lymph nodes; MLN, mesenteric lymph nodes; PP, Peyer's patches; FSC-A, forward scatter area.

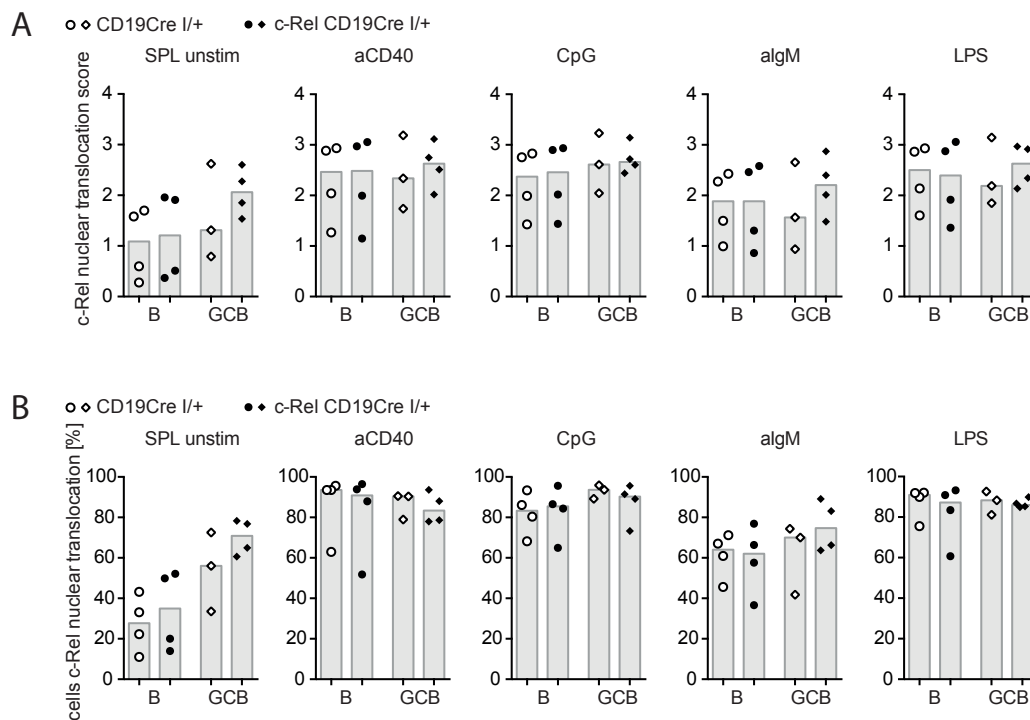


Figure S35: Quantification of c-Rel nuclear localization in splenic B cells and GC B cells by imaging flow cytometry. Splenocytes were stimulated with the indicated stimuli or left unstimulated (unstim) for 60 min in the presence of 10 μ M Q-VD to prolong the survival of GC B cells in culture. (A) Median c-Rel nuclear localization score and (B) percentage of cells with c-Rel nuclear translocation for splenic B cells and GC B cells from c-Rel CD19Cre^{1/+} and CD19Cre^{1/+} mice. Individual data points obtained in 3 independent experiments are plotted. GCB CD19⁺CD95^{high}CD38^{low}; B (non-GCB) CD19⁺CD95^{low}CD38^{high}.

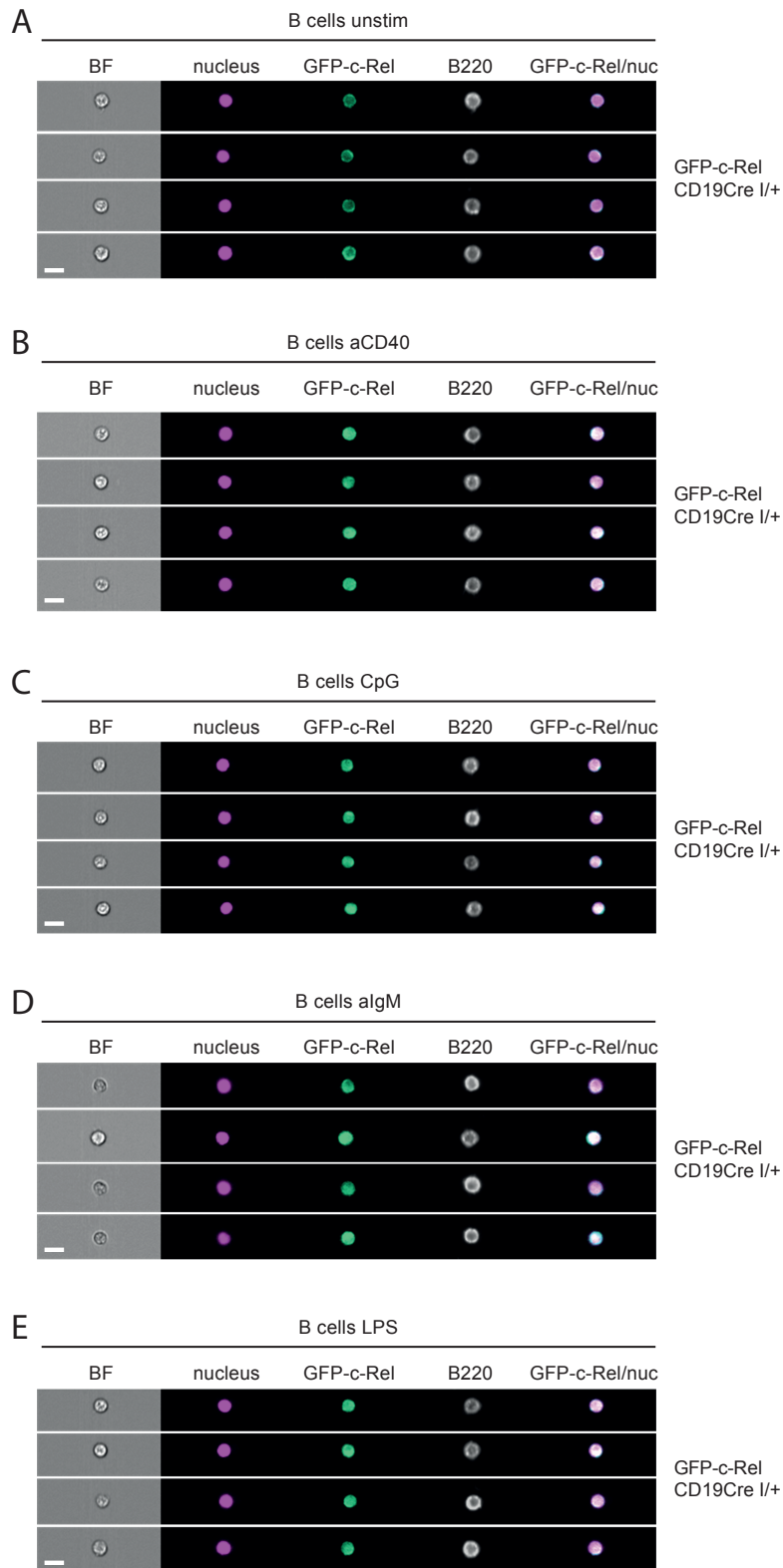
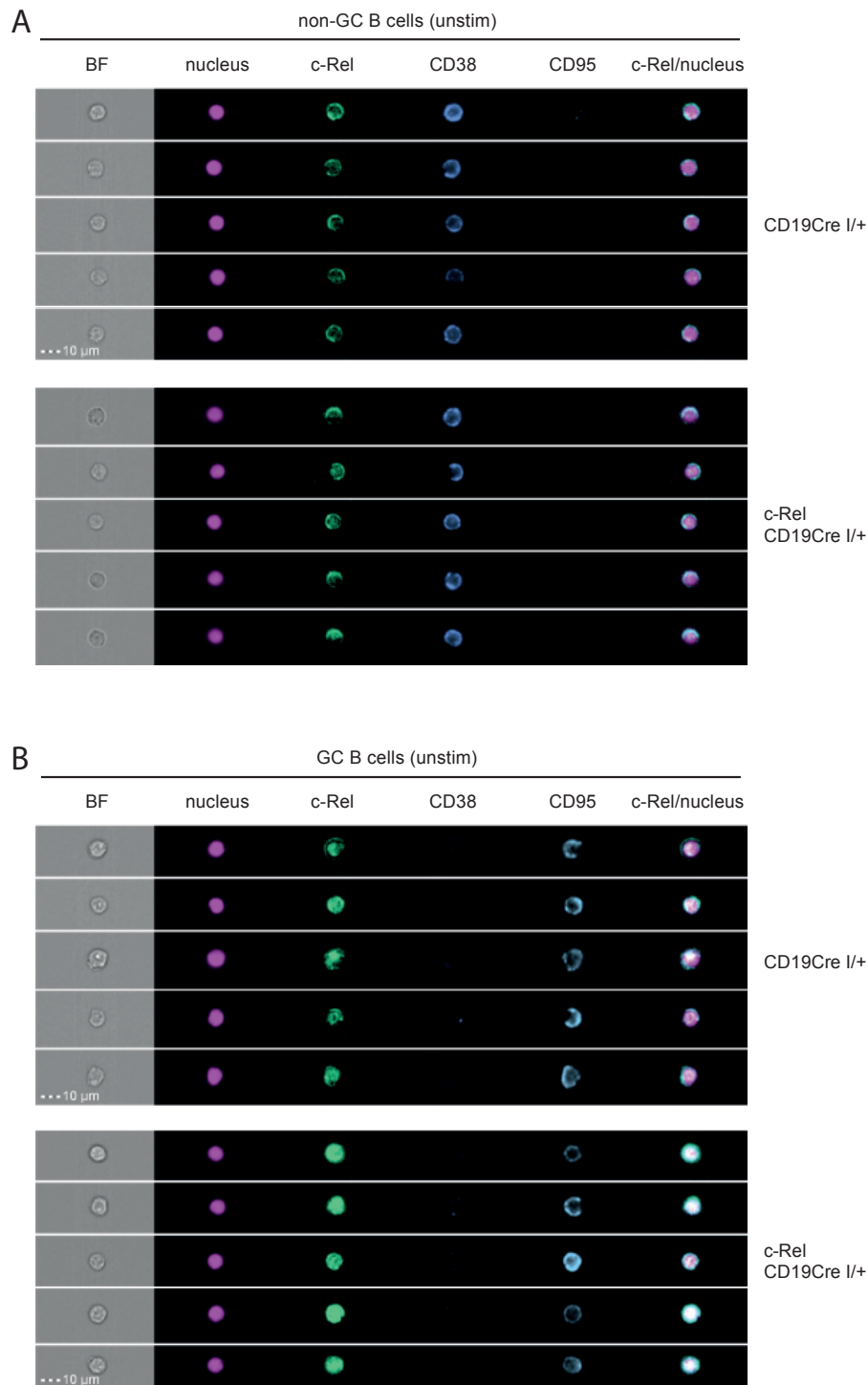


Figure S36: GFP-c-Rel nuclear localization in splenic B cells analyzed by imaging flow cytometry. Splenocytes were stimulated with the indicated stimuli or left unstimulated (unstim) for 60 min in the presence of 10 μ M Q-VD to prolong the survival of GC B cells in culture. Images representative for (A, B) 5 mice from 2 independent or (C, D, E) 3 mice from 1 experiments are shown. Exemplary cells were selected based on average nuclear localization scores. B (non-GCB) B220⁺CD95⁻CD38^{high}; white bar, 10 μ m; BF, bright field; nuc, nucleus.



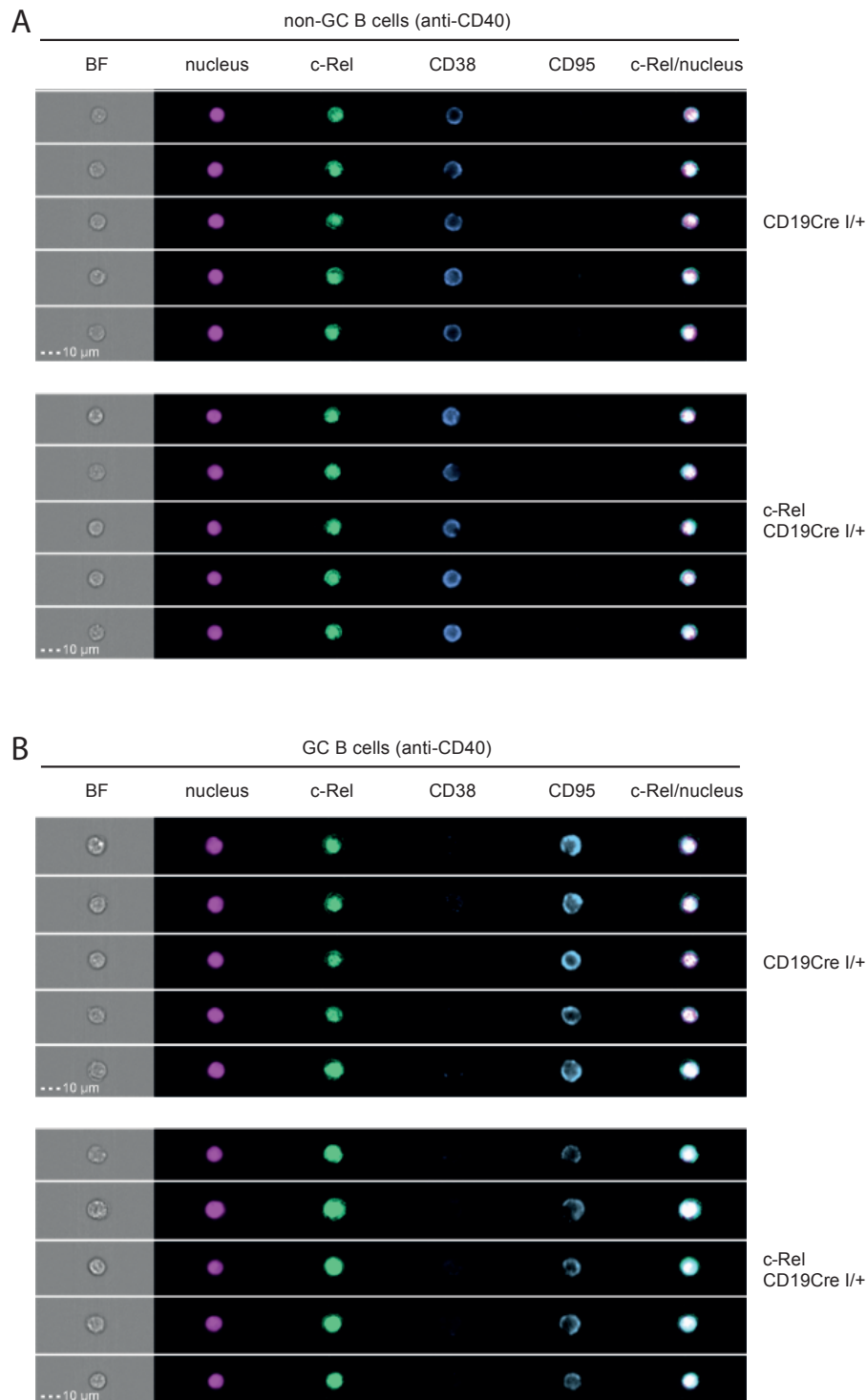


Figure S38: c-Rel nuclear translocation upon stimulation in B cells and GC B cells. Representative images for anti-CD40 stimulated (A) non-GC B cells and (B) GC B cells of lymph nodes from CD19Cre^{I/+} controls and c-Rel CD19Cre^{I/+} mice. A panel of images for indicated channels is shown for all merged c-Rel/nucleus magnified images displayed in Figure 27 for which the panel is not shown there. White bar, 10 μ m; BF, bright field.

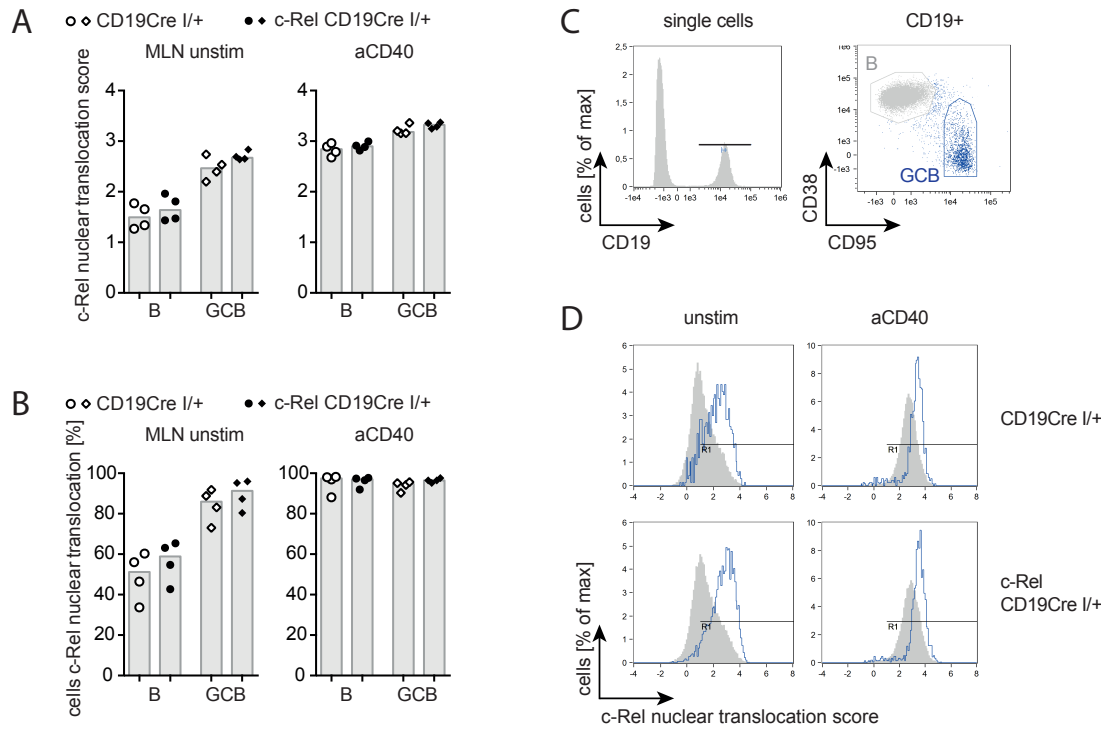


Figure S39: Quantification of c-Rel nuclear localization in B cells and GC B cells by imaging flow cytometry. Cells of mesenteric lymph nodes (MLN) were stimulated with anti-CD40 or left unstimulated (unstim) for 60 min in the presence of 10 μ M Q-VD to prolong the survival of GC B cells in culture. (A) Median c-Rel nuclear localization score and (B) percentage of cells with c-Rel nuclear translocation for B cells and GC B cells of MLN from c-Rel CD19Cre^{I/+} and CD19Cre^{I/+} mice. Individual data points obtained in 3 independent experiments are plotted. (C) Representative flow cytometry plots illustrating the gating strategy. (D) Representative histograms for c-Rel nuclear translocation score. Example images are provided in Figure S40-S43. GCB CD19⁺CD95^{high}CD38^{low}; B (non-GCB) CD19⁺CD95^{low}CD38^{high}.

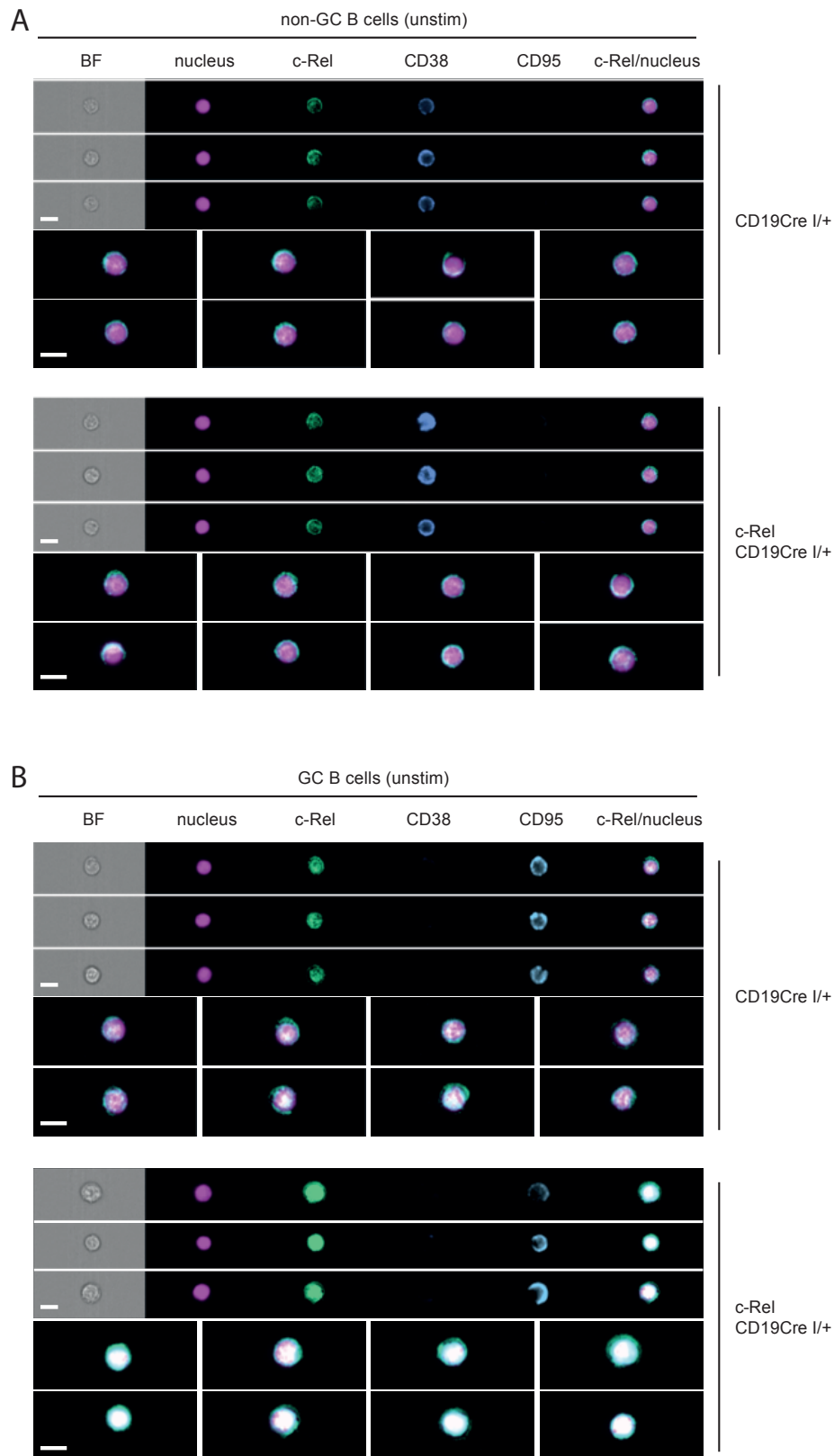


Figure S40: Higher c-Rel nuclear translocation in GC B cells in unstimulated state. Representative images for unstimulated (unstim) (A) non-GC B cells and (B) GC B cells of mesenteric lymph nodes from CD19Cre^{I/+} controls and c-Rel CD19Cre^{I/+} mice. A panel of images for indicated channels as well as magnified images of merged c-Rel/nucleus signals are displayed for each cell type and genotype. Exemplary cells were selected based on average nuclear localization scores. Quantification and gating strategy are displayed in Figure S39. White bar, 10 μ m; BF, bright field.

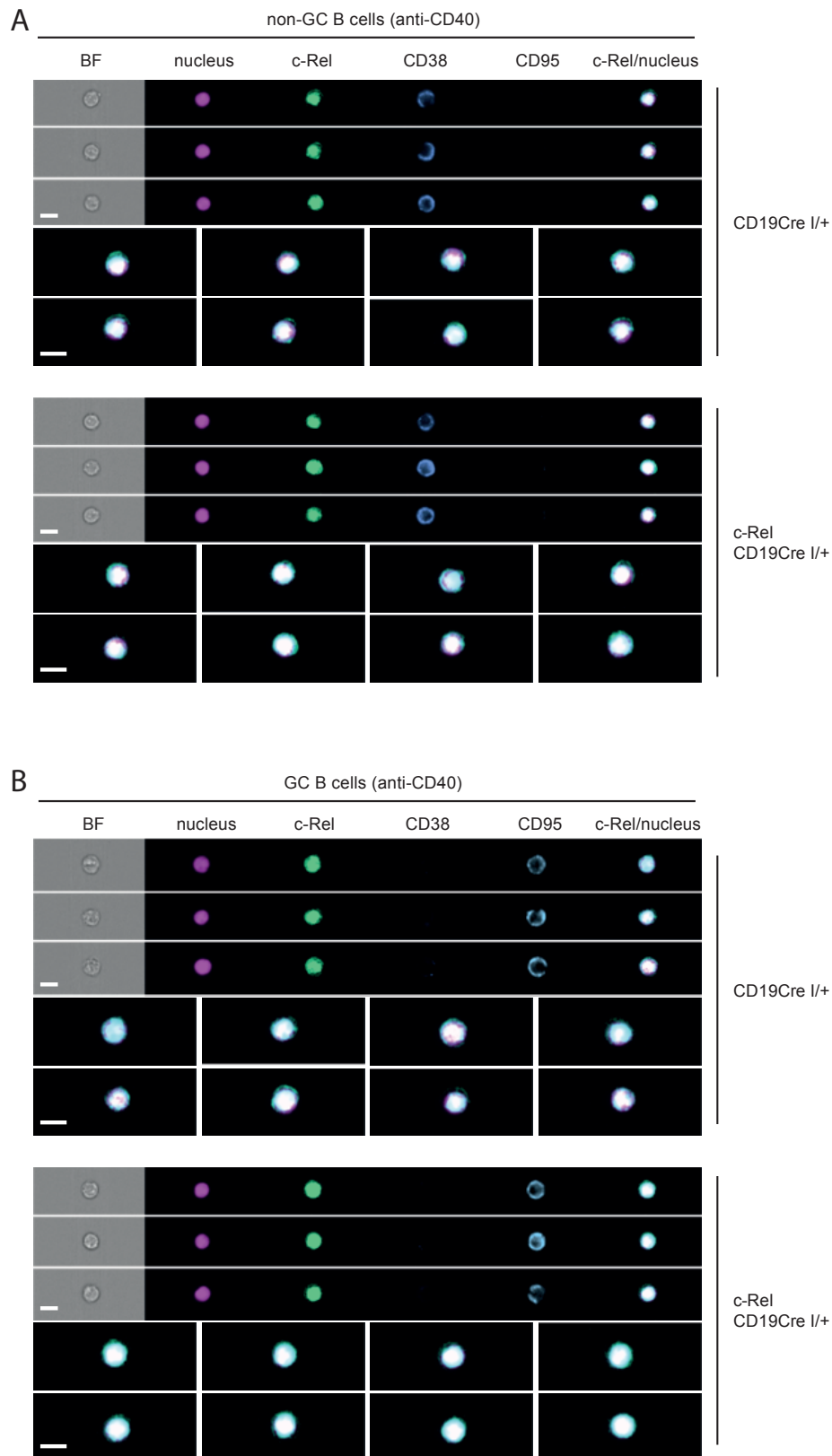
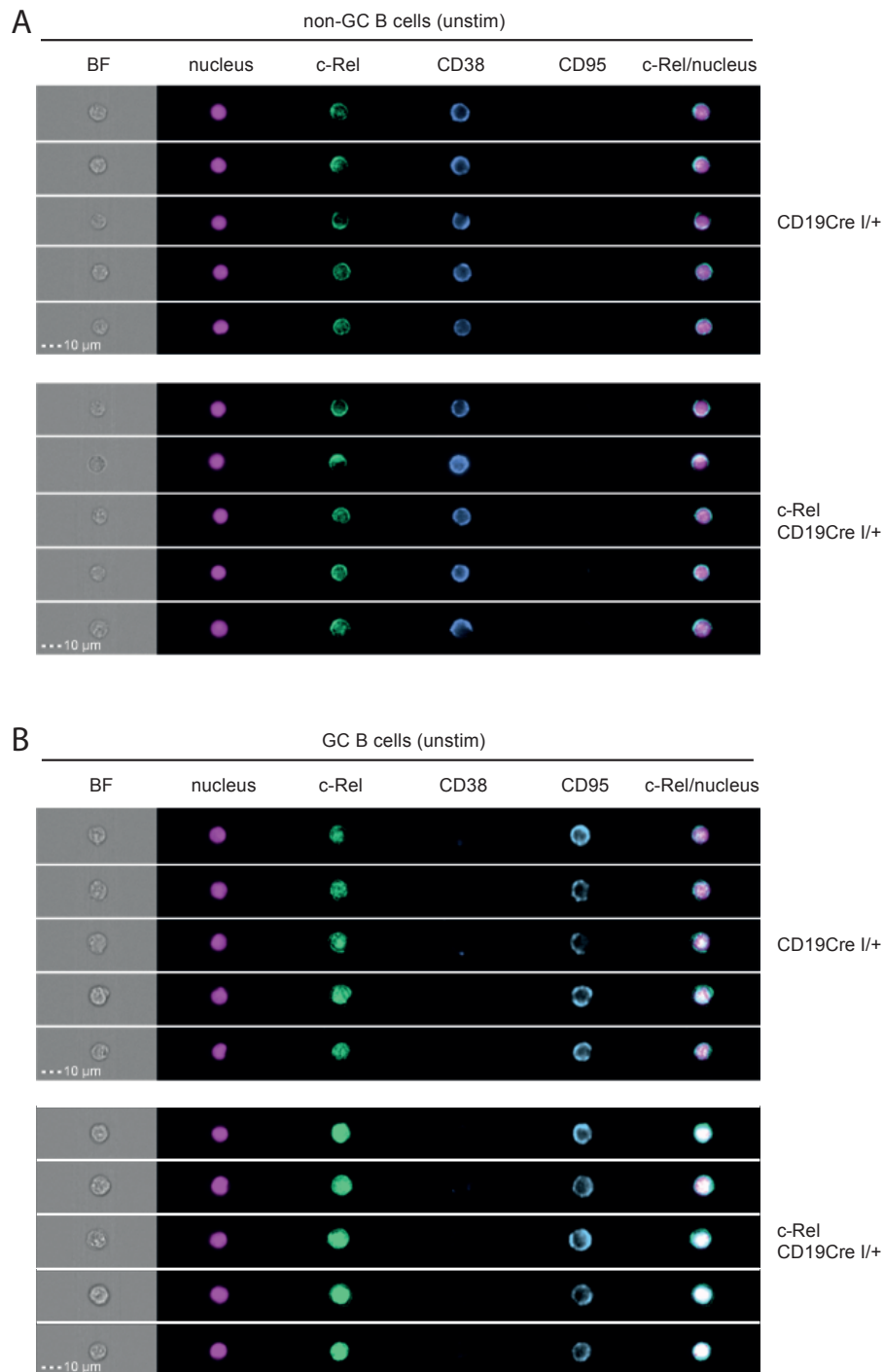


Figure S41: c-Rel nuclear translocation upon stimulation in B cells and GC B cells. Representative images for anti-CD40 stimulated (A) non-GC B cells and (B) GC B cells of mesenteric lymph nodes from CD19Cre^{I/+} controls and c-Rel CD19Cre^{I/+} mice. A panel of images for indicated channels as well as magnified images of merged c-Rel/nucleus signals are displayed for each cell type and genotype. Exemplary cells were selected based on average nuclear localization scores. Quantification and gating strategy are displayed in Figure S39. White bar, 10 μ m; BF, bright field.



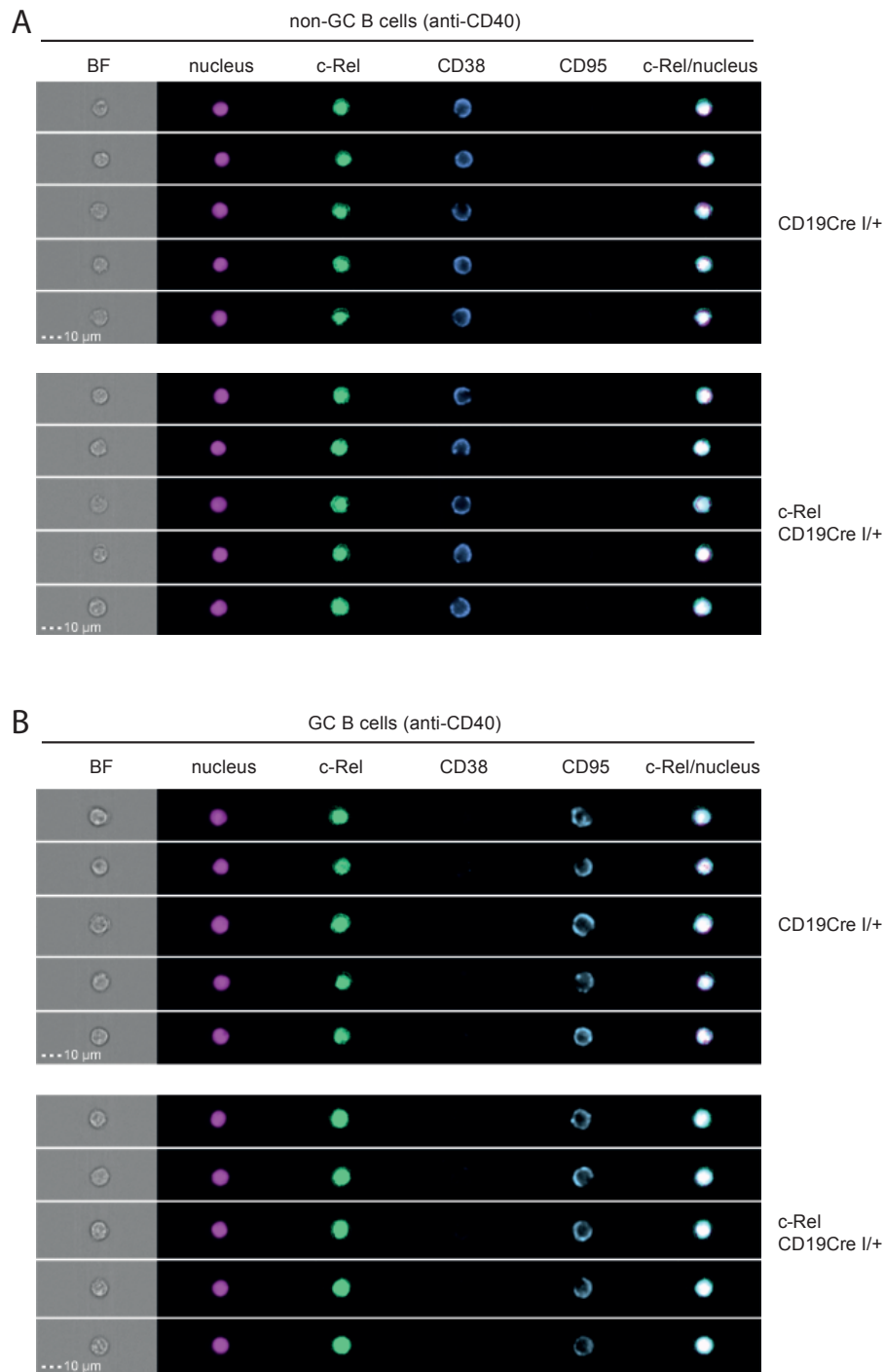


Figure S43: c-Rel nuclear translocation upon stimulation in B cells and GC B cells. Representative images for anti-CD40 stimulated (A) non-GC B cells and (B) GC B cells of mesenteric lymph nodes from CD19Cre^{I/+} controls and c-Rel CD19Cre^{I/+} mice. A panel of images for indicated channels is shown for all merged c-Rel/nucleus magnified images displayed in Figure S41 for which the panel is not shown there. White bar, 10 μ m; BF, bright field.

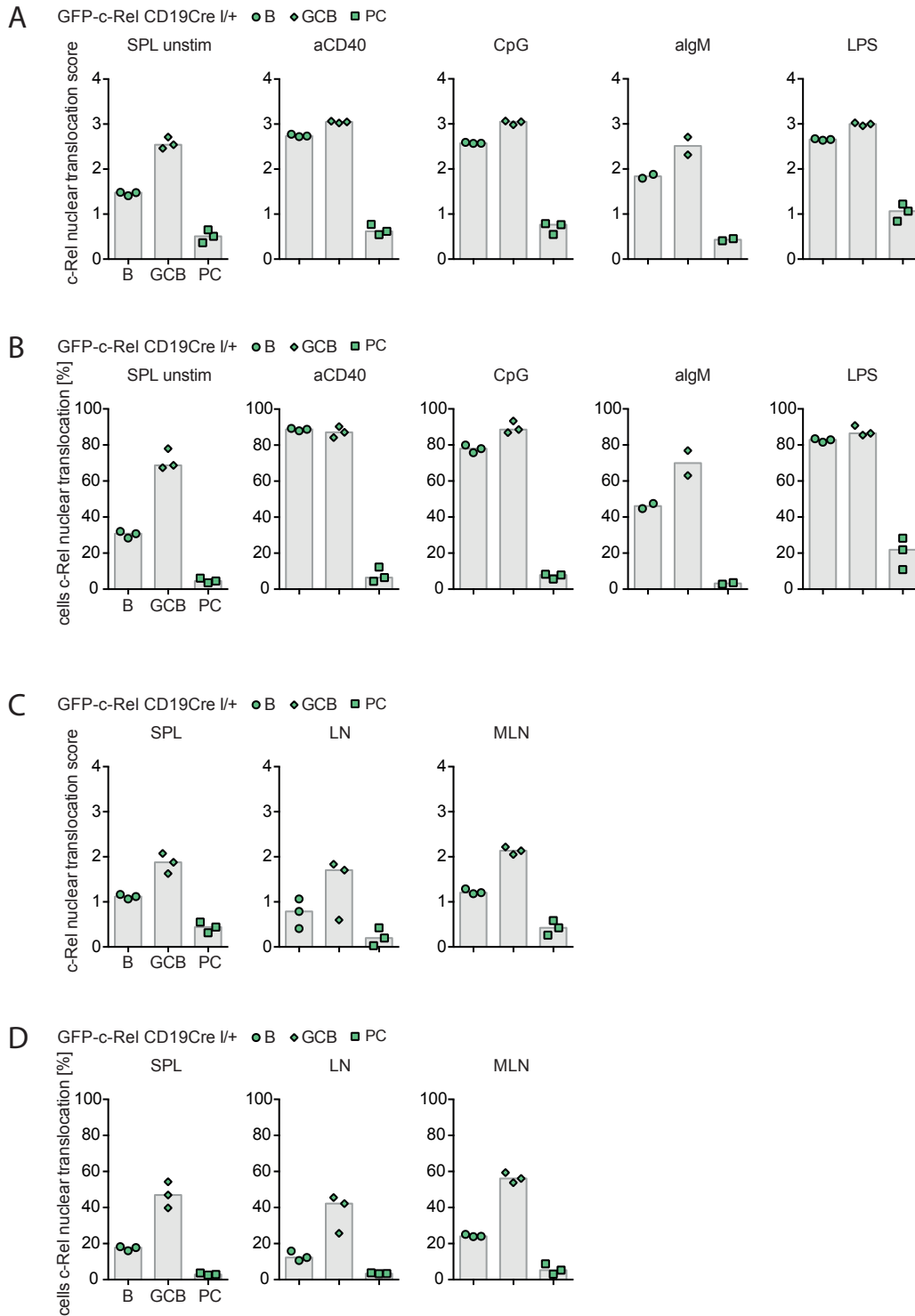


Figure S44: Quantification of c-Rel nuclear localization in B cell subsets of GFP-c-Rel CD19Cre^{1/+} mice by imaging flow cytometry. Intracellular c-Rel staining of total c-Rel levels in GFP-c-Rel CD19Cre^{1/+} mice. Individual data points obtained in 1 experiment are plotted. Bars represent median values. (A, B) Splenocytes were stimulated with the indicated stimuli or left unstimulated (unstim) for 60 min in the presence of 10 μ M Q-VD to prolong the survival of GC B cells in culture. (A) Median c-Rel nuclear localization score and (B) percentage of cells with c-Rel nuclear translocation for splenic B cells, GC B cells and plasma cells from GFP-c-Rel CD19Cre^{1/+} mice. (C) c-Rel nuclear translocation score and (D) percentage of cells with c-Rel nuclear translocation of directly *ex vivo* analyzed B cells, GC B cells and plasma cells of indicated organs from GFP-c-Rel CD19Cre^{1/+} mice. GCB CD19⁺CD95^{high}CD38^{low}; B (non-GCB) CD19⁺CD95⁻CD38^{high}; plasma cells (PC) B220^{low}CD138⁺; SPL, spleen; LN, lymph nodes; MLN, mesenteric lymph nodes.

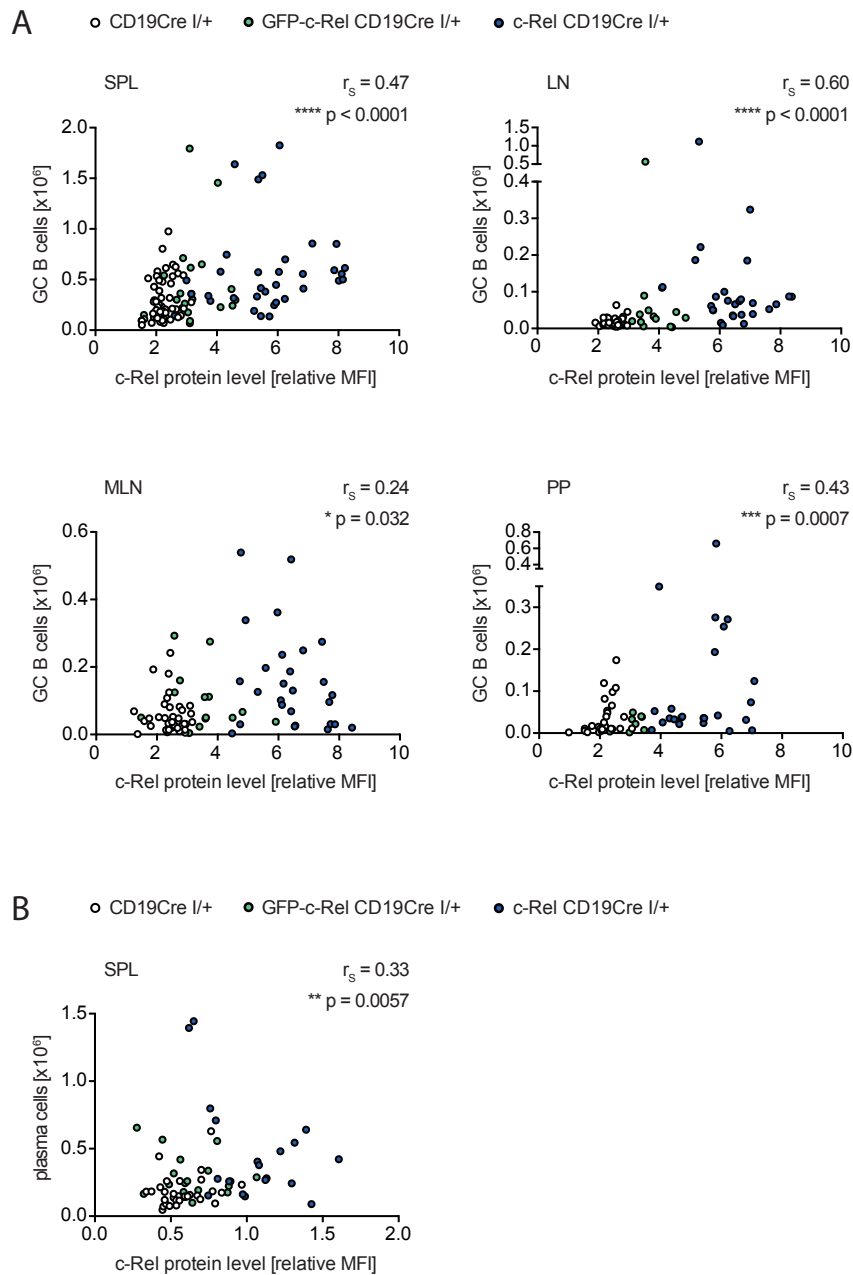


Figure S45: Strong positive correlation of c-Rel levels with cell numbers of GC B cells and plasma cells. Individual data points for c-Rel level and cell number of (A) GC B cells or (B) plasma cells is plotted. c-Rel levels are relative median fluorescence intensity (MFI) values normalized to the B cell population excluding GC B cells or plasma cells, respectively, of CD19Cre^{I/+} control mice in each experiment. Spearman correlation coefficient (r_s) and respective statistical significance analysis p values (two-tailed) are given for each dataset. GCB: $n_{SPL} = 110$; $n_{LN} = 77$; $n_{MLN} = 78$; $n_{PP} = 59$; PC $n_{SPL} = 70$; GCB CD19⁺/B220⁺CD95^{high}CD38^{low}; plasma cells (PC) B220^{low}CD138⁺; SPL, spleen; LN, lymph nodes; MLN, mesenteric lymph nodes; PP, Peyer's patches.

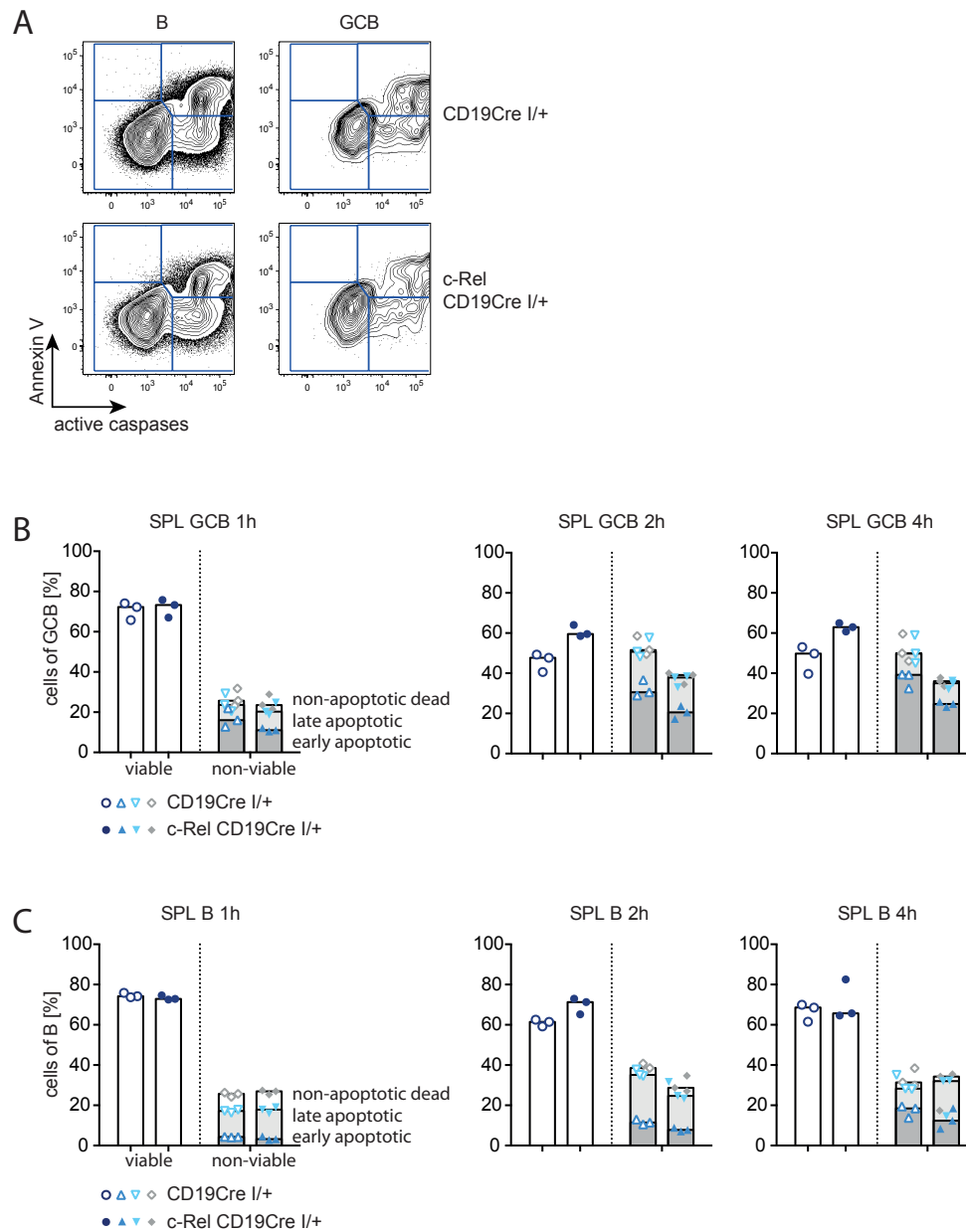


Figure S46: Assessment of apoptotic cells in $c\text{-Rel CD19Cre}^{I/+}$ mice. In order to stain active caspases splenocytes of SRBC-immunized mice were cultured for 1 h *in vitro*. For longer time periods of culture (2 h, 4 h) cells were stained during the last hour of culture. (A) Representative flow cytometry plots of Annexin V/active caspase staining in B cells and GC B cells. Quantification of viable and apoptotic cells in (B) GC B cell and (C) B cell population for indicated culture time periods. Individual data points obtained in 1 preliminary experiment and median values represented as bar graphs are plotted. Due to the preliminary character of the experiment, no statistical analysis was performed. viable: caspase⁻, Annexin V⁻, 7-AAD⁻; early apoptotic: caspase⁺ Annexin V⁻/caspase⁻ Annexin V⁺/caspase⁺ Annexin V⁺, 7-AAD⁻; late apoptotic: caspase⁺ Annexin V⁻/caspase⁻ Annexin V⁺/caspase⁺ Annexin V⁺, 7-AAD⁺; non-apoptotic dead: caspase⁻, Annexin V⁻, 7-AAD⁺; GCB CD19⁺B220⁺CD95^{high}CD38^{low}; B CD19⁺B220⁺; SPL, spleen.

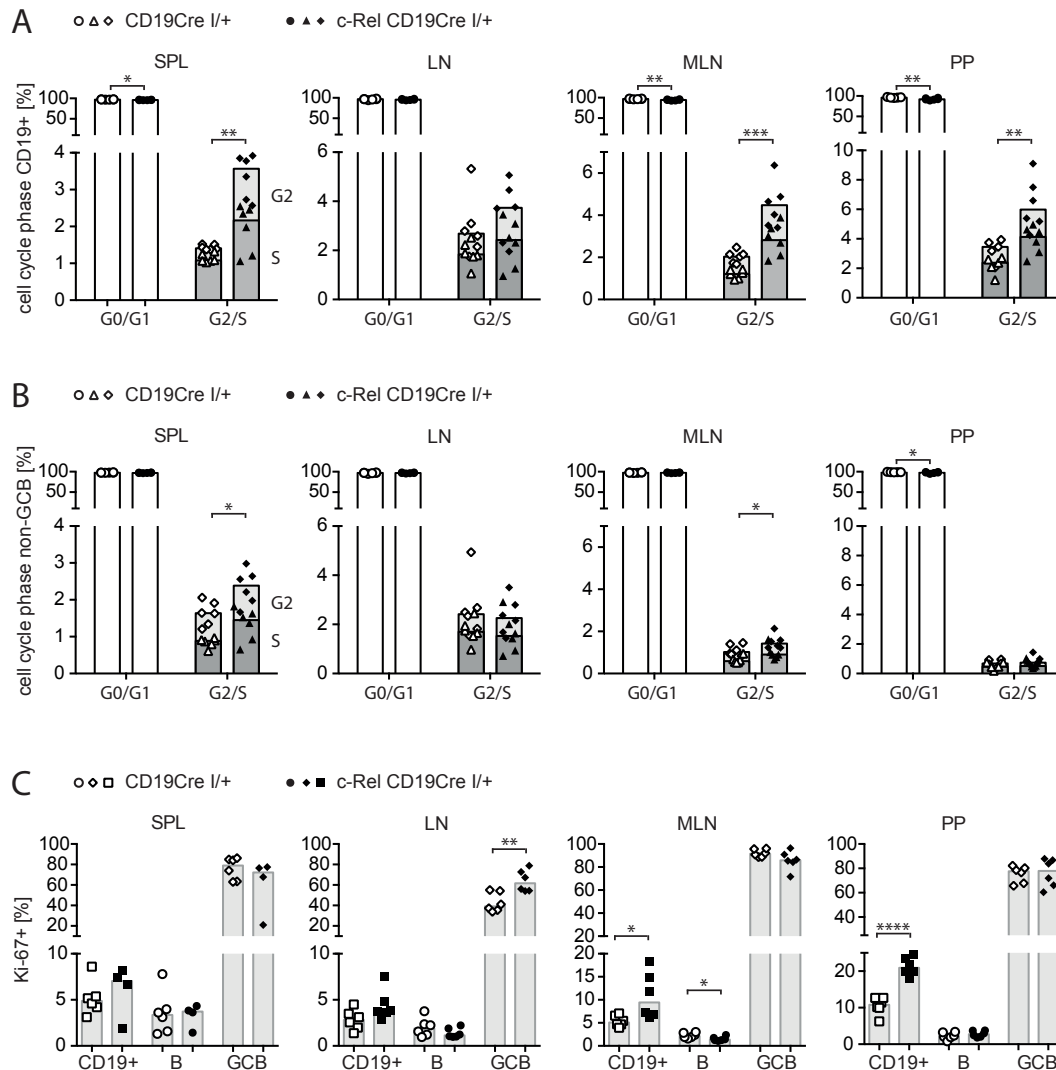


Figure S47: Cell cycle stages of B cells and Ki-67-expressing cells in c-Rel CD19Cre^{I/+} mice. Percentage of (A) total CD19⁺ B cells and (B) non-GC B cells in G0/G1 and G2/S phase of cell cycle for indicated organs from c-Rel CD19Cre^{I/+} or CD19Cre^{I/+} mice. (C) Percentage of Ki-67-expressing cells in indicated B cell populations. Individual data points obtained in 3 independent experiments are plotted and bars represent median values. * p ≤ 0.05, ** p ≤ 0.01, *** p ≤ 0.001, **** p ≤ 0.0001, unpaired t test. GCB CD19⁺CD95^{high}CD38^{low}; B (non-GCB) CD19⁺CD95^{low}CD38^{high}; SPL, spleen; LN, lymph nodes; MLN, mesenteric lymph nodes; PP, Peyer's patches.

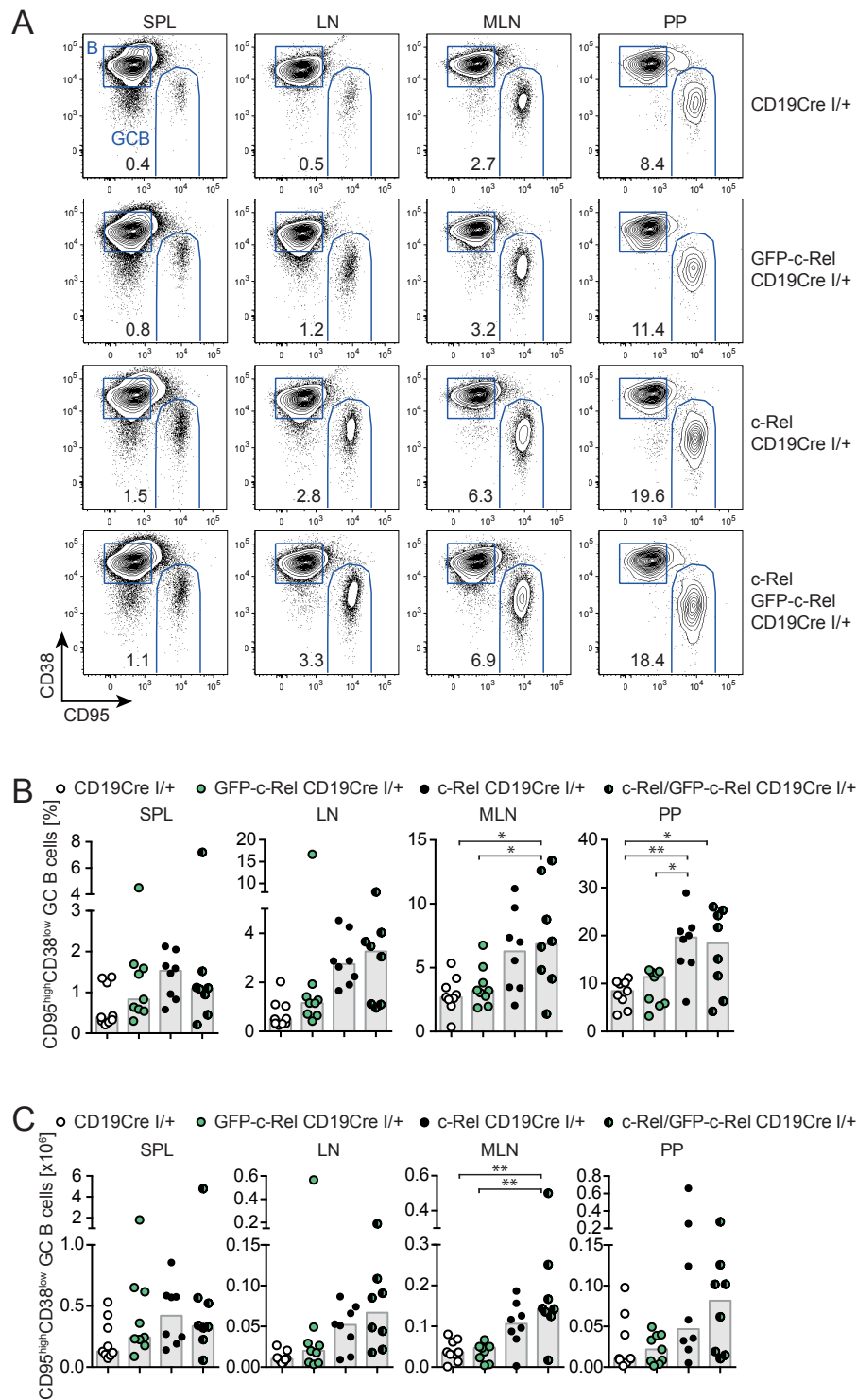


Figure S49: GC B cells in c-Rel/GFP-c-Rel CD19Cre^{I/+} double transgenic mice. (A) Representative flow cytometry plots of GC B cells. Numbers are median percentages of GC B cells of total B cells. (B) Percentages of GC B cells of total B cells and (C) GC B cell numbers. Individual data points obtained in 4 independent experiments are plotted. Bars and numbers below graphs are median values. * $p \leq 0.05$, ** $p \leq 0.01$, one-way ANOVA. GCB B220⁺CD95^{high}CD38^{low}; SPL, spleen; LN, lymph nodes; MLN, mesenteric lymph nodes; PP, Peyer's patches.

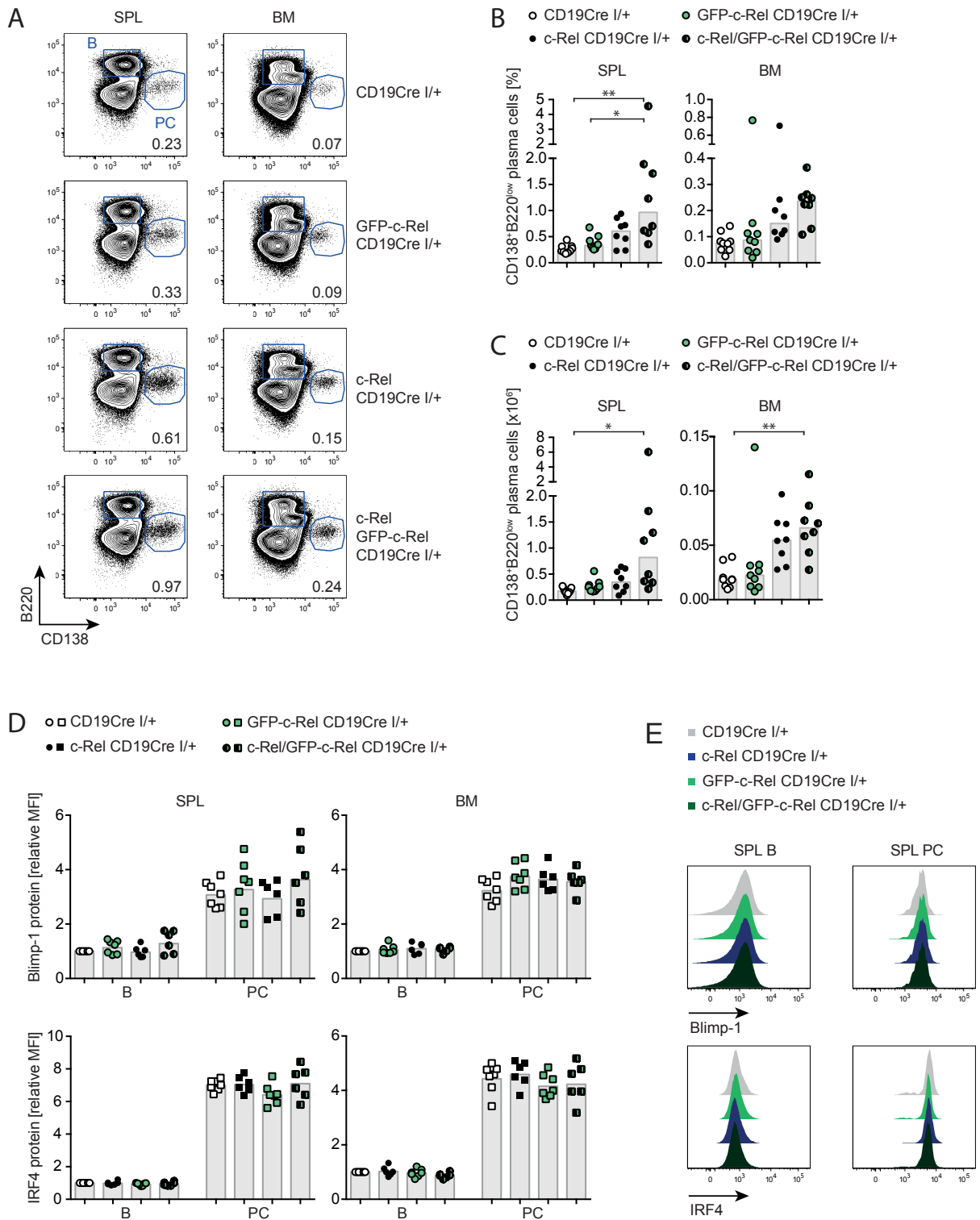


Figure S50: Plasma cells in c-Rel/GFP-c-Rel CD19Cre^{I/+} double transgenic mice. (A) Representative flow cytometry plots of plasma cells. Numbers are median percentages. Plasma cell (B) percentages and (C) cell numbers. Individual data points obtained in 4 independent experiments are plotted. Bars and numbers below graphs are median values. (D) Intracellular flow cytometry data of IRF4 and Blimp-1 protein levels in plasma cells normalized to the non-plasma cell B cell population of CD19Cre^{I/+} controls. Individual data points obtained in 3 independent experiments and the geometric mean represented as a bar are plotted. Three data points per genotype of IRF4 and Blimp-1 protein levels in BM of CD19Cre^{I/+} and c-Rel CD19Cre^{I/+} controls are also included in the data set shown in Figure 14C. (E) Representative histograms illustrate the bar graphs shown in (D). * $p \leq 0.05$, ** $p \leq 0.01$, one-way ANOVA. plasma cells (PC) B220^{low}CD138⁺; B (non-PC) B220⁺CD138⁻; SPL, spleen; BM, bone marrow.

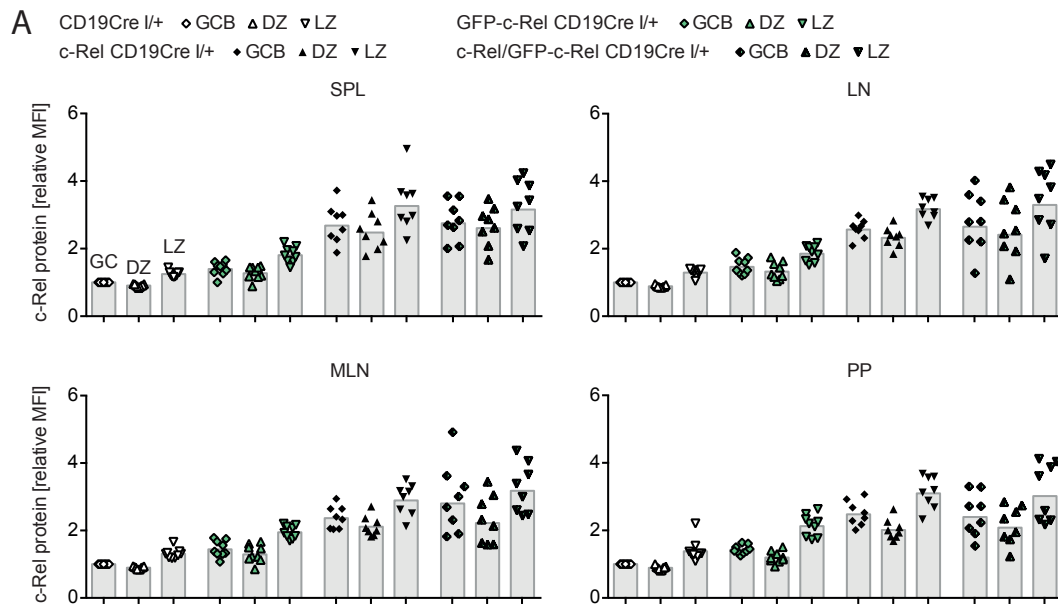


Figure S51: c-Rel levels in c-Rel/GFP-c-Rel CD19Cre^{I/+} double transgenic mice are comparable to GFP-c-Rel CD19Cre^{I/+} single transgenic mice. (A) Intracellular flow cytometry data of c-Rel protein levels in DZ and LZ of GC B cells. Median fluorescence intensities (MFI) were normalized to GC B cell population of CD19Cre^{I/+} controls. Individual data points obtained in ≥ 3 independent experiments and bars representing geometric means are plotted. GCB B220⁺CD95^{high}CD38^{low}; DZ CXCR4^{high}CD86^{low}; LZ CXCR4^{low}CD86^{high}; SPL, spleen; LN, lymph nodes; MLN, mesenteric lymph nodes; PP, Peyer's patches.

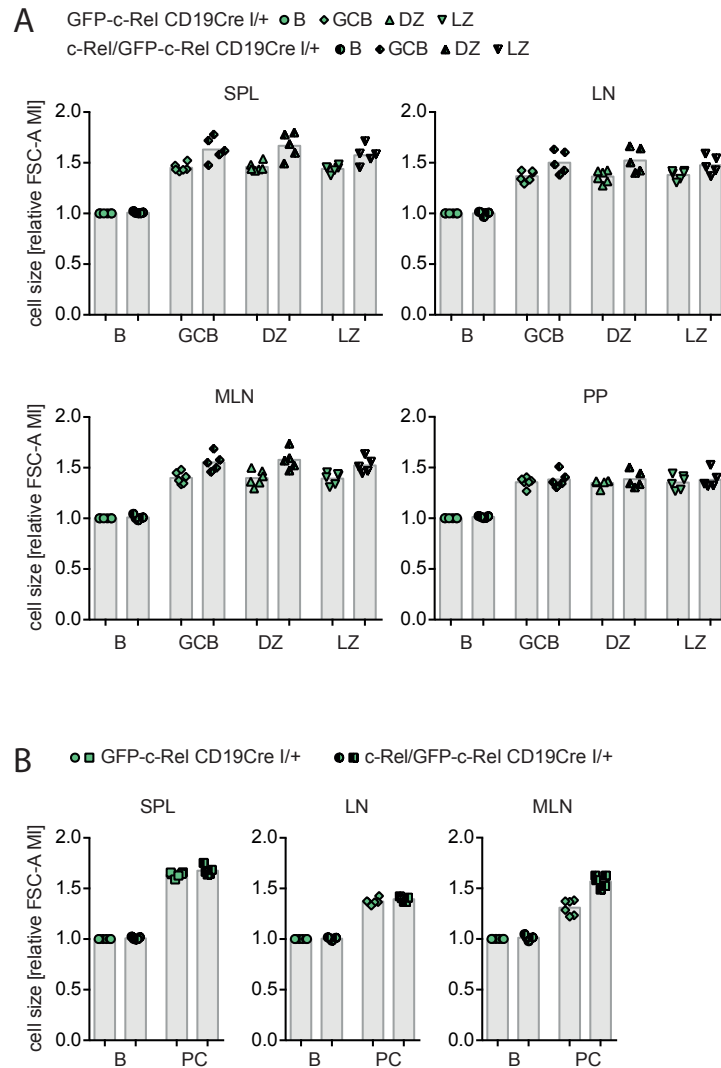


Figure S52: Cell size of GC B cells and plasma cells in $c\text{-Rel}/\text{GFP-c-Rel CD19Cre}^{I/+}$ double transgenic mice. Median intensities (MI) were normalized to $\text{GFP-c-Rel CD19Cre}^{I/+}$ mice. Individual data points obtained in 3 independent experiments and bars representing geometric means are plotted. (A) FSC-A median intensities for B cells and GC B cells normalized to non-GC B cells. (B) FSC-A median intensities for plasma cells normalized to non-PC. GCB $\text{B220}^+\text{CD95}^{\text{high}}\text{CD38}^{\text{low}}$; B (non-GCB) $\text{B220}^+\text{CD95}^-\text{CD38}^{\text{high}}$; DZ $\text{CXCR4}^{\text{high}}\text{CD86}^{\text{low}}$; LZ $\text{CXCR4}^{\text{low}}\text{CD86}^{\text{high}}$; plasma cells (PC) $\text{B220}^{\text{low}}\text{CD138}^+$; B (non-PC) $\text{B220}^+\text{CD138}^-$; SPL, spleen; LN, lymph nodes; MLN, mesenteric lymph nodes; PP, Peyer's patches; FSC-A, forward scatter area.

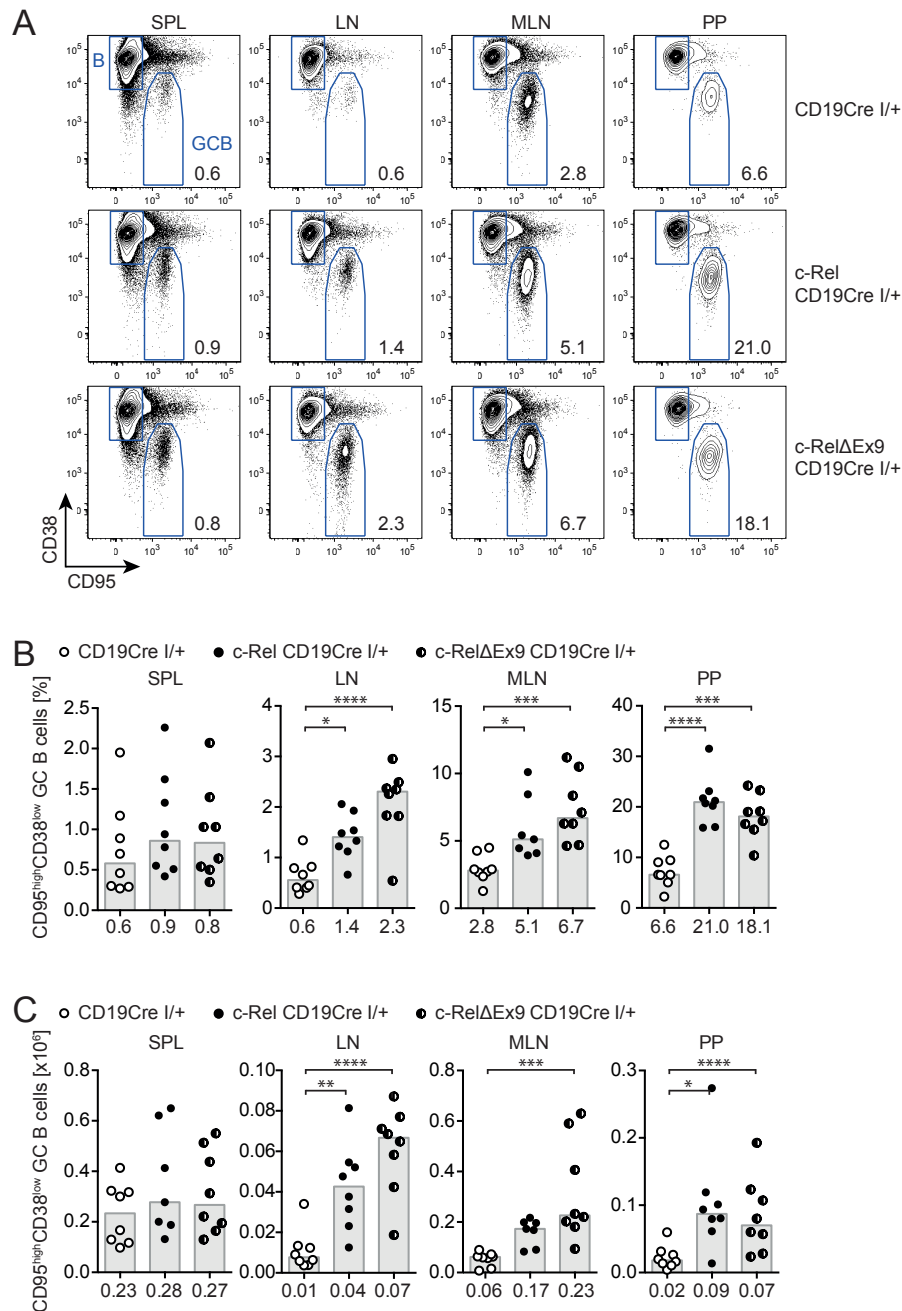


Figure S53: Expansion of GC B cells in *c-RelΔEx9 CD19Cre^{I/+}* mice. (A) Representative flow cytometry plots of GC B cells. Numbers are median percentages of GC B cells of total B cells. (B) Percentages of GC B cells of total B cells and (C) GC B cell numbers. Individual data points obtained in 3 independent experiments are plotted. Bars and numbers below graphs are median values. * $p \leq 0.05$, ** $p \leq 0.01$, *** $p \leq 0.001$, **** $p \leq 0.0001$, one-way ANOVA. GCB B220⁺CD95^{high}CD38^{low}; SPL, spleen; LN, lymph nodes; MLN, mesenteric lymph nodes; PP, Peyer's patches.

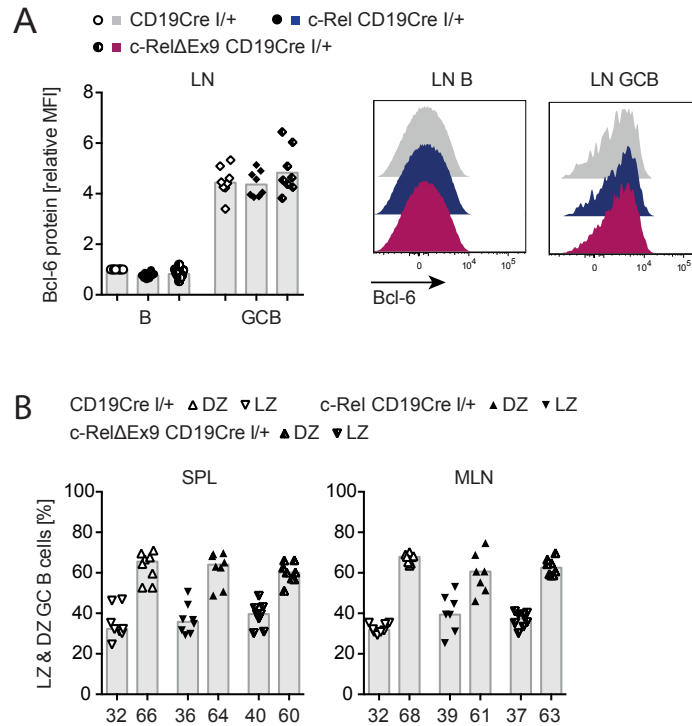


Figure S54: Bcl-6 expression and frequencies of dark zone and light zone GC B cells in c-RelΔEx9 CD19Cre^{I/+} mice. (A) Intracellular flow cytometry data of Bcl-6 protein levels in GC B cells normalized to the non-GC B cell population of CD19Cre^{I/+} controls. Representative histograms illustrate the bar graphs for which the geometric mean and individual data points obtained in 3 independent experiments are plotted. (B) Frequencies of dark zone (DZ) and light zone (LZ) GC B cells. Individual data points obtained in 3 independent experiments are plotted. Bars and numbers below graphs are median values. GCB B220⁺CD95^{high}CD38^{low}; B (non-GCB) B220⁺CD95^{high}CD38^{high}; DZ CXCR4^{high}CD86^{low}; LZ CXCR4^{low}CD86^{high}; SPL, spleen; LN, lymph nodes; MLN, mesenteric lymph nodes.

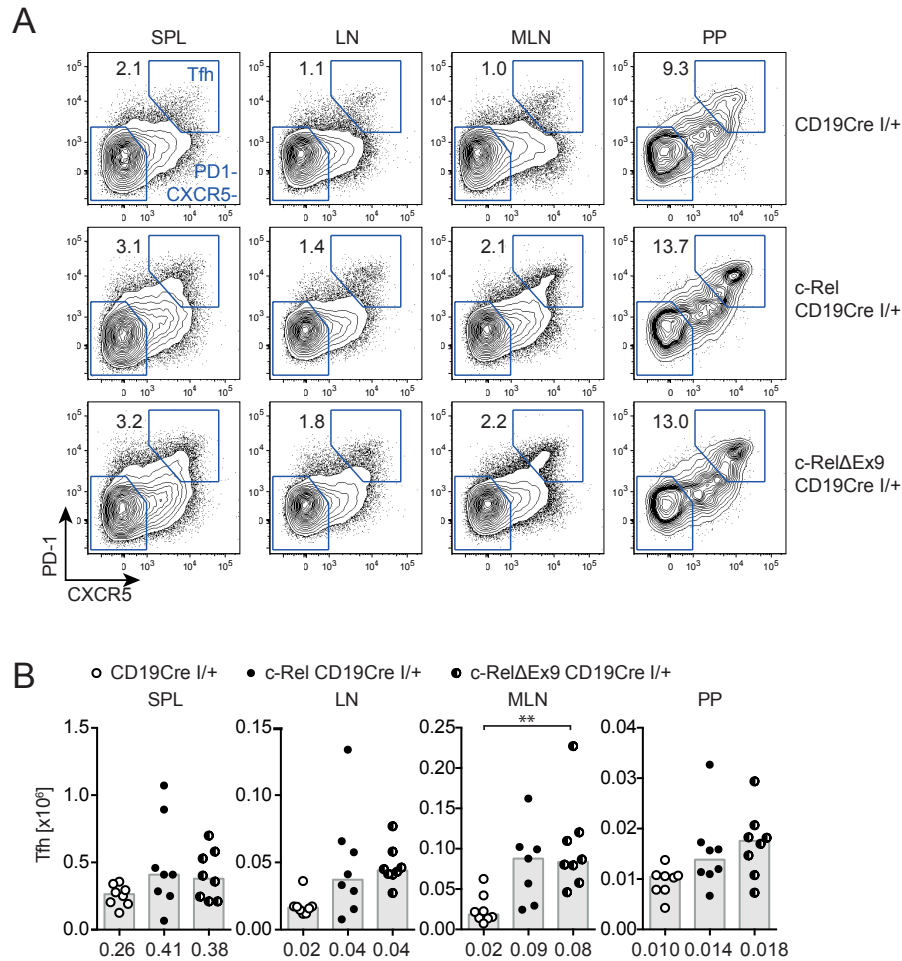


Figure S55: Expansion of T_{fh} cells in $c\text{-Rel}\Delta\text{Ex9 CD19Cre}^{I/+}$ mice. (A) Representative flow cytometry plots of follicular helper T (T_{fh}) cells. Numbers are median percentages of $\text{PD-1}^{\text{high}}\text{CXCR5}^{\text{high}}$ T_{fh} cells of $\text{TCR}\beta^+\text{CD4}^+$ T cells. (B) T_{fh} cell numbers. Individual data points obtained in 3 independent experiments are plotted. Bars and numbers below graphs are median values. ** $p \leq 0.01$, one-way ANOVA. T_{fh} $\text{TCR}\beta^+\text{CD4}^+\text{PD-1}^{\text{high}}\text{CXCR5}^{\text{high}}$; SPL, spleen; LN, lymph nodes; MLN, mesenteric lymph nodes; PP, Peyer's patches.

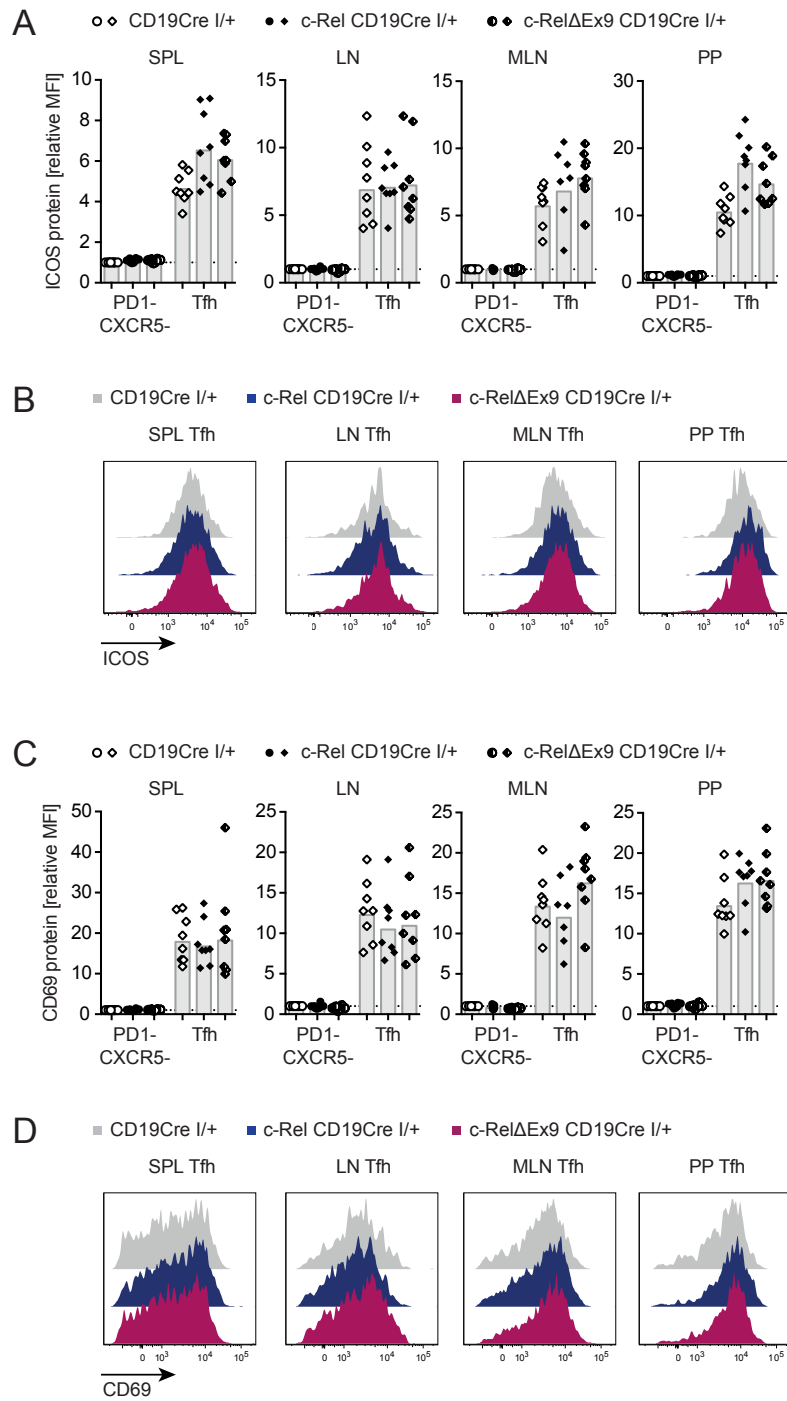
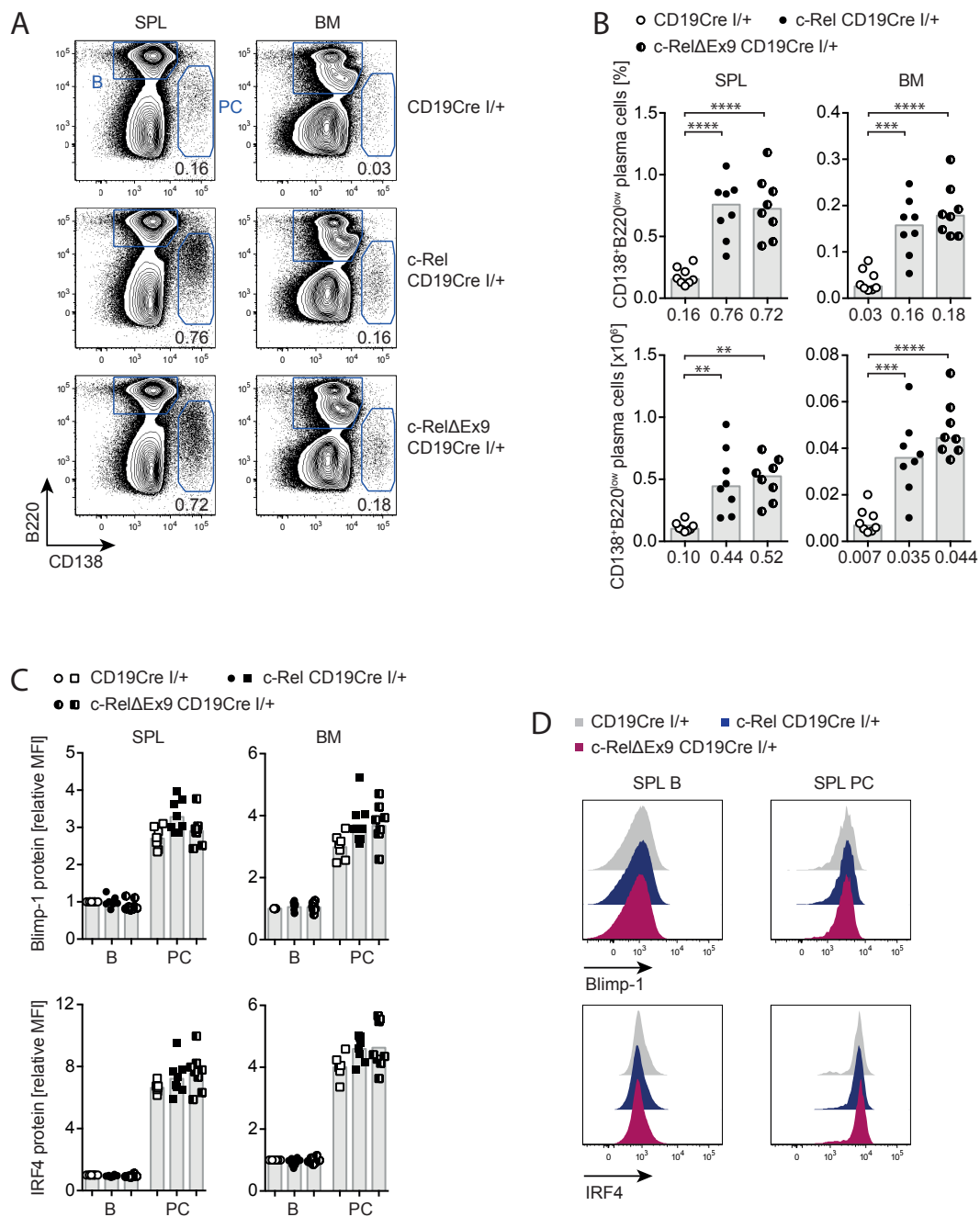


Figure S56: Characteristics of T_{fh} cells in c-RelΔEx9 CD19Cre^{I/+} mice. Flow cytometry data of (A) ICOS or (C) CD69 protein levels of T_{fh} cells normalized to the non-T_{fh} cell population of CD19Cre^{I/+} controls. Geometric mean and individual data points obtained in 3 independent experiments are plotted. (B) and (D) show representative histograms illustrating the bar graphs shown in (A) and (C), respectively. T_{fh} TCRβ⁺CD4⁺PD-1^{high}CXCR5^{high}; non-T_{fh} TCRβ⁺CD4⁺PD-1⁻CXCR5⁻; SPL, spleen; LN, lymph nodes; MLN, mesenteric lymph nodes; PP, Peyer's patches.



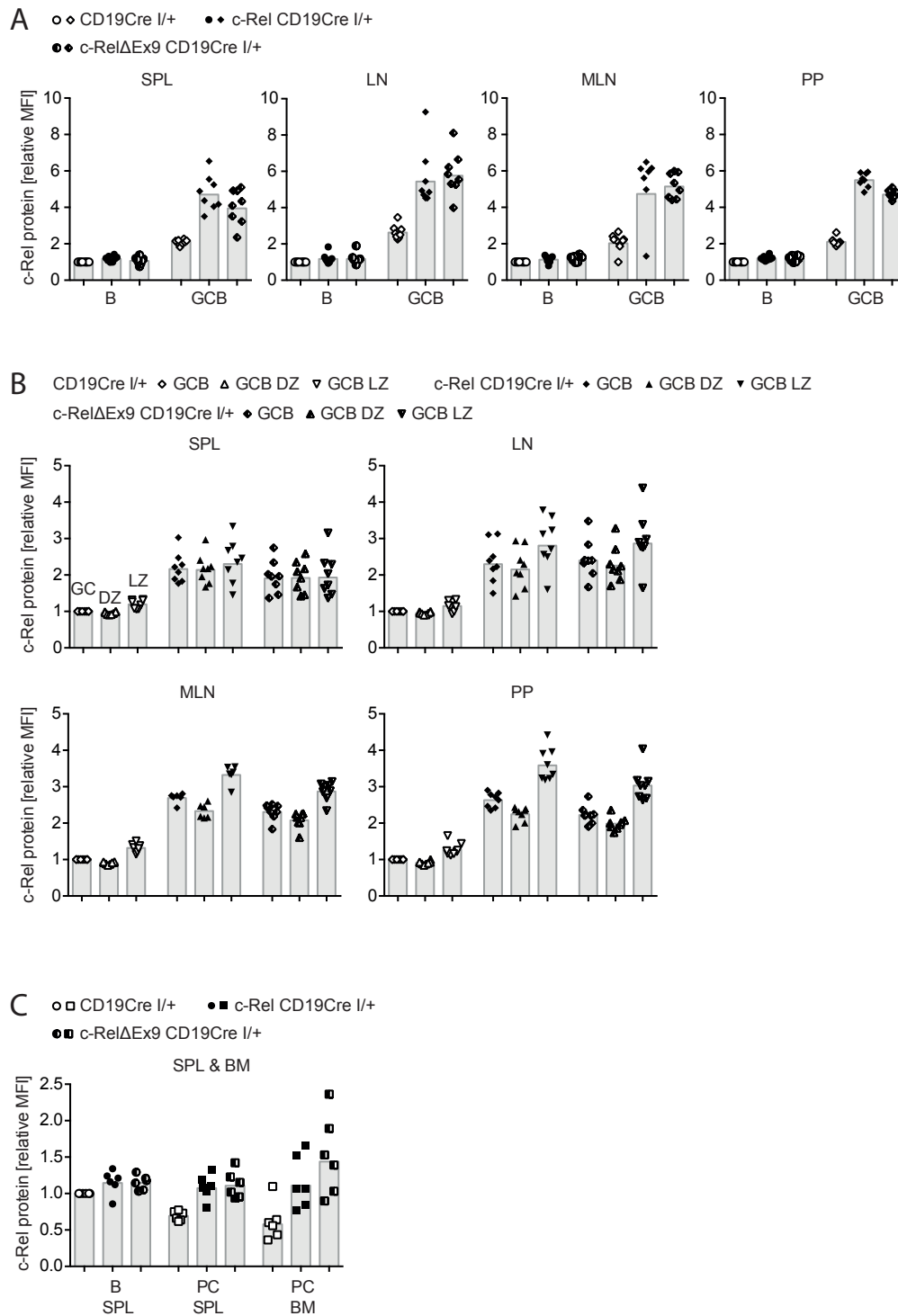


Figure S58: c-Rel levels in GC B cell and plasma cells of c-RelΔEx9 CD19Cre^{I/+} mice. Intracellular flow cytometry data of c-Rel protein levels in B cell subpopulations. Median fluorescence intensities (MFI) were normalized to CD19Cre^{I/+} controls. Individual data points obtained in 3 independent experiments and bars representing geometric means are plotted. (A) c-Rel level in B cells and GC B cells. MFIs were normalized to non-GCB of CD19Cre^{I/+} controls. (B) c-Rel level in DZ and LZ of GC B cells. MFIs were normalized to GCB of CD19Cre^{I/+} controls. (C) c-Rel level in plasma cells. MFIs were normalized to splenic B cells (non-PC) of CD19Cre^{I/+} controls. 6 data points per genotype for c-Rel level in BM of CD19Cre^{I/+} and c-Rel CD19Cre^{I/+} controls are also included in data set shown in Figure 22C. GCB B220⁺CD95^{high}CD38^{low}; B (non-GCB) B220⁺CD95⁻CD38^{high}; DZ CXCR4^{high}CD86^{low}; LZ CXCR4^{low}CD86^{high}; plasma cells (PC) B220^{low}CD138⁺; B (non-PC) B220⁺CD138⁻; BM, bone marrow; SPL, spleen; LN, lymph nodes; MLN, mesenteric lymph nodes; PP, Peyer's patches.

References

- Afshar-Sterle, S., Zotos, D., Bernard, N. J., Scherger, A. K., Rödling, L., Alsop, A. E., Walker, J., Masson, F., Belz, G. T., Corcoran, L. M., O'Reilly, L. A., Strasser, A., Smyth, M. J., Johnstone, R., Tarlinton, D. M., Nutt, S. L., and Kallies, A. (2014). Fas ligand-mediated immune surveillance by T cells is essential for the control of spontaneous B cell lymphomas. *Nature Medicine*, 20(3):283–290.
- Agresti, A. and Vercelli, D. (2002). c-Rel is a selective activator of a novel IL-4/CD40 responsive element in the human Ig γ 4 germline promoter. *Molecular Immunology*, 38(11):849–859.
- Aguzzi, A., Kranich, J., and Krautler, N. J. (2014). Follicular dendritic cells: origin, phenotype, and function in health and disease. *Trends in Immunology*, 35(3):105–113.
- Akashi, K., Kondo, M., Cheshier, S., Shizuru, J., Gandy, K., Domen, J., Mebius, R., Traver, D., and Weissman, I. L. (1999). Lymphoid development from stem cells and the common lymphocyte progenitors. *Cold Spring Harb Symp Quant Biol*, 64:1–12.
- Alizadeh, A. A., Eisen, M. B., Davis, R. E., Ma, C., Lossos, I. S., Rosenwald, A., Boldrick, J. C., Sabet, H., Tran, T., Yu, X., Powell, J. I., Yang, L., Marti, G. E., Moore, T., Hudson, J., Lu, L., Lewis, D. B., Tibshirani, R., Sherlock, G., Chan, W. C., Greiner, T. C., Weisenburger, D. D., Armitage, J. O., Warnke, R., Levy, R., Wilson, W., Grever, M. R., Byrd, J. C., Botstein, D., Brown, P. O., and Staudt, L. M. (2000). Distinct types of diffuse large B-cell lymphoma identified by gene expression profiling. *Nature*, 403(6769):503–511.
- Allen, C. D. C. (2015). Germinal center quality control: death by Fas. *Immunity*, 42(5):783–785.
- Allen, C. D. C., Ansel, K. M., Low, C., Lesley, R., Tamamura, H., Fujii, N., and Cyster, J. G. (2004). Germinal center dark and light zone organization is mediated by CXCR4 and CXCR5. *Nature Immunology*, 5(9):943–952.
- Allen, C. D. C. and Cyster, J. G. (2008). Follicular dendritic cell networks of primary follicles and germinal centers: Phenotype and function. *Seminars in Immunology*, 20(1):14–25.
- Allen, C. D. C., Okada, T., and Cyster, J. G. (2007a). Germinal-Center Organization and Cellular Dynamics. *Immunity*, 27(2):190–202.
- Allen, C. D. C., Okada, T., Tang, H. L., and Cyster, J. G. (2007b). Imaging of germinal center selection events during affinity maturation. *Science*, 315(5811):528–531.
- Allman, D., Lindsley, R. C., DeMuth, W., Rudd, K., Shinton, S. A., and Hardy, R. R. (2001). Resolution of three nonproliferative immature splenic B cell subsets reveals multiple selection points during peripheral B cell maturation. *The Journal of Immunology*, 167(12):6834–6840.
- Allman, D. and Pillai, S. (2008). Peripheral B cell subsets. *Current Opinion in Immunology*, 20(2):149–157.
- Almaden, J. V., Liu, Y. C., Yang, E., Otero, D. C., Birnbaum, H., Davis-Turak, J., Asagiri, M., David, M., Goldrath, A. W., and Hoffmann, A. (2016). B-cell survival and development controlled by the coordination of NF- κ B family members RelB and cRel. *Blood*, 127(10):1276–1286.
- Alves, B. N., Tsui, R., Almaden, J., Shokhirev, M. N., Davis-Turak, J., Fujimoto, J., Birnbaum, H., Ponomarenko, J., and Hoffmann, A. (2014). κ B ϵ is a key regulator of B cell expansion by providing negative feedback on cRel and RelA in a stimulus-specific manner. *The Journal of Immunology*, 192(7):3121–3132.
- Arbuckle, M. R., McClain, M. T., Rubertone, M. V., Scofield, R. H., Dennis, G. J., James, J. A., and Harley, J. B. (2003). Development of autoantibodies before the clinical onset of systemic lupus erythematosus. *The New England Journal of Medicine*, 349(16):1526–1533.
- Bain, G., Maandag, E., Izon, D. J., and Amsen, D. (1994). E2A proteins are required for proper B cell development and initiation of immunoglobulin gene rearrangements. *Cell*, 79(5):885–892.
- Balázs, M., Martin, F., Zhou, T., and Kearney, J. (2002). Blood dendritic cells interact with splenic marginal zone B cells to initiate T-independent immune responses. *Immunity*, 17(3):341–352.
- Baltimore, D. (2011). NF- κ B is 25. *Nature Immunology*, 12(8):683–685.
- Banerjee, A., Grumont, R., Gugasyan, R., White, C., Strasser, A., and Gerondakis, S. (2008). NF- κ B1 and c-Rel cooperate to promote the survival of TLR4-activated B cells by neutralizing Bim via distinct mechanisms. *Blood*, 112(13):5063–5073.
- Banerjee, D., Liou, H.-C., and Sen, R. (2005). c-Rel-Dependent Priming of Naive T Cells by Inflammatory Cytokines. *Immunity*, 23(4):445–458.
- Bannard, O., Horton, R. M., Allen, C. D. C., An, J., Nagasawa, T., and Cyster, J. G. (2013). Germinal center centroblasts transition to a centrocyte phenotype according to a timed program and depend on the dark zone for effective selection. *Immunity*, 39(5):912–924.
- Barbie, D. A., Tamayo, P., Boehm, J. S., Kim, S. Y., Moody, S. E., Dunn, I. F., Schinzel, A. C., Sandy, P., Meylan, E., Scholl, C., Fröhling, S., Chan, E. M., Sos, M. L., Michel, K., Mermel, C., Silver, S. J., Weir, B. A., Reiling, J. H., Sheng, Q., Gupta, P. B., Wadlow, R. C., Le, H., Hoersch, S., Wittner, B. S., Ramaswamy, S., Livingston, D. M., Sabatini, D. M., Meyerson, M., Thomas, R. K., Lander, E. S., Mesirov, J. P., Root, D. E., Gilliland, D. G., Jacks, T., and Hahn, W. C. (2009). Systematic RNA interference reveals that oncogenic KRAS-driven cancers require TBK1. *Nature*, 462(7269):108–112.
- Bargou, R. C., Leng, C., Krappmann, D., Emmerich, F., Mapara, M. Y., Bommert, K., Royer, H. D., Scheiderei, C., and Dörken, B. (1996). High-level nuclear NF- κ B and Oct-2 is a common feature of cultured Hodgkin/Reed-Sternberg cells.

- Blood*, 87(10):4340–4347.
- Barreto, V., Reina-San-Martin, B., Ramiro, A. R., McBride, K. M., and Nussenzweig, M. C. (2003). C-terminal deletion of AID uncouples class switch recombination from somatic hypermutation and gene conversion. *Molecular Cell*, 12(2):501–508.
- Barth, T. F., Leithäuser, F., Joos, S., Bentz, M., and Möller, P. (2002). Mediastinal (thymic) large B-cell lymphoma: where do we stand? *The Lancet Oncology*, 3(4):229–234.
- Barth, T. F. E., Martin-Subero, J. I., Joos, S., Menz, C. K., Hasel, C., Mechttersheimer, G., Parwaresch, R. M., Lichter, P., Siebert, R., and Möller, P. (2003). Gains of 2p involving the REL locus correlate with nuclear c-Rel protein accumulation in neoplastic cells of classical Hodgkin lymphoma. *Blood*, 101(9):3681–3686.
- Bassing, C. H., Swat, W., and Alt, F. W. (2002). The mechanism and regulation of chromosomal V(D)J recombination. *Cell*, 109(2):S45–S55.
- Basso, K. and Dalla-Favera, R. (2015). Germinal centres and B cell lymphomagenesis. *Nature Reviews Immunology*, 15(3):172–184.
- Basso, K., Klein, U., Niu, H., Stolovitzky, G. A., Tu, Y., Califano, A., Cattoretti, G., and Dalla-Favera, R. (2004). Tracking CD40 signaling during germinal center development. *Blood*, 104(13):4088–4096.
- Batista, F. D. and Harwood, N. E. (2009). The who, how and where of antigen presentation to B cells. *Nature Reviews Immunology*, 9(1):15–27.
- Baumgarth, N. (2011). The double life of a B-1 cell: self-reactivity selects for protective effector functions. *Nature Reviews Immunology*, 11(1):34–46.
- Bea, S., Colomo, L., López-Guillermo, A., Salaverria, I., Puig, X., Pinyol, M., Rives, S., Montserrat, E., and Campo, E. (2004). Clinicopathologic significance and prognostic value of chromosomal imbalances in diffuse large B-cell lymphomas. *Journal of Clinical Oncology*, 22(17):3498–3506.
- Bea, S., Zettl, A., Wright, G., Salaverria, I., Jehn, P., Moreno, V., Burek, C., Ott, G., Puig, X., Yang, L., López-Guillermo, A., Chan, W. C., Greiner, T. C., Weisenburger, D. D., Armitage, J. O., Gascoyne, R. D., Connors, J. M., Grogan, T. M., Braziel, R., Fisher, R. I., Smeland, E. B., Kvaloy, S., Holte, H., Delabie, J., Simon, R., Powell, J., Wilson, W. H., Jaffe, E. S., Montserrat, E., Muller-Hermelink, H.-K., Staudt, L. M., Campo, E., Rosenwald, A., and Lymphoma/Leukemia Molecular Profiling Project (2005). Diffuse large B-cell lymphoma subgroups have distinct genetic profiles that influence tumor biology and improve gene-expression-based survival prediction. *Blood*, 106(9):3183–3190.
- Bentz, M., Barth, T. F., Brüderlein, S., Bock, D., Schwerer, M. J., Baudis, M., Joos, S., Viardot, A., Feller, A. C., Müller-Hermelink, H. K., Lichter, P., Döhner, H., and Moller, P. (2001). Gain of chromosome arm 9p is characteristic of primary mediastinal B-cell lymphoma (MBL): comprehensive molecular cytogenetic analysis and presentation of a novel MBL cell line. *Genes, Chromosomes and Cancer*, 30(4):393–401.
- Berek, C., Berger, A., and Apel, M. (1991). Maturation of the immune response in germinal centers. *Cell*, 67(6):1121–1129.
- Bertoli, C., Skotheim, J. M., and de Bruin, R. A. M. (2013). Control of cell cycle transcription during G1 and S phases. *Nature Reviews Molecular Cell Biology*, 14(8):518–528.
- Bertossi, A., Aichinger, M., Sansonetti, P., Lech, M., Neff, F., Pal, M., Wunderlich, F. T., Anders, H.-J., Klein, L., and Schmidt-Suppran, M. (2011). Loss of Roquin induces early death and immune deregulation but not autoimmunity. *Journal of Experimental Medicine*, 208(9):1749–1756.
- Bizzaro, N. (2007). Autoantibodies as predictors of disease: the clinical and experimental evidence. *Autoimmunity Reviews*, 6(6):325–333.
- Bonizzi, G. and Karin, M. (2004). The two NF- κ B activation pathways and their role in innate and adaptive immunity. *Trends in Immunology*, 25(6):280–288.
- Bours, V., Villalobos, J., Burd, P. R., Kelly, K., and Siebenlist, U. (1990). Cloning of a mitogen-inducible gene encoding a κ B DNA-binding protein with homology to the rel oncogene and to cell-cycle motifs. *Nature*, 348(6296):76–80.
- Brink, R. (2014). The imperfect control of self-reactive germinal center B cells. *Current Opinion in Immunology*, 28:97–101.
- Brownell, E., Kozak, C. A., Fowle, J. R., Modi, W. S., Rice, N. R., and O’Brien, S. J. (1986). Comparative genetic mapping of cellular rel sequences in man, mouse, and the domestic cat. *American Journal of Human Genetics*, 39(2):194–202.
- Brownell, E., Mathieson, B., Young, H. A., Keller, J., Ihle, J. N., and Rice, N. R. (1987). Detection of c-rel-related transcripts in mouse hematopoietic tissues, fractionated lymphocyte populations, and cell lines. *Molecular and Cellular Biology*, 7(3):1304–1309.
- Brownell, E., Mittereder, N., and Rice, N. R. (1989). A human rel proto-oncogene cDNA containing an Alu fragment as a potential coding exon. *Oncogene*, 4(7):935–942.
- Brownell, E., O’Brien, S. J., Nash, W. G., and Rice, N. (1985). Genetic characterization of human c-rel sequences. *Molecular and Cellular Biology*, 5(10):2826–2831.
- Bull, P., Morley, K. L., Hoekstra, M. F., Hunter, T., and Verma, I. M. (1990). The mouse c-rel protein has an N-terminal regulatory domain and a C-terminal transcriptional transactivation domain. *Molecular and Cellular Biology*, 10(10):5473–5485.
- Bunting, K., Rao, S., Hardy, K., Woltring, D., Denyer, G. S., Wang, J., Gerondakis, S., and Shannon, M. F. (2007). Genome-wide analysis of gene expression in T cells to identify targets of the NF- κ B transcription factor c-Rel. *The Journal of Immunology*, 178(11):7097–7109.

- Butt, D., Chan, T. D., Bourne, K., Hermes, J. R., Nguyen, A., Statham, A., O'Reilly, L. A., Strasser, A., Price, S., Schofield, P., Christ, D., Basten, A., Ma, C. S., Tangye, S. G., Phan, T. G., Rao, V. K., and Brink, R. (2015). FAS Inactivation Releases Unconventional Germinal Center B Cells that Escape Antigen Control and Drive IgE and Autoantibody Production. *Immunity*, 42(5):890–902.
- Cabezas-Wallscheid, N., Klimmeck, D., Hansson, J., Lipka, D. B., Reyes, A., Wang, Q., Weichenhan, D., Lier, A., von Paleske, L., Renders, S., Wünsche, P., Zeisberger, P., Brocks, D., Gu, L., Herrmann, C., Haas, S., Essers, M. A. G., Brors, B., Eils, R., Huber, W., Milsom, M. D., Plass, C., Krijgsveld, J., and Trumpp, A. (2014). Identification of regulatory networks in HSCs and their immediate progeny via integrated proteome, transcriptome, and DNA methylome analysis. *Cell Stem Cell*, 15(4):507–522.
- Cabezas-Wallscheid, N. and Trumpp, A. (2016). Potency finds its niches. *Science*, 351(6269):126–127.
- Caganova, M., Carrisi, C., Varano, G., Mainoldi, F., Zanardi, F., Germain, P.-L., George, L., Alberghini, F., Ferrarini, L., Talukder, A. K., Ponzoni, M., Testa, G., Nojima, T., Doglioni, C., Kitamura, D., Toellner, K.-M., Su, I.-H., and Casola, S. (2013). Germinal center dysregulation by histone methyltransferase EZH2 promotes lymphomagenesis. *The Journal of Clinical Investigation*, 123(12):5009–5022.
- Calado, D. P., Sasaki, Y., Godinho, S. A., Pellerin, A., Köchert, K., Sleckman, B. P., de Alborán, I. M., Janz, M., Rodig, S., and Rajewsky, K. (2012). The cell-cycle regulator c-Myc is essential for the formation and maintenance of germinal centers. *Nature Immunology*, 13(11):1092–1100.
- Cambier, J. C., Gauld, S. B., Merrell, K. T., and Vilen, B. J. (2007). B-cell anergy: from transgenic models to naturally occurring anergic B cells? *Nature Reviews Immunology*, 7(8):633–643.
- Campbell, I. K., Gerondakis, S., O'Donnell, K., and Wicks, I. P. (2000). Distinct roles for the NF- κ B1 (p50) and c-Rel transcription factors in inflammatory arthritis. *The Journal of Clinical Investigation*, 105(12):1799–1806.
- Cariappa, A., Liou, H.-C., Horwitz, B. H., and Pillai, S. (2000). Nuclear Factor κ B Is Required for the Development of Marginal Zone B Lymphocytes. *The Journal of Experimental Medicine*, 192(8):1175–1182.
- Carmody, R. J., Ruan, Q., and Liou, H. C. (2007). Essential roles of c-Rel in TLR-induced IL-23 p19 gene expression in dendritic cells. *The Journal of Immunology*.
- Carrasco, D., Cheng, J., Lewin, A., Warr, G., Yang, H., Rizzo, C., Rosas, F., Snapper, C., and Bravo, R. (1998). Multiple hemopoietic defects and lymphoid hyperplasia in mice lacking the transcriptional activation domain of the c-Rel protein. *The Journal of Experimental Medicine*, 187(7):973–984.
- Carrasco, D., Rizzo, C. A., Dorfman, K., and Bravo, R. (1996). The v-rel oncogene promotes malignant T-cell leukemia/lymphoma in transgenic mice. *The EMBO Journal*, 15(14):3640–3650.
- Carrasco, D., Weih, F., and Bravo, R. (1994). Developmental expression of the mouse c-rel proto-oncogene in hematopoietic organs. *Development*, 120(10):2991–3004.
- Casola, S., Cattoretta, G., Uyttersprot, N., Koralov, S. B., Seagal, J., Segal, J., Hao, Z., Waisman, A., Egert, A., Ghitza, D., and Rajewsky, K. (2006). Tracking germinal center B cells expressing germ-line immunoglobulin γ 1 transcripts by conditional gene targeting. *Proceedings of the National Academy of Sciences*, 103(19):7396–7401.
- Casola, S. and Rajewsky, K. (2006). B cell recruitment and selection in mouse GALT germinal centers. *Current Topics in Microbiology and Immunology*, 308:155–171.
- Castro, I., Wright, J. A., Damdinsuren, B., Hoek, K. L., Carlesso, G., Shinnars, N. P., Gerstein, R. M., Woodland, R. T., Sen, R., and Khan, W. N. (2009). B Cell Receptor-Mediated Sustained c-Rel Activation Facilitates Late Transitional B Cell Survival through Control of B Cell Activating Factor Receptor and NF- κ B2. *The Journal of Immunology*, 182(12):7729–7737.
- Cerutti, A., Cols, M., and Puga, I. (2013). Marginal zone B cells: virtues of innate-like antibody-producing lymphocytes. *Nature Reviews Immunology*, 13(2):118–132.
- Chang, M., Jin, W., Chang, J.-H., Xiao, Y., Brittain, G. C., Yu, J., Zhou, X., Wang, Y.-H., Cheng, X., Li, P., Rabinovich, B. A., Hwu, P., and Sun, S.-C. (2011). The ubiquitin ligase Peli1 negatively regulates T cell activation and prevents autoimmunity. *Nature Immunology*, 12(10):1002–1009.
- Chaudhuri, J. and Alt, F. W. (2004). Class-switch recombination: interplay of transcription, DNA deamination and DNA repair. *Nature Reviews Immunology*, 4(7):541–552.
- Chen, C., Edelstein, L. C., and Gélinas, C. (2000). The Rel/NF- κ B Family Directly Activates Expression of the Apoptosis Inhibitor Bcl-xL. *Molecular and Cellular Biology*, 20(8):2687–2695.
- Chen, E., Hrdlicková, R., Nehyba, J., Longo, D. L., Bose, H. R., and Li, C. C. (1998). Degradation of proto-oncoprotein c-Rel by the ubiquitin-proteasome pathway. *Journal of Biological Chemistry*, 273(52):35201–35207.
- Chen, E. and Li, C. C. (1998). Association of Cdk2/cyclin E and NF- κ B complexes at G1/S phase. *Biochemical and Biophysical Research Communications*, 249(3):728–734.
- Chen, F. E. and Ghosh, G. (1999). Regulation of DNA binding by Rel/NF- κ B transcription factors: structural views. *Oncogene*, 18(49):6845–6852.
- Chen, G., Hardy, K., Bunting, K., Daley, S., Ma, L., and Shannon, M. F. (2010). Regulation of the IL-21 Gene by the NF- κ B Transcription Factor c-Rel. *The Journal of Immunology*, 185(4):2350–2359.
- Chen, G., Hardy, K., Pagler, E., Ma, L., Lee, S., Gerondakis, S., Daley, S., and Shannon, M. F. (2011). The NF- κ B transcription factor c-Rel is required for Th17 effector cell development in experimental autoimmune encephalomyelitis. *The Journal of Immunology*, 187(9):4483–4491.

- Chen, I. S., Mak, T. W., O'Rear, J. J., and Temin, H. M. (1981). Characterization of reticuloendotheliosis virus strain T DNA and isolation of a novel variant of reticuloendotheliosis virus strain T by molecular cloning. *Journal of Virology*, 40(3):800–811.
- Chen, I. S., Wilhelmson, K. C., and Temin, H. M. (1983). Structure and expression of c-rel, the cellular homolog to the oncogene of reticuloendotheliosis virus strain T. *Journal of Virology*, 45(1):104–113.
- Cheng, S., Hsia, C. Y., Leone, G., and Liou, H.-C. (2003). Cyclin E and Bcl-xL cooperatively induce cell cycle progression in c-Rel^{-/-} B cells. *Oncogene*, 22(52):8472–8486.
- Cheung, H. W., Cowley, G. S., Weir, B. A., Boehm, J. S., Rusin, S., Scott, J. A., East, A., Ali, L. D., Lizotte, P. H., Wong, T. C., Jiang, G., Hsiao, J., Mermel, C. H., Getz, G., Barretina, J., Gopal, S., Tamayo, P., Gould, J., Tsherniak, A., Stransky, N., Luo, B., Ren, Y., Drapkin, R., Bhatia, S. N., Mesirov, J. P., Garraway, L. A., Meyerson, M., Lander, E. S., Root, D. E., and Hahn, W. C. (2011). Systematic investigation of genetic vulnerabilities across cancer cell lines reveals lineage-specific dependencies in ovarian cancer. *Proceedings of the National Academy of Sciences*, 108(30):12372–12377.
- Chu, Y., Vahl, J. C., Kumar, D., Heger, K., Bertossi, A., Wojtowicz, E., Soberon, V., Schenten, D., Mack, B., Reutelshofer, M., Beyaert, R., Amann, K., van Loo, G., and Schmidt-Supprian, M. (2011). B cells lacking the tumor suppressor TNFAIP3/A20 display impaired differentiation and hyperactivation and cause inflammation and autoimmunity in aged mice. *Blood*, 117(7):2227–2236.
- Clark, J. M., Aleksiyadis, K., Martin, A., McNamee, K., Tharmalingam, T., Williams, R. O., Mémet, S., and Cope, A. P. (2011). Inhibitor of kappa B epsilon ($I\kappa B\epsilon$) is a non-redundant regulator of c-Rel-dependent gene expression in murine T and B cells. *PLoS ONE*, 6(9):e24504.
- Clark, M. R., Mandal, M., Ochiai, K., and Singh, H. (2014). Orchestrating B cell lymphopoiesis through interplay of IL-7 receptor and pre-B cell receptor signalling. *Nature Reviews Immunology*, 14(2):69–80.
- Compagno, M., Lim, W. K., Grunn, A., Nandula, S. V., Brahmachary, M., Shen, Q., Bertoni, F., Ponzoni, M., Scandurra, M., Califano, A., Bhagat, G., Chadburn, A., Dalla-Favera, R., and Pasqualucci, L. (2009). Mutations of multiple genes cause deregulation of NF- κ B in diffuse large B-cell lymphoma. *Nature*, 459(7247):717–721.
- Cooper, M. D. (2015). The early history of B cells. *Nature Reviews Immunology*, 15(3):191–197.
- Cooper, M. D., Peterson, R. D., and Good, R. A. (1965). Delineation of the Thymic and Bursal Lymphoid Systems in the Chicken. *Nature*, 205:143–146.
- Cortés, M. and Georgopoulos, K. (2004). Aiolos is required for the generation of high affinity bone marrow plasma cells responsible for long-term immunity. *The Journal of Experimental Medicine*, 199(2):209–219.
- Crotty, S. (2011). Follicular Helper CD4 T Cells (T_{FH}). *Annual Review of Immunology*, 29(1):621–663.
- Crotty, S. (2015). A brief history of T cell help to B cells. *Nature Reviews Immunology*, 15(3):185–189.
- Curry, C. V., Ewton, A. A., Olsen, R. J., Logan, B. R., Preti, H. A., Liu, Y.-C., Perkins, S. L., and Chang, C.-C. (2009). Prognostic impact of C-REL expression in diffuse large B-cell lymphoma. *Journal of Hematopathology*, 2(1):20–26.
- Dai, H., Ehrentraut, S., Nagel, S., Eberth, S., Pommerenke, C., Dirks, W. G., Geffers, R., Kalavalapalli, S., Kaufmann, M., Meyer, C., Faehnrich, S., Chen, S., Drexler, H. G., and MacLeod, R. A. F. (2015). Genomic Landscape of Primary Mediastinal B-Cell Lymphoma Cell Lines. *PLoS ONE*, 10(11):e0139663.
- Damdinsuren, B., Zhang, Y., Khalil, A., Wood, W. H., Becker, K. G., Shlomchik, M. J., and Sen, R. (2010). Single round of antigen receptor signaling programs naive B cells to receive T cell help. *Immunity*, 32(3):355–366.
- Daniel, J. A. and Nussenzweig, A. (2013). The AID-induced DNA damage response in chromatin. *Molecular Cell*, 50(3):309–321.
- de Boer, J., Williams, A., Skavdis, G., Harker, N., Coles, M., Tolaini, M., Norton, T., Williams, K., Roderick, K., Potocnik, A. J., and Kioussis, D. (2003). Transgenic mice with hematopoietic and lymphoid specific expression of Cre. *European Journal of Immunology*, 33(2):314–325.
- de Oliveira, K. A. P., Kaergel, E., Heinig, M., Fontaine, J.-F., Patone, G., Muro, E. M., Mathas, S., Hummel, M., Andrade-Navarro, M. A., Hübner, N., and Scheiderei, C. (2016). A roadmap of constitutive NF- κ B activity in Hodgkin lymphoma: Dominant roles of p50 and p52 revealed by genome-wide analyses. *Genome Medicine*, 8(1):28.
- De Silva, N. S. and Klein, U. (2015). Dynamics of B cells in germinal centres. *Nature Reviews Immunology*, 15(3):137–148.
- de Vries, C. G., Cook, M. C., Ball, J., Drew, M., Sunners, Y., Cascalho, M., Wabl, M., Klaus, G. G., and MacLennan, I. C. (2000). Germinal centers without T cells. *The Journal of Experimental Medicine*, 191(3):485–494.
- Delker, R. K., Fugmann, S. D., and Papavasiliou, F. N. (2009). A coming-of-age story: activation-induced cytidine deaminase turns 10. *Nature Immunology*, 10(11):1147–1153.
- Di Noia, J. M. and Neuberger, M. S. (2007). Molecular mechanisms of antibody somatic hypermutation. *Annual Review of Biochemistry*.
- Doi, T. S., Takahashi, T., Taguchi, O., Azuma, T., and Obata, Y. (1997). NF- κ B RelA-deficient lymphocytes: normal development of T cells and B cells, impaired production of IgA and IgG1 and reduced proliferative responses. *The Journal of Experimental Medicine*, 185(5):953–961.
- Dominguez-Sola, D., Kung, J., Holmes, A. B., Wells, V. A., Mo, T., Basso, K., and Dalla-Favera, R. (2015). The FOXO1 Transcription Factor Instructs the Germinal Center Dark Zone Program. *Immunity*, 43(6):1064–1074.
- Dominguez-Sola, D., Vitorica, G. D., Ying, C. Y., Phan, R. T., Saito, M., Nussenzweig, M. C., and Dalla-Favera, R. (2012). The proto-oncogene MYC is required for selection in the germinal center and cyclic reentry. *Nature Immunology*,

- 13(11):1083–1091.
- Donovan, C. E., Mark, D. A., He, H. Z., Liou, H. C., Kobzik, L., Wang, Y., De Sanctis, G. T., Perkins, D. L., and Finn, P. W. (1999). NF- κ B/Rel transcription factors: c-Rel promotes airway hyperresponsiveness and allergic pulmonary inflammation. *The Journal of Immunology*, 163(12):6827–6833.
- Dorshkind, K. and Montecino-Rodriguez, E. (2007). Fetal B-cell lymphopoiesis and the emergence of B-1-cell potential. *Nature Reviews Immunology*, 7(3):213–219.
- Doudna, J. A. and Charpentier, E. (2014). Genome editing. The new frontier of genome engineering with CRISPR-Cas9. *Science*, 346(6213):1258096.
- Dubois, P. C. A., Trynka, G., Franke, L., Hunt, K. A., Romanos, J., Curtotti, A., Zhernakova, A., Heap, G. A. R., Ádány, R., Aromaa, A., Bardella, M. T., van den Berg, L. H., Bockett, N. A., de la Concha, E. G., Dema, B., Fehrmann, R. S. N., Fernández-Arquero, M., Fiatal, S., Grandone, E., Green, P. M., Groen, H. J. M., Gwilliam, R., Houwen, R. H. J., Hunt, S. E., Kaukinen, K., Kelleher, D., Korponay-Szabo, I., Kurppa, K., MacMathuna, P., Mäki, M., Mazzilli, M. C., McCann, O. T., Mearin, M. L., Mein, C. A., Mirza, M. M., Mistry, V., Mora, B., Morley, K. I., Mulder, C. J., Murray, J. A., Núñez, C., Oosterom, E., Ophoff, R. A., Polanco, I., Peltonen, L., Platteel, M., Rybak, A., Salomaa, V., Schweizer, J. J., Sperandio, M. P., Tack, G. J., Turner, G., Veldink, J. H., Verbeek, W. H. M., Weersma, R. K., Wolters, V. M., Urcelay, E., Cukrowska, B., Greco, L., Neuhausen, S. L., McManus, R., Barisani, D., Deloukas, P., Barrett, J. C., Saavalainen, P., Wijmenga, C., and van Heel, D. A. (2010). Multiple common variants for celiac disease influencing immune gene expression. *Nature Genetics*, 42(4):295–302.
- Edelstein, L. C., Lagos, L., Simmons, M., Tirumalai, H., and Gélinas, C. (2003). NF- κ B-dependent assembly of an enhanceosome-like complex on the promoter region of apoptosis inhibitor Bfl-1/A1. *Molecular and Cellular Biology*, 23(8):2749–2761.
- Enciso-Mora, V., Broderick, P., Ma, Y., Jarrett, R. F., Hjalgrim, H., Hemminki, K., van den Berg, A., Olver, B., Lloyd, A., Dobbins, S. E., Lightfoot, T., van Leeuwen, F. E., Försti, A., Diepstra, A., Broeks, A., Vijayakrishnan, J., Shield, L., Lake, A., Montgomery, D., Roman, E., Engert, A., von Strandmann, E. P., Reiners, K. S., Nolte, I. M., Smedby, K. E., Adami, H.-O., Russell, N. S., Glimelius, B., Hamilton-Dutoit, S., de Bruin, M., Ryder, L. P., Molin, D., Sorensen, K. M., Chang, E. T., Taylor, M., Cooke, R., Hofstra, R., Westers, H., van Wezel, T., van Eijk, R., Ashworth, A., Rostgaard, K., Melbye, M., Swerdlow, A. J., and Houlston, R. S. (2010). A genome-wide association study of Hodgkin’s lymphoma identifies new susceptibility loci at 2p16.1 (REL), 8q24.21 and 10p14 (GATA3). *Nature Genetics*, 42(12):1126–1130.
- Engler, C., Gruetzner, R., Kandzia, R., and Marillonnet, S. (2009). Golden Gate Shuffling: A One-Pot DNA Shuffling Method Based on Type II Restriction Enzymes. *PLoS ONE*, 4(5):e5553.
- Engler, C., Kandzia, R., and Marillonnet, S. (2008). A One Pot, One Step, Precision Cloning Method with High Throughput Capability. *PLoS ONE*, 3(11):e3647.
- Engler, C. and Marillonnet, S. (2011). Generation of families of construct variants using golden gate shuffling. *Methods in Molecular Biology*, 729:167–181.
- Eyre, S., Hinks, A., Flynn, E., Martin, P., Wilson, A. G., Maxwell, J. R., Morgan, A. W., Emery, P., Steer, S., Hocking, L. J., Reid, D. M., Harrison, P., Wordsworth, P., Thomson, W., Worthington, J., and Barton, A. (2010). Confirmation of association of the REL locus with rheumatoid arthritis susceptibility in the UK population. *Annals of the Rheumatic Diseases*, 69(8):1572–1573.
- Fagerlund, R., Melén, K., Cao, X., and Julkunen, I. (2008). NF- κ B p52, RelB and c-Rel are transported into the nucleus via a subset of importin α molecules. *Cellular Signalling*, 20(8):1442–1451.
- Fan, G., Fan, Y., Gupta, N., Matsuura, I., Liu, F., Zhou, X. Z., Lu, K. P., and Gelinas, C. (2009). Peptidyl-Prolyl Isomerase Pin1 Markedly Enhances the Oncogenic Activity of the Rel Proteins in the Nuclear Factor- κ B Family. *Cancer Research*, 69(11):4589–4597.
- Fan, T., Wang, S., Yu, L., Yi, H., Liu, R., Geng, W., Wan, X., Ma, Y., Cai, L., Chen, Y. H., and Ruan, Q. (2016). Treating psoriasis by targeting its susceptibility gene Rel. *Clinical Immunology*, 165:47–54.
- Fan, Y. and Gelinas, C. (2007). An optimal range of transcription potency is necessary for efficient cell transformation by c-Rel to ensure optimal nuclear localization and gene-specific activation. *Oncogene*, 26(27):4038–4043.
- Fazilleau, N., Mark, L., McHeyzer-Williams, L. J., and McHeyzer-Williams, M. G. (2009). Follicular Helper T Cells: Lineage and Location. *Immunity*, 30(3):324–335.
- Ferch, U., Büschenfelde, C. M. z., Gewies, A., Wegener, E., Rauser, S., Peschel, C., Krappmann, D., and Ruland, J. (2007). MALT1 directs B cell receptor-induced canonical nuclear factor- κ B signaling selectively to the c-Rel subunit. *Nature Immunology*, 8(9):984–991.
- Ferch, U., Kloo, B., Gewies, A., Pfander, V., Duwel, M., Peschel, C., Krappmann, D., and Ruland, J. (2009). Inhibition of MALT1 protease activity is selectively toxic for activated B cell-like diffuse large B cell lymphoma cells. *Journal of Experimental Medicine*, 206(11):2313–2320.
- Feuerhake, F., Kutok, J. L., Monti, S., Chen, W., LaCasce, A. S., Cattoretti, G., Kurtin, P., Pinkus, G. S., de Leval, L., Harris, N. L., Savage, K. J., Neuberger, D., Habermann, T. M., Dalla-Favera, R., Golub, T. R., Aster, J. C., and Shipp, M. A. (2005). NF κ B activity, function, and target-gene signatures in primary mediastinal large B-cell lymphoma and diffuse large B-cell lymphoma subtypes. *Blood*, 106(4):1392–1399.
- Finn, P. W., He, H., Ma, C., Mueller, T., Stone, J. R., Liou, H.-C., Boothby, M. R., and Perkins, D. L. (2002). Molecular profiling of the role of the NF- κ B family of transcription factors during alloimmunity. *Journal of leukocyte biology*, 72(5):1054–1062.

- Fognani, C., Rondi, R., Romano, A., and Blasi, F. (2000). c-Rel-TD kinase: a serine/threonine kinase binding in vivo and in vitro c-Rel and phosphorylating its transactivation domain. *Oncogene*, 19(18):2224–2232.
- Fontan, L., Yang, C., Kabaleeswaran, V., Volpon, L., Osborne, M. J., Beltran, E., Garcia, M., Cerchietti, L., Shakhovich, R., Yang, S. N., Fang, F., Gascoyne, R. D., Martinez-Climent, J. A., Glickman, J. F., Borden, K., Wu, H., and Melnick, A. (2012). MALT1 Small Molecule Inhibitors Specifically Suppress ABC-DLBCL In Vitro and In Vivo. *Cancer Cell*, 22(6):812–824.
- Foy, T. M., Laman, J. D., Ledbetter, J. A., Aruffo, A., Claassen, E., and Noelle, R. J. (1994). gp39-CD40 interactions are essential for germinal center formation and the development of B cell memory. *The Journal of Experimental Medicine*, 180(1):157–163.
- Fu, L., Lin-Lee, Y.-C., Pham, L. V., Tamayo, A., Yoshimura, L., and Ford, R. J. (2006). Constitutive NF- κ B and NFAT activation leads to stimulation of the BlyS survival pathway in aggressive B-cell lymphomas. *Blood*, 107(11):4540–4548.
- Fukuhara, N., Tagawa, H., Kameoka, Y., Kasugai, Y., Karnan, S., Kameoka, J., Sasaki, T., Morishima, Y., Nakamura, S., and Seto, M. (2006). Characterization of target genes at the 2p15-16 amplicon in diffuse large B-cell lymphoma. *Cancer Science*, 97(6):499–504.
- Fuxa, M. and Skok, J. A. (2007). Transcriptional regulation in early B cell development. *Current Opinion in Immunology*, 19(2):129–136.
- Gapuzan, M.-E. R., Pitoc, G. A., and Gilmore, T. D. (2003). Mutations within a conserved protein kinase A recognition sequence confer temperature-sensitive and partially defective activities onto mouse c-Rel. *Biochemical and Biophysical Research Communications*, 307(1):92–99.
- Garbati, M. R., Alço, G., and Gilmore, T. D. (2010). Histone acetyltransferase p300 is a coactivator for transcription factor REL and is C-terminally truncated in the human diffuse large B-cell lymphoma cell line RC-K8. *Cancer Letters*, 291(2):237–245.
- George, T. C., Fanning, S. L., Fitzgerald-Bocarsly, P., Fitzgerald-Bocarsly, P., Medeiros, R. B., Highfill, S., Shimizu, Y., Hall, B. E., Frost, K., Basiji, D., Ortyrn, W. E., Morrissey, P. J., and Lynch, D. H. (2006). Quantitative measurement of nuclear translocation events using similarity analysis of multispectral cellular images obtained in flow. *Journal of Immunological Methods*, 311(1-2):117–129.
- Gerondakis, S., Grumont, R., Gugasyan, R., Wong, L., Isomura, I., Ho, W., and Banerjee, A. (2006). Unravelling the complexities of the NF- κ B signalling pathway using mouse knockout and transgenic models. *Oncogene*, 25(51):6781–6799.
- Gerondakis, S. and Siebenlist, U. (2010). Roles of the NF- κ B Pathway in Lymphocyte Development and Function. *Cold Spring Harbor Perspectives in Biology*, 2(5):a000182–a000182.
- Gerondakis, S., Strasser, A., Metcalf, D., Grigoriadis, G., Scheerlinck, J. Y., and Grumont, R. J. (1996). Rel-deficient T cells exhibit defects in production of interleukin 3 and granulocyte-macrophage colony-stimulating factor. *Proceedings of the National Academy of Sciences*, 93(8):3405–3409.
- Ghosh, S., Gifford, A. M., Riviere, L. R., Tempst, P., Nolan, G. P., and Baltimore, D. (1990). Cloning of the p50 DNA binding subunit of NF- κ B: Homology to rel and dorsal. *Cell*, 62(5):1019–1029.
- Ghosh, S. and Hayden, M. S. (2008). New regulators of NF- κ B in inflammation. *Nature Reviews Immunology*, 8(11):837–848.
- Gilmore, T. D. (1990). NF- κ B, KBF1, dorsal, and related matters. *Cell*, 62(5):841–843.
- Gilmore, T. D. (1999). Multiple mutations contribute to the oncogenicity of the retroviral oncoprotein v-Rel. *Oncogene*, 18(49):6925–6937.
- Gilmore, T. D., Cormier, C., Jean-Jacques, J., and Gapuzan, M. E. (2001). Malignant transformation of primary chicken spleen cells by human transcription factor c-Rel. *Oncogene*, 20(48):7098–7103.
- Gilmore, T. D. and Garbati, M. R. (2011). Inhibition of NF- κ B signaling as a strategy in disease therapy. *Current Topics in Microbiology and Immunology*, 349:245–263.
- Gilmore, T. D. and Gerondakis, S. (2011). The c-Rel Transcription Factor in Development and Disease. *Genes & Cancer*, 2(7):695–711.
- Gilmore, T. D., Kalaitzidis, D., Liang, M.-C., and Starczynowski, D. T. (2004a). The c-Rel transcription factor and B-cell proliferation: a deal with the devil. *Oncogene*, 23(13):2275–2286.
- Gilmore, T. D., Starczynowski, D. T., and Kalaitzidis, D. (2004b). RELevant gene amplification in B-cell lymphomas? *Blood*, 103(8):3243–4– author reply 3244–5.
- Gitlin, A. D., Mayer, C. T., Oliveira, T. Y., Shulman, Z., Jones, M. J. K., Koren, A., and Nussenzweig, M. C. (2015). T cell help controls the speed of the cell cycle in germinal center B cells. *Science*, 349(6248):643–646.
- Gitlin, A. D., Shulman, Z., and Nussenzweig, M. C. (2014). Clonal selection in the germinal centre by regulated proliferation and hypermutation. *Nature*, 509(7502):637–640.
- Gitlin, A. D., von Boehmer, L., Gazumyan, A., Shulman, Z., Oliveira, T. Y., and Nussenzweig, M. C. (2016). Independent Roles of Switching and Hypermutation in the Development and Persistence of B Lymphocyte Memory. *Immunity*, 44(4):769–781.
- Glineur, C., Davioud-Charvet, E., and Vandembunder, B. (2000). The conserved redox-sensitive cysteine residue of the DNA-binding region in the c-Rel protein is involved in the regulation of the phosphorylation of the protein. *Biochemical Journal*, 352(2):583–591.

- Goff, L. K., Neat, M. J., Crawley, C. R., Jones, L., Jones, E., Lister, T. A., and Gupta, R. K. (2000). The use of real-time quantitative polymerase chain reaction and comparative genomic hybridization to identify amplification of the REL gene in follicular lymphoma. *British Journal of Haematology*, 111(2):618–625.
- Grandien, A., Fucs, R., Nobrega, A., Andersson, J., and Coutinho, A. (1994). Negative selection of multireactive B cell clones in normal adult mice. *European Journal of Immunology*, 24(6):1345–1352.
- Gregersen, P. K., Amos, C. I., Lee, A. T., Lu, Y., Remmers, E. F., Kastner, D. L., Seldin, M. F., Criswell, L. A., Plenge, R. M., Holers, V. M., Mikuls, T. R., Sokka, T., Moreland, L. W., Bridges, S. L., Xie, G., Begovich, A. B., and Siminovitch, K. A. (2009). REL, encoding a member of the NF- κ B family of transcription factors, is a newly defined risk locus for rheumatoid arthritis. *Nature Genetics*, 41(7):820–823.
- Grootjans, J., Kaser, A., Kaufman, R. J., and Blumberg, R. S. (2016). The unfolded protein response in immunity and inflammation. *Nature Reviews Immunology*, 16(8):469–484.
- Grumont, R., Hochrein, H., O’Keeffe, M., Gugasyan, R., White, C., Caminschi, I., Cook, W., and Gerondakis, S. (2001). c-Rel regulates interleukin 12 p70 expression in CD8+ dendritic cells by specifically inducing p35 gene transcription. *The Journal of Experimental Medicine*, 194(8):1021–1032.
- Grumont, R. J. and Gerondakis, S. (1989). Structure of a mammalian c-rel protein deduced from the nucleotide sequence of murine cDNA clones. *Oncogene Research*, 4(1):1–8.
- Grumont, R. J. and Gerondakis, S. (1994). The subunit composition of NF- κ B complexes changes during B-cell development. *Cell Growth & Differentiation*, 5(12):1321–1331.
- Grumont, R. J. and Gerondakis, S. (2000). Rel induces interferon regulatory factor 4 (IRF-4) expression in lymphocytes: modulation of interferon-regulated gene expression by rel/nuclear factor κ B. *The Journal of Experimental Medicine*, 191(8):1281–1292.
- Grumont, R. J., Richardson, I. B., Gaff, C., and Gerondakis, S. (1993). rel/NF- κ B nuclear complexes that bind kB sites in the murine c-rel promoter are required for constitutive c-rel transcription in B-cells. *Cell Growth & Differentiation*, 4(9):731–743.
- Grumont, R. J., Rourke, I. J., and Gerondakis, S. (1999). Rel-dependent induction of A1 transcription is required to protect B cells from antigen receptor ligation-induced apoptosis. *Genes & Development*, 13(4):400–411.
- Grumont, R. J., Rourke, I. J., O’Reilly, L. A., Strasser, A., Miyake, K., Sha, W., and Gerondakis, S. (1998). B lymphocytes differentially use the Rel and nuclear factor κ B1 (NF- κ B1) transcription factors to regulate cell cycle progression and apoptosis in quiescent and mitogen-activated cells. *The Journal of Experimental Medicine*, 187(5):663–674.
- Grumont, R. J., Strasser, A., and Gerondakis, S. (2002). B cell growth is controlled by phosphatidylinositol 3-kinase-dependent induction of Rel/NF- κ B regulated c-myc transcription. *Molecular Cell*, 10(6):1283–1294.
- Han, S., Hathcock, K., Zheng, B., Kepler, T. B., Hodes, R., and Kelsoe, G. (1995). Cellular interaction in germinal centers. Roles of CD40 ligand and B7-2 in established germinal centers. *The Journal of Immunology*, 155(2):556–567.
- Hannink, M. and Temin, H. M. (1989). Transactivation of gene expression by nuclear and cytoplasmic rel proteins. *Molecular and Cellular Biology*, 9(10):4323–4336.
- Hao, Z., Duncan, G. S., Seagal, J., Su, Y.-W., Hong, C., Haight, J., Chen, N.-J., Elia, A., Wakeham, A., Li, W. Y., Liepa, J., Wood, G. A., Casola, S., Rajewsky, K., and Mak, T. W. (2008). Fas receptor expression in germinal-center B cells is essential for T and B lymphocyte homeostasis. *Immunity*, 29(4):615–627.
- Harling-McNabb, L., Deliyannis, G., Jackson, D. C., Gerondakis, S., Grigoriadis, G., and Brown, L. E. (1999). Mice lacking the transcription factor subunit Rel can clear an influenza infection and have functional anti-viral cytotoxic T cells but do not develop an optimal antibody response. *International Immunology*, 11(9):1431–1439.
- Harris, A. W., Pinkert, C. A., Crawford, M., Langdon, W. Y., Brinster, R. L., and Adams, J. M. (1988). The E μ -myc transgenic mouse. A model for high-incidence spontaneous lymphoma and leukemia of early B cells. *The Journal of Experimental Medicine*, 167(2):353–371.
- Harris, J., Oliére, S., Sharma, S., Sun, Q., Lin, R., Hiscott, J., and Grandvaux, N. (2006). Nuclear accumulation of cRel following C-terminal phosphorylation by TBK1/IKK epsilon. *The Journal of Immunology*, 177(4):2527–2535.
- Hartmann, S., Döring, C., Vucic, E., Chan, F. C., Ennishi, D., Tousseyn, T., de Wolf-Peeters, C., Perner, S., Wlodarska, I., Steidl, C., Gascoyne, R. D., and Hansmann, M.-L. (2015). Array comparative genomic hybridization reveals similarities between nodular lymphocyte predominant Hodgkin lymphoma and T cell/histiocyte rich large B cell lymphoma. *British Journal of Haematology*, 169(3):415–422.
- Hartmann, S., Gesk, S., Scholtysik, R., Kreuz, M., Bug, S., Vater, I., Döring, C., Cogliatti, S., Parrens, M., Merlio, J.-P., Kwiecinska, A., Porwit, A., Piccaluga, P. P., Pileri, S., Hoefler, G., Küppers, R., Siebert, R., and Hansmann, M.-L. (2010). High resolution SNP array genomic profiling of peripheral T cell lymphomas, not otherwise specified, identifies a subgroup with chromosomal aberrations affecting the REL locus. *British Journal of Haematology*, 148(3):402–412.
- Harwood, N. E. and Batista, F. D. (2010). Early events in B cell activation. *Annual Review of Immunology*, 28:185–210.
- Hauser, A. E., Junt, T., Mempel, T. R., Sneddon, M. W., Kleinstein, S. H., Henrickson, S. E., von Andrian, U. H., Shlomchik, M. J., and Haberman, A. M. (2007a). Definition of germinal-center B cell migration in vivo reveals predominant intrazonal circulation patterns. *Immunity*, 26(5):655–667.
- Hauser, A. E., Kerfoot, S. M., and Haberman, A. M. (2010). Cellular choreography in the germinal center: new visions from in vivo imaging. *Seminars in Immunopathology*, 32(3):239–255.
- Hauser, A. E., Shlomchik, M. J., and Haberman, A. M. (2007b). In vivo imaging studies shed light on germinal-centre

- development. *Nature Reviews Immunology*, 7(7):499–504.
- Hayden, M. S. and Ghosh, S. (2008). Shared Principles in NF- κ B Signaling. *Cell*, 132(3):344–362.
- Heesters, B. A., Myers, R. C., and Carroll, M. C. (2014). Follicular dendritic cells: dynamic antigen libraries. *Nature Reviews Immunology*, 14(7):495–504.
- Heger, K., Kober, M., Rieß, D., Drees, C., de Vries, I., Bertossi, A., Roers, A., Sixt, M., and Schmidt-Suppran, M. (2015). A novel Cre recombinase reporter mouse strain facilitates selective and efficient infection of primary immune cells with adenoviral vectors. *European Journal of Immunology*, 45(6):1614–1620.
- Heise, N., De Silva, N. S., Silva, K., Carette, A., Simonetti, G., Pasparakis, M., and Klein, U. (2014). Germinal center B cell maintenance and differentiation are controlled by distinct NF- κ B transcription factor subunits. *Journal of Experimental Medicine*, 211(10):2103–2118.
- Hilliard, B. A., Mason, N., Xu, L., Sun, J., Lamhamedi-Cherradi, S.-E., Liou, H.-C., Hunter, C., and Chen, Y. H. (2002). Critical roles of c-Rel in autoimmune inflammation and helper T cell differentiation. *The Journal of Clinical Investigation*, 110(6):843–850.
- Hodgkin, P. D., Lee, J. H., and Lyons, A. B. (1996). B cell differentiation and isotype switching is related to division cycle number. *The Journal of Experimental Medicine*, 184(1):277–281.
- Horwitz, B. H., Zelazowski, P., Shen, Y., Wolcott, K. M., Scott, M. L., Baltimore, D., and Snapper, C. M. (1999). The p65 subunit of NF- κ B is redundant with p50 during B cell proliferative responses, and is required for germline C_H transcription and class switching to IgG3. *The Journal of Immunology*, 162(4):1941–1946.
- Houldsworth, J., Mathew, S., Rao, P. H., Dyomina, K., Louie, D. C., Parsa, N., Offit, K., and Chaganti, R. S. (1996). REL proto-oncogene is frequently amplified in extranodal diffuse large cell lymphoma. *Blood*, 87(1):25–29.
- Houldsworth, J., Olshen, A. B., Cattoretti, G., Donnelly, G. B., Teruya-Feldstein, J., Qin, J., Palanisamy, N., Shen, Y., Dyomina, K., Petlakh, M., Pan, Q., Zelenetz, A. D., Dalla-Favera, R., and Chaganti, R. S. K. (2004). Relationship between REL amplification, REL function, and clinical and biologic features in diffuse large B-cell lymphomas. *Blood*, 103(5):1862–1868.
- Hozumi, N. and Tonegawa, S. (1976). Evidence for somatic rearrangement of immunoglobulin genes coding for variable and constant regions. *Proceedings of the National Academy of Sciences*, 73(10):3628–3632.
- Hsia, C. Y., Cheng, S., Owyang, A. M., Dowdy, S. F., and Liou, H.-C. (2002). c-Rel regulation of the cell cycle in primary mouse B lymphocytes. *International Immunology*, 14(8):905–916.
- Hu, C. J., Rao, S., Ramirez-Bergeron, D. L., Garrett-Sinha, L. A., Gerondakis, S., Clark, M. R., and Simon, M. C. (2001). PU.1/Spi-B regulation of c-rel is essential for mature B cell survival. *Immunity*, 15(4):545–555.
- Huang, D. B., Chen, Y. Q., Ruetsche, M., Phelps, C. B., and Ghosh, G. (2001). X-ray crystal structure of proto-oncogene product c-Rel bound to the CD28 response element of IL-2. *Structure*, 9(8):669–678.
- Hunter, J. E., Butterworth, J. A., Zhao, B., Sellier, H., Campbell, K. J., Thomas, H. D., Bacon, C. M., Cockell, S. J., Gewurz, B. E., and Perkins, N. D. (2015). The NF- κ B subunit c-Rel regulates Bach2 tumour suppressor expression in B-cell lymphoma. *Oncogene*.
- Hunter, J. E., Leslie, J., and Perkins, N. D. (2016). c-Rel and its many roles in cancer: an old story with new twists. *British Journal of Cancer*, 114(1):1–6.
- Hwang, J. K., Alt, F. W., and Yeap, L.-S. (2015). Related Mechanisms of Antibody Somatic Hypermutation and Class Switch Recombination. *Microbiology Spectrum*, 3(1):MDNA3-0037–2014.
- Izsvák, Z., Chuah, M. K. L., VandenDriessche, T., and Ivics, Z. (2009). Efficient stable gene transfer into human cells by the Sleeping Beauty transposon vectors. *Methods*, 49(3):287–297.
- Jacob, J., Kelsoe, G., Rajewsky, K., and Weiss, U. (1991). Intraclonal generation of antibody mutants in germinal centres. *Nature*, 354(6352):389–392.
- Jardin, F., Jais, J.-P., Molina, T.-J., Parmentier, F., Picquenot, J.-M., Ruminy, P., Tilly, H., Bastard, C., Salles, G.-A., Feugier, P., Thieblemont, C., Gisselbrecht, C., de Reynies, A., Coiffier, B., Haioun, C., and Leroy, K. (2010). Diffuse large B-cell lymphomas with CDKN2A deletion have a distinct gene expression signature and a poor prognosis under R-CHOP treatment: a GELA study. *Blood*, 116(7):1092–1104.
- Jaworski, M. and Thome, M. (2016). The paracaspase MALT1: biological function and potential for therapeutic inhibition. *Cellular and Molecular Life Sciences*, 73(3):459–473.
- Jeltsch, K. M., Hu, D., Brenner, S., Zöller, J., Heinz, G. A., Nagel, D., Vogel, K. U., Rehage, N., Warth, S. C., Edelmann, S. L., Gloury, R., Martin, N., Lohs, C., Lech, M., Stehklein, J. E., Geerlof, A., Kremmer, E., Weber, A., Anders, H.-J., Schmitz, I., Schmidt-Suppran, M., Fu, M., Holtmann, H., Krappmann, D., Ruland, J., Kallies, A., Heikenwälder, M., and Heissmeyer, V. (2014). Cleavage of roquin and regnase-1 by the paracaspase MALT1 releases their cooperatively repressed targets to promote T_H17 differentiation. *Nature Immunology*, 15(11):1079–1089.
- Jin, J., Xiao, Y., Hu, H., Zou, Q., Li, Y., Gao, Y., Ge, W., Cheng, X., and Sun, S.-C. (2015). Proinflammatory TLR signalling is regulated by a TRAF2-dependent proteolysis mechanism in macrophages. *Nature Communications*, 6:5930.
- Jinek, M., Chylinski, K., Fonfara, I., Hauer, M., Doudna, J. A., and Charpentier, E. (2012). A programmable dual-RNA-guided DNA endonuclease in adaptive bacterial immunity. *Science*, 337(6096):816–821.
- Joos, S., Granzow, M., Holtgreve-Grez, H., Siebert, R., Harder, L., Martin-Subero, J. I., Wolf, J., Adamowicz, M., Barth, T. F. E., Lichter, P., and Jauch, A. (2003). Hodgkin’s lymphoma cell lines are characterized by frequent aberrations on

- chromosomes 2p and 9p including REL and JAK2. *International Journal of Cancer*, 103(4):489–495.
- Joos, S., Küpper, M., Ohl, S., von Bonin, F., Mechttersheimer, G., Bentz, M., Marynen, P., Moller, P., Pfreundschuh, M., Trümper, L., and Lichter, P. (2000). Genomic imbalances including amplification of the tyrosine kinase gene JAK2 in CD30+ Hodgkin cells. *Cancer Research*, 60(3):549–552.
- Joos, S., Menz, C. K., Wrobel, G., Siebert, R., Gesk, S., Ohl, S., Mechttersheimer, G., Trümper, L., Möller, P., Lichter, P., and Barth, T. F. E. (2002). Classical Hodgkin lymphoma is characterized by recurrent copy number gains of the short arm of chromosome 2. *Blood*, 99(4):1381–1387.
- Joos, S. S., Otaño-Joos, M. I. M., Ziegler, S. S., Brüderlein, S. S., du Manoir, S. S., Bentz, M. M., Möller, P. P., and Lichter, P. P. (1996). Primary mediastinal (thymic) B-cell lymphoma is characterized by gains of chromosomal material including 9p and amplification of the REL gene. *Blood*, 87(4):1571–1578.
- Kaileh, M. and Sen, R. (2012). NF- κ B function in B lymphocytes. *Immunological Reviews*, 246(1):254–271.
- Kaisho, T., Takeda, K., Tsujimura, T., Kawai, T., Nomura, F., Terada, N., and Akira, S. (2001). I κ B Kinase α Is Essential for Mature B Cell Development and Function. *The Journal of Experimental Medicine*, 193(4):417–426.
- Kaku, H., Horikawa, K., Obata, Y., Kato, I., Okamoto, H., Sakaguchi, N., Gerondakis, S., and Takatsu, K. (2002). NF- κ B is required for CD38-mediated induction of C γ 1 germline transcripts in murine B lymphocytes. *International Immunology*, 14(9):1055–1064.
- Karin, M. (2011). *NF- κ B in Health and Disease*, volume 349 of *Current Topics in Microbiology and Immunology*. Springer, Berlin, Heidelberg.
- Kato, M., Sanada, M., Kato, I., Sato, Y., Takita, J., Takeuchi, K., Niwa, A., Chen, Y., Nakazaki, K., Nomoto, J., Asakura, Y., Muto, S., Tamura, A., Iio, M., Akatsuka, Y., Hayashi, Y., Mori, H., Igarashi, T., Kurokawa, M., Chiba, S., Mori, S., Ishikawa, Y., Okamoto, K., Tobinai, K., Nakagama, H., Nakahata, T., Yoshino, T., Kobayashi, Y., and Ogawa, S. (2009). Frequent inactivation of A20 in B-cell lymphomas. *Nature*, 459(7247):712–716.
- Kawabe, T., Naka, T., Yoshida, K., Tanaka, T., Fujiwara, H., Suematsu, S., Yoshida, N., Kishimoto, T., and Kikutani, H. (1994). The immune responses in CD40-deficient mice: Impaired immunoglobulin class switching and germinal center formation. *Immunity*, 1(3):167–178.
- Kepler, T. B. and Perelson, A. S. (1993). Cyclic re-entry of germinal center B cells and the efficiency of affinity maturation. *Immunology Today*, 14(8):412–415.
- Kerr, L. D., Ransone, L. J., Wamsley, P., Schmitt, M. J., Boyer, T. G., Zhou, Q., Berk, A. J., and Verma, I. M. (1993). Association between proto-oncogene Rel and TATA-binding protein mediates transcriptional activation by NF- κ B. *Nature*, 365(6445):412–419.
- Kieran, M., Blank, V., Logeat, F., Vandekerckhove, J., Lottspeich, F., Le Bail, O., Urban, M. B., Kourilsky, P., Baeuerle, P. A., and Israel, A. (1990). The DNA binding subunit of NF- κ B is identical to factor KBF1 and homologous to the rel oncogene product. *Cell*, 62(5):1007–1018.
- Kim, J. H., Lee, S.-R., Li, L.-H., Park, H.-J., Park, J.-H., Lee, K. Y., Kim, M.-K., Shin, B. A., and Choi, S.-Y. (2011). High Cleavage Efficiency of a 2A Peptide Derived from Porcine Teschovirus-1 in Human Cell Lines, Zebrafish and Mice. *PLoS ONE*, 6(4):e18556.
- Klein, U., Casola, S., Cattoretti, G., Shen, Q., Lia, M., Mo, T., Ludwig, T., Rajewsky, K., and Dalla-Favera, R. (2006). Transcription factor IRF4 controls plasma cell differentiation and class-switch recombination. *Nature Immunology*, 7(7):773–782.
- Klein, U. and Dalla-Favera, R. (2008). Germinal centres: role in B-cell physiology and malignancy. *Nature Reviews Immunology*, 8(1):22–33.
- Kleinhammer, A., Deussing, J., Wurst, W., and Kühn, R. (2011). Conditional RNAi in mice. *Methods*, 53(2):142–150.
- Kondo, M., Wagers, A. J., Manz, M. G., Prohaska, S. S., Scherer, D. C., Beilhack, G. F., Shizuru, J. A., and Weissman, I. L. (2003). Biology of hematopoietic stem cells and progenitors: implications for clinical application. *Annual Review of Immunology*, 21:759–806.
- Kontgen, F., Grumont, R. J., Strasser, A., Metcalf, D., Li, R., Tarlinton, D., and Gerondakis, S. (1995). Mice lacking the c-rel proto-oncogene exhibit defects in lymphocyte proliferation, humoral immunity, and interleukin-2 expression. *Genes & Development*, 9(16):1965–1977.
- Kramer, M. H., Hermans, J., Wijburg, E., Philippo, K., Geelen, E., van Krieken, J. H., de Jong, D., Maartense, E., Schuurin, E., and Kluin, P. M. (1998). Clinical relevance of BCL2, BCL6, and MYC rearrangements in diffuse large B-cell lymphoma. *Blood*, 92(9):3152–3162.
- Krappmann, D., Emmerich, F., Kordes, U., Scharschmidt, E., Dörken, B., and Scheidereit, C. (1999). Molecular mechanisms of constitutive NF- κ B/Rel activation in Hodgkin/Reed-Sternberg cells. *Oncogene*, 18(4):943–953.
- Kraus, M., Pao, L. I., Reichlin, A., Hu, Y., Canono, B., Cambier, J. C., Nussenzweig, M. C., and Rajewsky, K. (2001). Interference with immunoglobulin (Ig) α immunoreceptor tyrosine-based activation motif (ITAM) phosphorylation modulates or blocks B cell development, depending on the availability of an Ig β cytoplasmic tail. *The Journal of Experimental Medicine*, 194(4):455–469.
- Kunsch, C., Ruben, S. M., and Rosen, C. A. (1992). Selection of optimal κ B/Rel DNA-binding motifs: interaction of both subunits of NF- κ B with DNA is required for transcriptional activation. *Molecular and Cellular Biology*, 12(10):4412–4421.
- Küppers, R. (2005). Mechanisms of B-cell lymphoma pathogenesis. *Nature Reviews Cancer*, 5(4):251–262.

- Küppers, R. (2009). The biology of Hodgkin's lymphoma. *Nature Reviews Cancer*, 9(1):15–27.
- Küppers, R. (2012). New insights in the biology of Hodgkin lymphoma. *Hematology American Society of Hematology - Education Program*, 2012:328–334.
- Küppers, R. and Dalla-Favera, R. (2001). Mechanisms of chromosomal translocations in B cell lymphomas. *Oncogene*, 20(40):5580–5594.
- Küppers, R., Sonoki, T., Satterwhite, E., Gesk, S., Harder, L., Oscier, D. G., Tucker, P. W., Dyer, M. J. S., and Siebert, R. (2002). Lack of somatic hypermutation of IG VH genes in lymphoid malignancies with t(2;14)(p13;q32) translocation involving the BCL11A gene. *Leukemia*, 16(5):937–939.
- Kuraoka, M., Schmidt, A. G., Nojima, T., Feng, F., Watanabe, A., Kitamura, D., Harrison, S. C., Kepler, T. B., and Kelsoe, G. (2016). Complex Antigens Drive Permissive Clonal Selection in Germinal Centers. *Immunity*, 44(3):542–552.
- Kurosaki, T., Kometani, K., and Ise, W. (2015). Memory B cells. *Nature Reviews Immunology*, 15(3):149–159.
- Kurosaki, T. and Wienands, J. (2015). *B Cell Receptor Signaling*. Springer.
- Lawrence, T., Bebien, M., Liu, G. Y., Nizet, V., and Karin, M. (2005). IKK α limits macrophage NF- κ B activation and contributes to the resolution of inflammation. *Nature*, 434(7037):1138–1143.
- Leeman, J. R. and Gilmore, T. D. (2008). Alternative splicing in the NF- κ B signaling pathway. *Gene*, 423(2):97–107.
- Leeman, J. R., Weniger, M. A., Barth, T. F., and Gilmore, T. D. (2008). Deletion analysis and alternative splicing define a transactivation inhibitory domain in human oncoprotein REL. *Oncogene*, 27(53):6770–6781.
- Lentz, V. M. and Manser, T. (2001). Cutting Edge: Germinal Centers Can Be Induced in the Absence of T Cells. *The Journal of Immunology*, 167(1):15–20.
- Lenz, G., Wright, G. W., Emre, N. C. T., Kohlhammer, H., Dave, S. S., Davis, R. E., Carty, S., Lam, L. T., Shaffer, A. L., Xiao, W., Powell, J., Rosenwald, A., Ott, G., Muller-Hermelink, H.-K., Gascoyne, R. D., Connors, J. M., Campo, E., Jaffe, E. S., Delabie, J., Smeland, E. B., Rimsza, L. M., Fisher, R. I., Weisenburger, D. D., Chan, W. C., and Staudt, L. M. (2008). Molecular subtypes of diffuse large B-cell lymphoma arise by distinct genetic pathways. *Proceedings of the National Academy of Sciences*, 105(36):13520–13525.
- Li, L., Xu-Monette, Z. Y., Ok, C. Y., Tzankov, A., Manyam, G. C., Sun, R., Visco, C., Zhang, M., Montes-Moreno, S., Dybkaer, K., Chiu, A., Orazi, A., Zu, Y., Bhagat, G., Richards, K. L., Hsi, E. D., Choi, W. W. L., van Krieken, J. H., Huh, J., Ponzoni, M., Ferreri, A. J. M., Møller, M. B., Wang, J., Parsons, B. M., Winter, J. N., Piris, M. A., Pham, L. V., Medeiros, L. J., and Young, K. H. (2015). Prognostic impact of c-Rel nuclear expression and REL amplification and crosstalk between c-Rel and the p53 pathway in diffuse large B-cell lymphoma. *Oncotarget*, 6(27):23157–23180.
- Li, Z.-W., Omori, S. A., Labuda, T., Karin, M., and Rickert, R. C. (2003). IKK β is required for peripheral B cell survival and proliferation. *The Journal of Immunology*, 170(9):4630–4637.
- Lim, K.-H., Yang, Y., and Staudt, L. M. (2012). Pathogenetic importance and therapeutic implications of NF- κ B in lymphoid malignancies. *Immunological Reviews*, 246(1):359–378.
- Lin, H. and Grosschedl, R. (1995). Failure of B-cell differentiation in mice lacking the transcription factor EBF. *Nature*, 376(6537):263–267.
- Lin, K.-I., Angelin-Duclos, C., Kuo, T. C., and Calame, K. (2002). Blimp-1-dependent repression of Pax-5 is required for differentiation of B cells to immunoglobulin M-secreting plasma cells. *Molecular and Cellular Biology*, 22(13):4771–4780.
- Lin, S.-C., Wortis, H. H., and Stavnezer, J. (1998). The Ability of CD40L, but Not Lipopolysaccharide, To Initiate Immunoglobulin Switching to Immunoglobulin G1 Is Explained by Differential Induction of NF- κ B/Rel Proteins. *Molecular and Cellular Biology*, 18(9):5523–5532.
- Linterman, M. A., Beaton, L., Yu, D., Ramiscal, R. R., Srivastava, M., Hogan, J. J., Verma, N. K., Smyth, M. J., Rigby, R. J., and Vinuesa, C. G. (2010). IL-21 acts directly on B cells to regulate Bcl-6 expression and germinal center responses. *Journal of Experimental Medicine*, 207(2):353–363.
- Liou, H.-C. and Hsia, C. Y. (2003). Distinctions between c-Rel and other NF- κ B proteins in immunity and disease. *BioEssays*, 25(8):767–780.
- Liou, H. C., Sha, W. C., Scott, M. L., and Baltimore, D. (1994). Sequential induction of NF- κ B/Rel family proteins during B-cell terminal differentiation. *Molecular and Cellular Biology*, 14(8):5349–5359.
- Liu, J. and Ma, X. (2006). Interferon regulatory factor 8 regulates RANTES gene transcription in cooperation with interferon regulatory factor-1, NF- κ B, and PU.1. *Journal of Biological Chemistry*, 281(28):19188–19195.
- Liu, M., Duke, J. L., Richter, D. J., Vinuesa, C. G., Goodnow, C. C., Kleinstein, S. H., and Schatz, D. G. (2008). Two levels of protection for the B cell genome during somatic hypermutation. *Nature*, 451(7180):841–845.
- Liu, M. and Schatz, D. G. (2009). Balancing AID and DNA repair during somatic hypermutation. *Trends in Immunology*, 30(4):173–181.
- Liu, P., Keller, J. R., Ortiz, M., Tessarollo, L., Rachel, R. A., Nakamura, T., Jenkins, N. A., and Copeland, N. G. (2003). Bcl11a is essential for normal lymphoid development. *Nature Immunology*, 4(6):525–532.
- Loizou, L., Andersen, K. G., and Betz, A. G. (2011). Foxp3 Interacts with c-Rel to Mediate NF- κ B Repression. *PLoS ONE*, 6(4):e18670.
- Long, M., Park, S. G., Strickland, I., Hayden, M. S., and Ghosh, S. (2009). Nuclear factor- κ B modulates regulatory T cell development by directly regulating expression of Foxp3 transcription factor. *Immunity*, 31(6):921–931.

- MacLennan, I. C. M., Toellner, K.-M., Cunningham, A. F., Serre, K., Sze, D. M.-Y., Zúñiga, E., Cook, M. C., and Vinuesa, C. G. (2003). Extrafollicular antibody responses. *Immunological Reviews*, 194:8–18.
- Mader, A., Br uuml derlein, S., Wegener, S., Melzner, I., Popov, S., M uuml ller Hermelink, H. K., Barth, T. F., Viardot, A., and M ouml ller, P. (2007). U-HO1, a new cell line derived from a primary refractory classical Hodgkin lymphoma. *Cytogenetic and Genome Research*, 119(3-4):204–210.
- Mali, P., Aach, J., Stranges, P. B., Esvelt, K. M., Moosburner, M., Kosuri, S., Yang, L., and Church, G. M. (2013a). CAS9 transcriptional activators for target specificity screening and paired nickases for cooperative genome engineering. *Nature Biotechnology*, 31(9):833–838.
- Mali, P., Yang, L., Esvelt, K. M., Aach, J., Guell, M., DiCarlo, J. E., Norville, J. E., and Church, G. M. (2013b). RNA-guided human genome engineering via Cas9. *Science*, 339(6121):823–826.
- Martin, A. G. and Fresno, M. (2000). Tumor necrosis factor- α activation of NF- κ B requires the phosphorylation of Ser-471 in the transactivation domain of c-Rel. *Journal of Biological Chemistry*, 275(32):24383–24391.
- Martin, A. G., San-Antonio, B., and Fresno, M. (2001). Regulation of nuclear factor κ B transactivation. Implication of phosphatidylinositol 3-kinase and protein kinase C ζ in c-Rel activation by tumor necrosis factor α . *Journal of Biological Chemistry*, 276(19):15840–15849.
- Martin-Subero, J. I., Gesk, S., Harder, L., Sonoki, T., Tucker, P. W., Schlegelberger, B., Grote, W., Novo, F. J., Calasanz, M. J., Hansmann, M. L., Dyer, M. J. S., and Siebert, R. (2002). Recurrent involvement of the REL and BCL11A loci in classical Hodgkin lymphoma. *Blood*, 99(4):1474–1477.
- Martin-Subero, J. I., Klapper, W., Sotnikova, A., Callet-Bauchu, E., Harder, L., Bastard, C., Schmitz, R., Grohmann, S., Höppner, J., Riemke, J., Barth, T. F. E., Berger, F., Bernd, H.-W., Claviez, A., Gesk, S., Frank, G. A., Kaplanskaya, I. B., Möller, P., Parwaresch, R. M., Rüdiger, T., Stein, H., Küppers, R., Hansmann, M. L., Siebert, R., and Deutsche Krebshilfe Network Project Molecular Mechanisms in Malignant Lymphomas (2006). Chromosomal breakpoints affecting immunoglobulin loci are recurrent in Hodgkin and Reed-Sternberg cells of classical Hodgkin lymphoma. *Cancer Research*, 66(21):10332–10338.
- Martinez-Climent, J. A., Alizadeh, A. A., Se graves, R., Blesa, D., Rubio-Moscardo, F., Albertson, D. G., Garcia-Conde, J., Dyer, M. J. S., Levy, R., Pinkel, D., and Lossos, I. S. (2003). Transformation of follicular lymphoma to diffuse large cell lymphoma is associated with a heterogeneous set of DNA copy number and gene expression alterations. *Blood*, 101(8):3109–3117.
- Martomo, S. A. and Gearhart, P. J. (2006). Somatic hypermutation: subverted DNA repair. *Current Opinion in Immunology*, 18(3):243–248.
- Mátés, L., Chuah, M. K. L., Belay, E., Jerchow, B., Manoj, N., Acosta-Sanchez, A., Grzela, D. P., Schmitt, A., Becker, K., Matrai, J., Ma, L., Samara-Kuko, E., Gysemans, C., Pryputniewicz, D., Miskey, C., Fletcher, B., VandenDriessche, T., Ivics, Z., and Izsvák, Z. (2009). Molecular evolution of a novel hyperactive Sleeping Beauty transposase enables robust stable gene transfer in vertebrates. *Nature Genetics*, 41(6):753–761.
- Matsuda, S., Mikami, Y., Ohtani, M., Fujiwara, M., Hirata, Y., Minowa, A., Terauchi, Y., Kadowaki, T., and Koyasu, S. (2008). Critical role of class IA PI3K for c-Rel expression in B lymphocytes. *Blood*, 113(5):1037–1044.
- Matthews, A. J., Zheng, S., DiMenna, L. J., and Chaudhuri, J. (2014). Regulation of immunoglobulin class-switch recombination: choreography of noncoding transcription, targeted DNA deamination, and long-range DNA repair. *Advances in Immunology*, 122:1–57.
- McGovern, D. P. B., Gardet, A., Törkvist, L., Goyette, P., Essers, J., Taylor, K. D., Neale, B. M., Ong, R. T. H., Lagacé, C., Li, C., Green, T., Stevens, C. R., Beauchamp, C., Fleshner, P. R., Carlson, M., D’Amato, M., Halfvarson, J., Hibberd, M. L., Lördal, M., Padyukov, L., Andriulli, A., Colombo, E., Latiano, A., Palmieri, O., Bernard, E.-J., Deslandres, C., Hommes, D. W., de Jong, D. J., Stokkers, P. C., Weersma, R. K., NIDDK IBD Genetics Consortium, Sharma, Y., Silverberg, M. S., Cho, J. H., Wu, J., Roeder, K., Brant, S. R., Schumm, L. P., Duerr, R. H., Dubinsky, M. C., Glazer, N. L., Haritunians, T., Ippoliti, A., Melmed, G. Y., Siscovick, D. S., Vasilias, E. A., Targan, S. R., Annese, V., Wijmenga, C., Pettersson, S., Rotter, J. I., Xavier, R. J., Daly, M. J., Rioux, J. D., and Seielstad, M. (2010). Genome-wide association identifies multiple ulcerative colitis susceptibility loci. *Nature Genetics*, 42(4):332–337.
- McHeyzer-Williams, L. J., Milpied, P. J., Okitsu, S. L., and McHeyzer-Williams, M. G. (2015). Class-switched memory B cells remodel BCRs within secondary germinal centers. *Nature Immunology*, 16(3):296–305.
- McHeyzer-Williams, M., Okitsu, S., Wang, N., and McHeyzer-Williams, L. (2012). Molecular programming of B cell memory. *Nature Reviews Immunology*, 12(1):24–34.
- McKarns, S. C. and Schwartz, R. H. (2008). Biphasic regulation of Il2 transcription in CD4+ T cells: roles for TNF- α receptor signaling and chromatin structure. *The Journal of Immunology*, 181(2):1272–1281.
- Melchers, F. (2015). Checkpoints that control B cell development. *The Journal of Clinical Investigation*, 125(6):2203–2210.
- Melzner, I. (2005). Biallelic mutation of SOCS-1 impairs JAK2 degradation and sustains phospho-JAK2 action in the MedB-1 mediastinal lymphoma line. *Blood*, 105(6):2535–2542.
- Melzner, I., Weniger, M. A., Bucur, A. J., Brüderlein, S., Dorsch, K., Hasel, C., Leithäuser, F., Ritz, O., Dyer, M. J. S., Barth, T. F. E., and Möller, P. (2006). Biallelic deletion within 16p13.13 including SOCS-1 in Karpas1106P mediastinal B-cell lymphoma line is associated with delayed degradation of JAK2 protein. *International Journal of Cancer*, 118(8):1941–1944.
- Mémet, S., Laouini, D., Epinat, J. C., Whiteside, S. T., Goudeau, B., Philpott, D., Kayal, S., Sansonetti, P. J., Berche, P., Kanellopoulos, J., and Israel, A. (1999). I κ B ϵ -deficient mice: reduction of one T cell precursor subspecies and enhanced Ig isotype switching and cytokine synthesis. *The Journal of Immunology*, 163(11):5994–6005.

- Merrell, K. T., Benschop, R. J., Gauld, S. B., Aviszus, K., Decote-Ricardo, D., Wsocki, L. J., and Cambier, J. C. (2006). Identification of anergic B cells within a wild-type repertoire. *Immunity*, 25(6):953–962.
- Meyer-Bahlburg, A., Bandaranayake, A. D., Andrews, S. F., and Rawlings, D. J. (2009). Reduced c-myc expression levels limit follicular mature B cell cycling in response to TLR signals. *The Journal of Immunology*, 182(7):4065–4075.
- Meyer-Hermann, M., Mohr, E., Pelletier, N., Zhang, Y., Victora, G. D., and Toellner, K.-M. (2012). A theory of germinal center B cell selection, division, and exit. *Cell Reports*, 2(1):162–174.
- Meyer-Hermann, M. E., Maini, P. K., and Iber, D. (2006). An analysis of B cell selection mechanisms in germinal centers. *Mathematical Medicine and Biology*, 23(3):255–277.
- Meylan, E., Dooley, A. L., Feldser, D. M., Shen, L., Turk, E., Ouyang, C., and Jacks, T. (2009). Requirement for NF- κ B signalling in a mouse model of lung adenocarcinoma. *Nature*, 462(7269):104–107.
- Minnich, M., Tagoh, H., Bönelt, P., Axelsson, E., Fischer, M., Cebolla, B., Tarakhovskiy, A., Nutt, S. L., Jaritz, M., and Busslinger, M. (2016). Multifunctional role of the transcription factor Blimp-1 in coordinating plasma cell differentiation. *Nature Immunology*, 17(3):331–343.
- Miyamoto, S., Schmitt, M. J., and Verma, I. M. (1994). Qualitative changes in the subunit composition of κ B-binding complexes during murine B-cell differentiation. *Proceedings of the National Academy of Sciences*, 91(11):5056–5060.
- Moller, P., Brüderlein, S., Sträter, J., Leithäuser, F., Hasel, C., Bataille, F., Moldenhauer, G., Pawlita, M., and Barth, T. F. (2001). MedB-1, a human tumor cell line derived from a primary mediastinal large B-cell lymphoma. *International Journal of Cancer*, 92(3):348–353.
- Mombaerts, P., Iacomini, J., Johnson, R. S., and Herrup, K. (1992). RAG-1-deficient mice have no mature B and T lymphocytes. *Cell*, 68(5):869–877.
- Monti, S., Savage, K. J., Kutok, J. L., Feuerhake, F., Kurtin, P., Mihm, M., Wu, B., Pasqualucci, L., Neuberg, D., Aguiar, R. C. T., Dal Cin, P., Ladd, C., Pinkus, G. S., Salles, G., Harris, N. L., Dalla-Favera, R., Habermann, T. M., Aster, J. C., Golub, T. R., and Shipp, M. A. (2005). Molecular profiling of diffuse large B-cell lymphoma identifies robust subtypes including one characterized by host inflammatory response. *Blood*, 105(5):1851–1861.
- Mottok, A., Renne, C., Willenbrock, K., Hansmann, M. L., and Brauning, A. (2007). Somatic hypermutation of SOCS1 in lymphocyte-predominant Hodgkin lymphoma is accompanied by high JAK2 expression and activation of STAT6. *Blood*, 110(9):3387–3390.
- Muramatsu, M., Kinoshita, K., Fagarasan, S., Yamada, S., Shinkai, Y., and Honjo, T. (2000). Class switch recombination and hypermutation require activation-induced cytidine deaminase (AID), a potential RNA editing enzyme. *Cell*, 102(5):553–563.
- Muramatsu, M., Sankaranand, V. S., Anant, S., Sugai, M., Kinoshita, K., Davidson, N. O., and Honjo, T. (1999). Specific expression of activation-induced cytidine deaminase (AID), a novel member of the RNA-editing deaminase family in germinal center B cells. *Journal of Biological Chemistry*, 274(26):18470–18476.
- Murphy, K., Travers, P., and Walport, M. (2007). *Janeway’s Immunobiology*. Garland Publishing, New York, 7th edition.
- Nacheva, E., Dyer, M. J., Metivier, C., Jadayel, D., Stranks, G., Morilla, R., Heward, J. M., Holloway, T., O’Connor, S., and Bevan, P. C. (1994). B-cell non-Hodgkin’s lymphoma cell line (Karpas 1106) with complex translocation involving 18q21.3 but lacking BCL2 rearrangement and expression. *Blood*, 84(10):3422–3428.
- Nagasawa, T. (2006). Microenvironmental niches in the bone marrow required for B-cell development. *Nature Reviews Immunology*, 6(2):107–116.
- Natoli, G., Sacconi, S., Bosisio, D., and Marazzi, I. (2005). Interactions of NF- κ B with chromatin: the art of being at the right place at the right time. *Nature Immunology*, 6(5):439–445.
- Nemazee, D. (2006). Receptor editing in lymphocyte development and central tolerance. *Nature Reviews Immunology*, 6(10):728–740.
- Neo, W. H., Lim, J. F., Grumont, R., Gerondakis, S., and Su, I.-H. (2014). c-Rel regulates Ezh2 expression in activated lymphocytes and malignant lymphoid cells. *The Journal of Biological Chemistry*, 289(46):31693–31707.
- Nieuwenhuis, P. and Opstelten, D. (1984). Functional anatomy of germinal centers. *The American Journal of Anatomy*, 170(3):421–435.
- Nolan, G. P., Ghosh, S., Liou, H. C., Tempst, P., and Baltimore, D. (1991). DNA binding and I κ B inhibition of the cloned p65 subunit of NF- κ B, a rel-related polypeptide. *Cell*, 64(5):961–969.
- Nurieva, R. I., Chung, Y., Hwang, D., Yang, X. O., Kang, H. S., Ma, L., Wang, Y.-H., Watowich, S. S., Jetten, A. M., Tian, Q., and Dong, C. (2008). Generation of T follicular helper cells is mediated by interleukin-21 but independent of T helper 1, 2, or 17 cell lineages. *Immunity*, 29(1):138–149.
- Nutt, S. L., Heavey, B., Rolink, A. G., and Busslinger, M. (1999). Commitment to the B-lymphoid lineage depends on the transcription factor Pax5. *Nature*, 401(6753):556–562.
- Nutt, S. L., Hodgkin, P. D., Tarlinton, D. M., and Corcoran, L. M. (2015). The generation of antibody-secreting plasma cells. *Nature Reviews Immunology*, 15(3):160–171.
- Nutt, S. L., Taubenheim, N., Hasbold, J., Corcoran, L. M., and Hodgkin, P. D. (2011). The genetic network controlling plasma cell differentiation. *Seminars in Immunology*, 23(5):341–349.
- Ochiai, K., Maienschein-Cline, M., Simonetti, G., Chen, J., Rosenthal, R., Brink, R., Chong, A. S., Klein, U., Dinner, A. R., Singh, H., and Sciammas, R. (2013). Transcriptional Regulation of Germinal Center B and Plasma Cell Fates by

- Dynamical Control of IRF4. *Immunity*, 38(5):918–929.
- Odegard, V. H. and Schatz, D. G. (2006). Targeting of somatic hypermutation. *Nature Reviews Immunology*, 6(8):573–583.
- Odqvist, L., Montes-Moreno, S., Sánchez-Pacheco, R. E., Young, K. H., Martín-Sánchez, E., Cereceda, L., Sánchez-Verde, L., Pajares, R., Mollejo, M., Fresno, M. F., Mazorra, F., Ruíz-Marcellán, C., Sánchez-Beato, M., and Piris, M. A. (2014). NF κ B expression is a feature of both activated B-cell-like and germinal center B-cell-like subtypes of diffuse large B-cell lymphoma. *Modern Pathology*, 27(10):1331–1337.
- Oeckinghaus, A. and Ghosh, S. (2009). The NF- κ B family of transcription factors and its regulation. *Cold Spring Harbor Perspectives in Biology*, 1(4):a000034.
- Okkenhaug, K. and Vanhaesebroeck, B. (2003). PI3K in lymphocyte development, differentiation and activation. *Nature Reviews Immunology*, 3(4):317–330.
- O’Reilly, L. A., Hughes, P., Lin, A., Waring, P., Siebenlist, U., Jain, R., Gray, D. H. D., Gerondakis, S., and Strasser, A. (2015). Loss of c-REL but not NF- κ B2 prevents autoimmune disease driven by FasL mutation. *Cell Death and Differentiation*, 22(5):767–778.
- Ott, G., Rosenwald, A., and Campo, E. (2013). Understanding MYC-driven aggressive B-cell lymphomas: pathogenesis and classification. *Blood*, 122(24):3884–3891.
- Ouk, S., Liou, M.-L., and Liou, H.-C. (2009). Direct Rel/NF- κ B inhibitors: structural basis for mechanism of action. *Future Medicinal Chemistry*, 1(9):1683–1707.
- Owyang, A. M., Tumang, J. R., Schram, B. R., Hsia, C. Y., Behrens, T. W., Rothstein, T. L., and Liou, H. C. (2001). c-Rel is required for the protection of B cells from antigen receptor-mediated, but not Fas-mediated, apoptosis. *The Journal of Immunology*, 167(9):4948–4956.
- Palanisamy, N., Abou-Elella, A. A., Chaganti, S. R., Houldsworth, J., Offit, K., Louie, D. C., Terayu-Feldstein, J., Cigudosa, J. C., Rao, P. H., Sanger, W. G., Weisenburger, D. D., and Chaganti, R. S. K. (2002). Similar patterns of genomic alterations characterize primary mediastinal large-B-cell lymphoma and diffuse large-B-cell lymphoma. *Genes, Chromosomes and Cancer*, 33(2):114–122.
- Pasparakis, M. (2009). Regulation of tissue homeostasis by NF- κ B signalling: implications for inflammatory diseases. *Nature Reviews Immunology*, 9(11):778–788.
- Pasparakis, M., Luedde, T., and Schmidt-Supprian, M. (2006). Dissection of the NF- κ B signalling cascade in transgenic and knockout mice. *Cell Death and Differentiation*, 13(5):861–872.
- Pasparakis, M., Schmidt-Supprian, M., and Rajewsky, K. (2002). I κ B kinase signaling is essential for maintenance of mature B cells. *The Journal of Experimental Medicine*, 196(6):743–752.
- Pasqualucci, L., Neumeister, P., Goossens, T., Nanjangud, G., Chaganti, R. S., Küppers, R., and Dalla-Favera, R. (2001). Hypermutation of multiple proto-oncogenes in B-cell diffuse large-cell lymphomas. *Nature*, 412(6844):341–346.
- Pelanda, R. and Torres, R. M. (2012). Central B-cell tolerance: where selection begins. *Cold Spring Harbor Perspectives in Biology*, 4(4):a007146.
- Peled, J. U., Kuang, F. L., Iglesias-Ussel, M. D., Roa, S., Kalis, S. L., Goodman, M. F., and Scharff, M. D. (2008). The biochemistry of somatic hypermutation. *Annual Review of Immunology*, 26:481–511.
- Pelengaris, S., Khan, M., and Evan, G. (2002). c-MYC: more than just a matter of life and death. *Nature Reviews Cancer*, 2(10):764–776.
- Perkins, N. D. (2006). Post-translational modifications regulating the activity and function of the nuclear factor kappa B pathway. *Oncogene*, 25(51):6717–6730.
- Perkins, N. D. (2012). The diverse and complex roles of NF- κ B subunits in cancer. *Nature Reviews Cancer*, 12(2):121–132.
- Perkins, N. D., Felzien, L. K., Betts, J. C., Leung, K., Beach, D. H., and Nabel, G. J. (1997). Regulation of NF- κ B by Cyclin-Dependent Kinases Associated with the p300 Coactivator. *Science*, 275(5299):523–527.
- Perkins, N. D. and Gilmore, T. D. (2006). Good cop, bad cop: the different faces of NF- κ B. *Cell Death and Differentiation*, 13(5):759–772.
- Pham, L. V., Fu, L., Tamayo, A. T., Bueso-Ramos, C., Drakos, E., Vega, F., Medeiros, L. J., and Ford, R. J. (2011). Constitutive BR3 receptor signaling in diffuse, large B-cell lymphomas stabilizes nuclear factor- κ B-inducing kinase while activating both canonical and alternative nuclear factor- κ B pathways. *Blood*, 117(1):200–210.
- Pham, L. V., Tamayo, A. T., Yoshimura, L. C., Lin-Lee, Y.-C., and Ford, R. J. (2005). Constitutive NF- κ B and NFAT activation in aggressive B-cell lymphomas synergistically activates the CD154 gene and maintains lymphoma cell survival. *Blood*, 106(12):3940–3947.
- Pierce, S. K. (2002). Lipid rafts and B-cell activation. *Nature Reviews Immunology*, 2(2):96–105.
- Pillai, S. and Cariappa, A. (2009). The follicular versus marginal zone B lymphocyte cell fate decision. *Nature Reviews Immunology*, 9(11):767–777.
- R Core Team (2016). *R: A Language and Environment for Statistical Computing*. R foundation for Statistical Computing.
- Radbruch, A., Muehlinghaus, G., Luger, E. O., Inamine, A., Smith, K. G. C., Dörner, T., and Hiepe, F. (2006). Competence and competition: the challenge of becoming a long-lived plasma cell. *Nature Reviews Immunology*, 6(10):741–750.
- Rajewsky, K., Förster, I., and Cumano, A. (1987). Evolutionary and somatic selection of the antibody repertoire in the

- mouse. *Science*, 238(4830):1088–1094.
- Ramakrishnan, P., Clark, P. M., Mason, D. E., Peters, E. C., Hsieh-Wilson, L. C., and Baltimore, D. (2013). Activation of the Transcriptional Function of the NF- κ B Protein c-Rel by O-GlcNAc Glycosylation. *Science Signaling*, 6(290):ra75–ra75.
- Ramiscal, R. R. and Vinuesa, C. G. (2013). T-cell subsets in the germinal center. *Immunological Reviews*, 252(1):146–155.
- Ramos, J. C., Ruiz, P., Ratner, L., Reis, I. M., Brites, C., Pedrosa, C., Byrne, G. E., Toomey, N. L., Andela, V., Harhaj, E. W., Lossos, I. S., and Harrington, W. J. (2007). IRF-4 and c-Rel expression in antiviral-resistant adult T-cell leukemia/lymphoma. *Blood*, 109(7):3060–3068.
- Ranuncolo, S. M., Pittaluga, S., Evbuomwan, M. O., Jaffe, E. S., and Lewis, B. A. (2012). Hodgkin lymphoma requires stabilized NIK and constitutive RelB expression for survival. *Blood*, 120(18):3756–3763.
- Rao, P. H., Houldsworth, J., Dyomina, K., Parsa, N. Z., Cigudosa, J. C., Louie, D. C., Popplewell, L., Offit, K., Jhanwar, S. C., and Chaganti, R. S. (1998). Chromosomal and gene amplification in diffuse large B-cell lymphoma. *Blood*, 92(1):234–240.
- Rao, S., Gerondakis, S., Woltring, D., and Shannon, M. F. (2003). c-Rel is required for chromatin remodeling across the IL-2 gene promoter. *The Journal of Immunology*, 170(7):3724–3731.
- Raschka, S. (2013). *Instant Heat Maps in R*. How-To. Packt Publishing Ltd.
- Reader, J. C., Zhao, X. F., Butler, M. S., Rapoport, A. P., and Ning, Y. (2006). REL-positive double minute chromosomes in follicular lymphoma. *Leukemia*, 20(9):1624–1626.
- Reimold, A. M., Iwakoshi, N. N., Manis, J., Vallabhajosyula, P., Szomolanyi-Tsuda, E., Gravallese, E. M., Friend, D., Grusby, M. J., Alt, F., and Glimcher, L. H. (2001). Plasma cell differentiation requires the transcription factor XBP-1. *Nature*, 412(6844):300–307.
- Reth, M. and Wienands, J. (1997). Initiation and processing of signals from the B cell antigen receptor. *Annual Review of Immunology*, 15(1):453–479.
- Rickert, R. C., Roes, J., and Rajewsky, K. (1997). B lymphocyte-specific, Cre-mediated mutagenesis in mice. *Nucleic Acids Research*, 25(6):1317–1318.
- Rodig, S. J., Savage, K. J., LaCasce, A. S., Weng, A. P., Harris, N. L., Shipp, M. A., Hsi, E. D., Gascoyne, R. D., and Kutok, J. L. (2007). Expression of TRAF1 and nuclear c-Rel distinguishes primary mediastinal large cell lymphoma from other types of diffuse large B-cell lymphoma. *The American Journal of Surgical Pathology*, 31(1):106–112.
- Rodig, S. J., Savage, K. J., Nguyen, V., Pinkus, G. S., Shipp, M. A., Aster, J. C., and Kutok, J. L. (2005). TRAF1 expression and c-Rel activation are useful adjuncts in distinguishing classical Hodgkin lymphoma from a subset of morphologically or immunophenotypically similar lymphomas. *The American Journal of Surgical Pathology*, 29(2):196–203.
- Rodríguez, C. I., Buchholz, F., Galloway, J., Sequerra, R., Kasper, J., Ayala, R., Stewart, A. F., and Dymecki, S. M. (2000). High-efficiency deleter mice show that FLPe is an alternative to Cre-loxP. *Nature Genetics*, 25(2):139–140.
- Röhlich, K. (1930). Beitrag zur Cytologie der Keimzentren der Lymphknoten. *Z. Mikrosk. Anat. Forsch.*, 20:287–297.
- Rolink, A. G., Schaniel, C., Busslinger, M., Nutt, S. L., and Melchers, F. (2000). Fidelity and infidelity in commitment to B-lymphocyte lineage development. *Immunological Reviews*, 175:104–111.
- Romieu-Mourez, R., Kim, D. W., Shin, S. M., Demicco, E. G., Landesman-Bollag, E., Seldin, D. C., Cardiff, R. D., and Sonenshein, G. E. (2003). Mouse mammary tumor virus c-rel transgenic mice develop mammary tumors. *Molecular and Cellular Biology*, 23(16):5738–5754.
- Rosenwald, A., Wright, G., Chan, W. C., Connors, J. M., Campo, E., Fisher, R. I., Gascoyne, R. D., Muller-Hermelink, H. K., Smeland, E. B., Giltneane, J. M., Hurt, E. M., Zhao, H., Averett, L., Yang, L., Wilson, W. H., Jaffe, E. S., Simon, R., Klausner, R. D., Powell, J., Duffey, P. L., Longo, D. L., Greiner, T. C., Weisenburger, D. D., Sanger, W. G., Dave, B. J., Lynch, J. C., Vose, J., Armitage, J. O., Montserrat, E., López-Guillermo, A., Grogan, T. M., Miller, T. P., LeBlanc, M., Ott, G., Kvaloy, S., Delabie, J., Holte, H., Krajci, P., Stokke, T., Staudt, L. M., and Lymphoma/Leukemia Molecular Profiling Project (2002). The use of molecular profiling to predict survival after chemotherapy for diffuse large-B-cell lymphoma. *The New England Journal of Medicine*, 346(25):1937–1947.
- Rosenwald, A., Wright, G., Leroy, K., Yu, X., Gaulard, P., Gascoyne, R. D., Chan, W. C., Zhao, T., Haioun, C., Greiner, T. C., Weisenburger, D. D., Lynch, J. C., Vose, J., Armitage, J. O., Smeland, E. B., Kvaloy, S., Holte, H., Delabie, J., Campo, E., Montserrat, E., López-Guillermo, A., Ott, G., Muller-Hermelink, H. K., Connors, J. M., Braziel, R., Grogan, T. M., Fisher, R. I., Miller, T. P., LeBlanc, M., Chiorazzi, M., Zhao, H., Yang, L., Powell, J., Wilson, W. H., Jaffe, E. S., Simon, R., Klausner, R. D., and Staudt, L. M. (2003). Molecular diagnosis of primary mediastinal B cell lymphoma identifies a clinically favorable subgroup of diffuse large B cell lymphoma related to Hodgkin lymphoma. *The Journal of Experimental Medicine*, 198(6):851–862.
- Ruan, Q., Kameswaran, V., Tone, Y., Li, L., Liou, H.-C., Greene, M. I., Tone, M., and Chen, Y. H. (2009). Development of Foxp3+ regulatory t cells is driven by the c-Rel enhanceosome. *Immunity*, 31(6):932–940.
- Ruan, Q., Kameswaran, V., Zhang, Y., Zheng, S., Sun, J., Wang, J., DeVirgiliis, J., Liou, H.-C., Beg, A. A., and Chen, Y. H. (2011). The Th17 immune response is controlled by the Rel-ROR γ -ROR γ T transcriptional axis. *Journal of Experimental Medicine*, 208(11):2321–2333.
- Ruland, J. (2011). Return to homeostasis: downregulation of NF- κ B responses. *Nature Immunology*, 12(8):709–714.
- Saito, M., Gao, J., Basso, K., Kitagawa, Y., Smith, P. M., Bhagat, G., Pernis, A., Pasqualucci, L., and Dalla-Favera, R. (2007). A Signaling Pathway Mediating Downregulation of BCL6 in Germinal Center B Cells Is Blocked by BCL6 Gene

- Alterations in B Cell Lymphoma. *Cancer Cell*, 12(3):280–292.
- Salipante, S. J., Adey, A., Thomas, A., Lee, C., Liu, Y. J., Kumar, A., Lewis, A. P., Wu, D., Fromm, J. R., and Shendure, J. (2016). Recurrent somatic loss of TNFRSF14 in classical Hodgkin lymphoma. *Genes, Chromosomes and Cancer*, 55(3):278–287.
- Sambrook, J., Fritsch, E. F., and Maniatis, T. (1989). *Molecular Cloning: A laboratory manual*. Cold Spring Harbor Laboratory Press, 2nd edition.
- Sambrook, J. F. and Russell, D. W. (2001). *Molecular Cloning: A laboratory manual*. Cold Spring Harbor Laboratory Press, 3rd edition.
- Sánchez-Valdepeñas, C., Martin, A. G., Ramakrishnan, P., Wallach, D., and Fresno, M. (2006). NF- κ B-inducing kinase is involved in the activation of the CD28 responsive element through phosphorylation of c-Rel and regulation of its transactivating activity. *The Journal of Immunology*, 176(8):4666–4674.
- Sander, S., Chu, V. T., Yasuda, T., Franklin, A., Graf, R., Calado, D. P., Li, S., Imami, K., Selbach, M., Di Virgilio, M., Bullinger, L., and Rajewsky, K. (2015). PI3 Kinase and FOXO1 Transcription Factor Activity Differentially Control B Cells in the Germinal Center Light and Dark Zones. *Immunity*, 43(6):1075–1086.
- Sanjabi, S. (2005). A c-Rel subdomain responsible for enhanced DNA-binding affinity and selective gene activation. *Genes & Development*, 19(18):2138–2151.
- Sanjabi, S., Hoffmann, A., Liou, H. C., Baltimore, D., and Smale, S. T. (2000). Selective requirement for c-Rel during IL-12 P40 gene induction in macrophages. *Proceedings of the National Academy of Sciences*, 97(23):12705–12710.
- Sasaki, Y., Calado, D. P., Derudder, E., Zhang, B., Shimizu, Y., Mackay, F., Nishikawa, S.-i., Rajewsky, K., and Schmidt-Supprian, M. (2008). NIK overexpression amplifies, whereas ablation of its TRAF3-binding domain replaces BAFF:BAFF-R-mediated survival signals in B cells. *Proceedings of the National Academy of Sciences*, 105(31):10883–10888.
- Sasaki, Y., Casola, S., Kutok, J. L., Rajewsky, K., and Schmidt-Supprian, M. (2004). TNF family member B cell-activating factor (BAFF) receptor-dependent and -independent roles for BAFF in B cell physiology. *The Journal of Immunology*, 173(4):2245–2252.
- Sasaki, Y., Derudder, E., Hobeika, E., Pelanda, R., Reth, M., Rajewsky, K., and Schmidt-Supprian, M. (2006). Canonical NF- κ B Activity, Dispensable for B Cell Development, Replaces BAFF-Receptor Signals and Promotes B Cell Proliferation upon Activation. *Immunity*, 24(6):729–739.
- Sasaki, Y. and Iwai, K. (2016). Roles of the NF- κ B Pathway in B-Lymphocyte Biology. *Current Topics in Microbiology and Immunology*, 393:177–209.
- Satterwhite, E. (2001). The BCL11 gene family: involvement of BCL11A in lymphoid malignancies. *Blood*, 98(12):3413–3420.
- Savage, K. J. (2003). The molecular signature of mediastinal large B-cell lymphoma differs from that of other diffuse large B-cell lymphomas and shares features with classical Hodgkin lymphoma. *Blood*, 102(12):3871–3879.
- Savage, K. J. (2006). Primary mediastinal large B-cell lymphoma. *The Oncologist*, 11(5):488–495.
- Schaadt, M., Fonatsch, C., Kirchner, H., and Diehl, V. (1979). Establishment of a malignant, Epstein-Barr-virus (EBV)-negative cell-line from the pleura effusion of a patient with Hodgkin’s disease. *Blut*, 38(2):185–190.
- Schatz, D. G. and Ji, Y. (2011). Recombination centres and the orchestration of V(D)J recombination. *Nature Reviews Immunology*, 11(4):251–263.
- Schlissel, M. S. (2003). Regulating antigen-receptor gene assembly. *Nature Reviews Immunology*, 3(11):890–899.
- Schmidt-Supprian, M., Bloch, W., Courtois, G., Addicks, K., Israel, A., Rajewsky, K., and Pasparakis, M. (2000). NEMO/IKK γ -deficient mice model incontinentia pigmenti. *Molecular Cell*, 5(6):981–992.
- Schmidt-Supprian, M., Wunderlich, F. T., and Rajewsky, K. (2007). Excision of the Frt-flanked neo (R) cassette from the CD19cre knock-in transgene reduces Cre-mediated recombination. *Transgenic Research*, 16(5):657–660.
- Schmitz, R., Hansmann, M. L., Bohle, V., Martin-Subero, J. I., Hartmann, S., Mechttersheimer, G., Klapper, W., Vater, I., Giefing, M., Gesk, S., Stanelle, J., Siebert, R., and Küppers, R. (2009). TNFAIP3 (A20) is a tumor suppressor gene in Hodgkin lymphoma and primary mediastinal B cell lymphoma. *Journal of Experimental Medicine*, 206(5):981–989.
- Schneider, C. A., Rasband, W. S., and Eliceiri, K. W. (2012). NIH Image to ImageJ: 25 years of image analysis. *Nature Methods*, 9(7):671–675.
- Scholzen, T. and Gerdes, J. (2000). The Ki-67 protein: From the known and the unknown. *Journal of Cellular Physiology*, 182(3):311–322.
- Schreiber, J., Jenner, R. G., Murray, H. L., Gerber, G. K., Gifford, D. K., and Young, R. A. (2006). Coordinated binding of NF- κ B family members in the response of human cells to lipopolysaccharide. *Proceedings of the National Academy of Sciences*, 103(15):5899–5904.
- Schreiber, R. D., Old, L. J., and Smyth, M. J. (2011). Cancer Immunoediting: Integrating Immunity’s Roles in Cancer Suppression and Promotion. *Science*, 331(6024):1565–1570.
- Schwickert, T. A., Alabyev, B., Manser, T., and Nussenzweig, M. C. (2009). Germinal center reutilization by newly activated B cells. *Journal of Experimental Medicine*, 206(13):2907–2914.
- Schwickert, T. A., Lindquist, R. L., Shakhar, G., Livshits, G., Skokos, D., Kosco-Vilbois, M. H., Dustin, M. L., and

- Nussenzweig, M. C. (2007). In vivo imaging of germinal centres reveals a dynamic open structure. *Nature*, 446(7131):83–87.
- Sciammas, R., Shaffer, A. L., Schatz, J. H., Zhao, H., Staudt, L. M., and Singh, H. (2006). Graded expression of interferon regulatory factor-4 coordinates isotype switching with plasma cell differentiation. *Immunity*, 25(2):225–236.
- Scofield, R. H. (2004). Autoantibodies as predictors of disease. *Lancet*, 363(9420):1544–1546.
- Seifert, M., Przekopowicz, M., Taudien, S., Lollies, A., Ronge, V., Drees, B., Lindemann, M., Hillen, U., Engler, H., Singer, B. B., and Küppers, R. (2015). Functional capacities of human IgM memory B cells in early inflammatory responses and secondary germinal center reactions. *Proceedings of the National Academy of Sciences*, 112(6):E546–55.
- Sen, R. and Baltimore, D. (1986a). Inducibility of κ immunoglobulin enhancer-binding protein NF- κ B by a posttranslational mechanism. *Cell*, 47(6):921–928.
- Sen, R. and Baltimore, D. (1986b). Multiple nuclear factors interact with the immunoglobulin enhancer sequences. *Cell*, 46(5):705–716.
- Sen, R. and Smale, S. T. (2010). Selectivity of the NF- κ B Response. *Cold Spring Harbor Perspectives in Biology*, 2(4):a000257–a000257.
- Senftleben, U., Cao, Y., Xiao, G., Greten, F. R., Krähn, G., Bonizzi, G., Chen, Y., Hu, Y., Fong, A., Sun, S.-C., and Karin, M. (2001). Activation by IKK α of a Second, Evolutionary Conserved, NF- κ B Signaling Pathway. *Science*, 293(5534):1495–1499.
- Shaffer, A. L., Lin, K.-I., Kuo, T. C., Yu, X., Hurt, E. M., Rosenwald, A., Giltneane, J. M., Yang, L., Zhao, H., Calame, K., and Staudt, L. M. (2002a). Blimp-1 orchestrates plasma cell differentiation by extinguishing the mature B cell gene expression program. *Immunity*, 17(1):51–62.
- Shaffer, A. L., Rosenwald, A., Hurt, E. M., Giltneane, J. M., Lam, L. T., Pickeral, O. K., and Staudt, L. M. (2001). Signatures of the immune response. *Immunity*, 15(3):375–385.
- Shaffer, A. L., Rosenwald, A., and Staudt, L. M. (2002b). Lymphoid malignancies: the dark side of B-cell differentiation. *Nature Reviews Immunology*, 2(12):920–932.
- Shaffer, A. L., Shapiro-Shelef, M., Iwakoshi, N. N., Lee, A.-H., Qian, S.-B., Zhao, H., Yu, X., Yang, L., Tan, B. K., Rosenwald, A., Hurt, E. M., Petroulakis, E., Sonenberg, N., Yewdell, J. W., Calame, K., Glimcher, L. H., and Staudt, L. M. (2004). XBP1, downstream of Blimp-1, expands the secretory apparatus and other organelles, and increases protein synthesis in plasma cell differentiation. *Immunity*, 21(1):81–93.
- Shapiro-Shelef, M. and Calame, K. (2005). Regulation of plasma-cell development. *Nature Reviews Immunology*, 5(3):230–242.
- Shapiro-Shelef, M., Lin, K.-I., McHeyzer-Williams, L. J., Liao, J., McHeyzer-Williams, M. G., and Calame, K. (2003). Blimp-1 is required for the formation of immunoglobulin secreting plasma cells and pre-plasma memory B cells. *Immunity*, 19(4):607–620.
- Shen, H. M., Peters, A., Baron, B., Zhu, X., and Storb, U. (1998). Mutation of BCL-6 gene in normal B cells by the process of somatic hypermutation of Ig genes. *Science*, 280(5370):1750–1752.
- Shi, W., Liao, Y., Willis, S. N., Taubenheim, N., Inouye, M., Tarlinton, D. M., Smyth, G. K., Hodgkin, P. D., Nutt, S. L., and Corcoran, L. M. (2015). Transcriptional profiling of mouse B cell terminal differentiation defines a signature for antibody-secreting plasma cells. *Nature Immunology*, 16(6):663–673.
- Shindo, H., Yasui, K., Yamamoto, K., Honma, K., Yui, K., Kohno, T., Ma, Y., Chua, K. J., Kubo, Y., Aihara, H., Ito, T., Nagayasu, T., Matsuyama, T., and Hayashi, H. (2011). Interferon regulatory factor-4 activates IL-2 and IL-4 promoters in cooperation with c-Rel. *Cytokine*, 56(3):564–572.
- Shinkai, Y., Rathbun, G., Lam, K. P., Oltz, E. M., Stewart, V., Mendelsohn, M., Charron, J., Datta, M., Young, F., and Stall, A. M. (1992). RAG-2-deficient mice lack mature lymphocytes owing to inability to initiate V(D)J rearrangement. *Cell*, 68(5):855–867.
- Shinkura, R., Ito, S., Begum, N. A., Nagaoka, H., Muramatsu, M., Kinoshita, K., Sakakibara, Y., Hijikata, H., and Honjo, T. (2004). Separate domains of AID are required for somatic hypermutation and class-switch recombination. *Nature Immunology*, 5(7):707–712.
- Shinners, N. P., Carlesso, G., Castro, I., Hoek, K. L., Corn, R. A., Woodland, R. T., Woodland, R. L., Scott, M. L., Wang, D., and Khan, W. N. (2007). Bruton’s tyrosine kinase mediates NF- κ B activation and B cell survival by B cell-activating factor receptor of the TNF-R family. *The Journal of Immunology*, 179(6):3872–3880.
- Shipp, M. A., Ross, K. N., Tamayo, P., Weng, A. P., Kutok, J. L., Aguiar, R. C. T., Gaasenbeek, M., Angelo, M., Reich, M., Pinkus, G. S., Ray, T. S., Koval, M. A., Last, K. W., Norton, A., Lister, T. A., Mesirov, J., Neuberg, D. S., Lander, E. S., Aster, J. C., and Golub, T. R. (2002). Diffuse large B-cell lymphoma outcome prediction by gene-expression profiling and supervised machine learning. *Nature Medicine*, 8(1):68–74.
- Shlomchik, M. J. (2008). Sites and stages of autoreactive B cell activation and regulation. *Immunity*, 28(1):18–28.
- Shlomchik, M. J. and Weisel, F. (2012). Germinal center selection and the development of memory B and plasma cells. *Immunological Reviews*, 247(1):52–63.
- Shono, Y., Tuckett, A. Z., Liou, H.-C., Doubrovina, E., Derenzini, E., Ouk, S., Tsai, J. J., Smith, O. M., Levy, E. R., Kreines, F. M., Ziegler, C. G. K., Scallion, M. I., Doubrovin, M., Heller, G., Younes, A., O’Reilly, R. J., van den Brink, M. R. M., and Zakrzewski, J. L. (2016). Characterization of a c-Rel Inhibitor That Mediates Anticancer Properties in Hematologic Malignancies by Blocking NF- κ B-Controlled Oxidative Stress Responses. *Cancer Research*, 76(2):377–389.

- Shono, Y., Tuckett, A. Z., Ouk, S., Liou, H.-C., Altan-Bonnet, G., Tsai, J. J., Oyler, J. E., Smith, O. M., West, M. L., Singer, N. V., Doubrovina, E., Pankov, D., Undhad, C. V., Murphy, G. F., Lezcano, C., Liu, C., O'Reilly, R. J., van den Brink, M. R. M., and Zakrzewski, J. L. (2014). A small-molecule c-Rel inhibitor reduces alloactivation of T cells without compromising antitumor activity. *Cancer Discovery*, 4(5):578–591.
- Shulman, Z., Gitlin, A. D., Targ, S., Jankovic, M., Pasqual, G., Nussenzweig, M. C., and Victora, G. D. (2013). T follicular helper cell dynamics in germinal centers. *Science*, 341:673–677.
- Shulman, Z., Gitlin, A. D., Weinstein, J. S., Lainez, B., Esplugues, E., Flavell, R. A., Craft, J. E., and Nussenzweig, M. C. (2014). Dynamic signaling by T follicular helper cells during germinal center B cell selection. *Science*, 345(6200):1058–1062.
- Siebelt, F., Berberich, I., Shu, G., Serfling, E., and Clark, E. A. (1997). Role for CD40-mediated activation of c-Rel and maintenance of c-myc RNA levels in mitigating anti-IgM-induced growth arrest. *Cellular Immunology*, 181(1):13–22.
- Siebenlist, U., Brown, K., and Claudio, E. (2005). Control of lymphocyte development by nuclear factor- κ B. *Nature Reviews Immunology*, 5(6):435–445.
- Siggers, T., Chang, A. B., Teixeira, A., Wong, D., Williams, K. J., Ahmed, B., Ragoussis, J., Udalova, I. A., Smale, S. T., and Bulyk, M. L. (2012). Principles of dimer-specific gene regulation revealed by a comprehensive characterization of NF- κ B family DNA binding. *Nature Immunology*, 13(1):95–102.
- Singh, H., Medina, K. L., and Pongubala, J. M. R. (2005). Contingent gene regulatory networks and B cell fate specification. *Proceedings of the National Academy of Sciences*, 102(14):4949–4953.
- Smale, S. T. (2011). Hierarchies of NF- κ B target-gene regulation. *Nature Immunology*, 12(8):689–694.
- Snapper, C. M., Rosas, F. R., Zelazowski, P., Moorman, M. A., Kehry, M. R., Bravo, R., and Weih, F. (1996a). B cells lacking RelB are defective in proliferative responses, but undergo normal B cell maturation to Ig secretion and Ig class switching. *The Journal of Experimental Medicine*, 184(4):1537–1541.
- Snapper, C. M., Zelazowski, P., Rosas, F. R., Kehry, M. R., Tian, M., Baltimore, D., and Sha, W. C. (1996b). B cells from p50/NF- κ B knockout mice have selective defects in proliferation, differentiation, germ-line C_H transcription, and Ig class switching. *The Journal of Immunology*, 156(1):183–191.
- Srinivasan, L., Sasaki, Y., Calado, D. P., Zhang, B., Paik, J. H., DePinho, R. A., Kutok, J. L., Kearney, J. F., Otipoby, K. L., and Rajewsky, K. (2009). PI3 kinase signals BCR-dependent mature B cell survival. *Cell*, 139(3):573–586.
- Stadanlick, J. E. and Cancro, M. P. (2008). BAFF and the plasticity of peripheral B cell tolerance. *Current Opinion in Immunology*, 20(2):158–161.
- Starczynowski, D. T., Reynolds, J. G., and Gilmore, T. D. (2003). Deletion of either C-terminal transactivation subdomain enhances the in vitro transforming activity of human transcription factor REL in chicken spleen cells. *Oncogene*, 22(44):6928–6936.
- Starczynowski, D. T., Reynolds, J. G., and Gilmore, T. D. (2005). Mutations of tumor necrosis factor α -responsive serine residues within the C-terminal transactivation domain of human transcription factor REL enhance its in vitro transforming ability. *Oncogene*, 24(49):7355–7368.
- Starczynowski, D. T., Trautmann, H., Pott, C., Harder, L., Arnold, N., Africa, J. A., Leeman, J. R., Siebert, R., and Gilmore, T. D. (2007). Mutation of an IKK phosphorylation site within the transactivation domain of REL in two patients with B-cell lymphoma enhances REL's in vitro transforming activity. *Oncogene*, 26(19):2685–2694.
- Stasik, C. J., Nitta, H., Zhang, W., Mosher, C. H., Cook, J. R., Tubbs, R. R., Unger, J. M., Brooks, T. A., Persky, D. O., Wilkinson, S. T., Grogan, T. M., and Rimsza, L. M. (2010). Increased MYC gene copy number correlates with increased mRNA levels in diffuse large B-cell lymphoma. *Haematologica*, 95(4):597–603.
- Staudt, L. M. (2010). Oncogenic Activation of NF- κ B. *Cold Spring Harbor Perspectives in Biology*, 2(6):a000109–a000109.
- Stavnezer, J., Guikema, J. E. J., and Schrader, C. E. (2008). Mechanism and regulation of class switch recombination. *Annual Review of Immunology*, 26:261–292.
- Steidl, C., Telenius, A., Shah, S. P., Farinha, P., Barclay, L., Boyle, M., Connors, J. M., Horsman, D. E., and Gascoyne, R. D. (2010). Genome-wide copy number analysis of Hodgkin Reed-Sternberg cells identifies recurrent imbalances with correlations to treatment outcome. *Blood*, 116(3):418–427.
- Steward, R. (1987). Dorsal, an embryonic polarity gene in Drosophila, is homologous to the vertebrate proto-oncogene, c-rel. *Science*, 238(4827):692–694.
- Strange, A., Capon, F., Spencer, C. C. A., Knight, J., Weale, M. E., Allen, M. H., Barton, A., Band, G., Bellenguez, C., Bergboer, J. G. M., Blackwell, J. M., Bramon, E., Bumpstead, S. J., Casas, J. P., Cork, M. J., Corvin, A., Deloukas, P., Diltthey, A., Duncanson, A., Edkins, S., Estivill, X., Fitzgerald, O., Freeman, C., Giardina, E., Gray, E., Hofer, A., Hüffmeier, U., Hunt, S. E., Irvine, A. D., Jankowski, J., Kirby, B., Langford, C., Lascorz, J., Leman, J., Leslie, S., Mallbris, L., Markus, H. S., Mathew, C. G., McLean, W. H. I., McManus, R., Mössner, R., Moutsianas, L., Naluai, A. T., Nestle, F. O., Novelli, G., Onoufriadis, A., Palmer, C. N. A., Perricone, C., Pirinen, M., Plomin, R., Potter, S. C., Pujol, R. M., Rautanen, A., Riveira-Munoz, E., Ryan, A. W., Salmhofer, W., Samuelsson, L., Sawcer, S. J., Schalkwijk, J., Smith, C. H., Stähle, M., Su, Z., Tazi-Ahnini, R., Traupe, H., Viswanathan, A. C., Warren, R. B., Weger, W., Wolk, K., Wood, N., Worthington, J., Young, H. S., Zeeuwen, P. L. J. M., Hayday, A., Burden, A. D., Griffiths, C. E. M., Kere, J., Reis, A., McVean, G., Evans, D. M., Brown, M. A., Barker, J. N., Peltonen, L., Donnelly, P., Trembath, R. C., and Genetic Analysis of Psoriasis Consortium & the Wellcome Trust Case Control Consortium 2 (2010). A genome-wide association study identifies new psoriasis susceptibility loci and an interaction between HLA-C and ERAP1. *Nature Genetics*, 42(11):985–990.

- Strasser, A. (2005). The role of BH3-only proteins in the immune system. *Nature Reviews Immunology*, 5(3):189–200.
- Suzuki, H., Terauchi, Y., Fujiwara, M., Aizawa, S., Yazaki, Y., Kadowaki, T., and Koyasu, S. (1999). Xid-Like Immunodeficiency in Mice with Disruption of the p85 α Subunit of Phosphoinositide 3-Kinase. *Science*, 283(5400):390–392.
- Suzuki, K., Grigorova, I., Phan, T. G., Kelly, L. M., and Cyster, J. G. (2009). Visualizing B cell capture of cognate antigen from follicular dendritic cells. *Journal of Experimental Medicine*, 206(7):1485–1493.
- Szymczak, A. L., Workman, C. J., Wang, Y., Vignali, K. M., Dilioglou, S., Vanin, E. F., and Vignali, D. A. A. (2004). Correction of multi-gene deficiency in vivo using a single 'self-cleaving' 2A peptide-based retroviral vector. *Nature Biotechnology*, 22(5):589–594.
- Ta, V.-T., Nagaoka, H., Catalan, N., Durandy, A., Fischer, A., Imai, K., Nonoyama, S., Tashiro, J., Ikegawa, M., Ito, S., Kinoshita, K., Muramatsu, M., and Honjo, T. (2003). AID mutant analyses indicate requirement for class-switch-specific cofactors. *Nature Immunology*, 4(9):843–848.
- Tagawa, H. and Seto, M. (2005). A microRNA cluster as a target of genomic amplification in malignant lymphoma. *Leukemia*, 19(11):2013–2016.
- Tagawa, H., Suguro, M., Tsuzuki, S., Matsuo, K., Karnan, S., Ohshima, K., Okamoto, M., Morishima, Y., Nakamura, S., and Seto, M. (2005). Comparison of genome profiles for identification of distinct subgroups of diffuse large B-cell lymphoma. *Blood*, 106(5):1770–1777.
- Tam, W. F., Wang, W., and Sen, R. (2001). Cell-specific association and shuttling of I κ B α provides a mechanism for nuclear NF- κ B in B lymphocytes. *Molecular and Cellular Biology*, 21(14):4837–4846.
- Tan, J. B., Xu, K., Cretegnny, K., Visan, I., Yuan, J. S., Egan, S. E., and Guidos, C. J. (2009). Lunatic and manic fringe cooperatively enhance marginal zone B cell precursor competition for delta-like 1 in splenic endothelial niches. *Immunity*, 30(2):254–263.
- Tas, J. M. J., Mesin, L., Pasqual, G., Targ, S., Jacobsen, J. T., Mano, Y. M., Chen, C. S., Weill, J.-C., Reynaud, C.-A., Browne, E. P., Meyer-Hermann, M., and Victora, G. D. (2016). Visualizing antibody affinity maturation in germinal centers. *Science*, 351(6277):1048–1054.
- Tellier, J., Shi, W., Minnich, M., Liao, Y., Crawford, S., Smyth, G. K., Kallies, A., Busslinger, M., and Nutt, S. L. (2016). Blimp-1 controls plasma cell function through the regulation of immunoglobulin secretion and the unfolded protein response. *Nature Immunology*, 17(3):323–330.
- Teng, G. and Papavasiliou, F. N. (2007). Immunoglobulin somatic hypermutation. *Annual Review of Genetics*, 41:107–120.
- Tian, W. and Liou, H.-C. (2009). RNAi-Mediated c-Rel Silencing Leads to Apoptosis of B Cell Tumor Cells and Suppresses Antigenic Immune Response In Vivo. *PLoS ONE*, 4(4):e5028.
- Todd, D. J., McHeyzer-Williams, L. J., Kowal, C., Lee, A.-H., Volpe, B. T., Diamond, B., McHeyzer-Williams, M. G., and Glimcher, L. H. (2009). XBP1 governs late events in plasma cell differentiation and is not required for antigen-specific memory B cell development. *Journal of Experimental Medicine*, 206(10):2151–2159.
- Tonegawa, S. (1983). Somatic generation of antibody diversity. *Nature*, 302(5909):575–581.
- Trynka, G., Zhernakova, A., Romanos, J., Franke, L., Hunt, K. A., Turner, G., Bruinenberg, M., Heap, G. A., Platteel, M., Ryan, A. W., de Kovel, C., Holmes, G. K. T., Howdle, P. D., Walters, J. R. F., Sanders, D. S., Mulder, C. J. J., Mearin, M. L., Verbeek, W. H. M., Trimble, V., Stevens, F. M., Kelleher, D., Barisani, D., Bardella, M. T., McManus, R., van Heel, D. A., and Wijmenga, C. (2009). Coeliac disease-associated risk variants in TNFAIP3 and REL implicate altered NF- κ B signalling. *Gut*, 58(8):1078–1083.
- Tumang, J. R., Hsia, C. Y., Tian, W., Bromberg, J. F., and Liou, H.-C. (2002). IL-6 rescues the hyporesponsiveness of c-Rel deficient B cells independent of Bcl-xL, Mcl-1, and Bcl-2. *Cellular Immunology*, 217(1-2):47–57.
- Tumang, J. R., Owyang, A., Andjelic, S., Jin, Z., Hardy, R. R., Liou, M. L., and Liou, H. C. (1998). c-Rel is essential for B lymphocyte survival and cell cycle progression. *European Journal of Immunology*, 28(12):4299–4312.
- Uehata, T., Iwasaki, H., Vandenbon, A., Matsushita, K., Hernandez-Cuellar, E., Kuniyoshi, K., Satoh, T., Mino, T., Suzuki, Y., Standley, D. M., Tsujimura, T., Rakugi, H., Isaka, Y., Takeuchi, O., and Akira, S. (2013). Malt1-Induced Cleavage of Regnase-1 in CD4. *Cell*, 153(5):1036–1049.
- Urbánek, P., Wang, Z. Q., Fetka, I., and Wagner, E. F. (1994). Complete block of early B cell differentiation and altered patterning of the posterior midbrain in mice lacking Pax5BSAP. *Cell*, 79(5):901–912.
- Vallabhapurapu, S. and Karin, M. (2009). Regulation and Function of NF- κ B Transcription Factors in the Immune System. *Annual Review of Immunology*, 27(1):693–733.
- van Essen, D., Zhu, Y., and Saccani, S. (2010). A Feed-Forward Circuit Controlling Inducible NF- κ B Target Gene Activation by Promoter Histone Demethylation. *Molecular Cell*, 39(5):750–760.
- Vereecke, L., Beyaert, R., and van Loo, G. (2009). The ubiquitin-editing enzyme A20 (TNFAIP3) is a central regulator of immunopathology. *Trends in Immunology*, 30(8):383–391.
- Victora, G. D. (2014). SnapShot: the germinal center reaction. *Cell*, 159(3):700–700.e1.
- Victora, G. D., Dominguez-Sola, D., Holmes, A. B., Deroubaix, S., Dalla-Favera, R., and Nussenzweig, M. C. (2012). Identification of human germinal center light and dark zone cells and their relationship to human B-cell lymphomas. *Blood*, 120(11):2240–2248.
- Victora, G. D. and Nussenzweig, M. C. (2012). Germinal Centers. *Annual Review of Immunology*, 30(1):429–457.

- Victora, G. D., Schwickert, T. A., Fooksman, D. R., Kamphorst, A. O., Meyer-Hermann, M., Dustin, M. L., and Nussenzweig, M. C. (2010). Germinal center dynamics revealed by multiphoton microscopy with a photoactivatable fluorescent reporter. *Cell*, 143(4):592–605.
- Vinuesa, C. G., Linterman, M. A., Goodnow, C. C., and Randall, K. L. (2010). T cells and follicular dendritic cells in germinal center B-cell formation and selection. *Immunological Reviews*, 237(1):72–89.
- Vinuesa, C. G., Linterman, M. A., Yu, D., and MacLennan, I. C. M. (2016). Follicular Helper T Cells. *Annual Review of Immunology*, 34:335–368.
- Vinuesa, C. G., Sanz, I., and Cook, M. C. (2009). Dysregulation of germinal centres in autoimmune disease. *Nature Reviews Immunology*, 9(12):845–857.
- Visekruna, A., Linnerz, T., Martinic, V., Vachharajani, N., Hartmann, S., Harb, H., Joeris, T., Pfefferle, P. I., Hofer, M. J., and Steinhoff, U. (2015). Transcription factor c-Rel plays a crucial role in driving anti-CD40-mediated innate colitis. *Mucosal immunology*, 8(2):307–315.
- Viswanathan, M., Yu, M., Mendoza, L., and Yunis, J. J. (1996). Cloning and transcription factor-binding sites of the human c-rel proto-oncogene promoter. *Gene*, 170(2):271–276.
- Von Behring, E. and Kitasato, S. (1890). The mechanism of immunity in animals to diphteria and tetanus (Ueber das Zustandekommen der Diphtherie-Immunität und der Tetanus-Immunität bei Thieren). *Deutsche Medizinische Wochenschrift*, 16:1113–1114.
- Wang, X., Cho, B., Suzuki, K., Xu, Y., Green, J. A., An, J., and Cyster, J. G. (2011). Follicular dendritic cells help establish follicle identity and promote B cell retention in germinal centers. *Journal of Experimental Medicine*, 208(12):2497–2510.
- Wang, Y., Rickman, B. H., Poutahidis, T., Schlieper, K., Jackson, E. A., Erdman, S. E., Fox, J. G., and Horwitz, B. H. (2008). c-Rel is essential for the development of innate and T cell-induced colitis. *The Journal of Immunology*, 180(12):8118–8125.
- Wardemann, H., Yurasov, S., Schaefer, A., Young, J. W., Meffre, E., and Nussenzweig, M. C. (2003). Predominant autoantibody production by early human B cell precursors. *Science*, 301(5638):1374–1377.
- Wei, L., Fan, M., Xu, L., Heinrich, K., Berry, M. W., Homayouni, R., and Pfeffer, L. M. (2008). Bioinformatic Analysis Reveals cRel as a Regulator of a Subset of Interferon-Stimulated Genes. *Journal of Interferon & Cytokine Research*, 28(9):541–552.
- Weih, D. S., Yilmaz, Z. B., and Weih, F. (2001). Essential role of RelB in germinal center and marginal zone formation and proper expression of homing chemokines. *The Journal of Immunology*, 167(4):1909–1919.
- Weisel, F. J., Zuccarino-Catania, G. V., Chikina, M., and Shlomchik, M. J. (2016). A Temporal Switch in the Germinal Center Determines Differential Output of Memory B and Plasma Cells. *Immunity*, 44(1):116–130.
- Weniger, M. A., Gesk, S., Ehrlich, S., Martin-Subero, J. I., Dyer, M. J. S., Siebert, R., Möller, P., and Barth, T. F. E. (2007). Gains of REL in primary mediastinal B-cell lymphoma coincide with nuclear accumulation of REL protein. *Genes, Chromosomes and Cancer*, 46(4):406–415.
- Weniger, M. A., Melzner, I., Menz, C. K., Wegener, S., Bucur, A. J., Dorsch, K., Mattfeldt, T., Barth, T. F. E., and Moller, P. (2006a). Mutations of the tumor suppressor gene SOCS-1 in classical Hodgkin lymphoma are frequent and associated with nuclear phospho-STAT5 accumulation. *Oncogene*, 25(18):2679–2684.
- Weniger, M. A., Pulford, K., Gesk, S., Ehrlich, S., Banham, A. H., Lyne, L., Martin-Subero, J. I., Siebert, R., Dyer, M. J. S., Moller, P., and Barth, T. F. E. (2006b). Gains of the proto-oncogene BCL11A and nuclear accumulation of BCL11AXL protein are frequent in primary mediastinal B-cell lymphoma. *Leukemia*, 20(10):1880–1882.
- Wertz, I. E. and Dixit, V. M. (2010). Signaling to NF- κ B: regulation by ubiquitination. *Cold Spring Harbor Perspectives in Biology*, 2(3):a003350.
- Wessendorf, S., Barth, T. F. E., Viardot, A., Mueller, A., Kestler, H. A., Kohlhammer, H., Lichter, P., Bentz, M., Döhner, H., Moller, P., and Schwaenen, C. (2007). Further delineation of chromosomal consensus regions in primary mediastinal B-cell lymphomas: an analysis of 37 tumor samples using high-resolution genomic profiling (array-CGH). *Leukemia*, 21(12):2463–2469.
- Wilhelmsen, K. C., Eggleton, K., and Temin, H. M. (1984). Nucleic acid sequences of the oncogene v-rel in reticuloendotheliosis virus strain T and its cellular homolog, the proto-oncogene c-rel. *Journal of Virology*, 52(1):172–182.
- Wilhelmsen, K. C. and Temin, H. M. (1984). Structure and dimorphism of c-rel (turkey), the cellular homolog to the oncogene of reticuloendotheliosis virus strain T. *Journal of Virology*, 49(2):521–529.
- Wilson, A. and Trumpp, A. (2006). Bone-marrow haematopoietic-stem-cell niches. *Nature Reviews Immunology*, 6(2):93–106.
- Wright, G., Tan, B., Rosenwald, A., Hurt, E. H., Wiestner, A., and Staudt, L. M. (2003). A gene expression-based method to diagnose clinically distinct subgroups of diffuse large B cell lymphoma. *Proceedings of the National Academy of Sciences*, 100(17):9991–9996.
- Wuerzberger-Davis, S. M., Chen, Y., Yang, D. T., Kearns, J. D., Bates, P. W., Lynch, C., Ladell, N. C., Yu, M., Podd, A., Zeng, H., Huang, T. T., Wen, R., Hoffmann, A., Wang, D., and Miyamoto, S. (2011). Nuclear export of the NF- κ B inhibitor I κ B α is required for proper B cell and secondary lymphoid tissue formation. *Immunity*, 34(2):188–200.
- Xiao, C., Srinivasan, L., Calado, D. P., Patterson, H. C., Zhang, B., Wang, J., Henderson, J. M., Kutok, J. L., and Rajewsky, K. (2008). Lymphoproliferative disease and autoimmunity in mice with increased miR-17-92 expression in lymphocytes. *Nature Immunology*, 9(4):405–414.

- Xiao, Q., Shen, N., Hedvat, C. V., Moskowitz, C. H., Sussman, L. K., Filippa, D. A., Zelenetz, A. D., Houldsworth, J., Chaganti, R. S. K., and Teruya-Feldstein, J. (2004). Differential expression patterns of c-REL protein in classic and nodular lymphocyte predominant Hodgkin lymphoma. *Applied Immunohistochemistry & Molecular Morphology*, 12(3):211–215.
- Xu, H., Chaudhri, V. K., Wu, Z., Biliouris, K., Dienger-Stambaugh, K., Rochman, Y., and Singh, H. (2015). Regulation of bifurcating B cell trajectories by mutual antagonism between transcription factors IRF4 and IRF8. *Nature Immunology*, 16(12):1274–1281.
- Xu, J., Foy, T. M., Laman, J. D., Elliott, E. A., Dunn, J. J., Waldschmidt, T. J., Elsemore, J., Noelle, R. J., and Flavell, R. A. (1994). Mice deficient for the CD40 ligand. *Immunity*, 1(5):423–431.
- Xu, X., Prorock, C., Ishikawa, H., Maldonado, E., Ito, Y., and Gelinis, C. (1993). Functional interaction of the v-Rel and c-Rel oncoproteins with the TATA-binding protein and association with transcription factor IIB. *Molecular and Cellular Biology*, 13(11):6733–6741.
- Xu, Z., Zan, H., Pone, E. J., Mai, T., and Casali, P. (2012). Immunoglobulin class-switch DNA recombination: induction, targeting and beyond. *Nature Reviews Immunology*, 12(7):517–531.
- Yamada, T., Mitani, T., Yorita, K., Uchida, D., Matsushima, A., Iwamasa, K., Fujita, S., and Matsumoto, M. (2000). Abnormal Immune Function of Hemopoietic Cells from Alymphoplasia (aly) Mice, a Natural Strain with Mutant NF- κ B-Inducing Kinase. *The Journal of Immunology*, 165(2):804–812.
- Yamamoto, M., Horie, R., Takeiri, M., Kozawa, I., and Umezawa, K. (2008). Inactivation of NF- κ B components by covalent binding of (-)-dehydroxymethylepoxyquinomicin to specific cysteine residues. *Journal of Medicinal Chemistry*, 51(18):5780–5788.
- Yamazaki, T. and Kurosaki, T. (2003). Contribution of BCAP to maintenance of mature B cells through c-Rel. *Nature Immunology*, 4(8):780–786.
- Yang, H., Thomas, D., Boffa, D. J., Ding, R., Li, B., Muthukumar, T., Sharma, V. K., Lagman, M., Luo, G.-X., Kapur, S., Liou, H.-C., Hancock, W. W., and Suthanthiran, M. (2002). Enforced c-REL deficiency prolongs survival of islet allografts. *Transplantation*, 74(3):291–298.
- Yeo, A. T., Chennamadhavuni, S., Whitty, A., Porco, J. A., and Gilmore, T. D. (2015). Inhibition of Oncogenic Transcription Factor REL by the Natural Product Derivative Calafianin Monomer 101 Induces Proliferation Arrest and Apoptosis in Human B-Lymphoma Cell Lines. *Molecules*, 20(5):7474–7494.
- Yu, Y., Wang, D., Kaosaard, K., Liu, C., Fu, J., Haarberg, K., Anasetti, C., Beg, A. A., and Yu, X.-Z. (2013). c-Rel is an essential transcription factor for the development of acute graft-versus-host disease in mice. *European Journal of Immunology*, 43(9):2327–2337.
- Yusa, K., Zhou, L., Li, M. A., Bradley, A., and Craig, N. L. (2011). A hyperactive piggyBac transposase for mammalian applications. *Proceedings of the National Academy of Sciences*, 108(4):1531–1536.
- Zarnegar, B., He, J. Q., Oganessian, G., Hoffmann, A., Baltimore, D., and Cheng, G. (2004). Unique CD40-mediated biological program in B cell activation requires both type 1 and type 2 NF- κ B activation pathways. *Proceedings of the National Academy of Sciences*, 101(21):8108–8113.
- Zelazowski, P., Carrasco, D., Rosas, F. R., Moorman, M. A., Bravo, R., and Snapper, C. M. (1997). B cells genetically deficient in the c-Rel transactivation domain have selective defects in germline C_H transcription and Ig class switching. *The Journal of Immunology*, 159(7):3133–3139.
- Zelazowski, P., Shen, Y., and Snapper, C. M. (2000). NF- κ B/p50 and NF- κ B/c-Rel differentially regulate the activity of the 3'αE-hsl,2 enhancer in normal murine B cells in an activation-dependent manner. *International Immunology*, 12(8):1167–1172.
- Zhang, B., Kracker, S., Yasuda, T., Casola, S., Vanneman, M., Hömig-Hölzel, C., Wang, Z., Derudder, E., Li, S., Chakraborty, T., Cotter, S. E., Koyama, S., Currie, T., Freeman, G. J., Kutok, J. L., Rodig, S. J., Dranoff, G., and Rajewsky, K. (2012). Immune Surveillance and Therapy of Lymphomas Driven by Epstein-Barr Virus Protein LMP1 in a Mouse Model. *Cell*, 148(4):739–751.
- Zhang, Y., Meyer-Hermann, M., George, L. A., Figge, M. T., Khan, M., Goodall, M., Young, S. P., Reynolds, A., Falciani, F., Waisman, A., Notley, C. A., Ehrenstein, M. R., Kosco-Vilbois, M., and Toellner, K.-M. (2013). Germinal center B cells govern their own fate via antibody feedback. *Journal of Experimental Medicine*, 210(3):457–464.
- Zhao, B., Barrera, L. A., Ersing, I., Willox, B., Schmidt, S. C. S., Greenfield, H., Zhou, H., Mollo, S. B., Shi, T. T., Takasaki, K., Jiang, S., Cahir-McFarland, E., Kellis, M., Bulyk, M. L., Kieff, E., and Gewurz, B. E. (2014). The NF- κ B genomic landscape in lymphoblastoid B cells. *Cell Reports*, 8(5):1595–1606.
- Zheng, Y., Josefowicz, S., Chaudhry, A., Peng, X. P., Forbush, K., and Rudensky, A. Y. (2010). Role of conserved non-coding DNA elements in the Foxp3 gene in regulatory T-cell fate. *Nature*, 463(7282):808–812.
- Zhuang, Y., Soriano, P., and Weintraub, H. (1994). The helix-loop-helix gene E2A is required for B cell formation. *Cell*, 79(5):875–884.
- Zotos, D. and Tarlinton, D. M. (2012). Determining germinal centre B cell fate. *Trends in Immunology*, 33(6):281–288.
- Zuber, J., McJunkin, K., Fellmann, C., Dow, L. E., Taylor, M. J., Hannon, G. J., and Lowe, S. W. (2010). Toolkit for evaluating genes required for proliferation and survival using tetracycline-regulated RNAi. *Nature Biotechnology*, 29(1):79–83.

Abbreviations

aa	amino acid
ABC-DLBCL	activated B cell-like DLBCL
aCGH	array-based CGH
AID	activation-induced cytidine deaminase
ANA	anti-nuclear antibodies
APE	apurinic/aprimidinic endonucleases
APRIL	a proliferation inducing ligand
ATLL	adult T-cell leukemia/lymphoma
BAC	bacterial artificial chromosome
BACH2	BTB and CNC homolog 2
BAFF	B cell-activating factor belonging to TNF family
BATF	basic leucine zipper transcription factor ATF-like
BCAP	B cell adaptor for PI3K
Bcl-2A1	prosurvival Bcl-2 family member A1
Bcl-6	B cell lymphoma 6
BCMA	B cell maturation antigen
BCR	B cell receptor
BER	base excision repair
Bim	Bcl-2 interacting mediator of cell death
Blimp-1	B lymphocyte-induced maturation protein 1
BM	bone marrow
B-NHL	B cell non-Hodgkin lymphomas
Btk	Bruton's tyrosine kinase
Ca²⁺	calcium ion
CAG	CMV early enhancer/chicken β actin promoter
CAR	coxsackie/adenovirus receptor
CARD	caspase activation and recruitment domain
CARMA1	CARD-containing membrane-associated guanylate kinase-1
CD40L	CD40 ligand
CDK	cyclin-dependent kinase
CGH	comparative genomic hybridization
cHL	classical Hodgkin lymphoma
cIAP	cellular inhibitor of apoptosis
CMV	cytomegalovirus
c-Myc	myelocytomatosis oncogene cellular homolog
CNS	conserved non-coding DNA sequences
c-Rel	cellular v-Rel avian reticuloendotheliosis viral oncogene homolog
c-RelΔEx9	c-Rel splice variant devoid of Exon 9
CSR	class switch recombination
CXCL12	CXC-chemokine ligand 12
CXCR4	CXC-chemokine receptor 4
DHMEQ	dehydroxymethylepoxyquinomicin
DL1	Delta-like-1
DLBCL	diffuse large B cell lymphoma
DNA	deoxyribonucleic acid
DNA-PK	DNA-dependent protein kinase

DSB double strand breaks
DTT dithiothreitol
DZ dark zone
EAE experimental autoimmune encephalomyelitis
EBF early B cell factor
EF (cell) embryonic feeder (cell)
ELISA enzyme-linked immunosorbent assay
ES (cell) embryonic stem (cell)
ETS E twenty-six
Exo1 exonuclease 1
Ezh2 enhancer of zeste homolog 2
FDC follicular dendritic cells
FICTION fluorescence immunophenotyping and interphase cytogenetics as a tool for investigation of neoplasms
FISH fluorescence *in situ* hybridization
FL follicular lymphoma
Flp flippase
FLT3L FMS-like tyrosine kinase 3 ligand
FO follicular
FOXO1 forkhead box O1
FoxP3 forkhead box P3
Frt flippase recognition target
FSC-A/H forward scatter area/height
galK galactokinase
GC germinal center
GCB germinal center B cell
GCB-DLBCL germinal center B cell-like DLBCL
GFP green fluorescent protein
GVHD graft-versus-host disease
GM-CSF granulocyte macrophage colony-stimulating factor
GWAS genome-wide association study
H₂O_{dd} double-distilled water
H3K9 lysine 9 on histone H3
HoxC4 homeobox C4
HRP horseradish peroxidase
HRS Hodgkin and Reed-Sternberg
hyPB hyperactive piggyBac
ICOS inducible T cell co-stimulator
IFN γ interferon- γ
Ig immunoglobulin
IgH immunoglobulin heavy
IgL immunoglobulin light
I κ B inhibitor of κ B
IKK I κ B kinase
IL-7 interleukin-7
IMQ imiquimod
ITR inverted terminal repeat
i.p. intraperitoneal
IR infrared
IRES internal ribosomal entry site
IRF4 interferon regulatory factor 4
JAK2 Janus kinase 2

K48 lysine-48
LB lysogeny broth
LIF leukemia inhibitory factor
LN lymph nodes
LPS lipopolysaccharide
LZ light zone
MALT1 mucosa-associated lymphoid tissue protein 1
MEF mouse embryonic fibroblasts
MFI median fluorescence intensity
MHC-II major histocompatibility complex class II
miRNA microRNA
MLN mesenteric lymph nodes
MMC mitomycin C
MMR mismatch repair
MSH MutS protein homolog
MZ marginal zone
MZP marginal zone precursor
NEAA non-essential amino acids
NEMO NF- κ B essential modulator
NES nuclear export signal
NFAT nuclear factor of activated T cells
NF- κ B nuclear factor κ -light-chain-enhancer of activated B cells
NHEJ non-homologous end joining
NIK NF- κ B-inducing kinase
NLPHL nodular lymphocyte predominant Hodgkin lymphoma
NLS nuclear localization signal
NP-KLH 4-hydroxy-3-nitrophenyl acetyl-keyhole limpet hemocyanin
Oct octamer
O-GlcNAcylation O-linked β -N-acetyl-glucosamine
Pax5 paired box protein 5
PB plasmablast
PC plasma cell
PCR polymerase chain reaction
PD-1 programmed cell death 1
Peli1 Pellino E3 ubiquitin protein ligase 1
PerC peritoneal cavity
PGK phosphoglycerate kinase
PI3K phosphatidylinositol 3-kinase
Pin1 Peptidyl-prolyl cis/trans isomerase, NIMA interacting
PKA protein kinase A
PMBCL primary mediastinal B cell lymphoma
PMSF phenylmethanesulfonylfluorid
PNA peanut agglutinin
PP Peyer's patches
PTCL NOS peripheral T cell lymphoma, not otherwise specified
PVDF polyvinylidene fluoride
RAG recombination activation gene
RANKL receptor activator of nuclear factor- κ B ligand
Rb retinoblastoma protein
RBC red blood cell

Rev-T reticuloendotheliosis virus strain T
RF rheumatoid factor
RHD Rel homology domain
RNase A ribonuclease A
RID Rel inhibitory domain
RNA ribonucleic acid
ROR γ t retinoic acid-related orphan receptor γ t
rtTA reverse tetracycline transactivator
S switch
sb100x sleeping beauty 100x
SCF stem-cell factor
SDS-PAGE sodium dodecyl sulfate polyacrylamide gel electrophoresis
SHM somatic hypermutation
shRNA short hairpin RNA
siRNA small interfering RNA
SNP single nucleotide polymorphism
SOCS1 suppressor of cytokine signaling 1
SPL spleen
SRBC sheep red blood cells
SSB single strand breaks
SSC-A/H side scatter area/height
STAT signal transducer and activator of transcription
TACI transmembrane activator and calcium-modulating cyclophilin-ligand interactor
TAD transactivation domain
TBK1 TNFR-associated factor family member-associated NF- κ B activator (TANK)-binding kinase 1
TBP TATA-box-binding protein
TCR T cell receptor
TD T cell-dependent or thymus-dependent
tetO tet operator
tetR tetracycline repressor
T_{fh} follicular helper T cell
TFIIB transcription factor II B
TGF β transforming growth factor- β
TH thymus
THRLBCL T cell/histiocyte rich large B cell lymphoma
TI T cell-independent or thymus-independent
TLR toll-like receptor
TNF(R) tumor necrosis factor (receptor)
TRAF2 TNFR-associated factor 2
TRE tetracycline-responsive element
T_{reg} regulatory T cell
UNG uracil DNA glycosylase
UPR unfolded protein response
VLA4 very late antigen 4
XBP-1 X-box-binding protein 1
XRCC4 X-ray repair cross complementing protein 4
zVAD-fmk carbobenzoxy-valyl-alanyl-aspartyl-(O-methyl) fluoromethylketone
7-AAD 7-amino-actinomycin D
-/- homozygous knockout
-/+ heterozygous knockout
I/+ heterozygous insertion

Acknowledgements

First and foremost I would like to thank Marc Schmidt-Supprian. I am especially impressed by his incredible way of scientific thinking which caught me immediately when I first introduced myself as a PhD candidate and I am still grateful that I could join his laboratory. Ever since I have learned incredibly much from him and greatly value his brilliant ideas, exceptional support and encouraging mentoring.

I would like to thank my *Doktorvater* Matthias Mann for his continuous interest, advice and support. He always provided great input from a different perspective on my project. I also want to thank Daniel Krappmann for his helpful comments and input during my thesis advisory committee meetings and for being a member of my thesis committee. Furthermore, I thank PD Dr. Dietmar Martin, Prof. Dr. Olivia Merkel and Prof. Dr. Veit Hornung for taking the time to review my thesis and being members of my thesis committee.

I am greatly thankful to the former and current members of the Schmidt-Supprian laboratory. During the years of my PhD, I experienced more than countless scientific discussions, helpful suggestions and pleasant hours at the bench as this journey also contributed to building up many great memories and lasting friendship.

I thank Dilip Kumar who started the first steps of the c-Rel project in the Schmidt-Supprian laboratory, Arianna Bertossi and Paola Sansonetti who accompanied me during the first year of my PhD, Basma Abdel Motaal and Mayra Lorenz as well as Carina Steinecke and Sabrina Bortoluzzi who brought new spirit to the lab. I thank Tim Ammon for having an eye for things that need to be organized and for his sense of humor, Christoph Vahl for his helpfulness with regard to experiments and beyond the lab as well as his encouragement and positive way of thinking, Christoph Drees for being a great successor of Wal by likewise bringing along his positive point of view, Klaus Heger for his scientific expertise and many great conversations about data and experiments, scientific life and beyond, Yuanyuan Chu not only for providing me with experimental protocols but also for many conversations beyond science, David Rieß and Valeria Soberón – with whom I shared the life of a PhD student throughout the whole time – for conversations about everything and anything in scientific life and far beyond and Valeria in addition for being my bench and desk partner and roommate at conferences as well as for not hesitating to

visit art exhibitions with me. I am very grateful to Barbara Habermehl, Julia Knogler and Claudia Mugler not only for technical assistance during experiments but also for constantly keeping our laboratory up and running.

I also want to thank members of the Fässler department at the Max Planck Institute of Biochemistry who accompanied our laboratory during the first part of my PhD. Furthermore, I would like to thank Soo Jin Min-Weißenhorn from the transgenic core facility of the Max Planck Institute of Biochemistry. I also want to thank Nathalie Knies who offered great help during the first weeks after our relocation to the Technische Universität München.

In addition, I would like to thank Alison Dalfovo for her support. Likewise, I thank Hans-Joerg Schaeffer, Ingrid Wolf and Maximiliane Reif from the coordination office of the International Max Planck Research School for Molecular and Cellular Life Sciences for their support. I would also like to acknowledge the support from the Fonds der Chemischen Industrie.

Last but certainly not least, I want to thank my family and friends for their absolute support not only throughout the course of this work but during the last years. I deeply appreciate their patience and understanding for my dedication to this project. I particularly want to express my sincere gratitude to Nicolas who has been by my side all these years.